

Final Report

Design Synthesis Exercise AE3200

The redesign of an A320 using ammonia as the energy carrier

Group 10



Final Report

Design Synthesis Exercise AE3200

by

Group 10

Student Name	Student Number
Dean Amrane	4840771
Bhargava Sutar	4852052
Ilya Burdo	4532252
Justin Shi	4999630
Cristian Cotovanu	4644840
Witold Biegański	5024005
Deniz Rhode	5040051
Pim Haanen	5092795
Justin Brusche	4772571
Stijn Hersbach	4857054

Tutor: Dr. Arvind Gangoli Rao and Dr. Ivan Langella
Coaches: Federica Castino and Dr. Baris Kumru
Project Duration: April, 2022 - June, 2022
Faculty: Faculty of Aerospace Engineering, Delft
Cover: Airbus 2016 formation flight

Executive Overview

We are living in a constantly changing world and every generation faces its own problems. A challenge that is presently being tackled by engineers and scientists worldwide is reducing the negative impact that the human race has on Earth and its atmosphere. That negative impact stems from different industries and processes with aviation being one of the most polluting ones. A new generation of green aircraft has to be developed within the coming years to mitigate that effect. In order to contribute to this change, over the course of the Design Synthesis Exercise, Group 10 performed the theoretical design of a new generation of the a320 aircraft fuelled by ammonia: the A320-NH3.

Market Analysis

Airbus, as one of the world's leading aircraft manufacturers, expects its fleet size to exceed 46,700 aircraft by 2040. It presently has over 22,950 aircraft in operation. Furthermore, 15,250 planes will need to be replaced with modern planes. The A320 or A321 family is likely to account for the majority of these planes (76%) [16]. As public knowledge of climate change and environmental issues grows, so does the desire for a more environmentally friendly mode of transportation. When it comes to making airplanes more fuel efficient, the aviation industry is doing its part, but totally decarbonizing the sector remains a major challenge. In light of this, ammonia (NH_3) has a strong chance of replacing fossil fuels. Ammonia has a higher volumetric-energy density than other prominent energy carriers like liquid hydrogen (LH_2). Ammonia is a hydrogen-rich gas that is also easier to store and transport than liquid hydrogen since it does not require as much cooling. Liquid ammonia can be stored at a temperature of -33.4°C compared to -253°C in the case of liquid hydrogen at one atm. Overall, this would simplify infrastructure compared to other energy transporters while lowering pollutants such as CO_2 , NO_x , and other hydrocarbons. For an objective market analysis, the strengths, weaknesses, opportunities and threats needs to be compared. The most visual appealing way to compare these is using a SWOT diagram. Hereby the group analyzes the possible success of the future product on the market. The SWOT-diagram can be seen in Table 1.

Table 1: Market SWOT analysis.

Strengths	Weaknesses
<ul style="list-style-type: none">- Carbon-free, thus more eco-friendly, energy carrier<ul style="list-style-type: none">- Price not dependant on oil- Goes well with public opinion of sustainable aviation- Relatively easy storage of ammonium as fuel compared to other carbon-free energy carriers<ul style="list-style-type: none">- Growing supply and demand of ammonia- Ammonia is a non-finite fuel compared to fossil fuels<ul style="list-style-type: none">- Ammonia is not flammable, thus safer compared to kerosene or liquid hydrogen	<ul style="list-style-type: none">- Grey ammonia production- Conservative public opinion- Non-existing infrastructure for ammonia as fuel- Non-existing aircraft components for ammonia as fuel- Ammonia has a lower energy density compared to kerosene
Opportunities	Threats
<ul style="list-style-type: none">- New green-oriented government policies- Green ammonia production- Industry growth- Designing on a base of existing aircraft	<ul style="list-style-type: none">- Development costs- Operational costs- Fuel costs- Competition

Certain technical performance criteria are estimated during the early stages of an aircraft's design and

Table 2: Technical resource budget.

	A320-NH3
CAPACITY	
Pax Max seating	150-200
Typical seating 2-class min	150.00
Typical seating 2-class max	178.00
PERFORMANCE	
Range (km)	≥ 4000 km
Max take-off weight (tonnes)	83.0
Max fuel capacity (litres)	71,537.50
Max fuel mass (kg)	48,216.28
Max Payload weight (tonnes)	21.07
Takeoff length (m)	1,961.50
COST	
Development Costs (million €)	<5000
Unit Cost (million €)	118.45
EMISSIONS	
(NO_x + CO + CO₂ + Soot) emissions [g/kg fuel]	1585.51

can be expected to expand or vary as the project continues. It is a good idea to set a limit value for these adjustments to prevent them from spiraling out of control. Using reference aircraft identical to the A320neo, resource budgets for range, maximum take-off and fuel mass, maximum fuel capacity, payload weight, and take-off length are computed in Table 2.

Requirements & Design Space

In order to properly define the boundaries of the project and the design space for the new A320 generation, a set of requirements had to be devised. The novel aircraft was designed to be based on the a320 family, such that the required modifications are minimised. In terms of performance, the designed platform has to carry at least 150 passengers at a design range of 4000 km. To reduce the environmental impact, it is required that the overall operational emissions of the aircraft are reduced by 50% compared to the A320neo. This means, that the NO_x, CO, unburnt hydrocarbon, soot and water emissions combined will be cut by half. On top of these requirements, the aircraft has been designed in accordance with the latest safety and certification norms.

Risk Analysis

Identifying and comprehending risks is a vital part of every project. In order for the design work to be successful, the risks have to be determined, if possible mitigated, and taken into account during the course of the project. As such, a risk analysis has been performed on the A320-NH3 concept. Most of the risks can be attributed to the utilisation of ammonia as the energy carrier. As the substance is toxic, any leaks within the airframe are unacceptable. The ground operations will also be affected by the toxic properties of ammonia. These risks will be mitigated by adequate, safe design and adjusted ground procedures.

Propulsion

Possibly the biggest changes with respect to the original A320neo design can be seen in the propulsion subsystem of the newly developed aircraft. First of all, replacing kerosene with ammonia requires the implementation of a cracking system. This is done in order to obtain hydrogen, which can then be mixed with ammonia to obtain a mixture with satisfactory combustion characteristics. It was chosen to utilise a thermal catalytic reactor: a device that splits ammonia molecules into nitrogen and hydrogen by means of high temperature and a catalyst. The mixture can then be transferred to the engine, where

the second challenge arises.

Utilising such a fuel directly translates into an increase of NO_x emissions compared to traditional fuels. In order to offset this behavior it was chosen to implement a novel theoretical solution: an Inter-stage Turbine Burner (ITB). It is a second combustion chamber placed between the low pressure and high pressure turbine. Using an ITB promises a reduction in NO_x emissions due to reburning of the molecules. To further decrease the NO_x emissions, while sizing the engine, the possible engine designs are iterated to find the most optimum design point where the emission index of NO_x is the lowest while still generating enough thrust for the aircraft. Additionally, a heat exchanger is implemented within the engine, to provide the necessary heat for the cracking system.

In order for the system to work the ammonia has to be carried onboard the aircraft throughout its operation. It was chosen to store the fuel at an ambient pressure to avoid unnecessary structural reinforcements due to pressurization. In such case, the liquid fuel has a temperature of -33.3°C . In order to eliminate boil off when the aircraft is parked, both passive and active cooling was implemented. Passive insulation is provided by a polyurethane foam sprayed internally in the tanks and active cooling is achieved by circulating cold nitrogen gas through a network of pipes within the fuel tanks. In order to accommodate the necessary fuel two auxiliary tanks will be implemented within the fuselage, expanding the storage volume of the wing and center tanks.

Aircraft Design

Implementing the changes mentioned previously translates directly into an increase of the aircraft weight. Putting additional mass into an existing airframe dictates a change in its aerodynamic properties, geometry and stability characteristics. As such, the design of most of the A320neo components had to be reconsidered and adjusted properly. Major changes with respect to the original aircraft have been made to the wing, high lift devices, empennage and landing gear. The cabin layout was also revised due to the auxiliary fuel tank utilisation.

Operations & Logistic Concept

The infrastructure of ammonia as energy carrier is one of the highlights of this project. Not only the transportation of ammonia but also its production and storage need to be addressed. Since ammonia is one of the mostly produced inorganic chemicals, it has worldwide established methods of transportation and storage. The operational procedures and the regulations are already existing. This fact will simplify the design and production of on-airport transport and storage. Changing the propellant will also have an effect on, for example, existing fueling procedures. Ammonia is far less flammable than kerosene, but its leakage can cause big environmental problems. Prevention of these hazards and possible human casualties is regulated in existing protocols, such as protecting wear.

Sustainability

The ultimate goal of the project is to contribute to cleaner skies in the future. In order to do so, not only the operation of an aircraft has to be considered, but all the processes during its life have to be taken into account. It has been determined that outlined modifications can reduce the environmental impact of the aircraft by more than 50 %. Such a statement can only be true with appropriate sourcing of the fuel. Only if green ammonia is used can the impact be reduced both instantly and in the perspective of the coming years. This emphasizes the importance of importance of clean ammonia production. Evolving aircraft technology can be insufficient if it is not paired with improving the fuel production technology.

Contents

Executive Overview	i
Nomenclature	xi
1 Introduction	1
2 Market Analysis	2
2.1 Current Market Analysis	2
2.2 SWOT Analysis	3
2.2.1 Strengths	3
2.2.2 Weaknesses	4
2.2.3 Opportunities	4
2.2.4 Threats	4
3 Requirements and Constraints	7
3.1 Requirement Analysis	7
3.2 Requirement Discovery Tree	9
3.3 (Sub-)System Requirements	10
4 Technical Risk Assessment	17
4.1 SWOT Analysis	17
4.2 Risk Identification, Analysis and Resolution	17
4.3 RAMS Analysis	19
5 Engineering Design & Analysis	21
5.1 Aircraft configuration	21
5.2 Computation of weights	21
5.3 Wing sizing	22
5.4 Aerodynamic Performance	23
5.4.1 Airfoil design	23
5.4.2 Lift	24
5.4.3 High Lift devices	25
5.4.4 Profile Drag	26
5.4.5 Induced Drag	27
5.5 Tail sizing	29
5.5.1 Longitudinal stability	29
5.5.2 Lateral stability	31
5.6 Aircraft performance	32
5.6.1 Payload range	32
5.6.2 Flight profile diagram	33
5.6.3 Climb performance	33
5.7 Structures	34
5.7.1 Assumptions	34
5.7.2 Load diagrams	35
5.7.3 Loading	37
5.7.4 Layout	38
5.7.5 Stresses	38
5.8 Landing gear adjustments	39
5.9 Hydraulic System architecture	40
6 Propulsion Design	42
6.1 Internal Aircraft Configuration	42

6.1.1	Engine start-up procedure	42
6.1.2	Engine Design	42
6.2	Cracking System Design	48
6.2.1	Assumptions and Simplifications	48
6.2.2	Heat Exchangers and Reactor Design	49
6.2.3	Cracking System Insulation	52
6.2.4	Catalyst Mechanism, Safety, and Production	52
6.2.5	Engine Heat Exchanger	56
6.2.6	Fuel Storage Design	60
7	A320-NH3 Design Optimization	65
7.1	A320-NH3 Aircraft Architecture	65
7.2	Inputs	66
7.2.1	A320neo configuration	66
7.2.2	Propulsion system	66
7.2.3	Flight mission	67
7.3	Modules	67
7.3.1	The main	67
7.3.2	Weight class iteration	68
7.3.3	System sizing	68
7.4	Output	70
8	Final Design Parameters	71
9	Operations & Logistic Concept	75
9.1	Ammonia Infrastructure	75
9.1.1	Production of Ammonia	75
9.1.2	Transport of Ammonia as energy carrier	75
9.1.3	Airport storage	76
9.1.4	On-airport transport	78
9.1.5	Fuel storage sizing	78
9.2	Ground Operations & Regulations	79
9.2.1	Refueling operations & regulations	80
9.2.2	Leakages	81
9.2.3	Fires	81
9.2.4	Noise emissions	82
10	Material & Manufacturing	83
10.1	Materials	83
10.1.1	Material structures	83
10.1.2	Material fuel tank	84
10.2	Manufacturing	84
10.2.1	Parts	84
10.2.2	Assembly	85
10.2.3	Production Plan	85
11	Technical Resource Allocation & Budget Breakdown	87
11.1	Technical Budget Allocation	87
11.1.1	Contingency management	88
11.2	Cost Break-Down Structure	88
11.3	Return on Investment	89
11.3.1	Manufacturing company	89
11.3.2	Airline	91
12	Verification and Validation Procedures	94
12.1	Design program	94
12.2	Verification	94
12.2.1	Code verification	94
12.2.2	Unit tests	94

12.2.3 Discretization Error	95
12.2.4 Extreme values	95
12.3 Validation	95
12.3.1 Weight Iteration	95
12.3.2 Sizing	95
12.3.3 Structures	96
12.4 Verification and Validation plan	96
13 Reliability, Availability, Maintainability, and Safety (RAMS) characteristics	99
14 Sustainability	101
14.1 NO _x Emissions	101
14.1.1 A320-NH3 NO _x Emissions	101
14.1.2 A320neo NO _x Emissions	103
14.2 Carbon Dioxide Emissions	103
14.2.1 A320-NH3 Carbon Dioxide Emissions	103
14.2.2 A320neo CO ₂ Emissions	104
14.3 Water Vapour Emissions	104
14.4 Contrail Forming	104
14.5 Total Emissions	104
14.6 Effect on Climate	104
14.6.1 Weights method	104
14.6.2 CO ₂ - equivalent method	105
14.6.3 Results	106
14.6.4 Cruise altitude effect	107
14.7 Sustainability approach	108
14.7.1 Economical sustainability	108
14.7.2 Social sustainability	109
14.7.3 Environmental sustainability	109
14.7.4 Sustainability quantification	111
15 Sensitivity Analysis	112
15.1 Cracking System Design	112
15.2 Engine Heat Exchanger Design	112
15.2.1 Effect of nitrogen mass flow	112
15.2.2 Effect of combustion chamber temperature	112
15.3 Emissions Analysis	113
16 Requirements and Budgets Compliance	116
17 Conclusion	119
References	121
A Diagrams	125
B Design figures	128
C Task Division	132

List of Figures

2.1	A320neo family orders and deliveries by year (cumulative).	5
3.1	Requirement discovery tree with all the systems and subsystems.	9
5.1	Render of the fuselage.	21
5.2	Render of the wing.	23
5.3	The airfoil NACA4312.	23
5.4	Moment coefficient around the aerodynamic centre for an angle of attack range from -10 to 15 degrees.	24
5.5	The increased CL_{max} for the slats and flaps at different angles of attack.	26
5.6	Lift over drag at sea level conditions and clean configuration.	28
5.7	Minimum drag velocity at sea level conditions and clean configuration.	28
5.8	Loading diagram for the A320-NH3.	30
5.9	Scissor plot A320-NH3 for minimum tail size.	31
5.10	Render of empennage	32
5.11	Payload-Cruise range diagram A320-NH3.	32
5.12	Flight profile diagram.	33
5.13	Climb performance A320-NH3.	34
5.14	Load Diagrams.	36
5.16	FBD fuselage (dimensions are not to scale).	37
5.18	Bending stress of the wing box.	39
5.19	5° clearance and a dihedral angle which is fairly similar	39
5.20	Landing gear design.	40
5.21	A part of blue, green and yellow hydraulic systems visualized.	40
6.1	Model of the Simulated Engine.	43
6.2	General airflow pattern in a combustion chamber	44
6.3	Counter flow heat exchanger system [27].	49
6.4	Temperature profiles of double-pipe heat exchangers [27].	50
6.5	Schematics of cracking system	51
54figure.caption.63		
6.7	Performance of different catalysts on ammonia cracking [30]	54
6.8	Helical heat exchanger configuration used around the combustion chamber section of the engine[40].	58
6.9	Helical heat exchanger configuration used around the nozzle section of the engine[40].	59
6.10	Annular heat exchanger concept.	59
6.11	Internal fuel tank layout	62
6.12	Storage volume and mass in relation to the passive insulation thickness.	64
7.1	The software flowchart.	65
9.1	Diagram of a typical Railway Tank Car (RTC).	76
9.2	Tank with separate roofs and steel outside and interior walls.	77
9.3	Cross section of crack caused by SCC.	78
9.4	Two ways of refueling the aircraft on the airport	79
9.5	Refuel/Defuel Coupling on A320	80
9.6	Fuelling safety zones on an A320-NEO	81
9.7	Noise estimations visualized using 3DExperience software ¹⁵	82

84figure.caption.82

10.2 Cost vs unit production or complexity.	85
10.3 Buckling constants[39].	86
10.4 Production plan flow chart.	86
11.1 Cost breakdown structure.	90
11.2 Return of investment for the manufacturing company.	91
11.3 Return of investment for the airline, considering 120 passengers and a ticket price of \$60/flight hour.	92
11.4 Amount of years at which ROI is reached for different ticket prices, assuming sold out flights.	93
14.1 The relation between the mole fraction of NH_3/H_2 and emission factor	102
14.2 Normalized reduction in NO_x , emissions as the energy provided by ITB increases, I.E. the rise in ITB fractions [59].	102
14.3 Effective radiative forcing (ERF) for contrail cirrus forming and different emissions [6] . .	105
14.4 CO_2 -equivalents for contrail cirrus forming and different emissions [6]	106
14.5 Radiative forcing while flying 2000ft lower and 2000ft higher[7].	107
15.1 CO_2 -equivalents for contrail cirrus forming and different emissions[6].	113
15.3 Sensitivity of NO_x and soot in climate change relative to the A320neo, with green production, using the weight method (method 1)	115
A.1 Functional Flow Diagram.	125
A.2 Functional Breakdown Structure.	126
A.3 Gantt chart.	127
B.1 Top view of the A320-NH3.	128
B.2 Front-side view of the A320-NH3.	129
B.3 Back-side view of the A320-NH3.	129
B.4 Bottom view of the A320-NH3 while in flight.	130
B.5 Front view of the A320-NH3 while in flight.	130
B.6 Back view of the A320-NH3 while in flight.	130
B.7 The visualization of the placement of the cracking system with respect to the wing and the engine. Green: Evaporators, Orange: Preheaters, Red: Reactors, Black: Heat exchangers 2.	131

List of Tables

1	Market SWOT analysis.	i
2	Technical resource budget.	ii
2.1	Market SWOT analysis.	6
3.1	The system and subsystem requirements.	10
4.1	Technical SWOT analysis.	17
4.2	Risk analysis for various risk events. (P = Probability of event, C = Consequence of risk event).	18
4.3	Risk map for all identified technical risks before mitigation.	18
4.4	Legend.	18
4.5	Mitigation strategy medium to extreme level risks.	19
4.6	Risk map after mitigation. Refer to Table 4.4 for the legend.	19
4.7	Contingency management for risks identified close to moderate ranking after mitigation.	19
4.8	RAMS analysis	20
5.1	Fuselage parameters.	21
5.2	Parameters computed for the wing	23
5.3	Interference factor for every component.	27
5.4	Weight components and their respective CG location.	29
5.5	Input values for scissor plot	31
5.6	Parameters computed during tail sizing.	32
5.7	Points in the payload-range diagram with their values.	33
5.8	Relevant velocities as given in Figure 5.14(a) and Figure 5.14(b).	36
5.9	Wing box dimensions in mm.	38
5.10	Fuselage dimensions in cm.	38
5.11	Wing box dimensions.	39
6.1	Assumed Engine Design Parameters.	48
6.2	Engine Sizing Iteration Parameters.	48
6.3	Calculation parameters used in cracking system design	56
6.4	Calculation parameters used in the sizing of the engine heat exchangers.	57
6.5	Fuel storage calculation constants.	61
8.1	Final output values of the optimization system.	71
83table.caption.81		
11.1	Technical budget allocation based on reference aircraft data.	88
11.2	Contingency margins for technical resources.	88
11.3	Variables used in Equation 11.1	91
11.4	Variables used in Equation 11.2.	93
12.1	Verification and validation table.	97
13.1	RAMS analysis	100
14.1	NO _x emissions during different flight phases	103
14.2	CO ₂ emissions during ammonia production processes [52]	103
14.3	Total emissions per aircraft. CO ₂ and NO _x are given in [kg] and Contrails is dimensionless.	104
14.4	Relative climate impact of the A320-NH3 using method 1.	106

14.5 Relative climate impact of the A320-NH3 using method 2.	107
14.6 All sustainability priorities, the ways to measure them and importance.	111
15.1 Engine parameters used for engine heat exchanger size sensitivity analysis.	112
16.1 Requirements Compliance Matrix.	116
16.2 Technical budget compliance matrix	117
C.1 Distribution of the workload.	132

Nomenclature

If a nomenclature is required, a simple template can be found below for convenience. Feel free to use, adapt or completely remove.

Abbreviations

Abbreviation	Definition
ISA	International Standard Atmosphere
FL	Flight Level
SWOT	Strengths weakness opportunities and threats
ITB	Inter turbine burner
RAMS	Reliability, availability, maintainability and safety
EAS	Equivalent Airspeed
TAS	True Airspeed
MTOM	Maximum Takeoff Mass
MTOW	Maximum Takeoff Weight
MLW	Maximum Landing Weight
ZFW	Zero fuel Weight with maximum payload
PZAR	Primary zone air ratio in combustion chamber
TIT	Turbine Inlet Temperature
GPU	Ground power unit
LEAP	Leading Edge Aviation Propulsion
GENx-1B	General Electric Next-generation
PZAR	Primary zone air ratio
BPR	Bypass ratio
TEOS	Tetraethylorthosilicaat
HLD	High lift devices
2D	Two dimensional
3D	Three dimensional
LPC	Low pressure compressor
HPC	High pressure compressor
HPT	High pressure turbine
LPT	Low pressure turbine
NACA	National Advisory Committee for Aeronautics
TO	Take off
MAC	Mean aerodynamic chord
LE	Leading edge
TE	Trailing edge
LER	Leading edge radius
RTC	Railway tank car
SCC	Stress corrosion cracking
RAT	Engine-driven pump
EDP	Ram air turbine
CEPS	Centre for European Policy Studies
NATO	North-Atlantic Treaty Organization
ICAO	International civil aviation organization
CAD	Computer-aided design
NH ₃	Ammonia

Abbreviation	Definition
O ₂	Oxygen
N ₂	Nitrogen
H ₂	Hydrogen
LH ₂	Liquid hydrogen
CO ₂	Carbon dioxide
CO	Carbon monoxide
Al	Aluminium
Zn	Zinc
Mg	Magnesium
Cu	Copper
r	Root
t	Tip
v	Vertical tail
h	Horizontal tail
net	Netto
tot	Total
max	Maximum
ac	Aerodynamic center
c	Camber
cc	Combustion chamber
noz	Nozzle
ann	Annular
hel	Helical
cp	Center of pressure

Symbols

Symbol	Definition	Unit
EAS	Equivalent Airspeed	$[ms^{-1}]$
TAS	True Airspeed	$[ms^{-1}]$
MTOM	Maximum Takeoff Mass	$[kg]$
MTOW	Maximum Takeoff Weight	$[N]$
MLW	Maximum Landing Weight	$[N]$
T/W	Thrust to Weight ratio	$[-]$
ZFW	Zero fuel Weight with maximum payload	$[N]$
PZAR	Primary zone air ratio in combustion chamber	$[-]$
TIT	Turbine Inlet Temperature	$[K]$
a	Helical heat exchanger surface area per coil	$[m^2]$
A_0	Initial frontal area of single heat exchanger plane	$[m^2]$
W_0	Initial mass of single heat exchanger plane	$[kg]$
$A_{1,ann}$	Final frontal area of single heat exchanger plane	$[m^2]$
$W_{1,ann}$	Final mass of single heat exchanger plane	$[kg]$
A_s	Stringer area	$[m^2]$
A_{exch}	Heat exchanger surface area	$[m^2]$
b	Span	$[m]$
c	Chord length	$[m]$
C_p	Specific heat capacity	$[Jkg^{-1}K^{-1}]$
c_r	Root chord length	$[m]$
c_t	Tip chord length	$[m]$
C_L	Wing Lift coefficient	$[-]$
C_{L_α}	Lift curve slope	$[rad^{-1}]$
E	Young's Modulus	$[Pa]$

Symbol	Definition	Unit
G	Shear Modulus	$[Pa]$
h	Height	$[m]$
U	Heat Transfer Coefficient.	$[Wm^{-2}K^{-1}]$
I_{xx}	Second moment of area around x-axis	$[m^4]$
I_{yy}	Second moment of area around y-axis	$[m^4]$
I_{zz}	Second moment of area around z-axis	$[m^4]$
k	Thermal conductivity	$[Wm^{-1}K^{-1}]$
L	Lift	$[N]$
M	Mach number	$[-]$
M_x	Moment around x-axis	$[-]$
M_y	Moment around y-axis	$[-]$
M_z	Moment around z-axis	$[-]$
\dot{m}	Mass flow	$[kgs^{-1}]$
n	Load factor	$[-]$
n_{ult}	Ultimate load factor	$[-]$
N	Number of coils of helical heat exchanger	$[-]$
P	Pressure	$[Pa]$
T	Temperature	$[K]$
t_{sk}	Skin thickness	$[m]$
U	Overall heat transfer coefficient	$[W \cdot m^{-2} \cdot K^{-1}]$
V	Velocity	$[ms^{-1}]$
V_{EAS}	Equivalent Airspeed	$[ms^{-1}]$
V_{TAS}	True Airspeed	$[ms^{-1}]$
V_a	Design Manoeuvring Speed	$[ms^{-1}]$
V_b	Design Speed for maximum gust intensity	$[ms^{-1}]$
V_c	Design Cruise Speed	$[ms^{-1}]$
V_d	Design Dive Speed	$[ms^{-1}]$
V_s	Design Stall Speed	$[ms^{-1}]$
W/S	Wing loading	$[Nm^{-2}]$
w	Weight	$[kg]$
w_{1hel}	Mass per helical coil heat exchanger	$[kg]$
w_{1hel}	Mass per annular heat exchanger plane w	$[kg]$
α	Angle of attack	$[^\circ]$
π	Pressure ratio	$[^\circ]$
ρ	Density	$[kgm^{-3}]$
ρ_0	Density at sea level	$[kgm^{-3}]$
ω	Radial frequency	$[s^{-1}]$
λ	taper ratio	$[-]$
μ	Efficiency	$[-]$
ν	Poisson's ratio	$[-]$
σ	Stress	$[Pa]$
σ_y	Yield Stress	$[Pa]$
σ_t	Tensile Stress	$[Pa]$
σ_c	Compressive Stress	$[Pa]$
Γ	Dihedral	$[^\circ]$

This report starts with an analysis of the market in chapter 2. This analysis is followed by the requirements and constraints set for the design in chapter 3. After this, the possible risks are assessed in chapter 4. Next, the aircraft design is discussed in chapter 5. The engine and remaining parts of the propulsion system are designed in chapter 6. The code that was constructed to obtain all this data as well as optimize the design is explained in chapter 7. A sensitivity analysis for this system is provided in chapter 15. In order to use the actual A320-NH3, the ground operations & logistics need to be adjusted as well. This process is discussed in chapter 9. Following is the post-DSE project planning, for which a plan will be portrayed in chapter 10. The costs and revenues are also of great importance in the business. All of these resource allocations and budget estimations are provided in chapter 11. After this, the verification and validation procedures are given in chapter 12. It is important to perform a RAMS analysis to check the trust in the design, this is done in chapter 13. Next, the sustainable development strategy is given in chapter 14. At the end of the report, the compliance matrix is given in chapter 16. The report ends with a conclusion in chapter 17. In the appendices some of the diagrams shown in previous reports are provided such as the functional flow diagram, functional breakdown structure and Gantt chart. In addition, it includes the renderings of the ammonia-driven aircraft.

7602912/:text=%E2%80%9CGlasgow%20must%20be%20the%20start.a%20choice%20to%20do%20it.%E2%80%9D

Market Analysis

Understanding the possibilities of an A320neo with ammonia as an energy carrier necessitates research into the market for this aircraft type. In section 2.1 this market will be studied, including aspects such as the global economy, current supply and demand, the competitiveness and challenges with regard to sustainability trends. Furthermore, the future prospects are elaborated upon. As part of this analysis, Table 2.1 elaborates on the Strengths, Weaknesses, Opportunities and Threats when bringing this new aircraft to the market. Lastly, the resource allocation and budget breakdown is studied in section 11.1 based on data available of the A320neo as well as empirical data of similar aircraft.

2.1. Current Market Analysis

The need for air transportation is growing as economies expand and the desire for enabling international trade and tourism grows. The demand for air travel is predicted to expand rapidly in the future decades, with an estimated average annual growth rate of 4.3%.¹ If current trends continue, the industry will directly support almost 15 million employment, or 97.8 million if indirect jobs in the global tourist sector are taken into account. This entails balancing a number of aspects, including cost, sustainability, frequency, passenger comfort, and maintenance, to name a few. From this standpoint, it is critical to introduce an aircraft that is both cost-effective and high-performing in order for present airlines to compete and remain competitive in the future [29].

Airbus, as one of the world's leading aircraft manufacturers, expects its fleet size to surpass 46,700 aircraft by 2040. It presently has over 22,950 aircraft in service. Furthermore, 15,250 planes will need to be replaced with modern planes. The A320 or A321 family is likely to account for the majority of these planes, namely 76 percent. The A320neo is therefore a popular and attractive aircraft in terms of competition, particularly among short-to-medium-haul aircraft with a range of up to 6,300 km and a maximum capacity of 194 people. The A320neo has a market share of 60% when compared to the Boeing 737 MAX [4, 16].

The A320neo is in high demand among low cost carriers, particularly in Asia, where the aviation sector is emerging. IndiGo, China Southern Airlines and China Eastern Airlines are among the operators with the biggest fleets of this aircraft type but the overall orders for these and other operators continues to increase. As can be seen in Figure 2.1, the A320neo orders and deliveries have been consistently increasing in the last decade. However, due to a limited manufacturing capacity, the lead times are relatively long resulting into an accumulation of open orders.

Despite the aviation industry's bright prospects and the continued manufacture of the A320neo, the sector faces severe issues, including climate change, environmental effect, flight embarrassment, and airline ticket affordability, to name a few. Aviation, for example, is responsible for 2.1% of global carbon emissions, and nitrogen cycles are disrupted as a result of excessive NO_x emissions, damaging biodiversity. As public knowledge of climate change and environmental issues grows, so does the desire for a more environmentally friendly mode of transportation. When it comes to making airplanes more fuel efficient, the aviation industry is doing its part, but totally decarbonizing the sector remains a major

¹<https://www.icao.int/Meetings/FutureOfAviation/Pages/default.aspx>

challenge. Lithium batteries, biofuels, and liquid hydrogen are examples of alternative energy carriers that are either excessively heavy, inefficient, costly, or have practical constraints. To make a significant transition to a more sustainable mode of transportation, every stone must be turned and unconventional fuels must be examined.

When investigating carbon free fuel options, one may consider the option of utilizing hydrazine as it is already proven in the space industry. It is also utilised as an energy carrier for the emergency power unit in the F-16 fighter jets ². Hydrazine is a chemical compound that, due to its exothermic decomposition reactions, can be used as a monopropellant. When passed over a catalyst it breaks down into hydrogen, nitrogen and ammonia simultaneously releasing a large amount of heat. At a first glance this seems to be a promising solution, however, upon further investigation, the following problems arise. First of all, hydrazine is a highly toxic compound exposure to which can lead to damaging a human liver, kidneys or the central nervous system. Current studies point in the direction of classifying hydrazine as a carcinogenic substance. For this reason, handling the fuel on the ground and sufficiently isolating the passengers from possible exposure are crucial. It was deemed that due to those reasons, other concepts of carbon free energy carriers have to be investigated.

With this in mind, Ammonia (NH_3) has a high potential of replacing fossil fuels. In contrast to other popular energy carriers like liquid hydrogen (H_2), Ammonia has a better volumetric-energy density (141.68 MJ/kg compared to 18.6 MJ/kg at HHV). Ammonia is rich in hydrogen, and additionally it is easier to store and transport than liquid hydrogen since Ammonia needs to be cooled down significantly less. All in all, this would make the infrastructure less complex in comparison to other energy carriers whilst reducing emissions like CO_2 , NO_x and other hydrocarbons. In addition, Ammonia is widely accessible compared to scarce metals like lithium, and requires less volume. Therefore, making hydrogen combustion and Ammonia as energy carrier an interesting technological development which has the potential to be of added value in combating the main challenges faced today. However, when comparing ammonia to kerosene in regards to its supply, it's more difficult when comparing the technology readiness level. The price of completely new infrastructure can be a problem for investors. Also the price of ammonia per liter is higher than of the kerosene. That's respectively €7.54 per liter (99% ammonia) compared to €2.35 per liter this year. ³ In the following paragraphs the possible future changes will be discussed.

2.2. SWOT Analysis

As a part of market analysis a Strengths, Weaknesses, Opportunities & Threats should be compared. This is presented in a SWOT-diagram which can be found in Table 2.1. In this sections, the most important points will further be elaborated and explained.

2.2.1. Strengths

Current days are the times when global warming and environmental problems are ever-increasing, the environmental aspects of business missions are more important than ever. Additionally, more companies start to include environmental aspect in their vision statements and start pro-environmental initiatives as it becomes more and more important for a business to have an environmental friendly image. Therefore, if an environmental friendly solution is suggested, A320-NH3 will be preferred against the other kerosene fueled aircraft. Therefore this project will offer an aircraft which not only is helping decreasing the emissions but also offering a positive point of view for a company which uses it.

Furthermore, when compared to other carbon-free fuels, it is evident that NH_3 is a comparatively simple chemical to work with. In comparison to other sustainability initiatives that focus on storing hydrogen, this greatly simplifies the design of many components of this project.

Energy carriers based on fossil fuels are increasingly becoming an element of the geopolitical power game in the modern era. Countries who are fortunate enough to have oil under their soil can utilize it as a weapon of force. This might result in economic sanctions being imposed on certain countries. All of these events have an impact on the price of oil, resulting in uncertain economic outcomes for enterprises

²<https://www.hydrazine.com/propellants/h70>

³<https://www.lelystadairport.nl/pilot/brandstofprijzen>

that rely on it. Ammonia may also be made from the most fundamental components on the planet, such as water and air. As a result, unlike fossil fuels, the planet will never run out of ammonia. As a country you can't control the fact of having fossil fuels under your soil, however ammonia infrastructure and factories can always be build.

Furthermore, ammonia is gaining popularity around the world and is seen as a great carbon-free transportation fuel. By 2025, its market is expected to be worth more than \$150 billion [53].

2.2.2. Weaknesses

The public vision on an aircraft using Ammonia is very important. People can be very conservative as it comes to new technologies used in the aviation industry. Next to this, the public opinion regarding emitting nitrogen is negative. ⁴ In the Netherlands, the emission of nitrogen oxides is a huge problem because it affects the environment badly. However, nitrogen oxides are often confused with nitrogen, which does not affect the environment. Therefore the emission of nitrogen is often considered as bad by the public opinion.

Next to the costs of the Ammonia production, the pollution during this process is also an existing weakness. 99% of all ammonia is currently produced using Haber-Bosch process. Its a century old process that was mainly developed with low price and high production rate in mind, but without sustainability goals. A so-called 'Grey Ammonia production' uses methane (CH₄) and therefore emitting CO₂ during the process. Current ammonia synthesis is in fact responsible for 451 million metric tons of CO₂ emissions, which is 1% of global CO₂ emissions. ⁵ The goal of flying with Ammonia is to reduce pollution, but if a lot of pollution is emitted during the production phase, the net pollution is still high. Additionally, the non-existing infrastructure for Ammonia is also a weakness this project will have to deal with. Not only does the propulsion for such an aircraft needs to be designed & developed, this also holds for the fueling and preservation technologies at the airport. This can be seen as a weakness since it will cause higher development costs overall. Also, the fact that Ammonia has a lower energy density compared to kerosene and thus meaning the aircraft needs to be able to carry more fuel, which can cause a so-called 'snowball effect' known in aviation.

2.2.3. Opportunities

Politics plays a significant role on the policies regarding fossil fuels. When transportation with Ammonia as energy carrier will become available, it can be expected that the government will higher the taxes on fossil fuels and use grants on carbon-neutral fuels this project is focusing on. Furthermore there is a promising future for a sustainable production of Ammonia which will use renewable energy to produce it - a so-called 'Green Ammonia' [34].

The aviation industry in long-term predicts a significant amount of growth. Market forecast from Airbus suggests that while the number of fleet in service were 22,950 at the beginning of 2020, the fleet size at 2040 will hit 46,720. Additionally, 15,250 aircraft currently in service will need to be replaced by newer aircraft. Thus, 39,020 new deliveries are expected by 2040. 76% of these new deliveries are expected to be small aircraft resembling A320 and A321 family [16]. This is a great opportunity for A320-NH3 as its design, mission profile and market target will be resembling A320 and A321 family. Therefore, it has the opportunity to challenge its competitor small size aircraft's market.

2.2.4. Threats

The first threat is the costs. Both the development costs as the operational costs should be analyzed really well. Due to the current situation of Boeing and Airbus regarding competition, it is not possible to invest a lot of money in a new technology while taking the risk of loosing it in case of the concept turns out not to be feasible. Therefore, the companies should be convinced that investing in an aircraft using Ammonia as energy carrier is worth it. Next to threat that the companies do not want to invest in this technology, operational costs can be considered a threat as well. The fuel costs has a large influence on the operational costs and due to the fact that the production of Ammonia takes a lot of energy, the fuel costs will be higher compared to the one of kerosene. This increase in operational costs will result

⁴<https://www.boerenbusiness.nl/opinies/boerenbusiness/opinie/10894496/stikstofcrisis-wordt-steeds-onbegrijpelijker>

⁵<https://cen.acs.org/environment/green-chemistry/Industrial-ammonia-production-emits-CO2/97/i24>

in higher ticket prizes, which will have a negative impact on the market value. A way to encourage flying with a sustainable energy carrier is by putting taxes on kerosene. However, the government is in charge of this and therefore, the market value of Ammonia based aircraft is highly dependant on the decisions the government makes. This is considered a threat as this lies beyond the control of the Ammonia based aircraft industry.

Airbus A320neo is one of the most successful aircraft when looked at the number of orders. However, the manufacturing capacity and the delivery time leads to the accumulation of orders not being delivered. This accumulation is represented by the number of orders versus completed deliveries and can be seen in Figure 2.1.

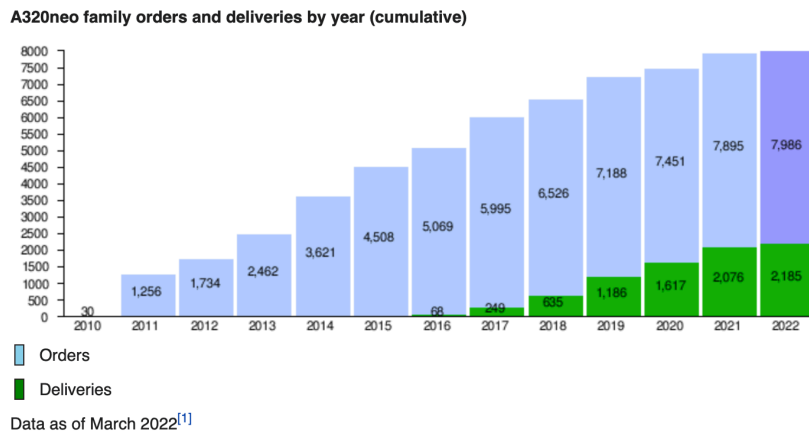


Figure 2.1: A320neo family orders and deliveries by year (cumulative).

6

The pace of number of deliveries increment is similar to the pace of new deliveries but not higher. As the pace of placed orders expected to rise, there is an opportunity that may arise from Airbus not being able to manufacture and deliver orders as expected. This may lead the clients of Airbus to order an alternative aircraft that resembles the mission profile of A320neo from an alternative manufacturer.

At this moment, several energy carriers are investigated to check whether they can be used for sustainable aviation. If another energy carrier turns out to be more applicable, flying with ammonia as energy carrier is not feasible anymore and can therefore lead in a loss of investment. Therefore, the competition between different ideals for the future of sustainable aviation is considered as a threat.

Table 2.1: Market SWOT analysis.

Strengths	Weaknesses
<ul style="list-style-type: none"> - Carbon-free, thus more eco-friendly, energy carrier <ul style="list-style-type: none"> - Price not dependant on oil - Goes well with public opinion of sustainable aviation - Relatively easy storage of ammonium as fuel compared to other carbon-free energy carriers <ul style="list-style-type: none"> - Growing supply and demand of Ammonia - Ammonia is a non-finite fuel compared to fossil fuels <ul style="list-style-type: none"> - Ammonia is not flammable, thus safer compared to kerosene or liquid hydrogen 	<ul style="list-style-type: none"> - Grey Ammonia production - Conservative public opinion - Non-existing infrastructure for Ammonia as fuel - Non-existing aircraft components for Ammonia as fuel - Ammonia has a lower energy density compared to kerosene
Opportunities	Threats
<ul style="list-style-type: none"> - New green-oriented government policies <ul style="list-style-type: none"> - Green Ammonia production - Industry growth - Designing on a base of existing aircraft 	<ul style="list-style-type: none"> - Development costs - Operational costs <ul style="list-style-type: none"> - Fuel costs - Competition

Requirements and Constraints

To give a design problem its first shape, requirements and constraints can be made to define the boundaries of the problem. In section 3.1 the first requirements, which were defined by the client, will be explained. Following are more detailed requirements that define the systems of the aircraft.

At the moment there is a social and a sustainable need for green aviation. Global emissions need to be reduced in order to combat climate change. This has activated researchers and engineers around the world to investigate alternative energy sources that reduce or completely mitigate the emission of green house gasses.

It is the mission to develop a new generation aircraft which will have engines powered by ammonia as energy carrier. The ammonia should be stored in the plane, cracked on board and fed the hydrogen to the combustion engine. The ammonia provides a safer and easier storing method for hydrogen than pure hydrogen. To implement the ammonia in an aircraft, the production, infrastructure and refueling need to be accessible as well. The question is if ammonia can take a plane in to the air and if the ammonia is not bad for the environment in different life stages or with different materials, which will be addressed in chapter 14 [44].

3.1. Requirement Analysis

The stakeholder requirements, also known as the user requirements, are given in section 3.1. These are stated by the client in their language, which are later transferred to technical requirements in section 3.3. The user requirements are negotiable with the client if they are unfeasible due to a high level of complexity or they do interfere with the mission statement. The identifier is structured as **US-[subgroup]-[#]** and are divided into subgroups, respectively: performance (PER), safety and reliability (SAR), sustainability (SUS), engineering budget (ENB) and cost (CST) [44].

US-PER-01: The students shall have a quantification of the performance gain due to ammonia usage.

US-PER-02: The aircraft shall have a refuelling system compatible with ammonia.

US-PER-03: The flight mechanics characteristics of the aircraft shall be evaluated.

US-PER-04: The flight performance of the aircraft shall be compared to the A320neo.

US-PER-05: The climate impact of the aircraft shall be compared to the A320neo.

US-PER-06: The operating cost of the aircraft shall be compared to the A320neo.

US-PER-07: The propulsion system shall be powered by ammonia.

US-PER-08: The aircraft shall satisfy the CS25 rules.

US-PER-09: The aircraft shall have a minimum range of 4000 km.

US-PER-10: The aircraft shall have a passenger capacity between 150-200 passengers.

US-PER-11: The impact of refuelling shall not add more than 30 min to the turnaround time.

US-SAR-01: The aircraft refuelling system shall be safe, following the CS-25 rules.

US-SAR-02: The NH₃ storage system shall be safely separated from the passenger cabin.

US-SAR-03: The safety of NH₃ refuelling system shall be addressed.

US-SAR-04: The storage of NH₃ at the airport shall be addressed.

US-SAR-05: The NH₃ storage system must be able to store the fuel for at least 48 hours without boil-off at an outside air temperature of 45°C.

US-SAR-06: The passenger evacuation time of 90s shall not be affected by the ammonia storage.

US-SUS-01: The supply and production of green hydrogen at the airport shall be investigated.

US-SUS-02: The life cycle of the aircraft shall be analysed.

US-SUS-03: The climate impact of the aircraft shall be at least 50% lower than A320neo.

US-SUS-04: The NO_x, CO, unburnt hydrocarbon and soot emission for the LTO cycle shall be reduced by at least 50% when compared to A320neo.

US-ENB-01: The TRL road-map for the development of the designed aircraft shall be made.

US-ENB-02: The EIS of the aircraft shall be in 2035.

US-CST-01: The total development cost of the aircraft must not exceed €5 billion.

US-CST-02: The cost of the A320-NH₃ aircraft shall not be 15% more than that of the A320neo.

3.2. Requirement Discovery Tree

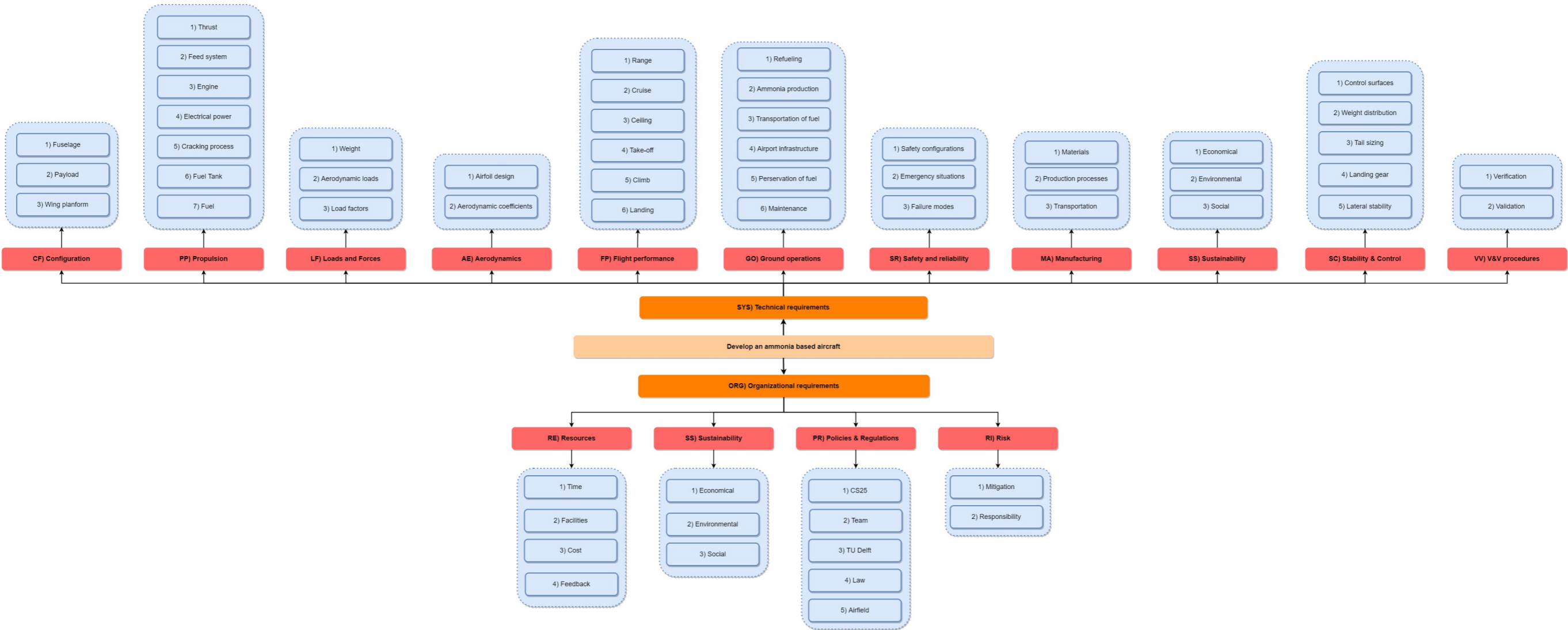






Figure 3.1: Requirement discovery tree with all the systems and subsystems.







3.3. (Sub-)System Requirements

The (Sub-)System Requirements are defined in Table 3.1, where the different codes are legible in Figure 3.1. There are system and organisational requirements, which are both divided in different systems or aspects. These systems have subsystems which are numbered, but also have a new layer of requirements explained in Table 3.1. The identifiers are structured as **SYS/ORG-[System]-[Subsystem]-[Sub-requirement]**. If a key is assigned it is a driving requirement, which is an important requirement for the design. If a skull is assigned it is a killer requirement, which could wipe-off the design of the table.





Table 3.1: The system and subsystem requirements.





Identifier	Key	Requirement
Configuration		
SYS-CF		The aircraft configuration shall be logical and safe.
SYS-CF-01		The fuselage shall be able to support all aircraft components in a safe manner.
SYS-CF-01-01		The fuselage shall host between 150 and 200 passengers including their luggage.
SYS-CF-01-02		The aircraft pressurised compartments shall withstand the flight loads specified in the manoeuvre and gust diagrams [5].
SYS-CF-02		The payload shall be hosted in the aircraft
SYS-CF-02-01		The payload mass shall be no more than 18,000 kg.
SYS-CF-02-02		The payload volume shall be no more than 33 m ³ .
SYS-CF-03		The wing shall generate lift.
SYS-CF-03-01		The aircraft shall not stall at operating velocities.
SYS-CF-03-02		The wing shall be able to generate a lift vector bigger than the weight vector.
Propulsion		
SYS-PP		The aircraft shall be propelled by a turbine [5].
SYS-PP-01		The thrust delivered by the engines shall be sufficient for every stage of the flight with maximum payload.
SYS-PP-02		The feed system shall safely transport the fuel from the tank to the engines.
SYS-PP-02-1		The energy carrier used by the aircraft shall be ammonia (NH ₃) which gives energy through Hydrogen (H ₂).
SYS-PP-02-2		The feed system shall be free of elements which react with ammonia; mercury, chlorine, iodine, bromine, calcium, silver oxide or hypochlorites to prevent explosive compounds. All equipment in contact with ammonia must be free of copper or copper containing alloys because of corrosive effects. Liquid ammonia shall not be combined with oxygen and carbon containing metals to prevent stress corrosion cracking.
SYS-PP-03		The engines shall provide thrust to the aircraft.
SYS-PP-03-01		The engines shall adhere to the CS-E regulations [5].
SYS-PP-03-02		The pylons shall be able to withstand 1g level flight loads acting simultaneously with the limit engine torque loads imposed during either maximum engine acceleration or deceleration [5].
SYS-PP-03-03		The engines and supporting structure shall be designed for a load factor in lateral direction of at least 1.33 or one-third of the limit load factor [5].
SYS-PP-03-04		The aircraft shall be able to withstand the unsymmetrical loads after failure of an engine




Identifier	Key	Requirement
Propulsion		
SYS-PP-04		The aircraft shall be able to give energy to all necessary electrical systems.
SYS-PP-05	☠	The aircraft shall be able to perform cracking of ammonia coming from the fuel tank.
SYS-PP-05-01		The aircraft shall provide hydrogen as fuel to the engine.
SYS-PP-05-02		The temperature range of the reactor shall be between 753.15 K and 1500 K.
SYS-PP-05-03		The energy from the reaction shall be reused to maximize the efficiency of the system.
SYS-PP-05-04		The weight of the cracking system as a whole shall not exceed 5000 kg.
SYS-PP-06		The fuel tank shall store the aircraft fuel.
SYS-PP-06-01		During fuel pumping between tanks the tanks shall not be damaged due to overfilling [5].
SYS-PP-06-02	🔑	The fuel tanks shall be able to withstand every operational load without failure.
SYS-PP-06-03		The fuel tanks shall be able to withstand a pressure of 1.1 atm.
SYS-PP-06-04		The fuel tanks shall be able to withstand a temperature of 333.15 K.
SYS-PP-06-05		The fuel tanks shall not allow fuel release in quantities sufficient to start a serious fire [5].
SYS-PP-06-06		The fuel tanks shall have an expansion space of at least 2% the tank capacity [5].
SYS-PP-06-07		Liquid ammonia shall not leak from the tank.
SYS-PP-06-08	🔑	The fuel tanks shall be able to carry liquefied ammonia at the corresponding liquid pressure and temperature.
SYS-PP-06-09		The fuel tank shall be free of elements which react with ammonia; mercury, chlorine, iodine, bromine, calcium, silver oxide or hypochlorites to prevent explosive compounds.
SYS-PP-06-10		All equipment in contact with ammonia shall be free of alloys containing copper (because of corrosive effects).
SYS-PP-06-11		Liquid ammonia shall not be combined with oxygen and carbon containing metals (prevent stress corrosion cracking).
SYS-PP-07		The aircraft shall carry its own fuel.
SYS-PP-07-01	🔑	The aircraft shall be able to use hydrogen as propellant.
Loads and Forces		
SYS-LO		The loads on the aircraft shall not create dangerous situations.
SYS-LO-01		The aircraft weight shall be lower than the Lift.
SYS-LO-01-01		The aircraft weight shall not be a factor 1.2 larger than the weight of the A320neo.
SYS-LO-02		The aerodynamic forces shall generate a force in upward direction w.r.t. the aircraft body.
SYS-LO-03	🔑	The aircraft shall withstand all applied load factors.
SYS-LO-03-01		The aircraft positive load factor shall not be less than $2 + \frac{24000}{MTOW+10000}$ or 2.5 [5].
SYS-LO-03-02		The aircraft positive load factor shall not exceed 3.8 [5].
SYS-LO-03-03		The aircraft shall have a factor of safety of 1.5 applied to the prescribed limit load [5].
SYS-LO-03-04		The aircraft shall be able to support limit loads without detrimental permanent deformation [5].
SYS-LO-03-05		The structure shall be able to support ultimate loads without failure for at least 3 seconds [5].
SYS-LO-03-06		The aircraft negative load factor shall not be less than -1.0 at speeds up to V_c [5].

Identifier	Key	Requirement
Aerodynamics		
SYS-AE		The aircraft aerodynamic properties shall be clearly defined.
SYS-AE-01		The airfoil shall generate lift.
SYS-AE-01-01		The airfoil shall have a resultant pressure distribution pointing upward.
SYS-AE-01-02		The airfoil shall generate a higher velocity on the top than the bottom.
SYS-AE-01-03		The airfoil shall host the wingbox.
SYS-AE-01-04		The airfoil shall host the high lift devices.
SYS-AE-02		The aerodynamic coefficients of the aircraft shall be clearly defined.
SYS-AE-02-01		The reference stall speed shall be larger or equal to $\frac{V_{CL_{max}}}{\sqrt{n_{zw}}}$, (n_{zw} being the load factor normal to the flight path) [5].
SYS-AE-02-02		The lift coefficient shall be positive [5].
SYS-AE-02-03		The maximum lift coefficient shall be found by using the $C_L - \alpha$ plot.
SYS-AE-02-04		The parasite drag (C_{d_0}) shall be optimised.
Flight performance		
SYS-FP		The flight performance shall fulfil the expected performance stated by the clients [45].
SYS-FP-01		The aircraft shall have a minimum design range of 4000 km [44].
SYS-FP-01-01		The average range shall be around 2500 km for the aircraft.
SYS-FP-01-02		The maximum aircraft range shall be 4000 km.
SYS-FP-02		The aircraft shall be able to perform the cruise phase.
SYS-FP-02-01		The aircraft shall have an optimal cruise velocity of at least 240 ms^{-1} .
SYS-FP-03		The aircraft shall be able to perform a safe landing manoeuvre.
SYS-FP-03-01		The landing distance shall be determined by the distance from 15m high from the landing surface and the point of complete stop [5].
SYS-FP-04		The aircraft shall be able to perform a safe take-off manoeuvre [5].
SYS-FP-04-01		V_C of the aircraft shall be sufficiently greater than V_b [5].
SYS-FP-04-02		V_R of the aircraft shall be greater than V_1 [5].
SYS-FP-04-03		The take off distance on a dry runway shall be at least the sum of the take off point to the point where the plane is 11 meters of the ground [5].
SYS-FP-05		The aircraft shall be able to perform a safe climb manoeuvre.
SYS-FP-05-01		The aircraft's climb performance should be designed to the most unfavourable centre of gravity [5].
Ground operations		
SYS-GO		The aircraft shall be able to cope with the operations on ground.
SYS-GO-01		The aircraft shall be refueled safely at the airport.
SYS-GO-01-1		The aircraft shall have a refuelling system with ammonia as energy carrier.
SYS-GO-01-2		The impact of refuelling shall not add more than 30 min to the turnaround time.
SYS-GO-02		Ammonia shall be produced for its propellant purposes.
SYS-GO-02-01		Production of ammonia shall be sustainable.

Identifier	Key	Requirement
Ground operations		
SYS-GO-03	🔑	The transportation of ammonia shall be safe and doable.
SYS-GO-03-01		Ammonia shall be transported safely from the factory to the airport for storing purposes.
SYS-GO-03-02	🔑	Ammonia shall be transported safely from the storing facilities at the airport to the aircraft for the refueling purposes.
SYS-GO-04		The ammonia fuel infrastructure shall be universal.
SYS-GO-05		The ammonia shall be stored safely at the airport.
SYS-GO-05-01		The ammonia storage system must be able to store the fuel for at least 48 hours without boil-off at an outside air temperature of 45°C.
SYS-GO-06		The aircraft shall allow for maintenance.
SYS-GO-06-01		The fuel tanks shall be placed in such a way that they have facilities to allow maintenance.
SYS-GO-06-02		The aircraft structure shall have a way such that every place can be entered.
Safety and reliability		
SYS-SR		The aircraft shall be safe and reliable.
SYS-SR-01		The systems shall be safely placed so that they do not interfere with passenger safety.
SYS-SR-01-01	🔑	The safety regulations of all operations shall adhere to the CS25 regulations [5].
SYS-SR-01-02		The ammonia storage system shall be safely separated from the passenger cabin.
SYS-SR-01-03		The aircraft parts interfering with passengers shall be fire-proof.
SYS-SR-01-04		The aircraft parts not interfering with passengers shall be fire-resistant.
SYS-SR-01-05		The aircraft shall be able to withstand a bird impact.
SYS-SR-02		The aircraft shall allow for safe continuation in emergency situations.
SYS-SR-02-01	🔑	The passenger evacuation time of 90 s shall not be affected by the ammonia storage.
SYS-SR-02-02		The aircraft shall be able to be totally evacuated in 90 seconds using only half of all the emergency exits [51].
SYS-SR-02-03		The aircraft shall be able to perform a safe landing when one of the engines shuts off [5].
SYS-SR-02-04		The aircraft shall have sufficient safety equipment for each passenger in case of a crash.
SYS-SR-02-05		The aircraft shall be able to float.
SYS-SR-02-06		The aircraft shall be lightning-resistant.
SYS-SR-03		The aircraft shall withstand all applied loads.
SYS-SR-03-01	🔑	Any permanent deformation due to the application of the ultimate load conditions should not prevent continued safe flight and landing [5].
SYS-SR-03-02		The ammonia refuelling system shall be designed for safety of the operators.
SYS-SR-03-03		Strict inspection shall be performed to control aircraft safety.
SYS-SR-03-04		Non-destructive tests shall be performed on the aircraft to check for flaws.
Manufacturing		
SYS-MA	🔑	The aircraft shall be manufacturable.
SYS-MA-01		The aircraft material choice shall support regular production.
SYS-MA-01-01	💀	The aircraft materials shall be available.
SYS-MA-01-02		The total aircraft materials costs shall be no more than 115% of the A320neo material costs.
SYS-MA-01-03		The aircraft materials integrated in the structure shall withstand all flight loads.
SYS-MA-01-04		The aircraft materials shall last at least until the break-even point of the individual parts are reached.
SYS-MA-01-05		The materials chosen shall be able to be produced using existing manufacturing methods.

Identifier	Key	Requirement
Manufacturing		
SYS-MA-02		The production processes used in manufacturing shall be feasible.
SYS-MA-02-01		The production process shall be available.
SYS-MA-02-02		The production process duration shall not exceed the production of the A320neo.
SYS-MA-02-03		The production process shall be sustainable.
SYS-MA-02-04		The EIS of the aircraft shall be at latest in 2035.
SYS-MA-02-05		For all new components of the aircraft the TRL shall be provided.
SYS-MA-03		The final parts shall be able to be transported by regular vehicles.
Sustainability		
SYS-SS		The aircraft design shall be optimised in sustainability.
SYS-SS-01		The aircraft design shall be kept economically sustainable.
SYS-SS-01-01		The resources for the production of the aircraft design shall not be scarce.
SYS-SS-01-02		The break even point shall be met after at most 500 number of aircraft.
SYS-SS-01-03		Lean manufacturing shall be executed to minimize waste and optimize activity.
SYS-SS-02		The aircraft design shall be kept environmentally sustainable.
SYS-SS-02-01		There shall be a sustainable option for every resource produced for production, operation and maintenance.
SYS-SS-02-02		The climate impact of the aircraft shall be at least 50% lower than A320neo
SYS-SS-02-03		The NO _x , CO, unburnt hydrocarbon and soot emission for the LTO cycle shall be reduced by at least 50% when compared to A320neo.
SYS-SS-02-04		The aircraft shall use "blue" or "green" ammonia.
SYS-SS-03		The aircraft design shall be kept socially sustainable.
SYS-SS-03-01		The aircraft controls shall act comparable for the pilot to the A320neo.
SYS-SS-03-02		The aircraft design shall have a green image.
Stability & Control		
SYS-SC		The aircraft shall be stable and controllable.
SYS-SC-01		The control surfaces shall support the aircraft's controllability
SYS-SC-01-01		The control surfaces shall be able to withstand the limit loads during all flight conditions.
SYS-SC-01-02		The wing flaps shall be designed for the critical loads occurring in the conditions prescribed in CS25-345.
SYS-SC-01-03		The control surfaces shall be able to be moved separately from each other.
SYS-SC-01-04		The control surfaces shall be able to generate a difference in pressure over the surface when the deflection changes.
SYS-SC-02		The aircraft shall have an even weight distribution.
SYS-SC-02-01		The aircraft design shall be supported by a loading diagram.
SYS-SC-02-02		The center of gravity range of the aircraft shall be small enough to not interfere with safety concerns.
SYS-SC-02-03		The center of gravity shall lie in front of the neutral point.
SYS-SC-02-04		The center of gravity shall be located such that 85-90% of weight is on the main landing gear, together with SYS-SC-02-02 and SYS-SC-02-03 this will ensure longitudinal stability and controllability.

Identifier	Key	Requirement
Stability & Control		
SYS-SC-03		The horizontal tail shall be sized such that it enhances longitudinal stability.
SYS-SC-03-1		The tail size shall allow for the rotation around the main landing gear.
SYS-SC-03-2		The short period eigenmotion shall be damped [5].
SYS-SC-04		The aircraft landing gear shall provide safe take-off and landing whilst not interfering with the controllability.
SYS-SC-04-01		The main landing gear loads shall not be greater than 103% of the critical design load for symmetrical loading conditions [5].
SYS-SC-04-02		The load on the nose landing gear should be between 8% and 15% of the aircraft maximum take off weight [5].
SYS-SC-04-03		The landing gear shall be positioned close enough behind the center of gravity to ensure a pitch up moment is possible during take-off.
SYS-SC-05		The aircraft shall have lateral stability.
SYS-SC-05-01		All stability derivatives shall have the right sign according to the flight dynamics guide [41].
SYS-SC-05-02		The vertical tail shall enhance lateral stability and controllability.
V&V procedures		
SYS-VV		The (sub)systems of the aircraft shall be verified and validated.
SYS-VV-01		The (sub)systems of the aircraft shall be verified for 100% of the requirements.
SYS-VV-01-01		The (sub)systems shall be verified using unit tests.
SYS-VV-01-02		The (sub)systems shall be verified through the analytical model.
SYS-VV-01-03		The (sub)systems shall be verified for disturbances from the ideal inputs.
SYS-VV-01-04		The (sub)systems shall be verified using extreme value tests.
SYS-VV-01-05		The (sub)systems shall be verified using module tests.
SYS-VV-02		The (sub)systems of the aircraft shall be validated according to the mission goal.
SYS-VV-02-01		The total aircraft performance shall be compared to that of the A320neo.
SYS-VV-02-02		The aircraft design range should be compared to the expected design range.
SYS-VV-02-03		The aircraft passenger capacity shall be compared to the expected amount of passengers.
SYS-VV-02-04		Safety checks shall be performed to check whether the aircraft adheres to the safety regulations.
Resources		
ORG-RE		The design shall stay within available resources.
ORG-RE-01		The design shall be finished within the specified time.
ORG-RE-01-01		The design shall be finished before the deadline specified in June.
ORG-RE-01-02		The design shall be finished with the group of 10 students working full-time.
ORG-RE-02		The design shall be finished using the available facilities.
ORG-RE-02-01		Only facilities at the TU Delft shall be used.
ORG-RE-03		The total cost made during of the aircraft shall not exceed the estimated budget.
ORG-RE-03-1		The total development cost of the aircraft shall not exceed 5 billion euros.
ORG-RE-03-2		The cost of the A320-H3N aircraft shall not be 115% of the A320neo.
ORG-RE-03-3		The annual costs of maintenance shall be no more than \$4,000,000.00 (around 15% of A320 family maintenance) [12].

Identifier	Key	Requirement
Resources		
ORG-RE-04		The feedback shall be implemented into the design.
ORG-RE-04-01		The internal feedback shall be read.
ORG-RE-04-02		The internal feedback shall be implemented in the design.
ORG-RE-04-03		The external feedback shall be read.
ORG-RE-04-04		The external feedback shall be implemented in the design.
Sustainability		
ORG-SS		The group should adhere to the sustainability plan.
ORG-SS-01		The group shall be kept economically sustainable.
ORG-SS-01-01		All group members shall work in the assigned working hours.
ORG-SS-01-02		The group shall work effectively to prevent work in unassigned hours.
ORG-SS-02		The group shall be kept environmentally sustainable.
ORG-SS-02-01		The group shall minimize the waste.
ORG-SS-02-02		The budget for printing shall not exceed 100 euros.
ORG-SS-02-03		Members shall travel by bike.
ORG-SS-03		The group shall be kept socially sustainable.
ORG-SS-03-01		Meetings shall be prepared.
ORG-SS-03-02		Group members shall propagate a good impression.
ORG-SS-03-03		Every group member shall not take a break alone
ORG-SS-03-04		The workloads shall be divided evenly.
ORG-SS-03-05		Recreational activities shall be planned to keep a good morale.
Policies & Regulations		
ORG-PR		Everyone shall adhere to the policies & regulations.
ORG-PR-01		The aircraft should adhere to the regulations stated in the CS25 of large aeroplanes.
ORG-PR-02		The team shall adhere to the rules made by themselves.
ORG-PR-02-01		The complete team shall be present everyday from 9:00 till 17:30.
ORG-PR-02-02		The team shall have a break of 30 minutes everyday.
ORG-PR-02-03		Each group member shall finish their tasks before the indicated deadlines.
ORG-PR-02-04		All the deliverables shall be delivered in the corresponding report.
ORG-PR-03		All team members shall adhere to the TU Delft rules.
ORG-PR-04		All actions taken by the team shall stay within the Dutch law.
ORG-PR-05		The aircraft should adhere to regulations stated by the airport.
Risk		
ORG-RI		All risks shall be assessed.
ORG-RI-01		All risks that can be mitigated and are in the so called 'red' region (high likelihood & impact) shall be mitigated.
ORG-RI-01-01		Risks in the red region shall be either removed or reduced.
ORG-RI-02		All risks that cannot be mitigated and are in the red region shall be handled differently.
ORG-RI-02-01		The responsibility for risks in the red region shall be shared among multiple parties.
ORG-RI-02-02		The risks in the red region that cannot be changed shall be accepted but closely monitored.

Technical Risk Assessment

Every design has risks which need to be managed and addressed if they are deemed as too dangerous. In this chapter, the risks are identified and addressed. By identifying and analysing risks, the impact on the project can be minimised. It starts with a 'strength, weakness, opportunity, and threats' (SWOT) analysis in section 4.1; section 4.2 identifies various risks of the aircraft, and those deemed too high are mitigated. Lastly, in section 4.3 for the aircraft is determined.

4.1. SWOT Analysis

Before analysing the risks, a SWOT-diagram is made in Table 4.1. Although there are a lot of 'harmful' problems, this is very logical when designing something new that has not been proven yet. Moreover, the advantages do outweigh the disadvantages, and the harmful aspects will slowly dissipate as the ammonia aircraft concept develops.

Table 4.1: Technical SWOT analysis.

	Helpful	Harmful
Internal	<ul style="list-style-type: none"> - Ammonia is less flammable than kerosene - No CO_2 emissions - Ammonia is more energy dense than hydrogen volume wise - Renewable fuel instead of finite - Not radically different than other passenger aircraft - Use of recyclable materials 	<ul style="list-style-type: none"> - Less passenger capacity - More complex fuel system - If hybrid, more engines needed - Ammonia is toxic - Produce nitrogen oxide gasses - Ammonia is less energy dense than kerosene
External	<ul style="list-style-type: none"> - Expand the use of ammonia for cheaper production - Less dependent on oil suppliers - There is an existing infrastructure for ammonia delivery 	<ul style="list-style-type: none"> - New airport infrastructure is needed - Costs more - Concept is not proven yet - Consistent green ammonia supply is dependent on the availability of a consistent green energy source

4.2. Risk Identification, Analysis and Resolution

With the SWOT-diagram created in section 4.1, the risks can be determined. In Table 4.2 the risks and causes are grouped in 3 categories: design (DE), general (GE) and operational (OP). Each cause is also given a score from 1 to 5 for its probability of occurrence, where 1 denotes the lowest probability and 5 the highest. Lastly, the consequence is stated for every risk in the last two columns of the table. Here, every consequence is also given a score of 1 to 5 with 1 the lowest consequence and 5 the highest.

Table 4.2: Risk analysis for various risk events. (P = Probability of event, C = Consequence of risk event).

Category	Risk event	Identifier	Cause	P	Consequence	C
Design	Budget overrun	DE-01	Improper budget allocation	2	Higher development cost	3
		DE-02	Longer development time	3		
	Higher weight than expected	DE-03	Improper trade-off criteria	2	May not be able to meet requirement for payload capacity	4
		DE-04	Ammonia system heavier than expected	2		
General	Ammonia contamination	GE-01	Leaks in aircraft tanks	2	Ammonia poisoning (towards passengers or operators); Damage towards environment	4
		GE-02	Aircraft crashes, accidents or incidents	1		
		GE-03	Leaks in airport storage	2		
		GE-04	Tank explosion	1		
	Fire	GE-05	Ammonia reacts violently with acidic compounds	2	Structural damage to the aircraft	5
		GE-06	Hydrogen has a relatively low auto-ignition point	3		
Operational	Insufficient engine thrust	OP-01	Insufficient ammonia cracking rate	5	Flame-out of the engine	3
		OP-02	Fuel pumps fail mid-flight	2	Engine surge	2
		OP-03	Clogging in the pipe system	2	Leakage due to pressure control valves, large amount of fuel losses	4
	Operational system failure	OP-04	Fuel storage cooler fails	2		

With the risks and causes analysed and documented in Table 4.2, a risk map can be created. This is done in Table 4.3. This is calculated by multiplying the 'probability score' with the 'consequence score'. As seen in the legend, the risk level with the corresponding score and color is explained. All the codes in Table 4.3 are the same cause codes as in Table 4.2. So for example, the cause: 'Hydrogen has a relatively low auto-ignition temperature' with code 'GE-06' has a probability score 'P' of 3 and consequence score 'C' of 5. This cause then has a score of 'High'.

Table 4.3: Risk map for all identified technical risks before mitigation.

		Consequence				
		1	2	3	4	5
Probability	1				GE-02, GE-04	
	2		OP-03	DE-01, OP-02	DE-03, DE-04, GE-01, GE-03, OP-04	GE-05
	3			DE-02		GE-06
	4					
	5			OP-01		

Table 4.4: Legend.

Legend	Risk Level
Negligible	1 to 4
Low	5 to 9
Moderate	10 to 14
High	15 to 19
Extreme	20 to 25

In Table 4.3, the causes that are labelled as moderate, high and extremely high need to be mitigated. This is done in Table 4.5. After the mitigation, the final risk map is given in Table 4.6. With the mitigation, there is only one final cause that have the label moderate risk. To minimize the damage (in terms of economics, social, environmental, and technical) caused by the risk events ranked close to moderate or higher when it occurs, contingency plans have to be made. This is then presented in Table 4.7.

Table 4.5: Mitigation strategy medium to extreme level risks.

Identifier	Mitigation strategy	Effect
GE-01	Use higher safety factors; Place tanks outside of pressure bulkheads in aircraft; These should reduce both the probability of ammonia leaking and the consequence for passengers	Probability decreases from 2 to 1; Consequence decreases from 4 to 3
GE-03	Use higher safety factors; This should reduce probability of ammonia leaking	Probability decreases from 2 to 1
GE-05	Increase the frequency of fuel tank inspections to ensure no contaminants that may degrade to acidic compounds in the fuel system remain; This should reduce the probability of the violent reaction occurring	Probability decreases from 2 to 1
GE-06	Use catalyst which needs lower temperature for cracking; Cool hydrogen to lower temperature after cracking and purge the fuel tanks of air using nitrogen before refuelling; This should reduce probability of hydrogen auto-igniting	Probability decreases from 3 to 2
OP-01	A reserve hydrogen tank will be installed for critical flight phases, this hydrogen tank will be able to supplement the hydrogen flow to the engine for a period of time. This should give the pilots time enough to change to a less fuel consuming flight configuration.	Probability decreases from 5 to 3
OP-04	A second cooling system will be installed in case the conventional cooling system fails. This will ensure the fuel has not to be disposed by the pressure valves due to the increasing temperature.	Consequence decreases from 4 to 2

Table 4.6: Risk map after mitigation. Refer to Table 4.4 for the legend.

		Consequence				
		1	2	3	4	5
Probability	1			GE-01	GE-02, GE-04 GE-03	GE-05
	2		OP-03, OP-04	DE-01, OP-02	DE-03, DE-04,	GE-06
	3			DE-02, OP-01		
	4					
	5					

Table 4.7: Contingency management for risks identified close to moderate ranking after mitigation.

Cause Identifier	Contingency strategy
DE-04	Resize the wing such that it incorporates a more complex high lift device for take-off
OP-01	Fly slower as this will require less thrust and less power
GE-05	Install firewall in regions where feed system vents to the atmosphere so that a potential fire does not spread to the cabin
GE-06	Install firewall around high temperature zones so that a potential fire does not spread to the cabin

4.3. RAMS Analysis

In a RAMS analysis the different aircraft components are analysed and their reliability, availability, maintainability and safety is determined. These values are given from a range of 1 to 5, 5 being the best and 1 being the worst. All of these numbers are estimated using different sources. The first four components, the fuselage, wings, empennage and landing gear will show quite some similarity to the A320neo. Therefore, the A320neo can be analysed for these components.

The reliability of the current A320neo is very high, considering that irregularities in the plane program are rare [13]. Furthermore the materials are all available, since the A320 series is one of the most common in air industry. The same holds for the maintainability. Lastly the safety of the A320neo is very high, this can be concluded from the extremely low hull-loss value compared to other aircraft ¹. Therefore all of these have been given a 5 out of 5. What should be noted is that a lot of the values in the RAMS analysis are high. This is because the different components have been chosen in the trade-off such that they are reliable, available, maintainable and safe. When a RAMS analysis would be performed in a preliminary stage the scores would be much lower.

The fuel tank will be made from aluminium, using insulation around it to control the temperature. Since this is a process that is very common in the aerospace industry the reliability and availability have been set high. The maintainability is acceptable, but more difficult since the fuel tank will be placed within the structure and is therefore harder to reach. Since the process is used more often, but there are some ways it could fail, the safety is expected to be sufficient. The safety is a bit less than the fuel tanks filled with kerosene, because of the new technologies.

For the engines the reliability is not so high, the reason for this is that the design has not yet been developed and therefore the reliability is hard to indicate. The availability is low, the concept does not exist yet and therefore is not available. The concept is however very promising and interesting. The maintainability is sufficient: the engine only has some extra volume which is added between the turbines compared to other engines. The chance that this adds extra difficulties is low. Lastly the safety is sufficient as well. The engine should not bring any difficulties in the design but it has also never been tested. Therefore it is difficult to estimate the outcome. The on ground fuel system is very reliable.

Most of the techniques are already available but need to be redesigned for ammonia use. Furthermore active cooling should be used, this will not be unreliable. The availability for the on ground fueling system is very low. These fueling systems do not yet exist for ammonia and need to be created first, therefore they are not yet available. Despite this, the maintainability is very high. There are a lot of testing methods and ways to maintain systems using ammonia. Some of these protocols use echos or infrared radiation. Lastly, the safety is high as well. Ammonia is not flammable and does not decrease the safety compared to kerosene.

The transportation scores very well on all the RAMS criteria. The reason for this is that all of the systems already exist. Ammonia is used in a lot of other industries and the transportation is happening on a daily basis. One drawback is that the transportation infrastructure might need to be scaled up. Last is the safety, which could be an issue since ammonia brings some difficulties when it leaks. However, all vehicles are designed to prevent leakage. No casualties have happened since the beginning of ammonia transportation.

The last property to discuss is the feed system, which also includes the cracking process. Since the process of thermal cracking will be used, this process is well established and therefore sufficiently reliable. The system exists and is currently available as well. It will be hard to maintain, since the system is extremely complex. Therefore, it will take time to repair broken parts and expertise is required. Despite this, it is still possible to do so. Lastly, the system is safe. No oxygen is required in the feed system and therefore there is very little risk of combustion. All of the analysis above led to Table 13.1.

Table 4.8: RAMS analysis

	Reliability (1-5)	Availability (1-5)	Maintainability (1-5)	Safety (1-5)
Fuselage	5	5	5	5
Wings	5	5	5	5
Empennage	5	5	5	5
Landing gear	5	5	5	5
Fuel tanks	5	5	4	4
Engines	2	1	4	3
On-ground fuel system	4	1	5	5
Transportation of fuel	5	5	5	5
Feed system	4	5	3	4

¹https://en.wikipedia.org/wiki/List_of_accidents_and_incidents_involving_the_Airbus_A320_family, 13-05-2022

Engineering Design & Analysis

In this chapter the aircraft design steps are explained. The aircraft is derived from the A320neo but a lot of parameters had to change. This chapter does not contain the propulsion design, which also includes the cracking system and fuel system. That design phase will be discussed in chapter 6.

5.1. Aircraft configuration

As the design objective states, the A320-NH3 will be derived from the A320neo. This means the aircraft dimensions are preferred to stay the same unless changing them is necessary. By removing passengers rows from the back the passenger requirement (150-200 pax) could still be met without changing the fuselage dimensions. This way space was indirectly freed up to compensate for the additional fuel. The fuselage dimensions for the A320-NH3 are given in Table 5.1. A render of this fuselage is given in Figure 5.1.

Table 5.1: Fuselage parameters.

Symbol	Value	Unit
L_{fus}	37.57	m
H_{fus}	4.14	m
W_{fus}	3.95	m
L_{cyl}	20.74	m
$L_{tailcone}$	11.97	m
$L_{nosecone}$	4.86	m

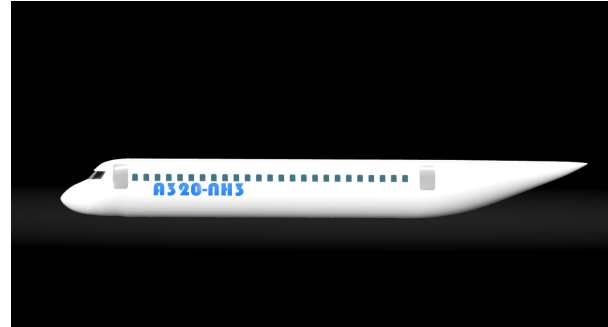


Figure 5.1: Render of the fuselage.

5.2. Computation of weights

The weight iteration block consists of two parts: a class 1 and a class 2 estimation. Class 1 covers the MTOW estimation and in class 2, the individual weights of aircraft parts are estimated in order to determine the OEW. As the OEW influences the MTOW (as well as the fuel fraction) and vice versa, the weight estimation is an iterative process. Class 2 uses aircraft dimensions together with the MZLW, MLW and MTOW to estimate the OEW. After this is done, this OEW is used as an input for the class 1 weight estimation. For this project, the class 1 weight iteration uses a different approach compared to the conventional class 1 weight estimation. For a conventional weight estimation, the mission profile together with some aerodynamic and fuel properties are used to estimate the MTOW based on statistical data. However, there are currently no aircraft in service which are fueled via ammonia. Therefore, no statistical data is available to perform the estimation. Therefore, another approach is used, which employs the following relation to determine the MTOW:

$$MTOW = OEW + W_{payload_{design}} + W_{fuel_{design}} + W_{extrafuel} \quad (5.1)$$

Here, $W_{extrafuel}$, is the reserve fuel taken on board which is used in case of a go-around. the minimum

amount for this is 5% ¹ of the fuel required for the mission. However, some mission profiles require more. Because of this, a value of 7.5 % of the fuel required for the mission will be taken for this weight estimation. To start the class 1 weight estimation, an initial estimation for the extra fuel is assumed. Then, the landing weight can be determined by:

$$LW = OEW + W_{payload_{design}} + W_{extrafuel} \quad (5.2)$$

As stated before, the mission profile data includes the flight conditions, altitude and velocity for every second in flight. When the weight of the aircraft is known, the thrust required and fuel mass flow can be determined. The only weight which is known by now is the landing weight. This means that the only moment during the flight where the thrust and mass flow can be determined is at the last second of the flight where the aircraft weight is equal to the landing weight. However, one should note that the mass flow of the fuel is actually the derivative of the mass of the aircraft. Therefore, as the mass flow during the last second of the flight can be determined, it is possible to calculate the mass of the aircraft a moment just before this last second. Since the aircraft mass is now known for this moment in time, it is possible to determine the mass flow and again the aircraft mass just before this moment. This process can be repeated in order to simulate the flight backwards in time up until the moment where the aircraft starts to accelerate for take-off. At this moment, the mass of the aircraft equals the MTOW and the fuel mass can be determined by the difference in weight between the beginning and the end of the flight. Now, the extra fuel fraction can be updated and the flight can be simulated backwards again. This process is iterated until the moment that the extra fuel weight does not change anymore and the system converged. At this moment, the weight iteration is not finished yet as the new MTOW influences the OEW. To check whether the OEW changes significant, the class 2 weight iteration is performed again and the previous and most recent OEW values are compared. If the difference between these values OEW is significantly small, the weight iteration is finished and the aircraft sizing block can begin. Else, the new OEW is inserted in the class 1 weight estimation and this iteration process is repeated till the system does converge.

5.3. Wing sizing

The wing sizing process consists of a few simple steps which convert the wing of the A320neo into a wing which is suitable for the A320-NH3. This starts by computing the wing loading of the A320neo. The wing loading is determined by dividing the A320neo MTOW by the wing surface area. This led to a wing loading of 6331.6 N/m².

Then, by dividing the new MTOW (of the A320-NH3) by this value, the new surface area is determined. This resulted in a wing surface area of 141.93 m². This also led to an increase in wing volume (fuel tank volume). The wing volume was assumed to increase according to Equation 5.3.

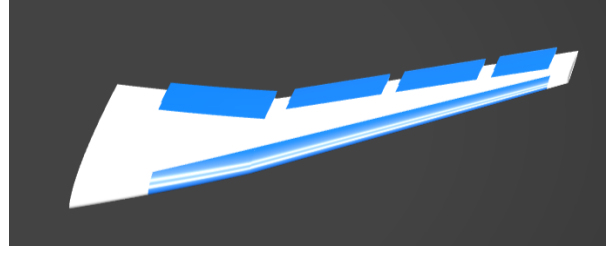
$$V_{A320NH3} = V_{A320neo} \cdot \left(\frac{S_{A320NH3}}{S_{A320neo}} \right)^{1.5} - V_{cracking} - V_{insulation} \quad (5.3)$$

This led to a wing volume (available for fuel tanks) of 32.47 m³. The shape of the wing stays constant, meaning the aspect ratio stays constant as well. This results in the wing geometry parameters given in Table 5.2. The design of the wing is given in Figure 5.2.

¹<https://www.eurocockpit.be/positions-publications/fuel-policy-safety-consistency#:~:text=Contingency%20fuel%20is%20carried%20to,routing%2025-05-2022>

Table 5.2: Parameters computed for the wing

Symbol	Value	Unit
S	141.93	m ²
V	32.47	m ³
Cr	7.55	m
Ct	1.68	m
b	36.72	m
λ	0.240	-
$\Lambda_{0.25}$	25	deg
Γ	5.3	deg
ϕ	-5	deg
A	9.5	-

**Figure 5.2:** Render of the wing.

5.4. Aerodynamic Performance

The airfoil of the A320neo is classified, which forced a method called reverse engineering to estimate the aerodynamic performance. In reality the airfoil geometry is not constant along the span of the wing. With morphing application multiple airfoils are used to optimize the airfoil performance along the span [37]. The aerodynamic performance parameters, could give an indication about these shapes used in the wing. Therefore is a software made to design for the 2D-airfoil performance, the 3D-wing performance, the effect of high lift devices, the profile drag and the induced drag created with the lift. The results of the software will be explained in subsection 5.4.1 to 5.4.5.

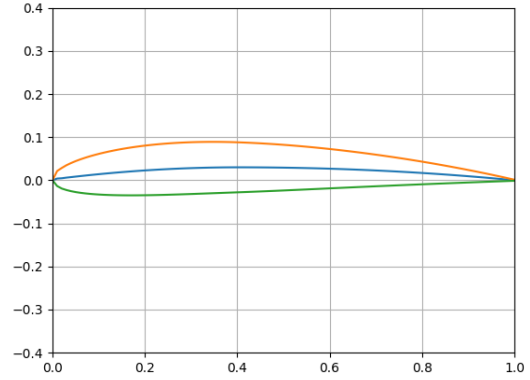
5.4.1. Airfoil design

To simplify the design we used a single airfoil along the span. This is done to have a solid idea of estimated performances. After iteration of different airfoils, the optimal final airfoil chosen for the current design is the NACA4312 ².

NACA4312 configuration summary.

- The maximum camber is 4% of the chord [t/c]
- The maximum camber position is 30% of the chord.
- The thickness to chord ratio is 12% of the chord.
- The max thickness ratio location is 30% of the chord.
- The leading edge ratio is 1.6% of the chord Calculated with Equation 5.4 [31].

$$\frac{LER}{c} = 1.1019 \cdot t/c^2 \quad (5.4)$$

**Figure 5.3:** The airfoil NACA4312.

The airfoil lift coefficient Equation 5.5 is dependent on the integration's over the chord of the airfoil, given by Equation 5.9, 5.10 and 5.11. With Equation 5.6, the center of pressure can be found where the c_l works on [23].

$$c_l(\alpha) = 2\pi \left(A_0(\alpha) + \frac{A_1}{2} \right) \quad (5.5) \quad \frac{x_{cp}}{c}(\alpha) = \frac{1}{4} \left(\frac{2A_0(\alpha) + 2A_1 - A_2}{2A_0 + A_1} \right) \quad (5.6)$$

Equation 5.7 is also computed with an integration over the chord in Equation 5.9, 5.10 and 5.11 we can find the $c_{m,ac}$ from equilibrium around the leading edge shown in Equation 5.8 [23].

²<http://airfoiltools.com/airfoil/naca4digit?MNaca4DigitForm%5Bcamber%5D=4&MNaca4DigitForm%5Bposition%5D=30&MNaca4DigitForm%5B>

$$c_{m,LE}(\alpha) = -\frac{\pi}{2} \left(A_0(\alpha) + A_1 - \frac{A_2}{2} \right) \quad (5.7)$$

$$c_{m,ac}(\alpha) = c_{m,LE} - c_l \frac{\frac{x_{cp}}{c}}{MAC} \quad (5.8)$$

The effect of the angle of attack on the moment around the aerodynamic center Equation 5.8 is shown in Figure 5.4.

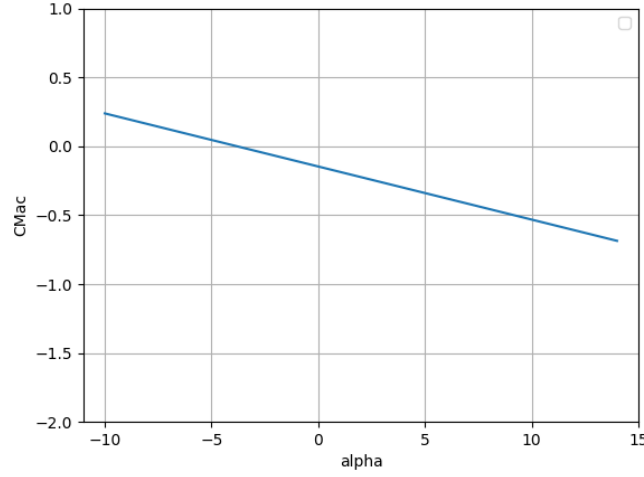


Figure 5.4: Moment coefficient around the aerodynamic centre for an angle of attack range from -10 to 15 degrees.

Cambered airfoils create more lift than symmetric airfoils for the same angle of attack, this increases the induced drag as consequences. To calculate what the effect is of the cambered airfoil, the camber slope is integrated over the length of the chord to find the three coefficients Equation 5.9, 5.10 and 5.11. These are solutions of the Fourier series to solve the A_n coefficients. A_0 is also dependent on the angle of attack [23].

$$A_0(\alpha) = \alpha - \frac{1}{\pi} \int_0^1 \frac{dz}{dx} \frac{-2}{\sqrt{1 - \left(1 - \frac{x}{c}\right)^2}} d\frac{x}{c} \quad (5.9)$$

$$A_1 = \frac{2}{\pi} \int_0^1 \frac{dz}{dx} \left(1 - 2\frac{x}{c}\right) \frac{-2}{\sqrt{1 - \left(1 - \frac{x}{c}\right)^2}} d\frac{x}{c} \quad (5.10)$$

$$A_2 = \frac{2}{\pi} \int_0^1 \frac{dz}{dx} \left(2\left(1 - 2\frac{x}{c}\right)^2 - 1\right) \frac{-2}{\sqrt{1 - \left(1 - \frac{x}{c}\right)^2}} d\frac{x}{c} \quad (5.11)$$

5.4.2. Lift

To design the C_{L_α} for the wing we need to estimate the influence from the finite wing effect. This effect is shown with Equation 5.13 and the C_{l_α} from the thin-airfoil theory shown in Equation 5.12 [23].

$$c_{l_\alpha}(\alpha) = 2\pi \quad [rad] \quad (5.12)$$

$$c_{L_\alpha}(\alpha) = \frac{c_{l_\alpha}}{1 + \frac{c_{l_\alpha}}{\pi A}} \quad (5.13)$$

To size the $C_{L,max, clean}$ in Equation 5.16, the 2D $c_{L,max, clean}$ in Equation 5.14 needs to be found, the 3D/2D ratio $\frac{C_{L,max}}{c_{L,max}}$ and the $\Delta C_{L,max}$.

To find the 2D $c_{L,max, clean}$, we need to find the base effect $(c_{L,max})_{base}$. This is a relation with $\Delta\gamma$ given in the DATCOM 1978 [18] in chapter 2.2.1-8. $\Delta_1 c_{L,max}$ is a correction term for the camber influenced by the position of maximum camber, with an initial location at 30% of the chord. $\Delta_2 c_{L,max}$ is a correction

term for only the position of maximum camber. $\Delta_3 C_{L,max}$ is a correction term for the influence of the Reynolds number. All the three correction terms are related to the leading edge sharpness $\Delta\gamma$ [18].

$$C_{L,max, clean} = (C_{L,max})_{base} + \Delta_1 C_{L,max} + \Delta_2 C_{L,max} + \Delta_3 C_{L,max} \quad (5.14)$$

Equation 5.15 gives a definition for the leading edge sharpness. This is the difference in thickness between the 0.15% and 6.0% of the chord locations. The shape is for all the NACA 4 digit the same, thus it only depends on the thickness over chord ratio [18].

$$\Delta\gamma = 26 \cdot (t/c) \quad \text{if : } NACA4 \text{ digit} \quad (5.15)$$

The $C_{L,max, clean}$ is defined by the $\frac{C_{L,max}}{C_{L,max}}$ ratio which is related to the sweep of the leading edge. $\Delta C_{L,max}$ is zero for mach < 0.2 and dependant on the leading edge sweep, mach and leading edge sharpness. Since we do not fly higher than 0.3 mach close to an angle of attack designed for the maximum lift angles it is almost negligible. This is visible in DATCOM1978 section 4.1.3.4 Method 2 [18].

$$C_{L,max, clean} = \left(\frac{C_{L,max}}{C_{L,max}} \right) \cdot C_{L,max, clean} + \Delta C_{L,max} \quad (5.16)$$

The $C_{L,max, clean}$ from Equation 5.16 is calculated for a straight wing. But the sweep has a influence on the angle of incidence of the free stream velocity in the lateral direction. Equation 5.17 shows effect of the quarter chord sweep in radians [18].

$$C_{L,max, swept} = C_{L,max, unswept} \cdot \cos\varphi_{25} \quad (5.17)$$

5.4.3. High Lift devices

The A320neo has single slotted flaps and slats. The new design A320-NH3 has double slotted flaps and slats to improve the high lift devices. The 2D effect of the flaps is defined by Equation 5.18 and the 2D effect of the slats is defined by Equation 5.19. Equation 5.20 and 5.22 define the effect of the flaps and slats along the wingspan. Equation 5.23 is the formula for the final $C_{L,max}$ that can be used for the take off performances. Most of the equations are originated from the DATCOM1978 aircraft design method section 6.1.1.3. [18].

$(\Delta C_{L,max})_{base}$ is a maximum increase in the lift coefficient for flaps with a 25% flap chord to chord ratio. It is dependent on the airfoil thickness ratio. k_1 is a correction factor for the flap chord to chord ratio, which is defined by the difference from 25%. k_2 is the correction factor for the flap deflection. k_3 is a factor for the flap kinematics. Since this is between internal and external angle differences it is taken as 1.0, so that it has no effect on the calculations and the actual flap deflection can be taken into account [18].

$$\Delta C_{L,max, f} = k_1 \cdot k_2 \cdot k_3 \cdot (\Delta C_{L,max})_{base} \quad (5.18)$$

$C_{l, \delta, max}$ is the maximum slat efficiency defined by the slat chord over chord ratio. η_{max} defines the slat efficiency dependent on the $\frac{LE}{c}$, from Equation 5.4, over the thickness ratio. η_δ gives the efficiency depending on the deflection angle of the slat. This angle is defined by the mid chord position and the difference of the leading edge positions at idle and deployment of the slat. δ_f is the deflection angle. $\frac{c'}{c}$ gives the slat chord over chord ratio [18].

$$\Delta C_{L,max, s} = C_{l, \delta, max} \cdot \eta_{max} \cdot \eta_\delta \cdot \delta_f \cdot \frac{c'}{c} \quad (5.19)$$

The effect of the flaps along the wing span is influenced by the wetted wing area of the flaps over the total wetted area, $\frac{S_{W, f}}{S_W}$. To take the wing sweep into account it is multiplied with K_Λ which is a function of the quarter-chord sweep, stated in Equation 5.21 [18].

$$\Delta C_{L,max, f} = \Delta C_{L,max, f} \cdot \frac{S_{W, f}}{S_W} \cdot K_\Lambda \quad (5.20)$$

$$K_\Lambda = (1 - 0.08 \cos^2 \Lambda c/4) \cos^{3/4} \Lambda c/4 \quad \Lambda c/4 = \varphi_{25} \quad (5.21)$$

The effect of the slats along the wing span is also influenced by the wetted wing area of the slats over the total wetted area, $\frac{S_{W,s}}{S_W}$. The slats are influenced by the sweep of the hinge line of the slats, this hinge line is estimated to be parallel to the quarter chord sweep. Thus $\cos\varphi_{H.L.} = \Lambda_{1/4}$ [47].

$$\Delta C_{L,max,s} = \Delta c_{L,max,s} \cdot \frac{S_{W,s}}{S_W} \cdot \cos\varphi_{H.L.} \quad (5.22)$$

All the $(\Delta)C_{L,max,i}$ components are summed to find the total $C_{L,max}$ stated in Equation 5.23 [18].

$$C_{L,max} = C_{L,max,clean} + \Delta C_{L,max,f} + \Delta C_{L,max,s} \quad (5.23)$$

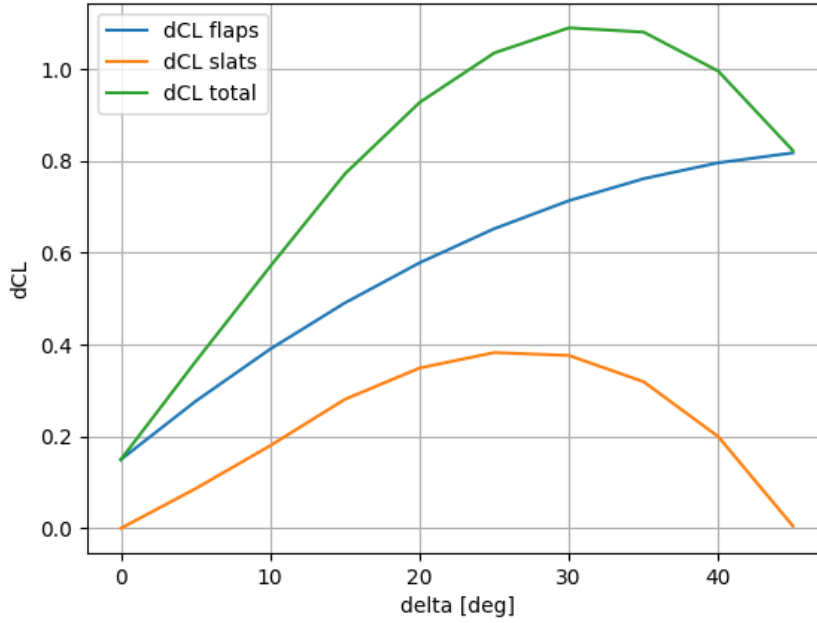


Figure 5.5: The increased CL_{max} for the slats and flaps at different angles of attack.

5.4.4. Profile Drag

The profile drag defined exists of the skin friction, form, trim and additional drag. In Equation 5.24 is defined what has influence on every component of the aircraft. The miscellaneous drag due to the landing gear and other alienated shapes are defined by $C_{D,misc}$. The effect of leakage due to pressure differences at doors or windows is defined by $C_{D,L+P}$, but since these values are marginal for now we neglect it in the design.

The form drag, $C_{f,c}$, takes the shapes into account. The friction coefficient, $C_{f,c}$, is dependent on the surface the flow travels along $\frac{S_{wet,c}}{S_{wet}}$. Multiplied they will give the friction drag coefficient. The interference factor defines the disturbance a components deals to the flow of other parts of the aircraft, general has the fuselage a value of 1.0 because it is taken as reference. The total is found by the summation of every component c. All the components evaluated with Equation 5.24 are the fuselage, nacelle, wings, vertical and horizontal tail and high lift devices [47].

$$C_{D0} = \sum_{c=1}^n \cdot C_{f,c} \cdot FF_c \cdot Q_c \cdot \frac{S_{wet,c}}{S_{wet}} + C_{D,misc} + C_{D,L+P} \quad (5.24)$$

The friction coefficient is defined by the ratio between laminar and turbulent flow, stated in Equation 5.27. The laminar and turbulent friction coefficients are given by Equation 5.25 and 5.26. The fraction of laminar flow is taken to be around 10% of the wing. A Reynolds number of $3.2e9$ is calculated for

cruise at the MAC of the wing [47].

$$C_{f,laminar} = \frac{1.328}{\sqrt{Re}} \quad (5.25)$$

$$C_{f,turbulent} = \frac{0.455}{(\log Re)^{2.58} \cdot (1 + 0.144 \cdot M^2)^{0.65}} \quad (5.26)$$

$$C_f = k_{laminar} \cdot C_{f,laminar} + (1 - k_{turbulent}) \cdot C_{f,turbulent} \quad (5.27)$$

The wetted areas have been determined by the method of Torenbeek1988 at page 150. These are defined by the dimensions ratios and curvature of different components of the fuselage, wing and components of the nacelle [55].

The form factor is defined for the wing and tail by Equation 5.28, for the fuselage it is defined by Equation 5.29 and for the nacelle it is defined by Equation 5.30. The nacelle and fuselage only depend on the shape, but the wing and empennage also take the mach into account [18] [47].

$$FF_{W,H,V} = \left[1 + \frac{0.6}{x_t} \left(\frac{t}{c} \right) + 100 \left(\frac{t}{c} \right)^4 \right] \cdot \left[1.34 \cdot M^{0.18} \cdot (\cos \theta_m)^{0.28} \right] \quad (5.28)$$

$$FF_F = 1 + \frac{60}{(l_f/d_f)^3} + \frac{(l_f/d_f)}{400} \quad (5.29)$$

$$FF_N = 1 + \frac{0.35}{l_N/d_N} \quad (5.30)$$

The interference factor for every component is shown in Table 5.3.

Aircraft part	Interference factor	Property
Fuselage	1.0	Reference
Wing	1.0	Wing with optimized wing-fuselage fairing
Nacelle	1.3	Engine mounted with a small distance from the wing
Vertical wing	1.03	conventional empennage
Horizontal wing	1.04	conventional empennage

Table 5.3: Interference factor for every component.

5.4.5. Induced Drag

The induced drag is caused by the lift created, defined in Equation 5.31. The squared lift is divided by pi, the aspect ratio and the oswald efficiency factor. The oswald efficiency factor is calculated by Equation 5.32. This is showing how the wing performs compared to an elliptical wing. Dennis Howe has researched this and found the equation stated. The influence from the taper ratio is defined in Equation 5.33. N_e is the amount of engines on the aircraft [28].

$$C_{D,i} = \frac{C_L^2}{\pi A e} \quad (5.31)$$

$$e = \frac{1}{(1 + 0.12 \cdot 2M^6) \left[1 + \frac{0.142 + f(\lambda)A(10t/c)^{0.33}}{(\cos \varphi_{25})^2} + \frac{0.1(3N_e + 1)}{(4 + A)^{0.8}} \right]} \quad (5.32)$$

$$f(\lambda) = 0.005 \left(1 + 1.5 (\lambda - 0.6)^2 \right) \quad (5.33)$$

The total drag is a summation of the profile drag and the induced drag. The wave drag is ignored, since the critical mach number is not reached in the designed flight mission. The significant variables for the performance of the design are the lift over drag and the minimum drag velocity.

$$C_D = C_{D,0} + C_{D,i}(C_L)[28] \quad (5.34)$$

The lift over drag is shown in Figure 5.6, the optimal $\frac{L}{D} = 18.11$ for the clean configuration without flaps or slats deployed with a deflection. The minimum drag velocity, $V_{D,min}$, is shown in Figure 5.7.

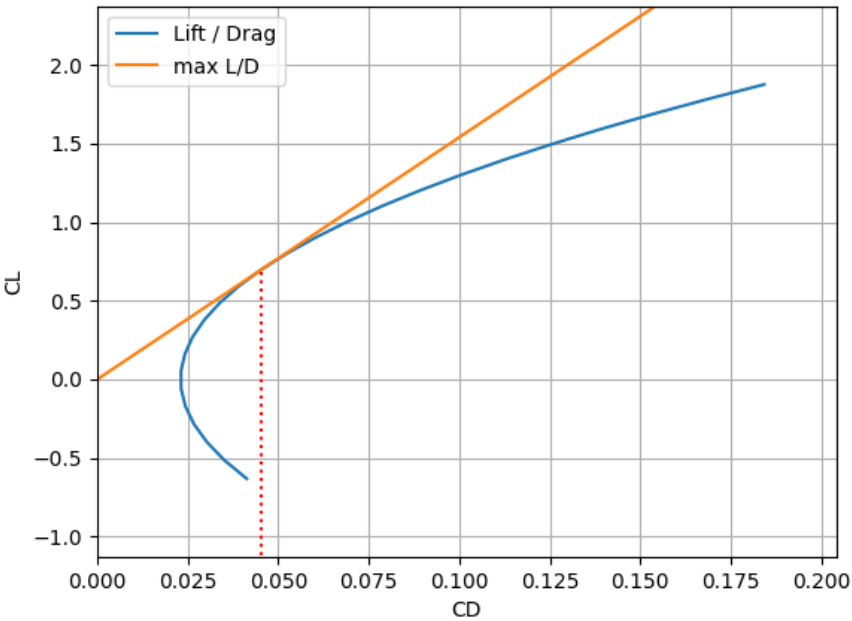


Figure 5.6: Lift over drag at sea level conditions and clean configuration.

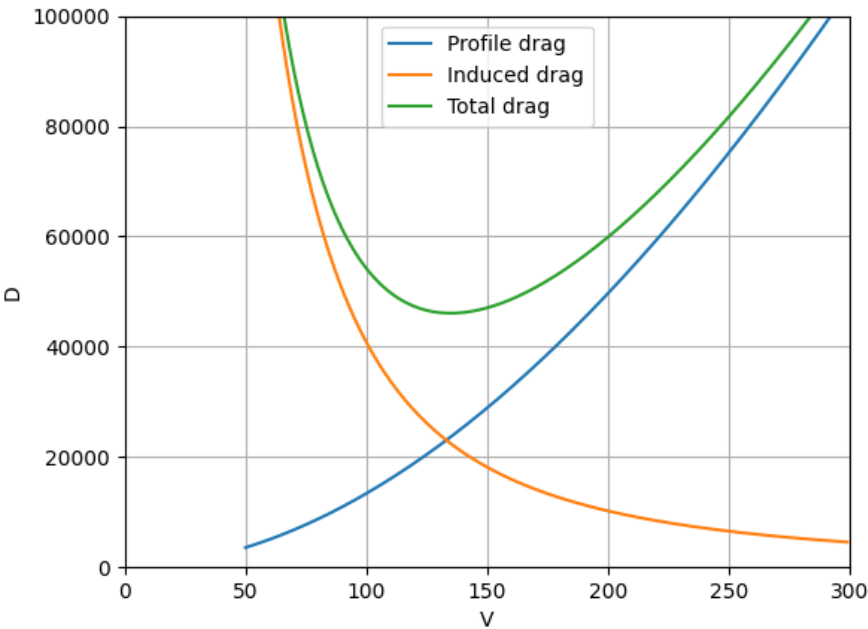


Figure 5.7: Minimum drag velocity at sea level conditions and clean configuration.

5.5. Tail sizing

The tail must be sized according to different characteristics. It is important to optimize the tail in order to save weight while still designing a stable and controllable aircraft. Otherwise this would interfere with the safety. An iterative process was implemented for this.

5.5.1. Longitudinal stability

The horizontal tail size is dependant on the centre of gravity range. In order to compute this range, first the centre of gravity of the empty aircraft must be determined. This was done by taking the separate weight components computed in the class I weight estimation, multiplied by their respective centre of gravity location (see Equation 5.35).

$$CG_{OEW} = \sum_1^n CG_n \frac{W_n}{OEW} \quad (5.35)$$

This also includes additional components like the cracking system, insulation or additional fuel tanks. The weight fractions computed during the weight iteration and their respective c.g. location is provided in Table 5.4. This also shows whether they are part of the fuselage or wing group, which indicates whether the components move when the wing placement changes or whether they stay fixed.

Table 5.4: Weight components and their respective CG location.

	Component	Group (Fuselage/Wing)	Weight (kg)	CG location (m from nose)
W1	Wing	Wing	9910	17.67
W2	Fuselage	Fuselage	8070	16.34
W3	Horizontal tail	Fuselage	970	33.84
W4	Vertical tail	Fuselage	623	33.93
W5	Wheels	Wing	4510	16.06
W6	Pylons	Wing	754	13.40
W7	Engine	Wing	5584	11.58
W8	Systems	Fuselage	7752	16.34
W9	Furnishing	Fuselage	3197	17.22
W10	Operational items	Fuselage	9838	16.34
W11	Cracking system	Wing	4127	17.61

The wing placement could be adjusted in order to optimise the final horizontal tail size. The entire process of the tail sizing was performed for multiple locations of the wing to determine the optimal size. The final centre of gravity for the aircraft's OEW is 19.78 meters from the nose.

This centre of gravity is the starting location of the loading diagram. This loading diagram shows the centre of gravity shift in different loading cases. The loading diagram is given in Figure 5.8

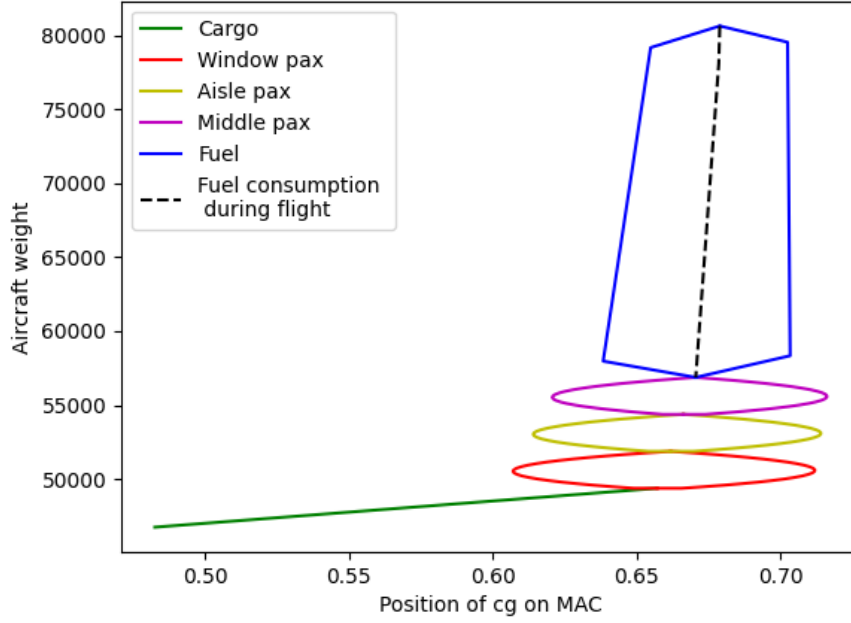


Figure 5.8: Loading diagram for the A320-NH3.

The bottom shows what happens when the cargo is loaded. The cargo hold is placed in the back of the aircraft. The holds which were previously used for cargo are now used to store the fuel. Next the passengers are loaded using the window-aisle rule. First the seats which are next to the window are filled (red), next the seats at the aisle (yellow) and lastly the passengers seated in the middle can take their place (purple). The last thing that is loaded is the fuel (blue). What can be seen is that the block corresponding to the fuel loading is quite odd. The reason for this is that, compared to an aircraft fueled regularly, much more fuel is required in the A320-NH3. Therefore, additional tanks are added in the fuselage, one in the front and one in the back. That is why the shape of the fuel block is a hexagon. The black dotted line represents the fuel usage during the flight. First the tanks in the fuselage will be emptied to keep relieving the wings with fuel weight for a longer time. After this the fuel in the wing will be emptied.

The top of the graph shows the MTOW, which is the weight when the aircraft is fully loaded. Furthermore the most left and right limit determine the centre of gravity range. This ranges from 0.48 to 0.72 %/ MAC. This range could be used in the scissor plot, which eventually determines the horizontal tail size. The scissor plot consists of one line resembling the controllability limit and one line resembling the stability limit. Within these two limits the aircraft is stable. The controllability curve is given in Equation 5.36 while the stability curve is given in Equation 5.37 [43].

$$\overline{x}_{cg} = \overline{x}_{ac} - \frac{C_{m_{ac}}}{C_{L_{A-h}}} + \frac{C_{L_h}}{C_{L_{A-h}}} \frac{S_h l_h}{S \bar{c}} \left(\frac{V_h}{V} \right)^2 \quad (5.36)$$

$$\overline{x}_{cg} = \overline{x}_{ac} + \frac{C_{L_{\alpha_h}}}{C_{L_{\alpha_{A-h}}}} \left(1 - \frac{d\epsilon}{d\alpha} \right) \frac{S_h l_h}{S \bar{c}} \left(\frac{V_h}{V} \right)^2 \quad (5.37)$$

These values could be computed using multiple estimation methods, as well as using values determined before this process. All of these values are given in Table 5.5.

Table 5.5: Input values for scissor plot

Symbol	Value
x_{ac}	0.25
$C_{m_{ac}}$	-0.05
$C_{L_{A-h}}$	1.775
C_{L_h}	-0.8
$\frac{l_h}{c}$	4.316
$\left(\frac{V_h}{V}\right)^2$	0.98
$C_{L_{\alpha_h}}$	4.898
$C_{L_{\alpha_{A-h}}}$	6.173
$\frac{d\epsilon}{d\alpha}$	0.348

Using these values the scissor plot could be determined. This plot is shown in Figure 5.9. As mentioned, the left curve shows the controllability limit and the right curve shows the stability limit. The horizontal line in the middle is the centre of gravity range computed before.

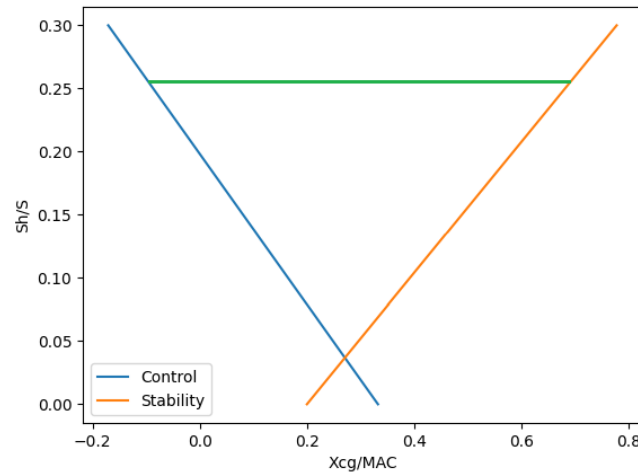
**Figure 5.9:** Scissor plot A320-NH3 for minimum tail size.

Figure 5.9 shows that the horizontal tail size is optimized. This can be concluded since the left and right hand side of the range touch both curves. This optimization process was performed for different wing locations, for which this curve shows the optimal result. The final horizontal tail size is 0.253 of the wing size, which is equal to 35.91 m². This tail size was reached with a wing from which the leading edge of the MAC was at a distance of 15.36 m from the nose ($X_{l_{emac}}$).

5.5.2. Lateral stability

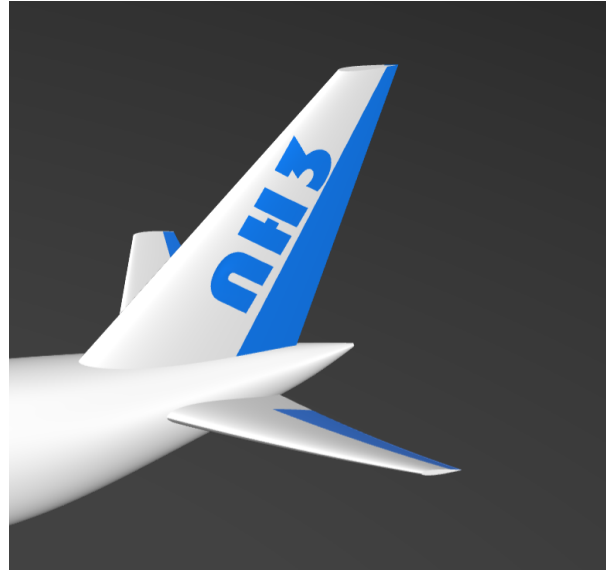
In order to achieve lateral stability, the vertical tail must be sized accordingly. The vertical tail is sized by following four main requirements which must all be met [22]. These requirements are:

1. The aircraft shall be able to withstand a crosswind of at least 20 knots.
2. The static directional and the dynamic stability shall be positive for any landing gear and flap position (Cn_{β}).
3. The aircraft shall be controllable after engine failure.
4. The tail shall provide a certain resistance for a spin manoeuvre.

Each of these requirements rendered a different tail size. In order to meet all of these requirements the largest vertical tail area of the four was taken. This resulted in $S_v = 21.48$ m². All of the important parameters computed in the tail sizing process are shown in Table 5.6. A CATIA render of the empennage is provided in Figure 5.10.

Table 5.6: Parameters computed during tail sizing.

Symbol	Horizontal tail	Vertical tail	Unit
S	35.91	21.48	m ²
Cr	4.27	5.27	m
Ct	1.09	1.60	m
b	13.40	6.26	m
λ	0.256	0.303	-
$\Lambda_{0.25}$	29	34	deg
t/c	0.12	0.15	-
A	5.00	1.82	-
Γ	6.843	0	-

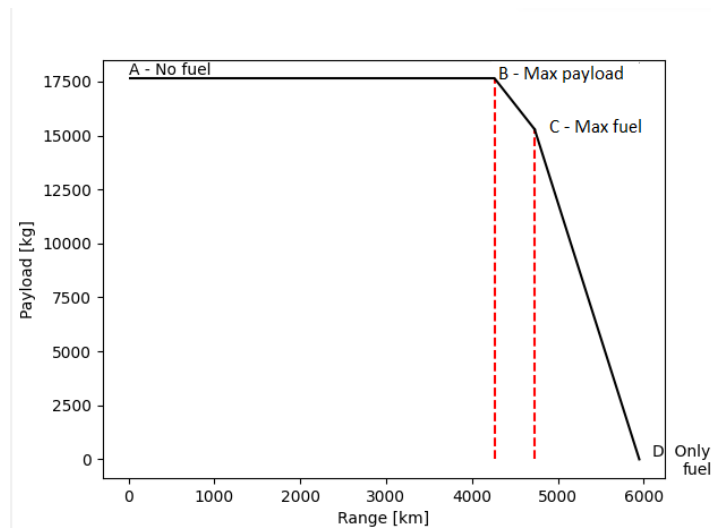
**Figure 5.10:** Render of empennage

5.6. Aircraft performance

In order to evaluate the aircraft performance multiple plots are constructed which give a clearer image of what the aircraft is able to do in the range, flight level and thrust sectors.

5.6.1. Payload range

The payload range diagram shows the range the aircraft is able to fly for different payload conditions. The heavier the aircraft is loaded the lower the range is and vice versa. The payload range diagram is provided in Figure 5.11.

**Figure 5.11:** Payload-Cruise range diagram A320-NH3.

The plot starts at point A, where no fuel is taken on the aircraft and the payload is maximised. Logically, without any fuel, the aircraft will not be able to take off. Hence, the range at this point is 0. The next point on the plot is point B. This edge shows the range for a flight where the maximum amount of payload is taken, the remaining weight is filled with fuel. At this point the range is around 4200 km. The next point on the diagram is point C. This point shows a flight where the maximum amount of fuel is taken whilst the rest of the weight is filled with payload. Here the range is around 4700 km. The last point on

the plot, plot D, shows the maximum range of the aircraft. This maximum range is equal to 5900 km. At this point no payload is taken aboard ($y=0$) and the aircraft only takes fuel. These points are also given in Table 5.7.

Table 5.7: Points in the payload-range diagram with their values.

Point	Payload (kg)	Range (km)
A	17630	0
B	17630	4200
C	15000	4700
D	0	5900

5.6.2. Flight profile diagram

The flight profile diagram shows the profile of a typical flight of the A320-NH3. The diagram shows the different flight phases during a typical flight. The flight starts with taxiing, followed by starting the engines, taking off and then climbing to a flight level of FL030. After this, it climbs to its cruise level of FL370. This is 20 flight levels under the theoretical ceiling. After the cruise phase it descends and subsequently lands. After this the engine shuts down and the aircraft is taxied again. This performance diagram is given in Figure 5.12.

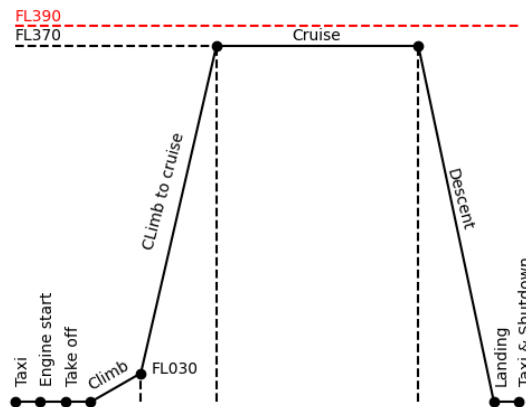


Figure 5.12: Flight profile diagram.

5.6.3. Climb performance

The climb performance diagram gives the amount of power, both available and required power versus the velocity. What this plot shows is the maximum velocity the aircraft can reach. At this point the required power curve crosses the available power curve. The power required to fly at this velocities is not available for this aircraft configuration. This plot is computed for sea level conditions and is given in Figure 5.13.

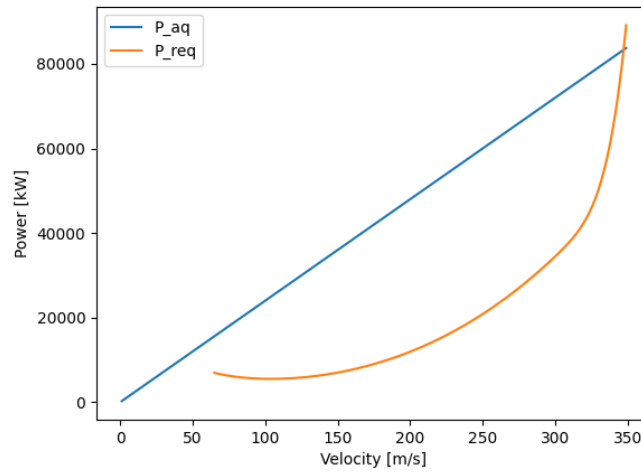


Figure 5.13: Climb performance A320-NH3.

The available power is a curve with constant slope given by equation Equation 5.38 whilst the required power curve does not have a constant slope as the equation is given by Equation 5.39.

$$P_{aq} = T_{aq} \cdot V \quad \text{with} \quad T_{aq} \perp V \quad (5.38)$$

$$P_{req} = D \cdot V \quad \text{with} \quad D \not\perp V \quad (5.39)$$

These two lines cross at a velocity of 343 ms⁻¹, which corresponds to a power of 82000 kW.

5.7. Structures

In this section the structural analysis is executed and explained. Firstly, in subsection 5.7.1, the assumptions are listed. In subsection 5.7.2 the load diagrams are calculated and therefore also the maximum load factor. Next, subsection 5.7.3 describes the loading of the wing and of the fuselage. Moreover, subsection 5.7.4 describes the layout of the wing box and how the fuselage is designed. Finally, subsection 5.7.5 explains how all the stresses are calculated and give the final dimensions of the wing box and fuselage structure.

5.7.1. Assumptions

In the list below, all the assumptions for the structural design are listed. These assumptions are made to simplify calculations and yet give accurate enough results. Moreover, it is also needed to make the computations less extensive, as than the computer will not be able to compute the calculations in the given time-frame.

1. The forces for the wing are at the beginning of cruise. This means that there is no acceleration. For the maximum stress, the maximum load is multiplied with the highest load factor found in subsection 5.7.2.
2. The wing is modelled as thin-walled beam subjected to pure bending. However, this can only be true if the bending moment is constant and thus shear forces are equal to zero.
3. The cross-sections of the wing and fuselage will remain longitudinal to the fibers of the beam. In reality the cross-sections do have a small deflection.
4. The wing is modelled as a cantilever beam, with one clamped end and one free end.
5. The wall thickness is assumed to be much smaller than the other representative dimensions of the cross-section.
6. Beam material is assumed to be homogeneous, isotropic and obey Hooke's Law, i.e. is linearly elastic.
7. Engine and pylon weight are assumed to be point loads on the wing. Moreover, the landing gear is also assumed to be a point load. All these loads are in the y-direction.

8. The thrust provided by the engine is assumed to be a point load in the x-direction.
9. The drag of the wing is assumed to be zero, so all the drag is at the end of the fuselage.
10. The weight of the wing is assumed to be linearly distributed, taking into account the local wing chord length.
11. The wing is assumed to have no sweep.
12. The wing is assumed to have a dihedral angle, however, the force in the y-direction of the lift is assumed to be zero.
13. The fuselage is modelled as a cantilever beam with two free ends.
14. The weight of the fuselage is assumed to be constant over the length of the fuselage
15. The weight of the cargo and fuel are assumed to be constant over their respective departments, and symmetrical so no torsion is created.
16. The diameter of the fuselage is assumed to be constant over the whole circle, while in reality, the horizontal diameter is slightly higher.
17. Hoop stresses on the fuselage due to pressurization are considered negligible when compared to the magnitude of direct stresses caused by bending loads.

5.7.2. Load diagrams

During a flight an aircraft encounters different load factors depending heavily on the speed, altitude and its weight. The critical load cases that the aircraft will bear will be determined in the content of this section. This will be done through the construction of V-n diagrams for manoeuvring and gust loading, however only symmetrical loading cases will be considered at this stage of the design process. These V-n diagrams will be used to determine the different load factors the structure of the wing will have to bear at different speeds for each different scenario considered. After determining the load factors it becomes easy to compute the maximum lift the wing box will carry.

To present a critical V-n diagram one has to take into account the varying velocities and load factors that the aircraft will experience during each flight phase from take-off to landing. The relevant velocities required to create the complete V-n diagrams for all scenarios are as follows:

- V_s indicates the stall speed
- V_a is the manoeuvring speed. It is the speed at which the wing structure will experience maximum stresses with the control surfaces fully deflected.
- V_c is then design cruise speed
- V_d indicates the design dive speed. It is the maximum velocity attainable by the aircraft without risking any structural damage or failure.

For the velocities mentioned above limitations are imposed by the European Aviation Safety Agency (EASA), which every design needs to adhere to [14]. These limitations are summarised below:

$$V_a > V_s \cdot \sqrt{n} \quad (5.40)$$

$$V_c \leq 0.8 \cdot V_d \quad (5.41)$$

Constraints on the maximum load factor (n_{\max}) are also set accordingly. To determine n_{\max} in the clean configuration Equation 5.42 must be used. In this case MTOW is expressed in lbs instead of kg. If the maximum load factor obtained from Equation 5.42 is less than 2.5, 2.5 must be set as a maximum in order to have a reasonable safety margin. For the A320-NH3, this was indeed the case.

$$n_{\max} = 2.1 + \frac{24000}{MTOW + 10000} \quad (5.42)$$

For the negative limit manoeuvring load factor (n_{\min}), it is stated that n_{\min} can not go lower than -1.0 for speeds up to V_c and finally to enclose the flight envelope n_{\min} varies linearly from V_c to V_d . In Figure 5.14(a), the manoeuvre diagram is showed with all the velocities and in Table 5.8 all the velocities are stated.

Another primary source for relevant symmetric load cases that the aircraft will experience during its mission is due to turbulence. This type of load cases will be analysed through the use of gust load diagrams. The A320neo must be designed to satisfy the CS-25 regulations, therefore one must ensure that it also meets the requirements set for gusts within the regulations.

$$V_b = V_s \cdot \sqrt{1 + \frac{K_G \cdot \rho_0 \cdot U_{ref} \cdot V_c \cdot C_{L\alpha}}{2 \cdot W/S}} \quad (5.43)$$

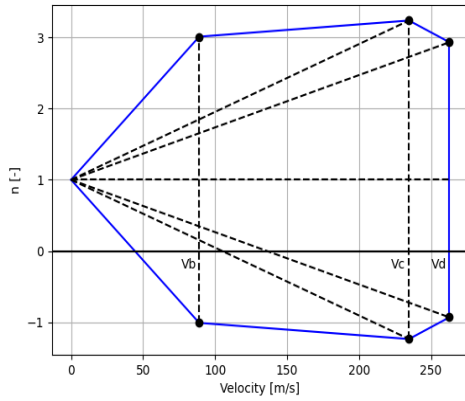
The reference gust velocity, U_{ref} is also defined by CS-25 regulations³. The U_{ref} formula for heights between FL 15 and FL 60 is given in Equation 5.44 and the gust velocity for FL 37 is

$$U_{ref} = (-0.5142 \cdot FL + 51.713) \cdot 0.3048 = 9.963 \quad (5.44)$$

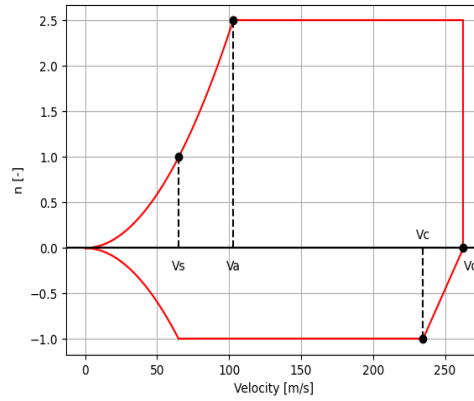
K_G is the empirical gust alleviation factor which was obtained from Equation 5.45 and the aircraft mass ratio, Equation 5.46. In here c is the MAC and ρ is at FL370. The final gust diagram is seen in Figure 5.14(b) and all final speed values are given in Table 5.8 for more clarity. It can be seen from the charts that the n_{max} is reached in the gust diagram at V_c and the value for this is 3.237 (be aware of the axis). This value will then be used for the calculations.

$$K_G = \frac{0.88 \cdot \mu}{5.3 + \mu} \quad (5.45)$$

$$\mu = \frac{2 \cdot W/S}{\rho \cdot c \cdot C_{L\alpha} \cdot g} \quad (5.46)$$



((a)) Gust diagram.



((b)) Manoeuvre diagram.

Figure 5.14: Load Diagrams.

Table 5.8: Relevant velocities as given in Figure 5.14(a) and Figure 5.14(b).

Symbol	EAS [ms^{-1}]
V_s	65.1
V_a	102.9
V_b	89.0
V_c	234.7
V_d	262.8

³https://www.law.cornell.edu/cfr/text/14/25.341#a_5, 12-05-2022

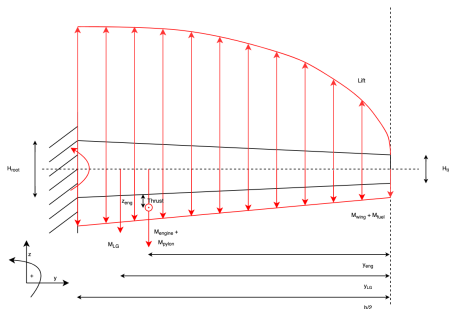
5.7.3. Loading

For calculating the needed structures and dimensions, the loading on the wing and fuselage need to be discussed. The free body diagrams (FBD) are seen in Figure 5.15(a) and Figure 5.16. As can be seen, the four forces are: the Lift force that is upwards, the weight of the aircraft downwards, the thrust at the engines, and the drag of the fuselage. For the the wings, it is assumed to be an trapezoidal beam with the chord length at every point of the wing span calculated with Equation 5.47. The weight distribution is then linearly calculated with respect to the chord length at a distance y . Which then gives an trapezoidal distribution over the area of the wing. The formula for this is Equation 5.48, where W is the total weight of the two wings which are calculated in class II weight estimation. The weight of the engine, pylon and landing gear are point loads on the structure. The aerodynamic wing loading is calculated as an elliptical distribution.

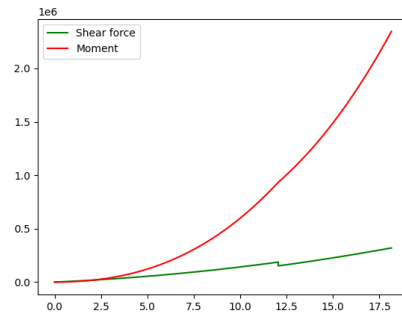
For the fuselage, the weight is distributed constant over the whole length of the fuselage. Furthermore, the weight of the fuel and cargo is evenly distributed over their respectively departments length. The weight of the nose gear is assumed to be a point load, and lastly, the internal load of the wing is also assumed to be a point load upwards, and counteracts the other loads.

$$c(y) = c_r \left[1 - \frac{2 \cdot y}{b} (1 - \lambda) \right] \quad (5.47)$$

$$W(y) = \frac{\frac{W}{2}}{\frac{b}{2} \cdot \frac{(c_r + c_t)}{2}} \cdot \frac{(c_r + c(y))}{2} \cdot y = \frac{W}{b \cdot (c_r + c_t)} \cdot (c_r + c(y)) \cdot y \quad (5.48)$$



((a)) FBD wing box (dimensions are not to scale).



((b)) Moment and shear diagram for wing box.

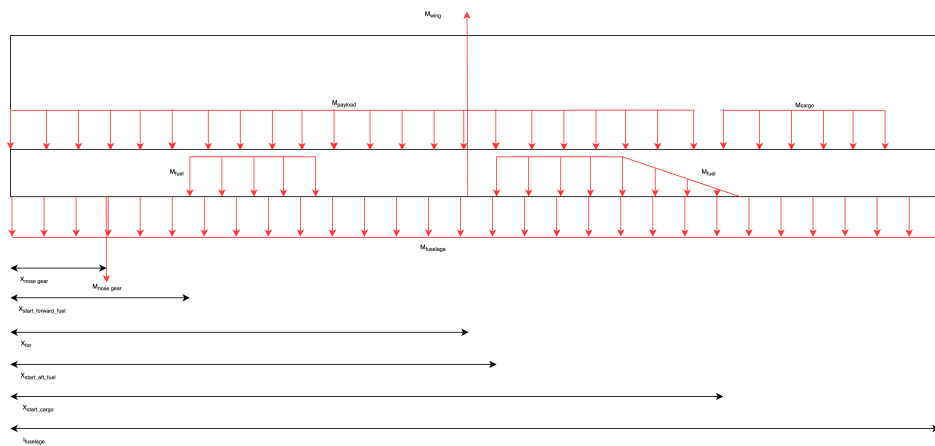
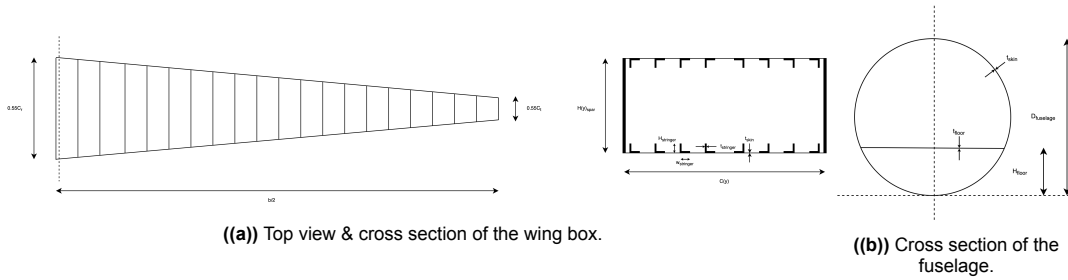


Figure 5.16: FBD fuselage (dimensions are not to scale).

5.7.4. Layout

Compared with the mid term report, the wing box is improved for reducing weight[19]. The wing box is divided into 20 sections. Every section of the wing box has the same spar thickness, however, the skin thickness will get reduced as the internal loads at the tip is less than at the root with a minimum of 2 [mm]. Moreover, Stringers are introduced to counter skin buckling and take over some of the bending moments. The number of stringers will also decrease each section Lastly, ribs are introduced to counteract torsion and give the wing form. An cross section view and top view of the wing box can be seen in Figure 5.17(a). The fuselage is assumed to be a beam with a circular cross section. In addition, the structure has a floor to handle the weight of the payload (passengers and cargo). The cross section of the fuselage can be seen in Figure 5.17(b)



5.7.5. Stresses

With the loadings defined and the layout defined, the stresses on the wing box and fuselage can be calculated. Different stresses are calculated to make sure that no failure will exist. The three equations below determine the critical values for the wing box and the fuselage, and to make sure that both structures do not fail. The bending stress is calculated with Equation 5.49. The maximum bending stress for the wing box is at the root of the wing box, as can be seen in Figure 5.18. The kink in the diagram can be explained by the fact that the skin thickness will increase with every section. For the fuselage, the maximum bending stress is where the wing is connected with the fuselage, as then the counter moment with the wing box is translated. Furthermore, Equation 5.50 provides Euler's critical load. This will estimate if the structure will fail in column buckling. Lastly, Equation 5.51 describes the skin buckling. It is a failure mode which does not involve the geometry of the stringer itself, except the spacing between stringers[39]. The final dimensions of the wing box is stated in Table 5.11 and Table 5.9 and of the fuselage in Table 5.10

$$\sigma = \frac{M_x h(y)}{I_{zz}} \quad (5.49)$$

$$P_{cr} = \frac{\pi^2 EI_{xx}}{l_e^2} \quad (5.50)$$

$$\sigma_{cr} = \frac{\pi^2 k E}{12(1 - \nu^2)} \left(\frac{t}{b} \right)^2 \quad (5.51)$$

Table 5.9: Wing box dimensions in mm.

Stringer length	60
Stringer height	60
Stringer thickness	3
Rib thickness	385

Table 5.10: Fuselage dimensions in cm.

Fuselage thickness	0.21
Floor thickness	0.78
Fuselage diameter	405

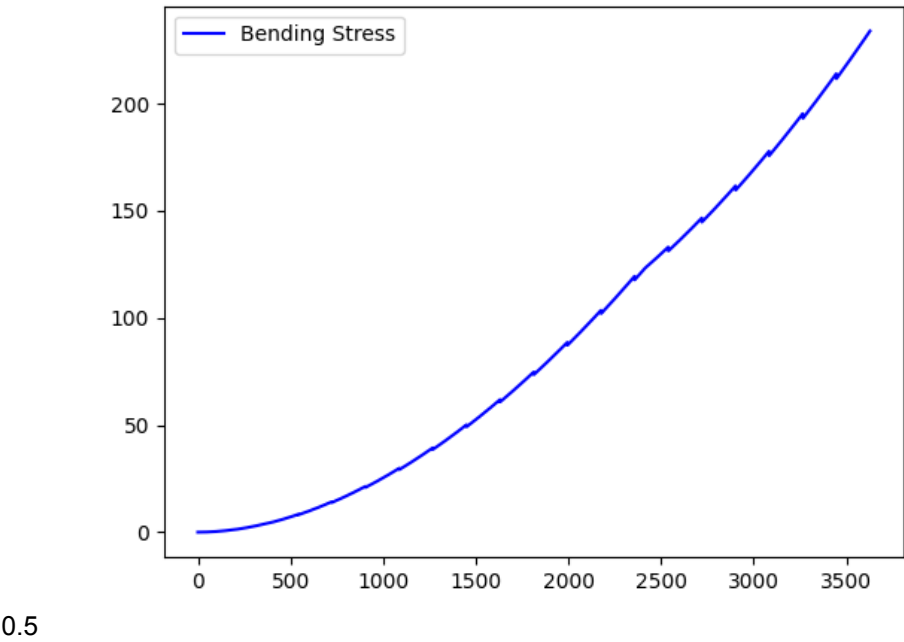


Figure 5.18: Bending stress of the wing box.

Table 5.11: Wing box dimensions.

Section	1	2	3	4	5	6	7	8	9	10
Thickness skin [mm]	2.0	2.0	2.0	2.0	2.0	2.6	3.0	3.8	4.6	5.4
Stringers [-]	4	4	5	6	6	7	8	9	9	10
Section	11	12	13	14	15	16	17	18	19	20
Thickness skin [mm]	6.1	6.9	7.7	8.2	8.7	9.2	9.7	10.3	10.9	11.5
Stringers [-]	11	11	12	12	13	13	14	15	16	16

5.8. Landing gear adjustments

The landing gear needs to be slightly adjusted to cope with the weight increase. The landing gear length are not necessary to be adjusted. Since the engines should have a 5° angle clearance from the ground, which is about similar to the dihedral, moving it around on the wing would make no difference. This can be seen in Figure 5.20, where A and B have a similar size.

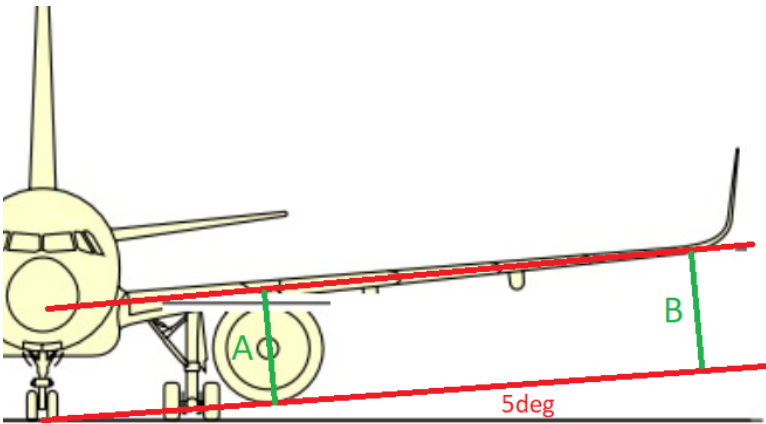


Figure 5.19: 5° clearance and a dihedral angle which is fairly similar

Since the engine size or location will not change compared to that of the A320neo, the landing gear length is sufficient to guarantee this 5° ground clearance angle.

Furthermore the struts cross-sectional area should increase to compensate for the additional aircraft weight. Because of this the cross-sections of the struts will be increased by a factor of $\frac{MTOW_{NH3}}{MTOW_{neo}} = 1.132$. A simplified design of the landing gear is given in Figure 5.20. The irrelevant aircraft components have been made transparent in the figure.

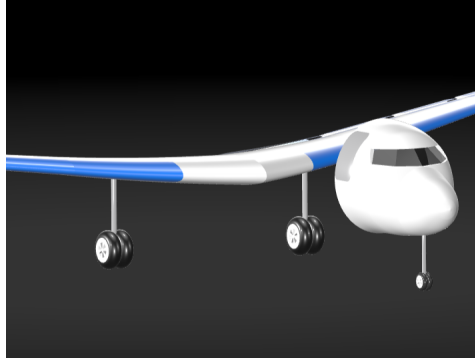


Figure 5.20: Landing gear design.

5.9. Hydraulic System architecture

To move and actuate flight control surfaces, high lift devices and other systems, hydraulics are used in modern commercial aircraft. A force is created and pressure is transmitted to the needed parts by means of pressurizing fluids in vessels. The Airbus A320 features three independent hydraulic systems; blue, green and yellow to minimize the chance of total hydraulic failure. As it can be seen in Figure 5.21 [50], each system has its own reservoir of hydraulic fluids and hydraulic fluids can not be transformed from one system into another. Normal operating pressure is 3000 PSI.⁴

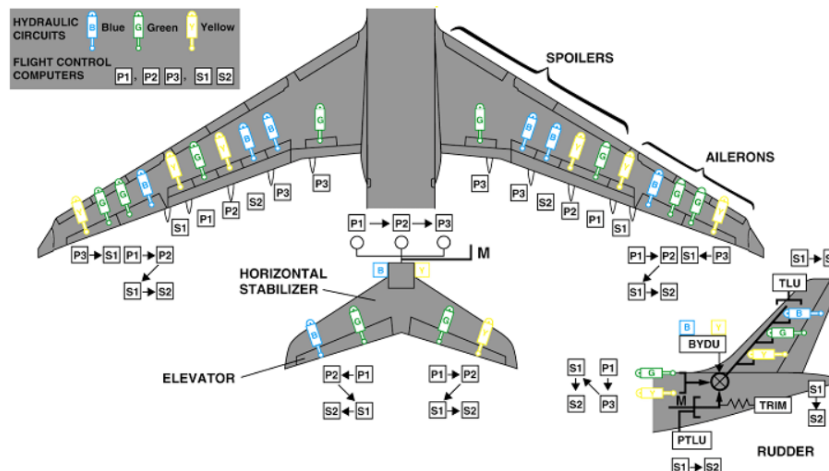


Figure 5.21: A part of blue, green and yellow hydraulic systems visualized.

The operation of these 3 systems is based on⁵;

- Green hydraulic system is powered by an engine-driven pump (EDP) on the engine number one.
- Yellow hydraulics are generally pressurized by an engine two driven pump (EDP 2). Even with engine number 2 turned off, the yellow hydraulic system may be driven by the yellow electric pump, allowing the yellow hydraulics to be pressured on the ground. The yellow system may

⁴<https://www.smartcockpit.com/docs/A320-Hydraulic.pdf>

⁵<https://www.aviationmatters.co/airbus-a320-hydraulic-system/>

also be inflated on the ground with a manual pump, allowing the ground crew to operate the cargo doors even if the aircraft is without electricity.

- The blue electric pump pressurizes the blue hydraulic system. The RAT (Ram Air Turbine) can provide pressure to the blue system in an emergency. In the event of a twin engine failure or a significant electrical malfunction, the RAT is a tiny propeller that may be released into the air stream to deliver hydraulic power to the blue hydraulic system.

These systems are not expected to undergo major change in the renewed A320-NH3 aircraft.

Propulsion Design

6.1. Internal Aircraft Configuration

6.1.1. Engine start-up procedure

At the start of every flight the aircraft must be able to perform the start-up of the systems. Often the aircraft can be found in the so-called 'Cold & Dark stage' at the beginning of the day. During preliminary cockpit preparations, exterior walk-around, briefing etc. the aircraft must produce adequate electrical power. This is usually provided by the Ground Power Unit (GPU). In this section the procedure for the engine start-up will be described.

In order to provide sufficient energy for the start-up procedures of the engines, Auxiliary Power Unit (APU) is used. In the A320-NH3 the fuel that will be burned in the APU will be hydrogen, which differs from the APU's in the normal commercial aircraft that produce electrical power by burning the kerosene from the fuel tanks. Since the A320-NH3 does not have a hydrogen tank, the needed hydrogen for the APU will be provided by starting up the cracking system. The amount of hydrogen that needs to be provided by the cracking system will be much lower than its normal operating capacity. Thus the temperature in the reactor that needs to be achieved will be lower. At this point in the design, there are multiple design solutions for this and the trade-off must be taken place. One of the solution would be initiate the cracking system using a battery in the aircraft or using the GPU (which is also can be used for engine start-up now days but is not a part of a normal procedure). After the start of the APU, the hydrogen will be burned to ensure adequate working of the necessary aircraft subsystems and also starting up the full-scale cracking process to produce the needed hydrogen for the engine start-up.

6.1.2. Engine Design

Assumptions and simplifications of the engine model

To size the engine and simulate its performance, several assumptions are made. These are given below.

- The engine inlet freestream Mach number is set to be 0.428 and stays constant for whole flight. This Mach number is found by reverse engineering the GEnx-1B and comparing the inlet air mass flow rate with the engine inlet fan diameter using Equation 6.2.
- The engine intake freestream is considered to be pure air with molar fractions of 0.21 for O₂ and 0.79 for N₂.
- The inlet fan diameter of the engine is set to be 2.0, very close to the current engine of A320 NEO, LEAP-1A, as this is decided to be the maximum design diameter the engine can have because of landing gear design limitations.
- The effect of shaft nose in the engine intake is not considered.
- The gearbox in the fan has an efficiency of 100% in transferring work.
- Combustion efficiencies and pressure ratios set to be constant during flight.
- The equivalence ratio in the primary zone of the combustion chamber is constant during flight and set to 1.02 [56].
- The calculation of the effect of heat exchanger system of cracking in the combustion chamber is simplified with equation Equation 6.19.

- The cooling down of combustion products in the secondary zone is simulated using Cantera in steady-state equilibrium, not including parameters such as residence time.
- The re-circulation of the combustion products between first zone and dilution zone are neglected.
- The fuel is assumed to be injected at the same temperature and pressure in combustion chamber inlet.

For the sizing of the engine, a simulation based approach is chosen. The following model is created via Python software.

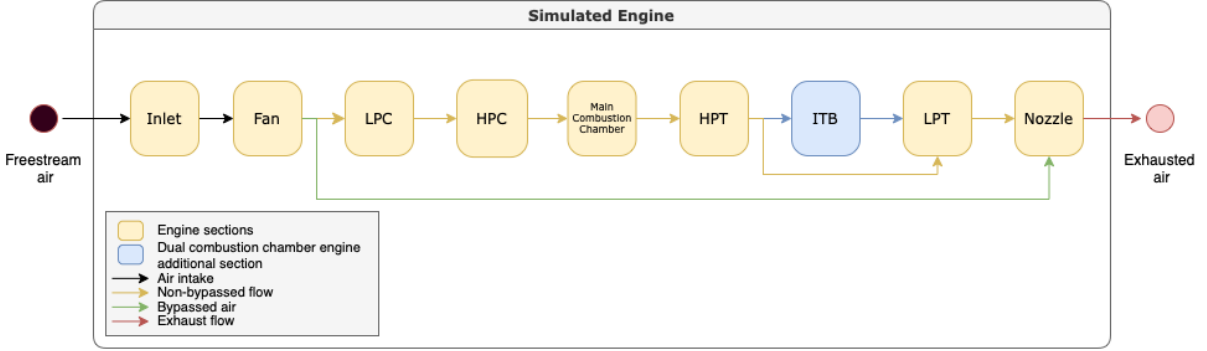


Figure 6.1: Model of the Simulated Engine.

The engine model

In Figure 6.1, the engine configuration simulated is given. LPC, HPC, HPT, ITB and LPT stand for low pressure compressor, high pressure compressor, high pressure turbine, inter-stage turbine burner and low pressure turbine, respectively. In this engine configuration, compared to conventional aero-engines, a second combustion chamber, namely an inter-stage turbine burner, is added.

Inlet

The engine model derives the engine intake air mass flow rate at any altitude from its relation to the corrected engine intake air mass flow rate at sea level conditions. This relation is given below.

$$V_{fan} = M_{fan} \sqrt{\gamma_{air} R T_{sea-level}} \quad (6.1) \quad \dot{m}_{corrected} = V_{fan} \rho_{sea-level} \frac{\pi D_{eng}^2}{4} \quad (6.2)$$

$$\dot{m}_{inlet} = \dot{m}_{corrected} \frac{\frac{P_{t,a}}{P_{sea-level}}}{\sqrt{\frac{T_{t,a}}{T_{sea-level}}}} \quad (6.3)$$

$$\dot{m}_{core} = \frac{\dot{m}_{inlet}}{1 + BPR} \quad (6.4) \quad \dot{m}_{bypassed} = \dot{m}_{inlet} - \dot{m}_{core} \quad (6.5)$$

The total temperature T_t and total pressure P_t used for mass flow rate calculations for any flight condition are derived using the equations below.

$$T_t = T_a \left(1 + \frac{\gamma_{air} - 1}{2} M^2\right) \quad (6.6) \quad P_t = P_a \left(\frac{T_t}{T_a}\right)^{\frac{\gamma_{air}}{\gamma_{air} - 1}} \quad (6.7)$$

The temperature at the inlet is set to equal total temperature T_t , whereas the pressure at the inlet is calculated using the following relation, taking the inlet efficiency into consideration.

$$P_{inlet} = P_a \left(1 + \frac{\eta_{inlet}(\gamma_{air} - 1)}{2} M^2\right)^{\frac{\gamma_{air}}{\gamma_{air} - 1}} \quad (6.8)$$

Fan

Fan is the initial compressor stage, where all the inlet air is being compressed. The resulting airflow pressure and temperature change resulted from the fan stage is simulated by the formulas given below.

$$P_{fan_{outlet}} = P_{fan_{inlet}} \cdot \pi_{fan} \quad (6.9) \quad T_{fan_{outlet}} = T_{fan_{inlet}} \left(1 + \frac{1}{\eta_{fan}} \left(\frac{P_{fan_{outlet}}}{P_{fan_{inlet}}}^{\frac{\gamma_{air}-1}{\gamma_{air}}} - 1 \right) \right) \quad (6.10)$$

In order to compress the airflow, work needs to be done on the flow. The work required for fan is calculated using equation below.

$$W_{fan} = \dot{m}_{inlet} C_{p,air} (\Delta T_{fan}) \quad (6.11)$$

Low pressure compressor

During LPC and HPC stages, the core airflow is being compressed. The pressure and temperature of the flow after LPC can be calculates using relations below.

$$P_{LPC_{outlet}} = P_{LPC_{inlet}} \cdot \pi_{LPC} \quad (6.12) \quad T_{LPC_{outlet}} = T_{LPC_{inlet}} \left(1 + \frac{1}{\eta_{LPC}} \left(\frac{P_{LPC_{outlet}}}{P_{LPC_{inlet}}}^{\frac{\gamma_{air}-1}{\gamma_{air}}} - 1 \right) \right) \quad (6.13)$$

To compress the flow, work is again required on the airflow. Compared to fan stage, the work required on the flow will be less because of the decrease in mass flow, regarding high bypass ratio.

$$W_{LPC} = \dot{m}_{core} C_{p,air} (\Delta T_{LPC}) \quad (6.14)$$

High pressure compressor

High pressure compressor is the compressor stage after LPC. The same relations used for LPC can be used again to find the flow characteristics just before entering combustion chamber.

$$P_{HPC_{outlet}} = P_{HPC_{inlet}} \cdot \pi_{HPC} \quad (6.15) \quad T_{HPC_{outlet}} = T_{HPC_{inlet}} \left(1 + \frac{1}{\eta_{HPC}} \left(\frac{P_{HPC_{outlet}}}{P_{HPC_{inlet}}}^{\frac{\gamma_{air}-1}{\gamma_{air}}} - 1 \right) \right) \quad (6.16)$$

$$W_{HPC} = \dot{m}_{core} C_{p,air} (\Delta T_{HPC}) \quad (6.17)$$

Combustion chamber

The general airflow pattern in a combustion chamber is shown in Figure 6.2 [54].

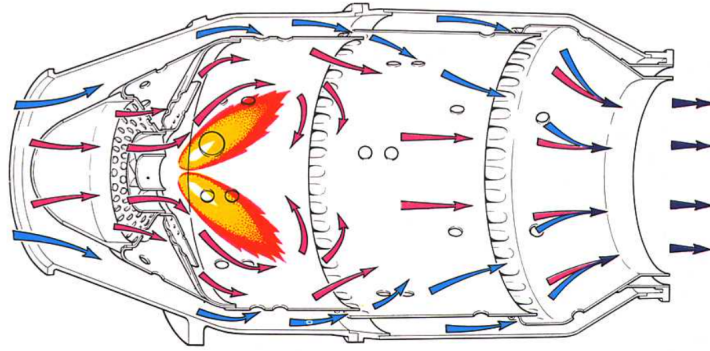


Figure 6.2: General airflow pattern in a combustion chamber

In general, a conventional combustion chamber can be divided to three zones: primary zone, intermediate zone, and dilution zone. The engine model created for this project simplifies the model by having two main zones: primary zone and secondary (dilution) zone [54]. The primary zone is where the fuel is injected and mixed sufficiently with some of the core airflow introduced to facilitate complete combustion and flame stabilisation. The secondary (dilution) zone is where the remaining air is introduced to cool the core flow down to the mean exit temperature required for entry to the turbine [56]. The ratio of the introduced core air flow in the primary zone to the total core air flow introduced is given by PZAR, primary zone air ratio.

In the simulation, a certain equivalence ratio for the primary zone has been chosen. This equals 0.9. With that information, the mass flow rate of the fuel added in the combustion chamber can be calculated using Equation 6.18, where $m_{frac,fuel}$ stands for the mass fraction of the fuel in the total gas flow in the primary zone. As the mass flow rate of the fuel is known, the temperature change inside the combustion chamber can be calculated by using Equation 6.19 and then simulating the cooling-down of the combustion products via Cantera, a thermodynamics simulator.¹ Equation 6.19 is used to calculate the temperature just before the cooling down, where the heat extracted $Q_{heat-exchange}$ for the heat-exchanger system of cracking is also taken into account.

$$\dot{m}_{fuel} = \frac{\dot{m}_{core} \cdot PZAR}{\frac{1}{m_{frac,fuel}} - 1} \quad (6.18)$$

$$TIT_{before-cooling} = T_{cc,inlet} + \frac{\dot{m}_{fuel} \mu_{cc} LHV_{fuel}}{\dot{m}_{core} \cdot PZAR \cdot C_{p,gas}} - \frac{Q_{heat-exchange}}{(\dot{m}_{core} \cdot PZAR + \dot{m}_{fuel}) C_{p,gas}} \quad (6.19)$$

$$\dot{m}_{cc,outlet} = \dot{m}_{core} + \dot{m}_{fuel} \quad (6.20)$$

Thermodynamics simulator: Cantera To simulate thermodynamic relations, Cantera is used. Cantera is an open-source suite of tools for problems involving chemical kinetics, thermodynamics, and transport processes.² Thermodynamic values such as C_p , LHV and γ for different conditions are simulated through Cantera. Cantera uses ideal gas law and assumption, NASA Polynomials Species Thermo entries and Maxwell relations to simulate ideal gas models and calculate thermodynamic coefficients.³ Cantera can also be used to simulate the mixing of gases, setting equivalence ratios and extracting mass fractions of molecules. $m_{frac,fuel}$ is extracted from Cantera where the equivalence ratio is set to the determined value before. Additionally, secondary zone air flow introduction and its cooling effect is also simulated through Cantera, depending on PZAR.

High pressure turbine

After the combustion, a high pressure turbine is introduced. The high pressure turbine lowers the pressure and temperature by extracting work from the flow. The work extracted is then provided to the compressors. The work extracted and new flow properties can be determined using following relations.

$$W_{HPT} = \frac{(W_{HPC})}{\mu_{mech}} \quad (6.21) \quad T_{HPT,outlet} = T_{HPT,inlet} - \frac{W_{HPT}}{\dot{m}_{cc,outlet} C_{p,gas}} \quad (6.22)$$

$$P_{HPT,outlet} = P_{HPT,inlet} \left(1 - \frac{1}{\mu_{HPT}} \left(1 - \frac{T_{HPT,outlet}}{T_{HPT,inlet}}\right)\right)^{\frac{\gamma_{gas}}{\gamma_{gas}-1}} \quad (6.23)$$

Inter-stage turbine burner

The inter-stage turbine burner is another combustion chamber placed between HPT and LPT. By adding extra fuel in ITB, the net thrust of the engine can be increased in cost of decreasing specific fuel consumption. $ITB_{energy-fraction}$ is the energy fraction of the fuel added in ITB to the fuel added in the first combustion chamber. The $ITB_{energy-fraction}$ is used as the parameter defining the added fuel in the ITB. The effect of having an ITB to the flow characteristics can be simulated using the following equations.

$$\dot{m}_{FITB} = \frac{\dot{m}_{fuel} LHV_{fuel} ITB_{energy-fraction}}{(1 - ITB_{energy-fraction}) LHV_{FITB}} \quad (6.24) \quad \dot{m}_{ITB,outlet} = \dot{m}_{cc,outlet} + \dot{m}_{FITB} \quad (6.25)$$

$$P_{ITB,outlet} = P_{ITB,inlet} \pi_{ITB} \quad (6.26) \quad T_{ITB,outlet} = T_{ITB,inlet} + \frac{\dot{m}_{FITB} \cdot \mu_{FITB} \cdot LHV_{FITB}}{(\dot{m}_{core} + \dot{m}_{fuel}) \cdot C_{p,gas,ITB}} \quad (6.27)$$

¹<https://cantera.org>

²<https://cantera.org>

³<https://cantera.org/science/thermodynamics.html>

Low pressure turbine

The low pressure turbine simulation use the same relations in HPT calculations. These are given below.

$$W_{LPT} = \frac{(W_{LPC} + W_{fan})}{\mu_{mech}} \quad T_{LPT_{outlet}} = T_{LPT_{inlet}} - \frac{W_{LPT}}{\dot{m}_{ITB_{outlet}} C_{p,gas,ITB}} \quad (6.28) \quad (6.29)$$

$$P_{LPT_{outlet}} = P_{LPT_{inlet}} \left(1 - \frac{1}{\mu_{LPT}} \left(1 - \frac{T_{LPT_{outlet}}}{T_{LPT_{inlet}}}\right)\right)^{\frac{\gamma_{gas,ITB}}{\gamma_{gas,ITB}-1}} \quad (6.30)$$

Nozzle

The nozzle is where the mass flow from the engine is exhausted. The flow characteristics of the exhausted flow generates thrust, namely the velocity and pressure of the flow. However, it is not possible to create an infinitely large pressure difference between the nozzle and atmosphere. Critical nozzle pressure ratio is when the pressure is so high that the nozzle becomes choked, the mach number at the smallest cross-section of the nozzle reaches 1 and the mass flow through the nozzle cannot increase more. Therefore, it is important to determine whether the nozzle for core and bypassed flow are choked or not. The core nozzle is choked if $\frac{P_{LPT_{outlet}}}{P_a} > \frac{P_{LPT_{outlet}}}{P_{crit_{core}}}$ and the bypassed nozzle is choked if $\frac{P_{fan_{outlet}}}{P_a} > \frac{P_{fan_{outlet}}}{P_{crit_{bypassed}}}$. These values can be obtained using the relation below.

$$\frac{P_{LPT_{outlet}}}{P_{crit_{core}}} = \frac{1}{\left(1 - \mu_{nozzle} \frac{\gamma_{FITB}-1}{\gamma_{FITB}+1}\right)^{\frac{\gamma_{FITB}}{\gamma_{FITB}-1}}} \quad (6.31) \quad \frac{P_{fan_{outlet}}}{P_{crit_{bypassed}}} = \frac{1}{\left(1 - \mu_{nozzle} \frac{\gamma_{air}-1}{\gamma_{air}+1}\right)^{\frac{\gamma_{air}}{\gamma_{air}-1}}} \quad (6.32)$$

Thrust for choked core nozzle Whether the nozzle is choked or not changes the thrust calculation attained from the flow. For a choked core, the thrust calculation scheme is given below.

$$P_{nozzle_{core}} = \frac{P_{LPT_{outlet}}}{P_{crit_{core}}} \quad (6.33) \quad T_{nozzle_{core}} = \frac{2 \cdot T_{LPT_{outlet}}}{\gamma_{ITB} + 1} \quad (6.34)$$

$$V_{nozzle_{core}} = \sqrt{\gamma_{ITB} \cdot R \cdot T_{nozzle_{core}}} \quad (6.35) \quad \rho_{nozzle_{core}} = \frac{P_{LPT_{outlet}}}{R \cdot T_{nozzle_{core}}} \quad (6.36)$$

$$A_{nozzle_{core}} = \frac{\dot{m}_{ITB_{outlet}}}{\rho_{nozzle_{core}} \cdot V_{nozzle_{core}}} \quad (6.37)$$

$$Thrust_{nozzle_{core}} = \dot{m}_{ITB_{outlet}} (V_{nozzle_{core}} - V_a) + A_{nozzle_{core}} (P_{nozzle_{core}} - P_a) \quad (6.38)$$

Thrust for unchoked core nozzle For unchoked core nozzle, the calculation scheme used is different. As the pressure now equals the atmospheric pressure, its contribution to thrust is neglected. The net thrust attained can be calculated using relations below.

$$P_{nozzle_{core}} = P_a \quad (6.39) \quad T_{nozzle_{core}} = T_{LPT_{outlet}} \left(1 - \mu_{nozzle} \left(1 - \frac{P_{nozzle_{core}}}{P_{LPT_{outlet}}}\right)^{\frac{\gamma_{FITB}-1}{\gamma_{FITB}}}\right) \quad (6.40)$$

$$V_{nozzle_{core}} = \sqrt{2C_{p,gas,ITB}(T_{LPT_{outlet}} - T_{nozzle_{core}})} \quad Thrust_{nozzle_{core}} = \dot{m}_{ITB_{outlet}} (V_{nozzle_{core}} - V_a) \quad (6.41) \quad (6.42)$$

Thrust for choked bypass nozzle A similar calculation is done for the bypassed flow as well by using bypassed airflow parameters. The thrust calculations for choked bypass nozzle are indicated below.

$$P_{nozzle_{bypassed}} = \frac{P_{fan_{outlet}}}{P_{crit_{bypassed}}} \quad (6.43)$$

$$T_{nozzle_{bypassed}} = \frac{2 \cdot T_{LPT_{outlet}}}{\gamma_{FITB} + 1} \quad (6.44)$$

$$V_{nozzle_{bypassed}} = \sqrt{\gamma_{FITB} \cdot R \cdot T_{nozzle_{bypassed}}} \quad (6.45) \quad \rho_{nozzle_{bypassed}} = \frac{P_{fan_{outlet}}}{R \cdot T_{nozzle_{bypassed}}} \quad (6.46)$$

$$A_{nozzle_{bypassed}} = \frac{\dot{m}_{bypassed}}{\rho_{nozzle_{bypassed}} \cdot V_{nozzle_{bypassed}}} \quad (6.47)$$

$$Thrust_{nozzle_{bypassed}} = \dot{m}_{bypassed}(V_{nozzle_{bypassed}} - V_a) + A_{nozzle_{bypassed}}(P_{nozzle_{bypassed}} - P_a) \quad (6.48)$$

Thrust for unchoked bypass nozzle The thrust calculations for unchoked bypass nozzle excludes the contribution of pressure difference, as in the the thrust calculations for unchoked core nozzle. All relations used to calculate net thrust for unchoked bypass nozzle are stated below.

$$P_{nozzle_{bypassed}} = P_a \quad (6.49)$$

$$T_{nozzle_{bypassed}} = T_{fan_{outlet}} \left(1 - \mu_{nozzle} \left(1 - \frac{P_{nozzle_{bypassed}}}{P_{fan_{outlet}}}\right)^{\frac{\gamma_{air}-1}{\gamma_{air}}}\right) \quad (6.50)$$

$$V_{nozzle_{bypassed}} = \sqrt{2C_{p,air}(T_{fan_{outlet}} - T_{nozzle_{core}})} \quad (6.51) \quad Thrust_{nozzle_{bypassed}} = \dot{m}_{bypassed}(V_{nozzle_{bypassed}} - V_a) \quad (6.52)$$

Total Thrust, Weight and Specific Fuel Consumption

As the each thrust generated by the core flow and the bypassed flow are calculated, the total thrust can be attained by summing them together. Additionally, the thrust specific fuel consumption of the engine can be calculated using the relation given in Equation 6.54.

$$Thrust_{total} = Thrust_{nozzle_{bypassed}} + Thrust_{nozzle_{core}} \quad (6.53)$$

$$SFC = \frac{\dot{m}_{fuel} + \dot{m}_{FITB}}{Thrust_{total}} \quad (6.54)$$

The weight calculation of the engine is estimated using the thrust to mass ratio of the current A320 NEO engine LEAP-1A. The ratio of the engine thrust to its mass is calculated to be 47.84 [Nkg⁻¹] [3]. All final design values of the engine can be found in Table 6.1.

Sizing of the Engine Model

During the sizing of the engine model, some engine parameters are iterated to find the optimum design point, whereas some other parameters are assumed to be constant. The engine parameters assumed to stay constant in the simulation are given in Table 6.1.

Table 6.1: Assumed Engine Design Parameters.

Component	Parameter	Notation	Value	Unit
Inlet	Polytropic efficiency	η_{inlet}	98	%
Fan	Polytropic efficiency	η_{fan}	92	%
LPC	Polytropic efficiency	η_{LPC}	92	%
HPC	Polytropic efficiency	η_{HPC}	92	%
Main combustion chamber	Combustion efficiency	η_{cc}	99.5	%
Main combustion chamber	Pressure ratio	π_{cc}	0.96	[-]
HPT	Polytropic efficiency	η_{HPT}	93	%
ITB	Combustion efficiency	η_{ITB}	99.5	%
ITB	Pressure ratio	π_{ITB}	0.97	[-]
LPT	Polytropic efficiency	η_{LPT}	93	%
HPT and LPT Shaft	Mechanical efficiency	η_{mech}	99	%
Nozzle	Polytropic efficiency	η_{nozzle}	98	%

During the engine sizing iteration, the model iterates through different BPR values, fan ratios, HPC ratios, LPC ratios, $PZAR$ values and $ITB_{energy-fraction}$ values. The iteration intervals of these parameters are given below.

Table 6.2: Engine Sizing Iteration Parameters.

Component	Parameter	Notation	Interval	Unit
[-]	Bypass ratio	BPR	[6,12]	[-]
Fan	Pressure ratio	π_{fan}	[1.6,1.9]	[-]
LPC	Pressure ratio	π_{LPC}	[1.4,2.0]	[-]
HPC	Pressure ratio	π_{HPC}	[8,20]	[-]
Combustion chamber	Primary zone air ratio	$PZAR$	[0.2,0.6]	[-]
ITB	ITB energy fraction	$ITB_{energy-fraction}$	[0.0,0.3]	[-]

The engine sizing iteration iterates through the possible design options. With each simulated engine design, the SFC of that engine is calculated. To choose the best engine design, an estimate of the fuel needed for the whole range of flight is calculated with the Breguet range equation given below.

$$Range = 2\sqrt{\frac{2}{\rho_{air}S}} \frac{1}{SFC} \frac{C_L^{\frac{1}{2}}}{C_D} (W_{initial}^{\frac{1}{2}} - W_{final}^{\frac{1}{2}}) \quad (6.55)$$

Using the formula above, the fuel consumption for certain flight scenario can be estimated. By multiplying the total fuel needed for the flight scenario by the emission index of NO_x , the amount of NO_x produced during the flight can be estimated. The engine sizing iteration aims to minimize the total NO_x emissions and chooses the best design parameters to achieve this.

6.2. Cracking System Design

6.2.1. Assumptions and Simplifications

Important assumptions have been made in order to simplify the cracking system design. The following assumptions are considered:

- It is assumed that the surface of the pellets of catalyst are linearly proportional to the reaction rate. This means that the pellet diameter can be reduced in order to increase the total catalytic surface area in the reactor. This subsequently reduces the residence time required and means that flow rates can increase to obtain higher yield.
- It is assumed that the density of the gasses involved have a constant density along all stages of the cracking system. This means that after evaporation of the ammonia the density of ammonia does not change.
- The amount of ammonia that is cracked prior to its introduction to the reactor is negligible.

- The gasses in this system are assumed to behave like ideal gasses.
- Some of the material and substance properties have been linearly extrapolated from available data on their characteristic behaviour based on a variation of temperatures and pressures.
- Heat losses have not been considered and perfect insulation of the system is assumed.
- Flow back does not take place as the gas heats up through multiple stages of the cracking system. The assumption is that the pump is able to compensate for this.

6.2.2. Heat Exchangers and Reactor Design

A cracking system is required in the aircraft for the decomposition of ammonia to hydrogen needed for the combustion process. The design of the reactor and other heat exchangers should ensure that sufficient hydrogen can be supplied at different flight conditions. Take-off, for instance, requires about three times the amount of hydrogen needed than for cruise conditions.

The design therefore utilizes 562 heat exchanging or reactor elements arranged in parallel. The use of a high number of reactors in parallel also increases the reliability of the system by reducing the impact of isolated heat exchanger or reactor failure. A tube-in-tube heat exchanger configuration is chosen for the system because of its efficient use of space, simplicity and heat exchanging performance. In addition to this, the heat exchangers and the reactor are designed for counter flow conditions; the schematics of a counter flow heat exchanger is shown in Figure 6.3 [27].

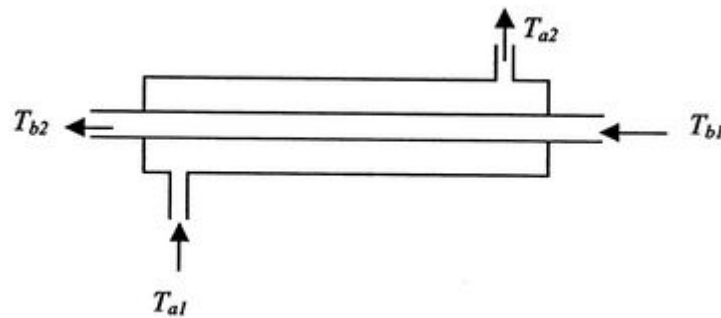


Figure 6.3: Counter flow heat exchanger system [27].

The disadvantage of the parallel flow design is the fact that the heat transfer drops over the length of the heat exchanger as the temperature of the concurrent gas flow approach each other as one gas heats up and the other cools down, as can be seen in Figure 6.4(a). This means that the heat transfer is not constant or linear but rather logarithmic. In order to accurately determine the heat transfer rate the logarithmic mean temperature difference (LMTD or ΔT_{LM}) has to be considered for which the parallel flow ΔT_{LM} is indicated by Equation 6.56 and counter flow ΔT_{LM} by Equation 6.57. In this cracking system design, the heat transfer rate of the counter flow configuration was up to 6.2 times higher compared to its counterpart. This significantly reduces the pipe surface area required to transfer the necessary heat for each compartment resulting in a higher performance of the overall system [27].

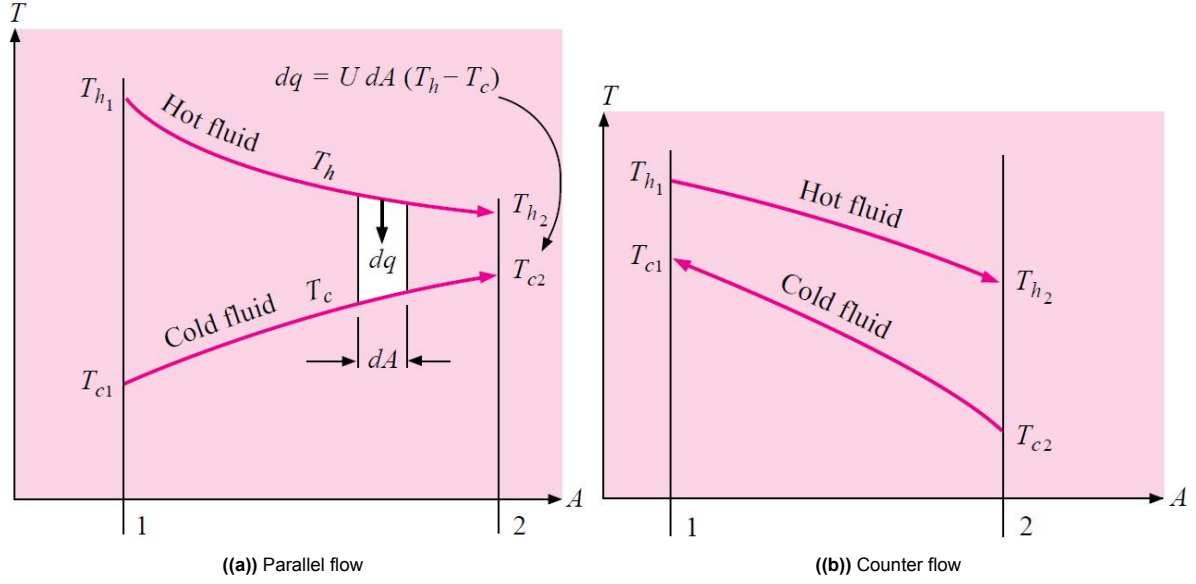
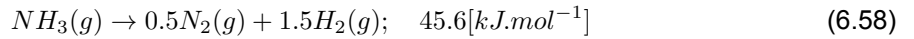


Figure 6.4: Temperature profiles of double-pipe heat exchangers [27].

$$\Delta T_{LM} = \frac{\Delta T_1 - \Delta T_2}{\ln \left(\frac{\Delta T_1}{\Delta T_2} \right)} \quad (6.56)$$

$$\Delta T_{LM} = \frac{(T_{a1} - T_{b2}) - (T_{a2} - T_{b1})}{\ln \left(\frac{T_{h1} - T_{c2}}{T_{h2} - T_{c1}} \right)} \quad (6.57)$$

The sizing of the reactor and heat exchangers is based on the maximum amount of hydrogen required for the engine fuel blend, which is estimated to be 0.79 [kgs⁻¹]. The flow rate of hydrogen needed determines the power requirement for the decomposition of ammonia (Equation 6.58) and heating up of the gas, and the mass of the catalyst. With the determination of the overall heat transfer coefficient (which is elaborated upon in a later part of this section) combined with the power requirement and gas properties, the required surface area is determined which is used to compute the length, weight and volume of the exchanger.



The inner diameter, d_{in} of the reactor system is set at 0.01 [m], while the outer diameter, d_{out} is 0.017 [m] in size. These parameters affect the characteristic lengths which are required for the determination of the overall heat transfer coefficient. The length of the system is then calculated based on the surface area required. Surface area required is calculated with the heat transfer equation, Equation 6.61. A represents the surface area required for heat transfer, and U is the overall heat transfer coefficient determined with Equation 6.62.

$$A = \frac{\dot{Q}}{h \cdot (T_{N_2} - T_{NH_3})} \quad (6.59) \quad \frac{1}{U} = \frac{1}{h_{air}} + \frac{t_{pipe}}{k_{pipe}} + \frac{1}{h_{N_2}} \quad (6.60)$$

$$A = \frac{\dot{Q}}{U \cdot \Delta T_{LM}} \quad (6.61) \quad \frac{1}{U} = \frac{1}{h_{NH_3}} + \frac{t_{pipe}}{k_{steel}} + \frac{1}{h_{N_2}} \quad (6.62)$$

Carbon steel has been selected as material of the inner and outer piping of the cracking system. This material has been chosen due to its high temperature tolerance, strength and cost per kg. The melting temperature (1800 K) has been one of the leading factors for the material selection due to the high temperature of the nitrogen gas required to enter the reactor (1500 K). In addition it is not a rare metal compared to alternative metals with similar or higher temperature tolerances. Chromium could be a good alternative because the melting point is higher than carbon steel but this was not considered

due to its cost which is estimated to be approximately 25 times higher. Thermal conductivity is also an important parameter that needs to be considered but since the structure of the cracking system is thin-walled, the contribution to the overall heat transfer coefficient can be neglected [30].

The cracking system consists of four main compartments: the evaporator, preheater, reactor and heat exchanger. These compartments can be studied in Figure 6.5. In essence the mechanisms are the same: the structure of each compartment is a tube-in-tube configuration. Each section has its own purpose. The evaporator evaporates the entering liquid ammonia from the fuel tank to its gaseous state. The energy required to evaporate liquid ammonia is $23.35 \cdot 10^3 \text{ Jmol}^{-1}$ and is calculated by Equation 6.63. Subsequently the gas is heated up from -33.34°C to 480°C (753.15 K) for which the heat transfer rate is computed by Equation 6.64. \dot{Q} represents the amount of heat per second needed by the respective system in W, and n the amount of ammonia needed by the aircraft in $[\text{mols}^{-1}]$ [30].

$$\dot{Q}_{\text{evaporator}} = n \cdot \Delta H_{\text{vap}} \quad (6.63)$$

$$\dot{Q}_{\text{preheater}} = n \cdot C \cdot \Delta T \quad (6.64)$$

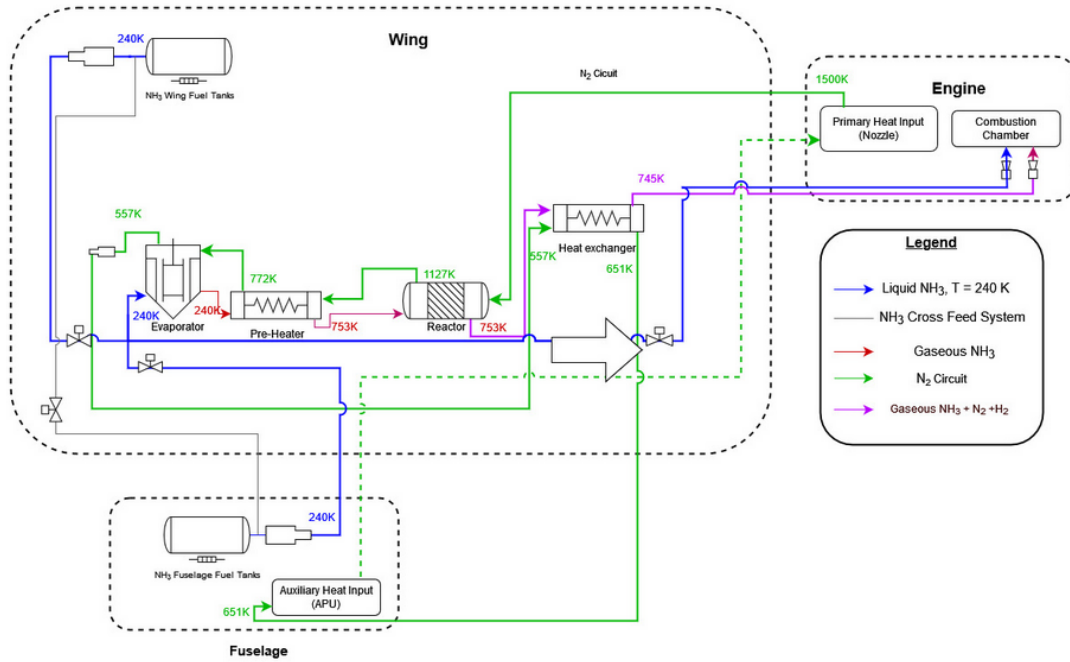


Figure 6.5: Schematics of cracking system

At a temperature of 753.15 K the ammonia is decomposed by means of thermal catalysis up to 97% using a lithium amide catalyst which is further elaborated upon in subsection 6.2.4. Afterwards the gas is conducted towards the reactor where the gaseous ammonia and the products from cracking enter and leave the reactor at a temperature of 753.15 K. Ultimately the final products are conducted through a heat exchanger in order to cool down, and to heat up the N_2 circuit prior to its introduction to the next heat exchanger in the combustion chamber. The final step enables some of the heat of the fuel to be reused for cracking purposes. Since the incoming flow of N_2 into the heat exchanger is already at a higher temperature, the heat transfer requirement to bring the nitrogen gas up to the desired temperature of 1500 K is lower. This reduces the overall energy cost for the operation of the cracking system [30].

The heat required for each component of the cracking system is then used to calculate pipe length, l_p and (if applicable) coil length of the components l_c with Equation 6.65 and Equation 6.66, respectively.

$$l_p = \frac{A}{\pi \cdot d_{in}} \quad (6.65)$$

$$l_c = \frac{l_p \cdot d_{out}}{\sqrt{\pi \cdot d_c^2 + d_{out}^2}} \quad (6.66)$$

Subsequently, the required thickness of the reactor and heat exchangers is determined by pressure of the nitrogen circuit, which is set at 564 [atm]. Pressure in the circuit introduces stress in the reactor as shown in Equation 6.67, and the wall of the nitrogen circuit has to be able to withstand this pressure. σ refers to the yield strength of steel; p refers to the pressure of the nitrogen circuit, while d and t refer to diameter of the outer reactor pipe and thickness of the pipe.

$$\sigma_h = \frac{p \cdot d}{2t} \quad (6.67)$$

With the dimensions of the cracking system set, volume and mass of the cracking system can be calculated. These are performed with simple geometrical calculations shown in Equation 6.68 and Equation 6.69.

$$m = \frac{\pi \cdot ((d+1)^2 - d^2) \cdot l_p \cdot \rho_{steel}}{4} \quad (6.68)$$

$$V = d_c^2 \cdot l_p \cdot Reactor\ number \quad (6.69)$$

6.2.3. Cracking System Insulation

With the ammonia stored in the wings under a temperature of -33.34 °C as well as the cracking system functioning with temperatures up to 1226.85 °C, there are conflicting interests. Where the energy carrier is required to remain cooled during flight in order to minimize the pressure inside the fuel tank, the cracking system requires high heat to ensure enough ammonia is cracked into hydrogen and nitrogen gas. The structure of the wing is made of aluminium, and the highest temperature involved in this system is beyond the melting point of the latter material (660.3 °C or 933.45 K). In order to make sure that the elevated temperatures of the cracking system do not melt other metals in the wing and to ensure the energy carrier is not heated by the cracking system, proper insulation is paramount to the success of the cracking system.

In the search for the right insulating material, aerogel was selected. Aerogel has the main advantage of having an extremely low thermal conductivity (e.g. 0.013 W/(m²K)) due to its porosity and being lightweight. The heat exchangers and reactor are covered by this material which has a layer of about 4 cm. This density is relatively low compared to its counter parts such as polystyrene and polyurethane. The latter have a relatively low melting temperature which makes these materials unsuitable for this use case. Aerogel does not melt within the temperature range of the cracking system [46].

When considering the maintenance required, polymers do have an advantage over aerogel as these are easily applicable through spraying extra material on the insulating surface. Aerogel often has to be replaced entirely. However considering its relative low cost, and minimal increase in complexity, this is not considered to be a problem.

6.2.4. Catalyst Mechanism, Safety, and Production

Catalysts plays an important role in decomposition of ammonia. It helps increase the rate of reaction by reducing activation energy required for the reaction. This is illustrated in Figure 6.6.⁴ Using a catalyst is therefore paramount to the successful cracking of ammonia. Without it the temperatures that are required to reach high conversion rates a significantly higher than with the use of catalyst. This is illustrated by Figure 6.7 in which the blank reactor can be compared with other catalysts. The blank reactor has a higher power consumption for the same conversion rates compared to its alternatives. This comes with a penalty for the engine sizing as both the engine and its heat exchanger become bigger and thus heavier. This increases the overall aircraft weight [30].

Catalysts that are currently being used for the thermal catalytic decomposition of ammonia are predominantly ruthenium or nickel-based. Ruthenium is popular because of its high conversion rate at lower

⁴<http://ch302.cm.utexas.edu/kinetics/catalysts/catalysts-all.php>, accessed 14 June 2022

temperatures, and its overall reliability and safety. On a larger scale this catalyst is not appealing due to its rarity and high price per kg of substance. These disadvantages do not occur with the use of nickel-based catalysts which are generally cheaper and abundant. Unfortunately due to the relatively low effectiveness of this catalyst, the amount of catalyst that is required needs to be significantly higher compared to its counterparts or the temperatures that need to be achieved are notably more elevated [30, 10].

For this cracking system, lithium amide (LiNH_2) was selected as catalyst due to its high performance and exceptionally low activation energy compared to other alternatives. In addition to this, the substance is low in cost, significantly lighter in weight than other catalysts and highly functioning at lower temperatures as shown in Figure 6.7. The usage of this catalyst is starting to gain more traction in the academic field. Studies are predominantly performed on small scale experiments and the catalyst is not yet widely used for this purpose. In general terms, the thermal catalytic cracking of ammonia always happens on a smaller scale. The production rates that are required for this aircraft do not exist on an industrial scale. The challenge is sustaining the desired conversion rates at relatively low temperatures whilst achieving higher flow rates for increased yield. Since the catalytic process depends on the residence time, the higher flow rates result in a lower yield. The conventional way of increasing the output of the cracking system is therefore by numbering up, however, there are design parameters that could be optimized such as choosing the right catalyst, adjusting the pellet size, increasing the temperature, adjust the residence time etc. [30].

The mechanism of this catalyst is rather interesting, and raises the question of its practicality upon its implementation. The equilibrium reaction that occurs shows that chemical kinetics of the lithium amide catalyst in use (Equation 6.70). Once lithium amide is beyond its melting point (375°C) the substance starts decomposing into lithium imide and ammonia. It is tempting to think that the substance would be in liquid form after it has reached this temperature, however, the outer layer that decomposes into lithium imide contains the lithium amide particle. A phase boundary layer is formed through which the ammonia diffuses. The diffusion of NH_3 through the lithium imide is controlling the rate of decomposition. The decomposition of LiNH_2 increases the growth of the shell of Li_2NH . Since the melting temperature of lithium imide is above 600°C , the integrity of the pellets are maintained [30, 35].



The melting temperature of LiNH_2 is about 375°C , considering the operating temperature of the reactor one would suggest that the catalyst is liquid rather than solid.

Lithium amide is manufactured in industrial scale by allowing a stream of ammonia to react with heated lithium metal or lithium hydride.⁵ This is then ground into smaller particle size, often through ball-milling. This is necessary to aid the decomposition of LiNH_2 to Li_2NH , but lowers purity of the catalyst because of contamination [9]. An alternative, newer method of LiNH_2 is through the reaction of *n*-butyllithium with ammonia under nitrogen atmosphere; the reaction is shown in Equation 6.71. The reaction has to be stirred for 18 hours, filtered, washed and dried in vacuum for 24 hours [9]. With this method, small granules of LiNH_2 can be produced, and complete decomposition to LiNH_2 can be reached with temperature as low as 600°C [9].



⁵<https://pubchem.ncbi.nlm.nih.gov/compound/Lithium-amide#section=Stability-Shelf-Life>, accessed 15 June 2022

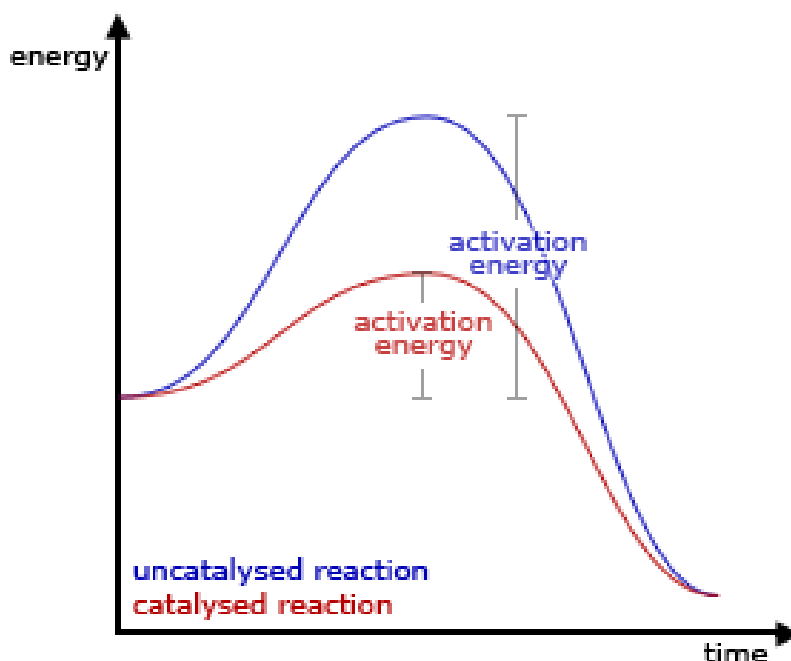


Figure 6.6: Catalyst effect on activation energy⁶

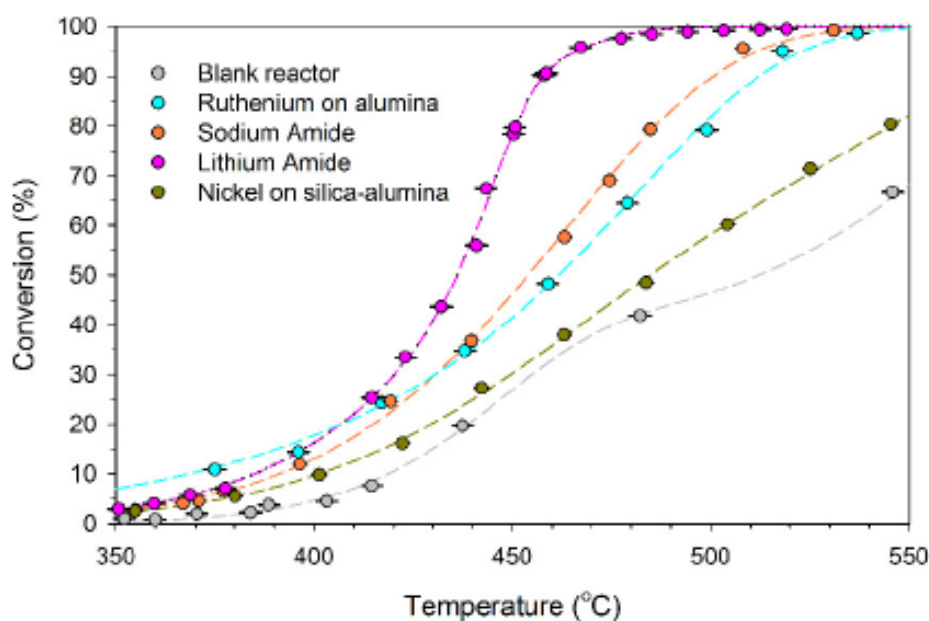


Figure 6.7: Performance of different catalysts on ammonia cracking [30]

There are several challenges with regard to the use of Lithium Amide as catalyst. This includes its low melting temperature and highly reactive nature; this makes lithium amide less safe compared to the traditional, well-established catalysts. LiNH_2 starts to melt at 375 [°C], which means that there is a risk that the catalyst may be turn into liquid during the reaction. This is problematic because liquid typically result in significant catalyst lost [57]. However, LiNH_2 also starts to decompose at 320 [°C]; the decomposition forms Lithium Imide (Li_2NH) [36], which only further decomposes at temperature 750 [°C] ⁷.

⁷<https://pubchem.ncbi.nlm.nih.gov/compound/Lithium-amide#section=Stability-Shelf-Life>, accessed 15 June 2022

The temperature at which LiNH_2 starts to decompose to form Li_2NH can be reduced by decreasing the particle size of the catalyst [36]. This has an added benefit of increasing rate of ammonia decomposition reaction as smaller catalyst size increases the surface area of catalyst in contact with ammonia. In addition, the reactivity of LiNH_2 means that the commonly used catalyst supports including aluminium oxide and magnesium oxide are difficult to incorporate to the catalyst [57]. Because of this, the system will not be using any support for the catalyst.

The amount of catalyst needed by the cracking system is determined by the amount of ammonia needed by the aircraft per second. The relation used for the calculations are presented in Equation 6.72 [30] and Equation 6.73, which represents the catalyst constant and mass needed, respectively. In the equations, p refers to the pressure of the ammonia cracking system in bars, mf_{NH_3} mass fraction of ammonia in the system, T the temperature in the reactor, and mol_{NH_3} the number of moles needed by the aircraft for every second. The mass calculated using these equations are included in the mass of the reactor.

$$r = 2.92 \cdot 10^6 \cdot p \cdot mf_{\text{NH}_3} \cdot e^{\frac{-17020}{T}} \quad (6.72)$$

$$m_{\text{catalyst}} = \frac{\text{mol}_{\text{NH}_3}}{r} \quad (6.73)$$

Aside from lithium amide, NiSiO_2 is also a viable alternative that is already commonly used in the industry. The use of this catalyst in an aircraft should not introduce additional challenges for the cracking system in terms of phase change or safety. The disadvantage of using NiSiO_2 however, is its lower catalyst efficiency, which lowers conversion rate for the cracking system. This means that a higher flow rate of ammonia is required for the reactor to obtain the same amount of hydrogen needed by the aircraft. Because a higher amount of ammonia has to be heated up for the decomposition reaction, leading a higher heat requirement for the cracking system. A higher heat requirement means a higher surface area is required for the reactor as shown by Equation 6.61, leading to a higher volume needed, and mass penalty as well.

NiSiO_2 can be synthesized through several methods, including the use of homogeneous precipitation in wet gel (HPG) or in combination with phase separation [11]. In literature [11, 25], the synthesis of NiSiO_2 always requires the use of an alkoxide, usually tetraethylortosilicate (TEOS) ($\text{Si}(\text{OC}_2\text{H}_5)_4$); an acid, usually Hydrochloric acid (HCl) or Nitric acid HNO_3 ; a compound containing nickel, usually $(\text{Ni}(\text{NO}_3)_2 \cdot 6\text{H}_2\text{O})$; and ethanol.

One example of NiSiO_2 preparation is by first mixing two solutions; the first a solution of TEOS and ethanol, and the second a solution of acid. The two solutions have to be stirred while mixing, and temperature has to be maintained at 50°C during the process. This product is then mixed with two additional solutions, namely $(\text{Ni}(\text{NO}_3)_2 \cdot 6\text{H}_2\text{O})$ and solution of NH_4OH in ethanol. This is conducted at room temperature and a firm, clear gel will be instantaneously formed. The gel has to be stored at room temperature before it is then dried and calcined to obtained NiSiO_2 . Because of the potential challenges and uncertainties involved from using LiNH_2 , it was decided to use NiSiO_2 instead because of its reliability.

Effect of the change in catalyst on the aircraft system

The change from the use of LiNH_2 to NiSiO_2 as catalyst has some effects on other subsystems of the aircraft. The lower efficiency if the cracking system caused by the switch means that at the same temperature of 480°C , ammonia decomposition rate is lower. The conversion rate decreases from close to 97% to about 48%. This means that the cracking system will not be able to generate sufficient H_2 for the fuel blend required by the aircraft. Modifications in the cracking system design are required to generate convert sufficient amount of ammonia. This may include the use of a separator and recycling system or higher temperature at the reactor.

The effect of this is an increase in cracking system weight and volume, which will lead to a snowball effect on other aircraft subsystems. This means that further iteration is required for the design. However, this is not performed because of time constraint in the project. The switch was made late in the project, and it was concluded that too many parameters will change with the iteration at this stage of the project.

The parameters used in the cracking system design and values obtained out of the calculations are tabulated in Table 6.3.

Table 6.3: Calculation parameters used in cracking system design

Parameter	Symbol	Value	Unit
Carbon steel thermal conductivity	k_{steel}	45	$[W/mK]$
Reactor inner diameter	d_{in}	0.010	$[m]$
Reactor outer diameter	d_{out}	0.0170	$[m]$
Reactor pipe thickness	t_{steel}	0.00137	$[m]$
Reactor temperature	$T_{reactor}$	753.15	$[K]$
Evaporator temperature	$T_{evaporator}$	240	$[K]$
Pre-heater temperature	$T_{pre-heater}$	240 to 753.15	$[K]$
Specific heat capacity of ammonia	$C_{ammonia}$	3080	$[J/kgK]$
Specific heat capacity of nitrogen	$C_{nitrogen}$	1098	$[J/kgK]$
Enthalpy of Vaporization of ammonia	ΔH	23.35	$[kJ/mol]$
Density carbon steel	ρ_{steel}	7850	$[kg/m^3]$

6.2.5. Engine Heat Exchanger

Since the ammonia cracking system is a thermal system, a heat source is required to supply the thermal power needed for each of the cracking components. Here, the method used to size this heat exchanger is discussed along with all the assumptions made during the sizing process.

The sizing method is based on the temperature of the Nitrogen exiting the heat exchanger ($T_{N2,o} = 1500$ [K]) and the heat transfer coefficient for the 3-component-system consisting of: the engine core air flow, the piping of the Nitrogen circuit and the Nitrogen in the Nitrogen circuit. All heat extracted from the core flow is assumed to be absorbed by the Nitrogen in the Nitrogen circuit, thus, the heat balance between the 3-component system is given by Equation 6.74. The area needed for the heat exchange to occur is given by Equation 6.76 with U being calculated using Equation 6.77⁸. All known, assumed or calculated parameters are given in Table 6.4[1] [61]^{9 10 11 12}.

⁸<https://web.mit.edu/16.unified/www/FALL/thermodynamics/notes/node123.html>, accessed 07/06/2022

⁹ <https://www.engineeringtoolbox.com/>, accessed 08-06-2022

¹⁰<https://top-seiko.com/guide/characteristic/>, accessed 13-06-2022

¹¹https://commonchemistry.cas.org/detail?cas_rn=24304-00-5, accessed 13-06-2022

¹²https://commonchemistry.cas.org/detail?cas_rn=11121-90-7&search=Carbon%20Steel, accessed 13-06-2022

Table 6.4: Calculation parameters used in the sizing of the engine heat exchangers.

Parameter	Value	Unit	Remark
$C_{p,gas}$	1160	[J kg ⁻¹ K ⁻¹]	Assumed
μ_{air}	$4.111 \cdot 10^{-5}$	[Pa s]	
k_{air}	$68 \cdot 10^{-3}$	[W m ⁻¹ K ⁻¹]	
$D_{cc,outer}$	60	[cm]	Assumed
$D_{cc,inner}$	30	[cm]	Assumed
D_{lpt}	1.084	[m]	
$L_{1,ann}$	5	[mm]	
dL	5	[mm]	
dD	5	[mm]	
A_0	0	[m ²]	
W_0	0	[kg]	
$C_{p,N2}$	1098	[J kg ⁻¹ K ⁻¹]	
μ_{N2}	$40.3 \cdot 10^{-6}$	[Pa s]	
k_{N2}	$63.11 \cdot 10^{-3}$	[W m ⁻¹ K ⁻¹]	
\dot{m}_{N2}	11.625	[kg s ⁻¹]	
ρ_{N2}	70	[kg m ⁻³]	
D_{N2}	7	[m]	
$T_{N2,o}$	1500	[K]	
$T_{N2,i}$	651	[K]	
$t_{pipe,cc}$	1	[mm]	Assumed
$k_{pipe,cc}$	170	[W m ⁻¹ K ⁻¹]	Aluminium Nitride
$\rho_{pipe,cc}$	3203	[kg m ⁻³]	Aluminium Nitride
$t_{pipe,noz}$	1	[mm]	Assumed
$k_{pipe,noz}$	45	[W m ⁻¹ K ⁻¹]	Carbon Steel
$\rho_{pipe,noz}$	7850	[kg m ⁻³]	Carbon Steel

$$\dot{Q} = \dot{m}_{N2} \cdot C_{p,N2} \cdot (T_{N2,o} - T_{N2,i}) = \dot{m}_{core} \cdot C_{p,gas} \cdot (T_{air,i} - T_{air,o}) = U \cdot A \cdot (T_{air,i} - T_{N2,i}) \quad (6.74)$$

$$T_{air,o} = T_{air,i} - \frac{\dot{Q}}{\dot{m}_{core} \cdot C_{p,gas}} \quad (6.75)$$

$$A_{exch} = \frac{\dot{Q}}{U \cdot (T_{N2,o} - T_{air,i})} \quad (6.76)$$

$$\frac{1}{U} = \frac{1}{h_{0,air}} + \frac{t_{pipe}}{k_{pipe}} + \frac{1}{h_{0,N2}} \quad (6.77)$$

Since the heat transfer coefficients h_{air} & h_{N2} are a function of the Reynolds Number, Nusselt Number and the Prandtl Number of the respective systems, these are defined first, as done in Equation 6.78, Equation 6.80 and Equation 6.79 respectively.

$$Re_D = \frac{\rho \cdot V \cdot D}{\mu} \quad (6.78) \quad Pr = \frac{\mu \cdot C_p}{k} \quad (6.79) \quad Nu = \frac{h \cdot D}{k} \quad (6.80)$$

Nitrogen Circuit Heat Transfer Coefficient

The Nitrogen heat transfer coefficient will be calculated assuming turbulent flow within the pipes. The Prandtl Number is calculated from known parameters and Equation 6.79 and is constant. The Nitrogen circuit flow velocity V_{N2} , is calculated from the known parameters using the continuity equation for mass flow of Nitrogen. From this, the Reynolds Number of the Nitrogen flow is calculated using Equation 6.78. With the Reynolds Number and Prandtl Number of the Nitrogen flow determined, the Nusselt Number can be calculated from the following relation [33]:

$$Nu = 0.023 \cdot Re^{0.8} \cdot Pr^n \begin{cases} n = 0.4, & \text{fluid is heated} \\ n = 0.3, & \text{fluid is cooled} \end{cases} \quad (6.81)$$

With $n=0.4$, the Nusselt Number for Nitrogen is known - the convective heat transfer coefficient for Nitrogen, $h_{0,N2}$, can then be calculated by re-ordering Equation 6.80.

Engine Core Flow Heat Transfer Coefficient

The values for $T_{air,i}$, \dot{m}_{core} , U , $h_{0,air}$ depend on the architecture of the heat transfer system, the section of the engine from which the required heat is extracted and the flight phase at which these parameters are obtained. As such, only the calculation methods used are presented here; accurate values will be used as part of an iterative optimization process for the mass estimation and sizing of the aircraft, which is discussed in chapter 7. 3 heat exchange configurations are considered during the design process and will now be analysed.

The first heat exchanger setup considered is that of a helical heat exchanger coil wrapped along the outer wall of the flow channel in the combustion chamber section of the engine. This is depicted in Figure 6.8. Since the expected temperatures in the combustion chamber can go as high as 2300 K for the engines used in the design, and the melting point of this material is $\approx 1698 \text{ K}^{13}$, carbon steel is not used. Instead, for the heat exchanger in the combustion chamber section, Aluminium Nitride shall be used. The low pressure turbine outlet in the Leap 1A engine has a diameter of 1.084 m [1], which is used to come up with values for $D_{cc,outer}$ and $D_{cc,inner}$. This gives a hydraulic diameter, D_h , of 15 cm. This hydraulic diameter is used in place of D in Equation 6.78 and Equation 6.80. The Reynolds Number and Prandtl Number are computed in the same manner as done for the Nitrogen flow in the Nitrogen circuit, but using the airflow properties in the combustion chamber of the engine. The computation of the Nusselt Number uses Equation 6.82 [24] for a Reynolds Number range of $(1 \cdot 10^4, 5 \cdot 10^6)$ and a Prandtl Number range of $[0.5, 2000]$ and Equation 6.81 for a Reynolds Number higher than $1 \cdot 10^4$ and a Prandtl Number range of $[0.7, 16700]$, but with $n=0.3$. From these, the heat transfer coefficient of air, $h_{0,air}$, is calculated. With all parameters in Equation 6.77 known, the overall heat transfer coefficient, U , can then be calculated.

$$Nu = \frac{\left(\frac{f}{8}\right) \cdot (Re - 2000) \cdot Pr}{1 + 12.7 \cdot \left(\frac{f}{8}\right)^{0.5} \cdot Pr} \quad (6.82)$$

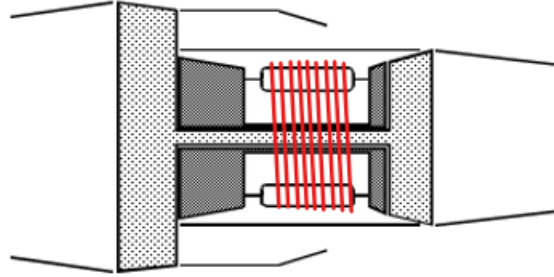


Figure 6.8: Helical heat exchanger configuration used around the combustion chamber section of the engine[40].

$$a_{hel} = \pi \cdot \left(\frac{D_{N2}}{2} + t_{pipe,cc}\right) \cdot \pi \cdot D_{cc,outer} \quad (6.83)$$

$$w1_{hel} = \rho_{pipe,cc} \cdot \pi \cdot D_{cc,outer} \cdot \left(\pi \cdot \left(\left(\frac{D_{N2}}{2} + t_{pipe,cc}\right)^2 - \left(\frac{D_{N2}}{2}\right)^2\right)\right) \quad (6.84)$$

$$N_{hel} = A_{exch}/a_{hel} \quad (6.85)$$

The sizing of the helical heat exchanger uses the heat exchanger area, given by Equation 6.76, as a starting point. The heat exchange surface area per coil is then calculated using Equation 6.83, from which the number of coils are then calculated using Equation 6.85. The mass per coil is a product of the pipe material density and the cross-sectional area of 1 coil, as shown in Equation 6.84. Finally the

¹³https://www.engineeringtoolbox.com/melting-temperature-metals-d_860.html, accessed 09-06-2022

total mass and length of the heat exchangers are found by multiplying the number of coils to the mass and length per coil respectively. This is shown in Equation 6.86 and Equation 6.87 respectively.

$$W_{tot, hel} = N_{hel} \cdot w_{1_{hel}} \quad (6.86)$$

$$L_{tot, hel} = N_{hel} \cdot D_{N2} \quad (6.87)$$

The second heat exchanger setup is very similar to the first - instead of placing the helical coil in the combustion chamber section, it is placed in the nozzle section of the engine. This is depicted in Figure 6.9. The calculation scheme for this configuration remains the same as it was for the first configuration; the only changes being the use of airflow properties of the section after the low pressure turbine section instead of the combustion chamber section, the use of D_{lpt} instead of D_h & $D_{cc, outer}$ and the material of the heat exchanger pipes being Carbon Steel.

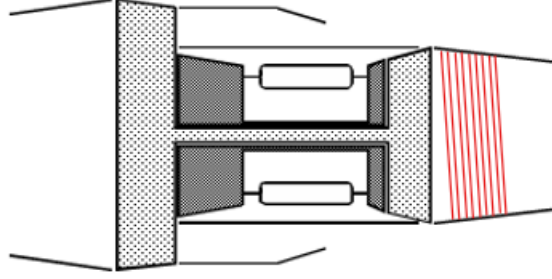
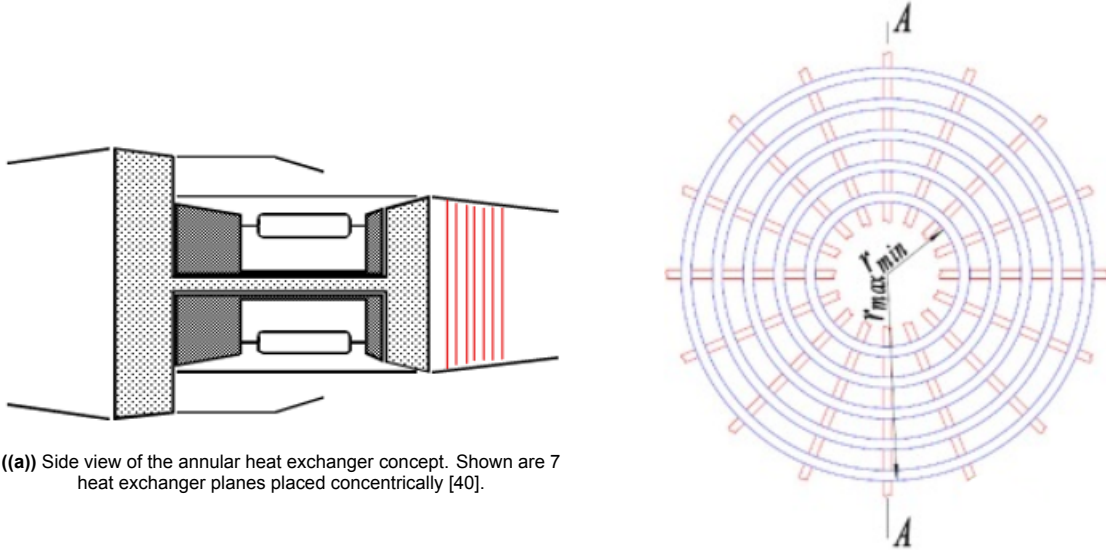


Figure 6.9: Helical heat exchanger configuration used around the nozzle section of the engine[40].

The third heat exchanger setup considered is that of multiple planes of concentric annular heat exchangers, with the planes of each heat exchanger being perpendicular to the engine shaft. These heat exchangers extract heat from the air exiting the low pressure turbine section of the engine. This is depicted in Figure 6.10.



((a)) Side view of the annular heat exchanger concept. Shown are 7 heat exchanger planes placed concentrically [40].

((b)) Front view of the annular heat exchanger concept (single heat exchanger plane)[58].

Figure 6.10: Annular heat exchanger concept.

The computation of the Reynolds Number is performed using the low pressure turbine outlet diameter, D_{lpt} , as the characteristic length of the channel and the already presented known parameters. The Prandtl Number for air in this setup also follows simply from Equation 6.79. Since temperatures in

this engine section are lower than the combustion chamber, carbon steel shall be used as the heat exchanger material. The Nusselt Number for this setup is given by Equation 6.88 [33] and the heat transfer coefficient of air, $h_{0,air}$, follows from Equation 6.80. The overall heat transfer coefficient, U , is then calculated as per Equation 6.77.

$$Nu = 0.3 + \frac{0.62 \cdot Re^{0.5} \cdot Pr^{0.3}}{(1 + (0.4/Pr)^{0.6})^{0.25}} \cdot \left[1 + \left(\frac{Re}{282000} \right)^{5/8} \right]^{4/5} \quad (6.88)$$

The sizing of this heat exchanger is more elaborate compared to the sizing of the helical heat exchanger. The frontal area of each annular heat exchanger plane has been set to a maximum of 40% of the cross-sectional area of the turbine section (See Equation 6.89). This shall be the value that the total area of the rings seen in Figure 6.10(b) cannot exceed, for a single heat exchanger plane. This is to allow sufficient uninterrupted flow in the engine so it is capable of generating sufficient thrust. The actual area of these heat exchanger rings is calculated in Python using the algorithm described by Equation 6.90. In a similar manner, the mass of 1 heat exchanger plane is calculated in Python using the algorithm described by Equation 6.91. The number of heat exchanger planes is calculated using Equation 6.92 which rounds up the right hand side to the nearest integer value greater than or equal to the parameter in parentheses. The total mass and length of this heat exchanger configuration is simply given by Equation 6.94 and Equation 6.93 respectively. The pressure loss factor of each heat exchanger plane is assumed to be 0.998, thus the total pressure loss factor for this heat exchanger configuration is given by Equation 6.95.

$$A_{max} = 0.4 \cdot \pi \cdot \frac{D_{lpt}^2}{4} \quad (6.89)$$

While($A_{i+1} < A_{max}$):

$$A_{i+1} = A_i + \pi \cdot (D_{lpt} - i \cdot dD) \cdot (D_{N2} + 2 \cdot t_{pipe,noz}) \quad (6.90)$$

$$W_{i+1} = W_i + \rho_{pipe,noz} \cdot \pi \cdot (D_{lpt} - i \cdot dD) \cdot (\pi \cdot ((\frac{D_{N2}}{2} + t_{pipe,noz})^2 - (\frac{D_{N2}}{2})^2)) \quad (6.91)$$

$$n_{heat} = \left\lceil \frac{A_{exch}}{A_{1,ann}} \right\rceil_{ceil} \quad (6.92) \quad L_{tot,ann} = n_{heat} \cdot (L + dL) \quad (6.93)$$

$$W_{tot,ann} = n_{heat} \cdot W_{1,ann} \quad (6.94)$$

$$dP_{tot,ann} = 0.998^{n_{heat}} \quad (6.95)$$

With the sizing method now described, the most optimal design is chosen based on values of the mass and the length of the heat exchangers that will be required. The working of the iteration process used to choose the most optimal design option is described in chapter 7. The final dimensions of the chosen heat exchanger are presented in chapter 8.

6.2.6. Fuel Storage Design

In order to fly an aircraft it is necessary to bring the required amount of fuel on board. In case of this design, it is challenging due to the specific density of ammonia: the fuel will have to occupy a larger volume than kerosene would for a similar mission. Additionally, the aircraft is required to be able to store the fuel for 48 hours at an ambient temperature of 45 °C. In order to fulfill these requirements, an optimized fuel storage system had to be designed.

It was chosen to store ammonia at the atmospheric pressure to avoid heavy reinforcements of the structure needed to sustain a pressure differential. In such case, the liquid fuel has a temperature of -33.3 °C, thus a sufficient thermal insulation will have to be implemented. It was chosen to insulate the tank both

actively and passively. Either option alone yielded unsatisfactory performance with respect to its mass.

Fuel Storage Thermal Insulation

Passive insulation, the simpler of the two, has been well investigated and is applied across the industry. In case of this design polymer foams were considered due to their simple application, reliability and compatibility with ammonia. Such foams have already been used in cryogenic storage applications with the Space Shuttle External Tank being one of the examples [20]. Upon research it was found that the insulation options available offer thermal conductivity in the range $k = 0.02 - 0.03 \frac{\text{W}}{\text{m}\cdot\text{K}}$ and density in the range of $\rho = 30 - 40 \frac{\text{kg}}{\text{m}^3}$ ¹⁴. In further calculations it will thus be taken that $k_{\text{foam}} = 0.02$ and $\rho_{\text{foam}} = 34$. The thickness of the insulation will be optimized to minimize the weight of the entire storage system. Aside from reducing the heat inflow into the tanks, the passive insulation also serves the purpose of reducing the temperature difference across the tank walls. This is done in order to avoid icing problems on the skin of the aircraft.

Alongside the passive insulation, an active cooling system will have to be implemented as well. It was chosen to place heat exchanging pipes inside the fuel tanks. The heat exchangers will be made out of the same aluminum as the structure of the wing to avoid thermal expansion stress problems. As a first approximation the pipes were assumed to be 100 mm in diameter with a 1 mm wall thickness. The thermal conductivity was taken to be $k_{\text{aluminum}} = 95.3 \frac{\text{W}}{\text{m}\cdot\text{K}}$. At this point it has to be mentioned, that this assumption reduces the accuracy of the calculations. The thermal conductivity is dependant on the temperature and will change along the length of the pipe as the temperature changes. This design however assumes a small difference between the inlet and outlet temperatures, so that the assumption can be taken without invalidating the results.

In order to cool the ammonia as efficiently as possible, it was chosen to utilise a coolant at a temperature slightly higher than the ammonia freezing temperature. In that case, the highest temperature difference can be created without freezing the ammonia which has a positive influence on the heat transfer coefficient. During this design iteration, pressurized gaseous nitrogen at $T_{\text{coolant}} = 200 \text{ K}$ was used. The relevant coolant parameters at this temperature, as well as other significant parameters for the following calculations are summarized in Table 6.5

Parameter	Symbol	Value	Unit
Foam Insulation Thermal Conductivity	k_{foam}	0.02	$\text{W m}^{-1} \text{K}^{-1}$
Foam Insulation Density	ρ_{foam}	34	kg m^{-3}
Aluminum Thermal Conductivity	k_{al}	95.3	$\text{W m}^{-1} \text{K}^{-1}$
Cooling Pipe Diameter	$d_{\text{pipe,outer}}$	100	mm
Cooling Pipe Thickness	t_{pipe}	1	mm
Coolant Temperature	T_{coolant}	200	K
Coolant Thermal Conductivity	k_{coolant}	0.01828	$\text{W m}^{-1} \text{K}^{-1}$
Coolant Prandtl Number	Pr_{coolant}	0.7366	[-]
Coolant Dynamic Viscosity	μ_{coolant}	0.00001313	$\text{kg m}^{-1} \text{s}^{-1}$
Coolant Density	ρ_{coolant}	1.689	kg m^{-3}
Coolant Specific Heat Capacity	cp_{coolant}	1039	$\text{J kg}^{-1} \text{K}^{-1}$
Fuel Prandtl Number	Pr_{fuel}	2.15	[-]
Fuel Kinematic Viscosity	ν_{fuel}	0.387	$\text{m}^2 \text{s}^{-1}$

Table 6.5: Fuel storage calculation constants.

Fuel Storage Volume

During early stages of the design it became apparent that the ammonia will not fit in the currently existing wing and center tank. An approach was therefore taken to put as much fuel as possible within the wing and utilize two auxiliary tanks in the cargo holds, placed such that the cg range is not affected negatively. In order to do so, the volume available within the wing had to be estimated. With the initial A320neo wing area and volume being 122.4 m^2 and 15.49 m^3 respectively, the new volume is:

¹⁴<https://www.jm.com/en/industrial-insulation/insulation-for-cryogenic-and-lng-systems-/?nocache=true>

$$V_{new,wing} = \left(\frac{S_{new}}{122.4}\right)^{\frac{3}{2}} \cdot 15.49 \quad (6.96)$$

And the wing tank surface area:

$$S_{wing,tank} = 2 \cdot 0.55 \cdot S_{new} \cdot 1.1 \quad (6.97)$$

Where the 0.55 factor is to account for the fact that the tank is to be placed between the spars. The tank top area area is therefore about 55 % of the total wing area. The 1.1 factor is to take into account the side surfaces of the tank. The tank layout within the wing can be seen in Figure 6.11. The thickness of the skin and the passive insulation is indicated in white.

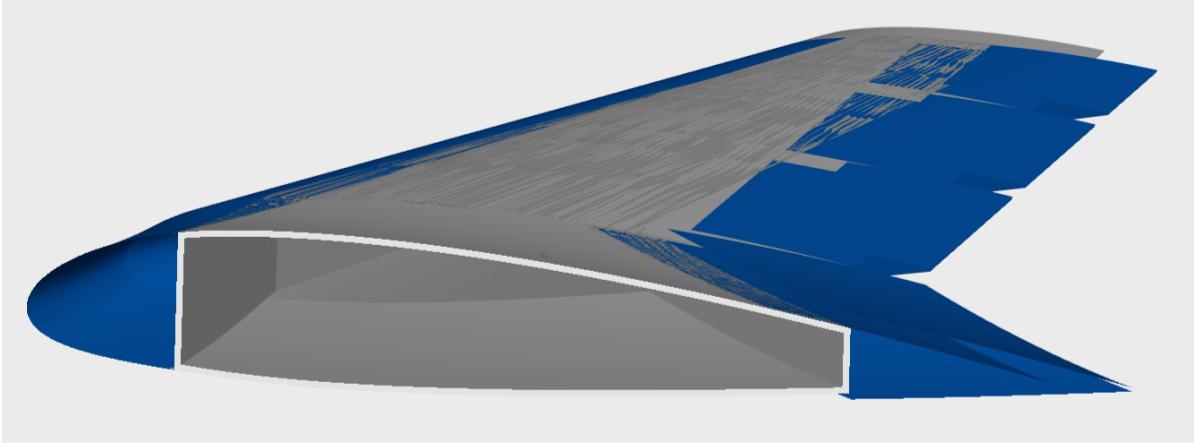


Figure 6.11: Internal fuel tank layout

With this information, the heat inflow to the wing fuel tank can be estimated. To simplify calculations at this stage, it was chosen to neglect radiation. In order to have a precise estimation for the heat balance, deeper studies into the heat transfer mechanisms have to be conducted. Nevertheless, the presented method provides sufficient accuracy for this design iteration. As such, the heat inflow is:

$$q_{in} = \frac{T_{amb} - T_{fuel}}{\frac{t_{foam}}{k_{foam} \cdot S_{wing,tank}} + \frac{t_{skin}}{k_{skin} \cdot S_{wing,tank}}} \quad (6.98)$$

In order to avoid any fuel boil off, the heat inflow will have to be offset by the active cooling system. The heat inflow obtained for a certain insulation and tank wall thickness thus defines the design space for the active cooling system. With all the given parameters, the required cooling pipe length and volume can be estimated. There are three heat transfer components that have to be regarded: convection in the fuel, conduction through pipe walls and forced convection in the coolant. For each of the aforementioned modes thermal resistance coefficients have to be determined. Starting with the simplest one, thermal resistance for conduction in the pipe is:

$$R_{pipe} = \frac{\log\left(\frac{d_{pipe,outer}}{d_{pipe,inner}}\right)}{2 \cdot \pi \cdot k_{pipe}} \quad (6.99)$$

The thermal resistances for the fuel and nitrogen are not as simple to calculate. Starting with the fuel, we have to estimate three significant numbers: the Grashof number, Nusselt number and Prandtl number. They can be obtained as follows:

$$Gr_{fuel} = \frac{g \cdot \beta_{NH3} \cdot (T_{NH3} - T_{coolant}) \cdot d_{pipe,outer}^3}{v_{NH3}^2} \quad (6.100)$$

$$Nu_{fuel} = 1.02 \cdot (Gr_{fuel} \cdot Pr_{fuel})^{0.148} \quad (6.101)$$

With the Prandtl number being a constant for the set fuel temperature and equal to $Pr_{fuel} = 2.15$. With that the thermal resistance of the fuel can be readily obtained from:

$$h_{fuel} = \frac{Nu_{fuel} \cdot k_{fuel}}{d_{pipe,outer}} \quad (6.102)$$

$$R_{fuel} = \frac{1}{h_{fuel} \cdot \pi \cdot d_{pipe,outer}} \quad (6.103)$$

The only coefficient left to be estimated is the coolant thermal resistance. In this case, a method specific to forced convection in a flowing fluid has to be applied. The relevant parameters can be estimated as follows:

$$Re_{coolant} = \frac{\rho_{N2} \cdot v \cdot d_{pipe,inner}}{\mu_{N2}} \quad (6.104)$$

$$Nu_{coolant} = 0.023 \cdot Re_{coolant}^{0.8} \cdot Pr_{coolant}^{0.4} \quad (6.105)$$

With the coolant Prandtl number again being a constant equal to $Pr_{coolant} = 0.7366$. The coolant thermal resistance then follows from:

$$h_{coolant} = \frac{Nu_{coolant} \cdot k_{N2}}{d_{pipe,inner}} \quad (6.106)$$

$$R_{coolant} = \frac{1}{h_{coolant} \cdot \pi \cdot d_{pipe,inner}} \quad (6.107)$$

With all the relevant resistances estimated, the heat extracted by the cooling pipes can be obtained from:

$$q_{out} = \frac{(T_{fuel} - T_{coolant}) \cdot \pi \cdot d_{pipe,outer}}{R_{pipe} + R_{fuel} + R_{coolant}} \quad (6.108)$$

The length of the pipe was omitted from the formula in order to obtain the heat outflow per unit length. Knowing the total heat inflow and heat outflow per unit length of pipe, the total cooling pipe length can be obtained:

$$L_{cooling,pipe} = \frac{q_{in}}{q_{out}} \quad (6.109)$$

This result enables the calculation of the additional mass and volume required to accommodate the piping.

$$V_{cooling,pipe} = \frac{\pi}{4} \cdot d_{pipe,outer}^2 \cdot L_{cooling,pipe} \quad (6.110)$$

$$m_{cooling,pipe} = \rho_{aluminum} \cdot \frac{\pi}{4} \cdot (d_{pipe,outer}^2 - d_{pipe,inner}^2) \cdot L_{cooling,pipe} \quad (6.111)$$

With this result, the final calculations can be done. The volume available for fuel storage within the wing and center tank can be estimated as follows:

$$V_{fuel,wing} = V_{new,wing} - S_{wing,tank} \cdot t_{foam} - V_{cooling,pipe} \quad (6.112)$$

As such, the volume required for the two auxiliary tanks is:

$$V_{fuel,aux} = \frac{m_{fuel,total}}{\rho_{fuel}} - V_{fuel,wing} \quad (6.113)$$

The shown calculation scheme can then be repeated for the auxiliary tanks to obtain the additional volume of the cooling pipes and insulation.

Adding auxiliary tanks requires additional volume within the fuselage as well as additional mass taken aboard. It is thus desired to find the optimal relation between the mass and volume. The above calculations allow to determine the optimal foam insulation thickness, such that the volume and mass are

minimized. A program in Python has been utilized to obtain this result. A plot showing the thickness volume and mass relation can be seen in Figure 6.12.

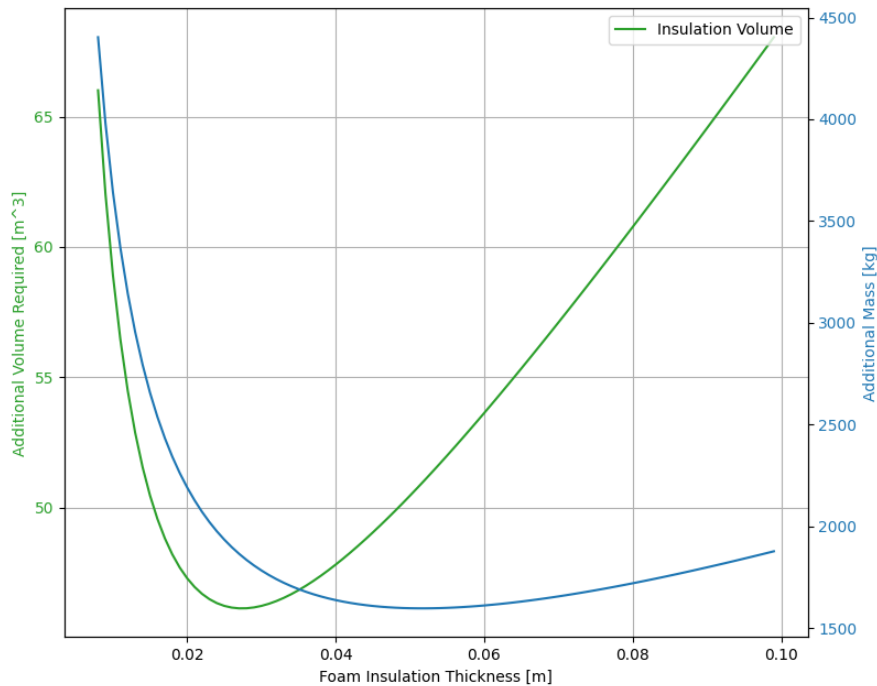


Figure 6.12: Storage volume and mass in relation to the passive insulation thickness.

The plot depicts a sample calculation done for the fuel mass of 35 tonnes and wing surface area of 175 m². Three significant points can be seen on the graph: mass and volume minima, and the intersection of the two lines. Depending on other limitations, each can be chosen as the optimal point. For this design, it was chosen to take the point with the minimal mass and volume possible (the intersection point) as the most optimal insulation thickness. With the most optimal thickness determined, the fuel storage system mass and total volume can be determined as shown previously. The auxiliary tanks can then be sized and placed such that the cg range is not affected negatively during operation. As the tanks are not pressurized the placement within the fuselage is mostly determined by its stability limits. The tank structure can be designed to be conformal with the structure at the required location.

The outlined calculation method definitely has limitations. First of all, accurate heat transfer analysis would require the evaluation of thermal conductivity's and other parameters at every temperature in the system and take into account the expansion and contraction of the working gasses with different temperatures. Such an approach would require developing a finite difference method, which would greatly increase the runtime of the overall program. Due to the low assumed temperature difference between coolant inlet and outlet the outlined method provides satisfactory accuracy. As the parameters are overestimated due to the assumptions taken, a safety factor can be imposed on the additional volume to account for the expected lower performance of the cooling system.

The remaining aspect of the fuel storage system design is the refrigerant and its utilisation. As the boil-off requirement is significant only during prolonged parking periods, it was chosen to base the refrigeration system on the ground. Carrying unnecessary mass to facilitate flight during the flying phase of aircraft operation would simply reduce the performance of the platform. The design of the said refrigeration system is not treated in this work, as there are already existing cryocoolers that offer sufficient performance for this application.

A320-NH3 Design Optimization

The designing methods and results of the aircraft systems are explained in chapter 5 and 6. To optimize the design, multiple iteration loops are made. the optimization process is needed to decrease the weight and increase the performance. It could be seen as the reversed snowball affect.

7.1. A320-NH3 Aircraft Architecture

The system exists of inputs, modules and outputs which all assemble in the main. The inputs exist of dictionaries that can be updated within modules. Where every module can import the main inputs to modify. The main regulates the sequence of the modules in the right order, defines the iteration loops and checks the results with the optimization criteria. After the iteration the updated inputs, outputs and resulting graphs are plotted. The general outline is visible in the software flowchart in Figure 7.1.

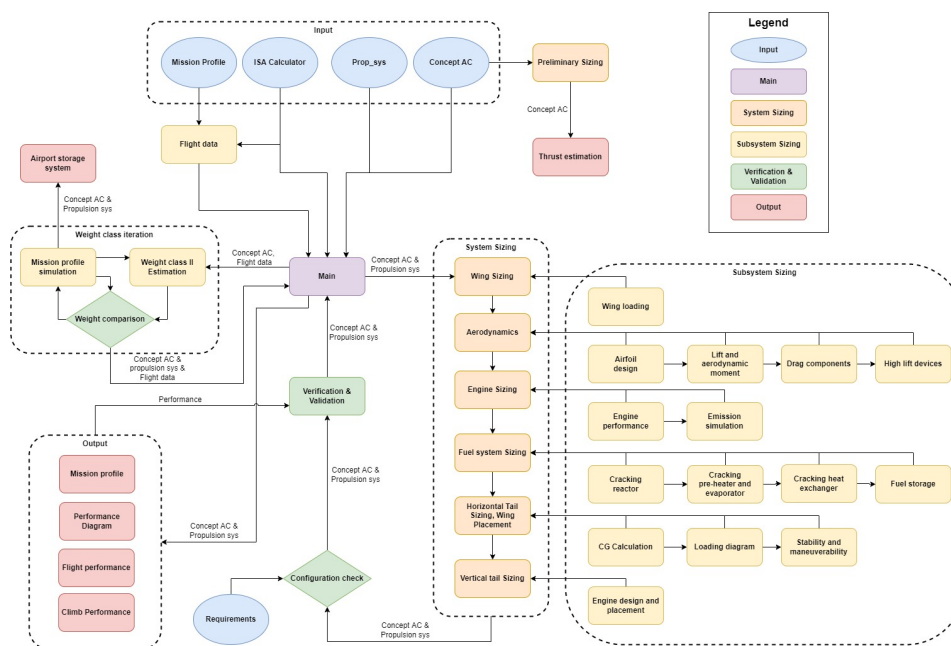


Figure 7.1: The software flowchart.

There is a large iteration loop containing all the systems of the aircraft and a smaller iteration loop to size the operation weights and take off thrust of the aircraft. The main iteration starts the small iteration loop to collect the maximum take off weight and thrust back to the main. Then all the systems are sized from the following order; *wing, aerodynamics, engine, fuel system, empennage*. The weight class II estimation is called again to update the system weights. The performance and configuration of the systems are checked with the requirements.

The weight iteration loop starts with a weight class II estimation and sizes all the system weights to find the operational weights. These operational weights will be used in the mission profile simulation to

update the weights depending on the performance. Both resulting operational weights are compared. If the weights differ too much from each other the modules are called again with the updated operational weights as input.

The performance of the architecture of the software is depending on the cohesion, coupling and modularity. The software has a high cohesion which makes it complex, but the reusability makes it easier to use for optimization. Modules can be used multiple times and can be integrated within the complete program. On macro level has the program a medium coupling level to make it easier to use and understand clearly which values are updated. When zoomed in on systems and sub-systems the coupling increases due to the complicated calculations. The system has an average modularity which makes it friendly to use. Every module can be tested with a unique input and most modules can be removed from the main without interrupting the iteration loops. There are modules which deliver highly ordered parameters and functions which are used in multiple systems. This is mostly on the level of subsystems.

7.2. Inputs

The optimization process has three large data inputs to process. The A320neo data, the propulsion unit data and the design flight mission profile. The A320neo consists of a collection of dictionaries which consist of all needed data for calculations of the aircraft design. The propulsion unit data contains all the data of the systems that store, transport, process or burn the fuel. The design flight mission profile describes the designed flight path determined by the requirements stated in chapter 3.

7.2.1. A320neo configuration

The A320neo is used as example for an aircraft that can be used as input. Since the class with all the information in the dictionaries is independent from the code, a comparable aircraft can be implemented with the same variables but different data. Next to that it is also possible to design for different concepts of the A320 at the same time and compare the results.

Aircraft sub-systems:

- **Weights:** All the aircraft operation weights are saved in this dictionary.
- **Configuration:** A dictionary with all the sizes and distances of the fuselage.
- **Capacity:** The dictionary for all the payload weights and amounts.
- **Wing:** A dictionary consisting of all the wing configuration parameters.
- **Performance:** A dictionary consisting of speeds, heights and distances.
- **Airfoil:** This is a dictionary with only the airfoil defined, the designed airfoil performance characteristics will be stored after calculations.
- **Aerodynamics:** This is an empty dictionary where the designed wing performance characteristics will be stored.
- **HLD:** A dictionary for the configuration of the flaps and the slats.
- **Flaps:** A dictionary for the angles the flaps make for different flight phases.
- **Slats:** A dictionary for the angles the slats make for different flight phases.
- **Cd0:** A dictionary for the zero induced drag coefficient for different flight phases and the surface roughness.
- **Stability:** A dictionary for significant data needed to calculate longitudinal stability and controllability.
- **Horizontal tail:** A dictionary consisting of all the data needed to shape the horizontal tail.
- **Vertical tail:** A dictionary consisting of all the data needed to shape the vertical tail.
- **Misc:** A dictionary consisting of the Wheel friction and crew number.

7.2.2. Propulsion system

The propulsion system exists of multiple systems, the engine the cracking system, the heat exchange and the fuel storage. This input is particular designed for the new A320-NH3 design to fit in. A different

aircraft would need a new personal design.

Propulsion sub-systems:

- **Engine:** A dictionary with all the sizes and general information about the engine.
- **Combustion:** All the parameters of combustion, compression, expansion and acceleration phases in the engine are saved in one dictionary.
- **Heat exchanger:** In the dictionary are all the sizes of the system and thermodynamic constants of the heat exchange performance saved.
- **Cracker:** The dictionary consists of the temperatures at the inlet and outlet of all the subsystems in the cracker. The total system performance is defined after calculations.
- **Pipe system:** The pipe design in the cracking system is elaborated, since it needs to be optimized for cracking. In this dictionary are all the material and configuration properties saved together with the chemical properties of N_2 and NH_3 .
- **Fuel:** To compare the design of different fuel properties of; kerosene, hydrogen, liquid ammonia and gaseous ammonia, all the chemical properties are saved in this dictionary.
- **Storage:** The storage system is dependent on the engine and cracker performance, this dictionary is empty to save the design parameters of the storage system.

7.2.3. Flight mission

It consists of a mission characteristic input and a module to convert the mission into a data set that saves the mission conditions for every time interval. This data set will later be used to simulate the flight backwards and calculate the needed performance for every time step.

Mission characteristics:

- **General:** The range, landing weight and choice of fuel is saved.
- **Take off:** The take off is defined by the runway length and the take off speed.
- **Climb phase:** The climb phase is parted in four phases with the starting height, indicated air speed, vertical speed and the acceleration.
- **Cruise:** The cruise mach and height is defined.
- **Descent:** The descent is parted in two phases, starting with a descending cruise phase. The second phase is from FL240 with the indicated airspeed, vertical speed and the deceleration.
- **Approach:** From FL100 an approach phase is defined similar to the second descent phase.
- **Landing phase:** The final phase consists of the landing speed and required runway distance.

Flight data module: The mission is used to define for every time step the following parameters; *flight phase, time, distance, height, speed, horizontal speed, vertical speed, temperature, pressure, density, profile drag and mach*. A large data set is created where every column is defined by a parameter and every row defines a new time interval of the simulation. This data set will be used to simulate the required performance of the designed aircraft which is required to perform the design mission.

7.3. Modules

The program exists of a collection of system and subsystem modules, which all assemble in the main. The modules are briefly explained and the inputs(In:) and outputs(Out:) are briefly stated for understanding. Methods are not explained, these can be found in the related design chapters.

7.3.1. The main

The main calls the input data from the A320neo, the propulsion system and the flight profile twice. One set for the simulation of the A320-NH3 design and another set for the A320neo that can be used as validation model. Then the airfoil gets integrated for the aerodynamic performance.

Main iteration loop: The iteration process is started, before updating systems, old values are saved to monitor the large changes. After the weight iteration process the wing, aerodynamics, engine, cracking and heat exchange, fuel system and empennage are updated in the stated order. The weight is

updated with the weight II class estimation since the configuration of the systems are adjusted. A flight simulation is not needed, since it is already calibrated with the weight II class.

Configuration check: The starting values saved for the configuration check are verified for large changes. The following parameters are checked, if they do not diverge according the stated percentages and relations. If one parameter diverged to many, the iteration loop is started again.

- Operating empty weight: 0.13%
- Wing surface: 0.5%
- Max thrust: 0.5%
- Max thrust required < Engine number · Max thrust
- Vertical tail surface: 0.5%
- Horizontal tail surface: 0.5%
- Cracking system mass: 0.5%
- Fuel mass: 0.5%
- Heat exchange area: 0.5%

Climate impact: For the impact the difference between the A320neo and the new design are compared for the total and CO₂-equivalent emissions. A sensitivity analysis is performed on the results to find the maximum allowed emissions for the A320-NH3 in order to meet the requirements stated by the client.

In: *Emissions from; CO₂, NO_x, H₂O; fuel, MTOW, Wing surface, Specific fuel consumption, cruise height.*

Out: *Climate impact results for different FL, ammonia production*

7.3.2. Weight class iteration

The weight iteration loop contains 2 modules, weight class II estimation and the flight simulation. In these modules are two ways used to approach the aircraft weight. The first depends on the system configurations and the second on the performance. The maximum take off weight is saved at the beginning, when both weight estimations have been performed to update the maximum take off weight is compared with the starting value. If the difference is less then 100 kg the weight iteration is done.

Weight class II estimation: In the weight class II estimation the configuration defines all the weights of different main systems of the aircraft. In: *MTOW, MZFW, MLW, Payload weight, span, wing surface, wing thickness ratio, quarter chord sweep, Dive dynamic pressure, fuselage dimensions, empennage surfaces, engine weight and number, passengers and crew amount, payload configuration*

Out: *MZFW, MLW, OEW, System weights*

Flight simulation: In the flight simulation is the designed mission simulated backwards and retrieved in time order. The flight and engine performances and conditions are simulated for a constant time step. The simulation runs through the design mission to have a approach the required performances.

In: *Engine performances, cracker performances, fuel composition, MTOW, max lift, profile drag, take off distance and speed, max thrust experience, wing configuration*

Out: *Flight data, engine validity, weight, lift required, thrust required, fuel mass flow, specific fuel consumption, mass flow hydrogen, NO_x, CO₂, engine core mass flow, Pressure combustion,*

7.3.3. System sizing

Wing sizing: The wing is updated by keeping the wing loading the same. A ratio between the new and old wing surface is calculated to increase the wing dimensions.

In: *MTOW, Wing loading and surface.*

Out: *Surface, span, root chord, Mean aerodynamic chord, engine-fuselage offset.*

Aerodynamics: The aerodynamics is split up in 5 sub modules; airfoil design, lift, high lift devices(HLD), profile drag and induced drag. The airfoil is updated before, as following the lift generated by the airfoil is calculated with the other moment coefficients and center of pressure. The effect of a finite wing is implemented for the 3D lift coefficients to find the wing lift slope. The high lift devices are then calculated and sized, which have influence on the profile drag. The profile drag is calculated for different flight phases. At last is the induced drag and total drag calculated. From here the highest L/D could be found.

In: *airfoil, AoA, cruise conditions, flight phase, mach, engine dimensions, fuselage dimensions, empennage dimensions, wing dimensions, flap and slat deflection.*

Out: *airfoil integration constants, thickness ratio, leading edge radius, location max thickness and camber, center of pressure, lift coefficient 2D and 3D, lift slope 2D and 3D, maximum lift coefficient, HLD effect, moment coefficient around aerodynamic center, profile drag, Oswald efficiency factor, induced drag, wave drag, lift over drag, minimum drag velocity.*

Engine sizing: The engine simulation is used to simulate the engine performance for different engine design parameters. It sizes the engine by aiming to reduce NO_x emissions during whole flight.

In: *Inlet pressure, temperature and velocity, engine performance constants, chemical fuel and air characteristics, cracking system performance.*

Out: *Thrust, specific fuel consumption, fuel mass flow, engine validity, mass flow core engine, temperatures and pressures, conversion fraction.*

Fuel system sizing: The fuel system exists of 4 subsystems; the cracking reactor, the cracking pre-heater and evaporator, the cracking heat exchanger and the fuel storage. The reactor is sized to the required performance of the engine. The required hydrogen is the main design parameter. The temperatures in the reactor and material choices in the system, define the required performance of the pre-heater, evaporator and heat exchanger. After sizing all the cracking subsystems, the required power, mass and volume of the subsystems are found.

In: *Hydrogen mass flow, material properties of the piping system, conversion performance catalyst, process temperatures, ammonia chemical properties, hydrogen chemical properties, fuel storage material properties, insulation material properties, storage temperature.*

Out: *Required power, mass and volume of the cracking system, required mass, volume and thickness of the fuel storage, boil off ratio, insulation mass and volume.*

Horizontal tail sizing & wing placement: The horizontal tail is sized with the required stability performance. The center of gravity is determined, from there the loading diagram and finally a scissor plot to check the stability and maneuverability. From the plot the location and size can be found for the horizontal tail. The new size and location define a growth factor, where the other parameters are also sized with.

In: *systems center of gravity and weights, wing parameters, payload and passenger mass and location, fuel weight and location, aerodynamic properties of the wing and tail*

Out: *Horizontal tail; surface, span, MAC, tip and root chord, volume.*

Vertical tail sizing: The tail is sized to lateral stability requirements like engine failure and gust loads. A new vertical tail growth factor is required. It is sized linearly with the old surface.

In: *Fuselage and wing sizes, max thrust, lateral engine location.*

Out: *Vertical tail; surface, span, MAC, tip and root chord, volume.*

Verification & Validation The verification and validation is done by checking the system for the original aircraft and the new designed aircraft. In this case the A320neo and the A320-NH3 are compared and the values of the A320neo are verified.

In: *(Sub-)System modules, aircraft input, propulsion system input.*

Out: *Pass or no pass*

7.4. Output

The output is structured in 2 groups, the graphs and the final updated data. The final data exists of all the dictionaries with the updated parameters. These are structured in the same way as the input. In the next chapter 8, the results are presented from the A320-NH3 and the new propulsion system. The final graphs are presented in the corresponding chapters.

Final Design Parameters

Table 8.1: Final output values of the optimization system.

Component:	Parameter	Notation	Value	Unit
<i>Configuration</i>				
Payload	Passenger capacity	pax	150	[—]
Weights	Maximum ramp weight	MRW	92067.636	[kg]
Weights	Maximum take-off weight	$MTOW$	91603.819	[kg]
Weights	Maximum landing weight	MLW	70910.889	[kg]
Weights	Maximum zero-fuel weight	$MZFW$	66897.065	[kg]
Weights	Operating empty weight	OEW	49267.065	[kg]
Payload	Weight	W_{weight}	17630.0	[kg]
Payload	Passenger weight	W_{pax}	15000.0	[kg]
Payload	Cargo weight	W_{cargo}	2630.0	[kg]
Fuel	Weight	W_{fuel}	24696.761	[kg]
Fuel	Volume	$Volume_{fuel}$	39.839	[m ³]
Fuselage	Total length	$Length_{fuselage}$	37.57	[m]
Fuselage	Width	$Width_{fuselage}$	3.95	[m]
Fuselage	Height	$Height_{fuselage}$	4.14	[m]
Tail cone	Length	$Length_{tail-cone}$	11.97	[m]
Cockpit	Length	$Length_{cockpit}$	4.86	[m]
Cabin	Length	$Length_{cabin}$	27.51	[m]
Cabin	Width	$Width_{cabin}$	3.63	[m]
Cabin	Seating rows	n_{rows}	25	[—]
Cabin	Length per row	l_{row}	0.77	[m]
Cargo	Volume	$Volume_{cargo}$	37.42	[m ³]
Cargo	Volume for	$Volume_{cargo-for}$	13.28	[m ³]
Cargo	Volume aft	$Volume_{cargo-aft}$	18.26	[m ³]
Cargo	Volume aft bulk	$Volume_{cargo-aft-bulk}$	5.88	[m ³]
Cargo	Water volume for	$Volume_{water,cargo-for}$	15.56	[m ³]
Cargo	Water volume aft	$Volume_{water,cargo-aft}$	20.77	[m ³]
Cargo	Water volume aft bulk	$Volume_{water,cargo-aft-bulk}$	7.76	[m ³]
Wing	Span	b	36.72	[m]
Wing	Surface	S	141.93	[m ²]
Wing	Aspect ratio	A	9.5	[—]
Wing	Inner wing span ratio	b_{inner}	0.37	[m]
Wing	Sweep leading edge	Λ_{LE}	0.475	[rad]
Wing	Quarter chord sweep	$\Lambda_{1/4}$	0.436	[rad]
Wing	Half chord sweep	$\Lambda_{1/2}$	0.370	[rad]
Wing	Taper ratio	λ	0.24	[—]
Wing	Mean aerodynamic chord	MAC	4.62	[m]

Wing	Leading edge MAC	le_{mac}	14.44	[m]
Wing	Root chord	C_r	7.55	[m]
Wing	Tip chord	C_t	1.68	[m]
Wing	Dihedral	Γ	0.0873	[rad]
Wing	Wetted surface	S_{wet}	92.3	[m ²]
Vertical tail	airfoil	$NACA_{xxxx}$	0015	[—]
Vertical tail	Thickness ratio	t/c_v	0.15	[—]
Vertical tail	Leading edge MAC	l_v	18.435	[m]
Vertical tail	Mean aerodynamic chord	MAC_v	4.256	[m]
Vertical tail	Height	b_v	6.255	[m]
Vertical tail	Surface	S_v	21.484	[m ²]
Vertical tail	Root chord	$C_{r,v}$	5.268	[m]
Vertical tail	Tip chord	$C_{t,v}$	1.596	[m]
Vertical tail	Taper ratio	v	0.303	[—]
Vertical tail	Aspect ratio	A_v	1.82	[—]
Vertical tail	Sweep leading edge	$\Lambda_{LE,v}$	0.708	[rad]
Vertical tail	Quarter chord sweep	$\Lambda_{1/4,v}$	0.593	[rad]
Vertical tail	Surface ratio to wing	$\frac{S_v}{S_w}$	0.151	[—]
Vertical tail	Vertical tail volume	$\frac{\bar{S}_v l_h}{S_c}$	0.076	[—]
Horizontal tail	airfoil	$NACA_{xxxx}$	0012	[—]
Horizontal tail	Thickness ratio	t/c_h	0.12	[—]
Horizontal tail	Leading edge MAC	l_h	17.53	[m]
Horizontal tail	Mean aerodynamic chord	MAC_h	2.716	[m]
Horizontal tail	Span	b_h	13.4	[m]
Horizontal tail	Surface	S_h	35.908	[m ²]
Horizontal tail	Root chord	$C_{r,h}$	4.267	[m]
Horizontal tail	Tip chord	$C_{t,h}$	1.092	[m]
Horizontal tail	Taper ratio	h	0.256	[—]
Horizontal tail	Aspect ratio	A_h	5.0	[—]
Horizontal tail	Sweep leading edge	$\Lambda_{LE,h}$	0.519	[rad]
Horizontal tail	Quarter chord sweep	$\Lambda_{1/4,h}$	0.506	[rad]
Horizontal tail	Half chord sweep	$\Lambda_{1/2,h}$	0.412	[rad]
Horizontal tail	Surface ratio to wing	$\frac{S_h}{S_w}$	0.253	[—]
Horizontal tail	Horizontal tail volume	$\frac{\bar{S}_h l_h}{S_c}$	1.092	[—]
Performance:				
Performance	Range	<i>Range</i>	4000	[km]
Performance	Cruise mach number	M_{cruise}	0.78	[—]
Performance	Cruise height	H_{cruise}	11277.6	[m]
Performance	Take off speed	V_{TO}	73.686	[m/s]
Performance	Take off length	$Length_{TO}$	1951	[m]
Performance	Maximum take off thrust	$Thrust_{T/O}$	257764	[N]
Performance	CO2 emissions	m_{CO_2}	0	[kg]
Performance	NOx emissions	m_{NO_x}	38.337	[kg]
Performance	H2O emissions	m_{CO_2}	28960.775	[kg]
Engine:				
Intake	Bypass ratio	BPR	9.75	[—]
Fan	Pressure ratio	π_{fan}	1.816	[—]
LPC	Pressure ratio	π_{LPC}	1.5	[—]
HPC	Pressure ratio	π_{HPC}	8.0	[—]
ITB	ITB energy fraction	$ITB_{energy-fraction}$	0.213	[—]
Main combustion chamber	Primary zone air ratio	$PZAR$	0.2	[—]
Engine	Maximum thrust	$Thrust$	133585	[N]

Combustion chamber Engine	Specific fuel consumption of ammonia Mass	SFC m_{engine}	26.0 2539.634	[g/kN/s] [kg]
<i>Fuel Tanks:</i>				
Wing tank	Tank Volume	$V_{tank,wing}$	21.6	[m ³]
Wing tank	Fuel Volume	$V_{fuel,wing}$	15.6	[m ³]
Auxiliary tanks	Tank Volume	$V_{tank,aux}$	34.7	[m ³]
Auxiliary tanks	Fuel Volume	$V_{fuel,aux}$	21	[m ³]
Total	Tank Volume	$V_{tank,total}$	56.3	[m ³]
<i>Cracker</i>				
Evaporator	Weight	$m_{Evaporator}$	574.4	[kg]
Evaporator	Volume	$V_{Evaporator}$	0.1429	[m ³]
Evaporator	Power	$P_{Evaporator}$	7.25	[MW]
Preheater	Weight	$m_{Preheater}$	613.7	[kg]
Preheater	Volume	$V_{Preheater}$	0.1527	[m ³]
Preheater	Power	$P_{Preheater}$	8.36	[MW]
Reactor	Weight	$m_{Reactor}$	2830	[kg]
Reactor	Volume	$V_{Reactor}$	0.3913	[m ³]
Reactor	Power	$P_{Preheater}$	25.7	[MW]
Reactor	Catalyst Weight	m_{Cat}	1254	[kg]
Heat exchanger	Weight	$m_{exchanger}$	112.4	[kg]
Heat exchanger	Volume	$V_{exchanger}$	0.02797	[m ³]
Heat exchanger	Power	$P_{exchanger}$	0.472	[MW]
Cracking System	Weight	$m_{cracking}$	4127	[kg]
Cracking System	Volume	$V_{cracking}$	0.7149	[m ³]
Cracking System	Power	$P_{cracking}$	40.9	[MW]
Cracking System	Number of Reactors	$n_{reactors}$	581	[—]
Combustion chamber heat exchanger	Helix Length Mass	$L_{tot,hel,cc}$ $W_{tot,hel,cc}$	0.56 12.37	[m] [kg]
<i>Aerodynamics</i>				
Airfoil	name	$NACA_{xxxx}$	4312	[—]
Airfoil	thickness ratio	t/c	12	[%]
Airfoil	Leading edge radius	$\frac{LER}{c}$	0.01587	[—]
Airfoil	max thickness location	x_t	30	[%]
Airfoil	Max camber location	x_c	30	[%]
Airfoil	camber	$\frac{dz}{dx}$	4	[%]
Airfoil	Center of pressure	X_{cp}	0.271	[—]
Airfoil	Airfoil lift slope	$C_{l,\alpha}$	0.1097	[—]
Airfoil	Airfoil max lift	$C_{l,max}$	1.91	[—]
Airfoil	Moment around aerodynamic center	$C_{m,ac}$	-0.1468	[—]
Airfoil	Airfoil technology factor	κ_A	0.95	[—]
Wing	Lift slope	$C_{L,\alpha}$	0.109	[rad]
Wing	Maximum lift	$C_{L,max}$	2.74	[—]

Wing	Maximum lift over drag	$\frac{L}{D}$	18.11	[—]
Wing	Lift @L/D maximum	$C_{L,max,L/D}$	0.597	[—]
Wing	Drag @L/D maximum	$C_{D,max,L/D}$	0.033	[—]
HLD	Inner flap span ratio	$b_{f,inner}$	0.9	[—]
HLD	Outer flap span ratio	$b_{f,outer}$	0.7	[—]
HLD	Slat span ratio	b_s	0.95	[—]
HLD	Inner flap tip chord ratio	$\left(\frac{cf}{c}\right)_{inner,tip}$	0.35	[—]
HLD	Outer flap chord ratio	$\left(\frac{cf}{c}\right)_{outer}$	0.3	[—]
HLD	Slat root chord	$c_{s,root}$	0.75	[m]
HLD	Slat tip chord	$c_{s,tip}$	0.5	[m]
Profile drag	Clean	$C_{D0,clean}$	0.0158	[—]
Profile drag	Take off	$C_{D0,Takeoff}$	0.0473	[—]
Profile drag	Climb	$C_{D0,Climb}$	0.0218	[—]
Profile drag	Approach	$C_{D0,Approach}$	0.0324	[—]
Profile drag	Landing	$C_{D0,Landing}$	0.0677	[—]
Induced drag	Oswald efficiency factor	e	0.732	[—]

Operations & Logistic Concept

9.1. Ammonia Infrastructure

The infrastructure for ammonia as an energy carrier for a renovated Airbus A320 will be discussed in this section.

9.1.1. Production of Ammonia

Once the renewed aircraft A320-NH₃ will be operational, a new infrastructure will be required for ammonia. The inorganic chemical NH_3 is already one of the most widely produced - 175 million tonnes of ammonia were produced in 2016 alone. This is mostly utilized in agriculture, although it is also employed in the manufacturing of other materials. Nowadays, a Haber Bosch method is used to produce ammonia, which was primarily developed to maximize economic profit and production rate without regard for the process's long-term sustainability. As a result, industrial ammonia synthesis generates more CO₂ than any other chemical process, accounting for around 1% of total CO₂ emissions.¹ By creating a demand for ammonia as propellant, its supply needs to be increased as well. The choice of this production definitely goes to the so-called "Green ammonia". The electrically driven Haber Bosch process is predicted to boost energy efficiency in the synthesis loop by 50% and reduce CO₂ emissions by 78% using this technology [52].

The green Haber Bosch process uses sustainable energy from the wind or the sun to perform electrolysis instead of methane. Some countries have a lot of potential to generate big amounts of green energy from the solar powers and are planning to use it for ammonia production in the future. Australia is one of those countries, but also Spain has these kind of plans. The closer the production to the airport - the lower the price of ammonia as fuel. Just like it holds for other fuels - ammonia must be pure and uncontaminated when used as propellant, requiring high standards for production and transportation.

9.1.2. Transport of Ammonia as energy carrier

Ammonia is a common chemical. The infrastructure to transport ammonia is already in place, and the restrictions have been well tested over time. Ammonia is generally transported by ship or rail across the world. Because of its relative complexity, the last is chosen to be described in this section.

Railway tank cars (RTCs) used to transport anhydrous ammonia must meet both national and international norms in terms of design and construction. A typical design of a RTC can be seen in Figure 9.1

¹<https://cen.acs.org/environment/green-chemistry/Industrial-ammonia-production-emits-CO2/97/i24>

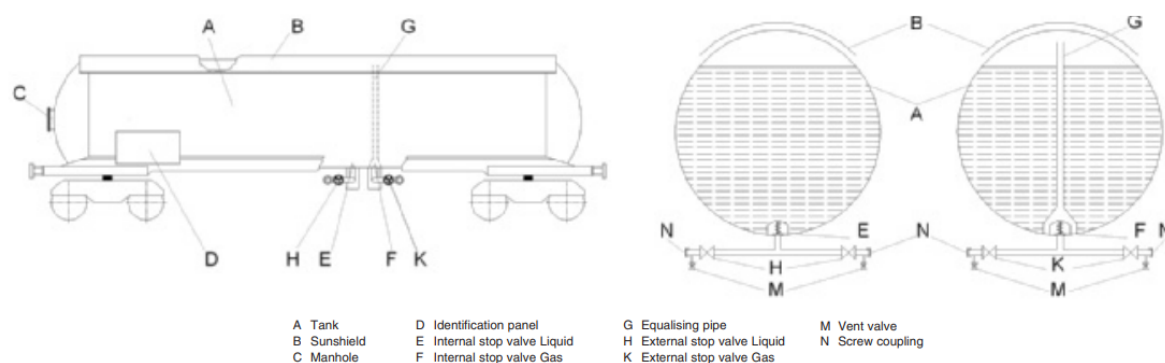


Figure 9.1: Diagram of a typical Railway Tank Car (RTC).

By adopting the correct design, materials, and construction, stress corrosion cracking may be prevented. The likelihood of SCC rises as the yield strength of the plate material, weld metal strength, and local hardness in the welds increase. These variables should be taken into account. Despite the fact that ammonia is created without oxygen, air can infiltrate the system during transportation from the factory to the user. If there is enough oxygen available, stress corrosion cracking can develop in tanks used to transport liquid ammonia. As a result, air must not enter the tank, and tanks must be purged with nitrogen before being used to carry ammonia. RTCs typically have storing capacities of 50 to 110 [m³]. As it be explained further in the chapter, this means that 1 RCT of 50 [m³] is enough to fully fuel the A320-NH₃ for 1 flight. RCTs must be designed and built with the material selected and the wall thickness established by considering the minimum and maximum filling and operating temperatures. Any tank thermal insulation should be either a sun shield or fully covered insulating materials of sufficient thickness. All items in touch with ammonia, including component materials, must be devoid of chemicals that might cause it to react violently. Copper or copper-containing materials, in particular, should not be used. Shells must be composed of appropriate metallic materials that are resistant to brittle fracture and stress corrosion cracking at temperatures ranging from -20 to +50 [°C]. Pipelines, huge seagoing boats, river barges, rail tank cars, and tank trucks are examples of alternate means of transport (except in Germany due to its regulations). Ammonia is carried throughout Europe through river barges, rail tank trains, and tank trucks. There are no ammonia long-distance pipeline networks in Europe. ².

Two different ways ways of transporting the fuel to the airport can be discussed. For example Amsterdam Airport Schiphol (EHAM) is connected to the 'Central Europe Pipeline System', one of several NATO pipeline systems that transports gasoline for ground and air vehicles throughout Europe. It was first designed for military use, to help in the speedy and safe transportation of petroleum for military reasons throughout Europe. Over 5,314 km of pipeline make up the system, which passes through Belgium, France, Germany, Luxembourg, and the Netherlands. The system is utilized by the military of the United States in addition to these host nations.³ However there are 15 fuel tanks of different sizes present on EHAM, these only serve as a buffer for the supply through the pipeline. The other example of fuel transport is being used at Rotterdam The Hague Airport (EHRD), this airport is not connected to the CEPS and has multiple Shell fuel trailers there that are occasionally driven to Shell Pernis to be refilled. Pipeline infrastructure for ammonia can be build, also being the most favorable solution. Until that moment, transportation by road will be the optimal way to go.

9.1.3. Airport storage

After the transportation to the airport facilities, ammonia shall safely be stored. Since the ammonia will be stored at the temperature of approximately -33 [°C] in the fuel tank, this temperature must be achieved before being fueled into the aircraft. This means that the fuel storage facilities at the airport have to designed to cool and sustain the needed temperature for ammonia. The fact that the energy carrier will be stored at that temperature, makes it to be stored at the atmospheric pressure.

²https://cefic.org/app/uploads/2018/12/Transporting-Ammonia_ByRail-by-EFMA-2007-GUIDELINES-ROAD-SUBSTANCE.pdf

³<https://www.nspa.nato.int/about/ceps>

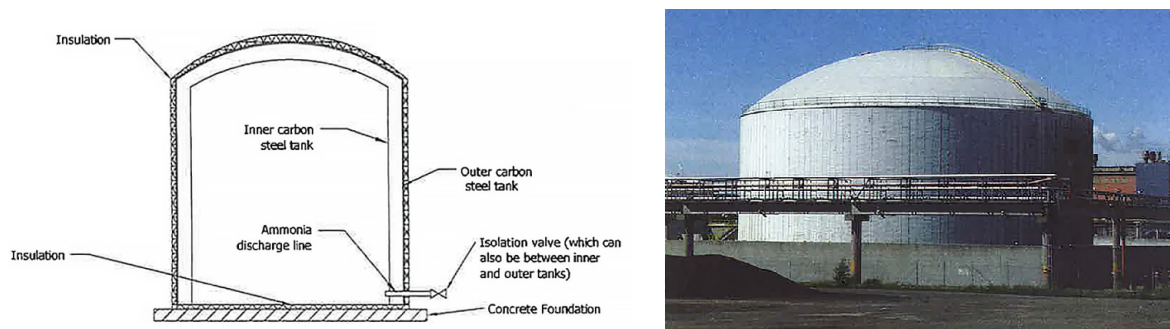


Figure 9.2: Tank with separate roofs and steel outside and interior walls.

In Figure 9.2 an example of a ammonia storage tank can be seen. In such a tank the ground beneath the tank base does not need to be heated since the foundation is sitting on concrete and the earth below is not exposed to freezing temperatures due to ammonia. The materials used in atmospheric ammonia tanks must be chosen to meet the design regulations' criteria. Low temperature certified carbon manganese steel, impact tested at or near -40 [$^{\circ}\text{C}$], is the standard kind of material. With increased yield strength, the steel's vulnerability to stress corrosion cracking rises. Typically, materials having a minimum yield strength of 290 to 360 MPa are employed. The inner and outside tanks should be made of normalized carbon-manganese steel and constructed entirely by welding.

To prevent against over pressuring or vacuum situations, each atmospheric storage tank should have at least two pressure release valves and two vacuum relief valves installed. Acoustic emission testing should be the principal non-destructive testing method utilized on the NH_3 tank during its life. Furthermore, earthing bosses should be installed on all tanks, and tanks larger than 30 meters in diameter should have three. To avoid ammonia contact, the earthing bosses should be made of stainless steel for the studs and washers and covered copper conductor strips. Earthing bosses must be uniformly distributed throughout the tank.⁴ It is assumed that during the transportation by train, truck or a pipeline will not be cooled ammonia will not be cooled and the tank will be pressurized. The cooling shall be performed before entering the tank. Warm ammonia inbounding is commonly accomplished by running the product through a flash tank to improve efficiency. Refrigeration capacity limits the rate (usually 5-20 tons per hour) [21].

As already mentioned in subsection 9.1.2, stress corrosion cracking (SCC) is a phenomenon that may develop in metals subjected to a corrosive environment under stress. In this section this phenomenon will be elaborated. Under some conditions, the corrosive environment will destabilize the protective oxide layer without triggering widespread corrosion. In carbon steels, liquid ammonia in the presence of oxygen can induce SCC. Some storage tanks operating at -33 [$^{\circ}\text{C}$] have been showing signs of stress corrosion cracking since the late 1980s. It appears that commissioning and, to a lesser extent, recommissioning are crucial phases in the creation of fractures, based on findings and substantial worldwide study work. This is due to the possibility of increasing oxygen levels inside the tank as well as temperature fluctuations generating additional stress. In Figure 9.3 an example of a rupture caused by SCC can be seen.⁵

⁴<https://ammoniaknowhow.com/ammonia-storage-tanks/>

⁵https://www.fertilizerseurope.com/wp-content/uploads/2019/08/Guidance_for_inspection_of_atmospheric_refrigerated_ammonia_storage_tanksVJ_website.pdf

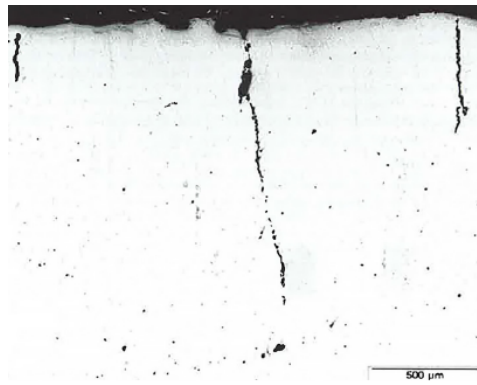


Figure 9.3: Cross section of crack caused by SCC.

Due to the necessity for oxygen to catalyze the process and the slowing effect of the low temperature, SCC is uncommon in low temperature tanks. The principal internal deterioration process in fully refrigerated ammonia storage tanks is SCC, which must be considered while developing and implementing an inspection program. Exterior variables for degradation, such as external corrosion, settling, and so on, must also be taken into account.

9.1.4. On-airport transport

After being stored at the airport, the fuel needs to be transported to the aircraft. This can be divided in two different ways. Fueling can be done by an equipped refueling truck which can be seen in Figure 9.4(b). A refueling truck is quite similar to a traditional fuel tanker. It has a pumping system, fuel hoses for connecting to an aircraft's fuel receptacle, safety and protection mechanisms for gasoline risks, and a metering device for measuring the volume of fuel transported from the truck to the aircraft so that the airline could be billed. Some other airports, like for example Amsterdam Airport Schiphol, can sometimes invest in a pipeline which runs through underground network of tubes to the gates. Connection between the airport pipelines and the wing of the aircraft where the fuel is stored is then made by a truck carrying the connecting extendable pipes, a so-called 'Fuel Hydrant Dispenser'. This can be seen in Figure 9.4(a). This method is also called 'transporting kerosene via a hydrant'. The pipeline infrastructure is fast and reliable. In Amsterdam Airport Schiphol the hydrant is used transport more than 85% of total fuel delivered to the airplanes.⁶

However fuel hydrants are more expensive infrastructure compared to refueling trucks, because of the danger of collisions with other vehicles and ground support equipment that might result in gasoline spills, a refuel truck poses a higher safety risk. This risk is lower for the hydrant dispensers. The cost-benefit analysis determines whether to use fuel hydrant dispensers or refuel trucks. It is not adopted if the additional expense of developing an underground fuel supply network does not equal the advantages of employing the simpler trucking method. For this project also the price of the active cooling that the underground system of the hydrant must have, needs to be taken into the account.

9.1.5. Fuel storage sizing

A preliminary decision for airport storage may be generated based on the amount of fuel required for the aircraft. The following estimates are provided for the A320(-NH₃) aircraft's design range:

- 10,384kg of kerosene would be needed, which is equal to approximately 13,000 liters using the density of 0.804 kg l⁻¹ for Jet-A1 1
- 35,000kg of ammonia is needed, this results in 51,320 liters of liquid ammonia using the density 0.682 kg l⁻¹ at -33.3 °C

Choosing the right amount of storage space is a challenging job. Each airport has its own set of fuel supply and demand issues. Mathematical models may be unable to optimize constraints that are not measurable. Different priorities exist among stakeholders, which can be difficult to reconcile. However,

⁶<https://blog.klm.com/this-is-how-we-refuel-at-schiphol-airport-handy-hydrant/>



((a)) Fueling the aircraft using kerosene pipeline



((b)) Fueling the aircraft using a refueling truck

Figure 9.4: Two ways of refueling the aircraft on the airport

defining a thought process framework for improved communication and informed perspectives among stakeholders and regulators is beneficial. It will also be critical that the final strategy considers all aspects of safety, quality control, and engineering. It will be necessary to obtain professional safety, quality control, and technical guidance to design particular projects after the optimum capacity has been identified.⁷

Before beginning the quantification process, it's essential to have a thorough understanding of the airport's present profile. This may be accomplished by responding to the following questions

1. Forecast of demand (current daily/monthly average, peak daily/monthly demand, and demand profile for the day).
2. The modalities and capacity of supply (road tank trucks, pipeline, rail cars, barges, and so on).
3. Fuel delivery to the airport depot operational hours of the supply modes
4. Operating hours of the Airport Depot
5. Offloading facilities, limits, and more at the airport depot (For example, the number of off-loading islands in use, the size of the pipeline receiving station, and so on)

Furthermore other parameters should be taken into account. The current and future demand (growth) should be accommodated. The normal current supply, the buffer normal supply and future supply developments need to be handled. Additionally quality control should be allowed, e.g. time for settling and quality control tests prior to re-certification, maintenance requirements and allowing for recirculation and filtering of product from any tank. When compared to the present kerosene scenario, the size of the airport fuel tank may be projected to be about doubled at this point in the design.

Consider Rotterdam Airport and Amsterdam Schiphol Airport. The first one mainly focuses on recreational flights and narrow-body aircraft flying through Europe. This does not apply to Schiphol - it has a big worldwide hub function and is home to both wide- and narrow-body aircraft. At this moment, this project is the only one redesigning the aircraft using ammonia as fuel. There are no plans at this moment of creating wide-body aircraft using ammonia whose design will come with new problems. Most likely future of the aviation will not lie in one new energy carrier, rather than multiple sources of propulsion. These are the reasons why a precise estimation for a particular airport is rather complex. However, using the estimations explained in this section that on average on this stage of the design it is predicted that for the same flight 4 times more ammonia will be needed compared to kerosene in terms of volume, one can use this number to make some forecasts.

9.2. Ground Operations & Regulations

In this section the renewed operations for the aircraft using ammonia as propellant will be discussed. This would mean that differences shall be made compared to the current energy carriers operations in the aviation.

⁷<https://www.iata.org/contentassets/4eae6e82b7b948b58370eb6413bd8d88/guidance-fuel-storage-may08.pdf>

9.2.1. Refueling operations & regulations

Safe refueling operations now need close attention to safety measures not just by refueling operators, but also by flight crews, cabin crews, and other ground operators. The reason for this is the danger posed by extremely flammable jet fuel. Historically, this perilous process has resulted in many of the regulations aimed at preventing harmful circumstances from occurring. The majority of laws governing airplane refueling and propellant handling are based on the extremely high flammability of these energy carriers and much less by the potential health risks.⁸ Consider the 'Bonding,' which is required before the refueling hose can be connected to the airplane. Bonding ensures electrical continuity between the aircraft and the refueling truck when the ground operator connects the refueling line to the aircraft coupler, eliminating any spark. The bonding wire must be linked to one of the grounding (earthing) points, such as those on landing gears or wings. This is an excellent example of a variety of fuel rules in place to avoid unmanageable fires.

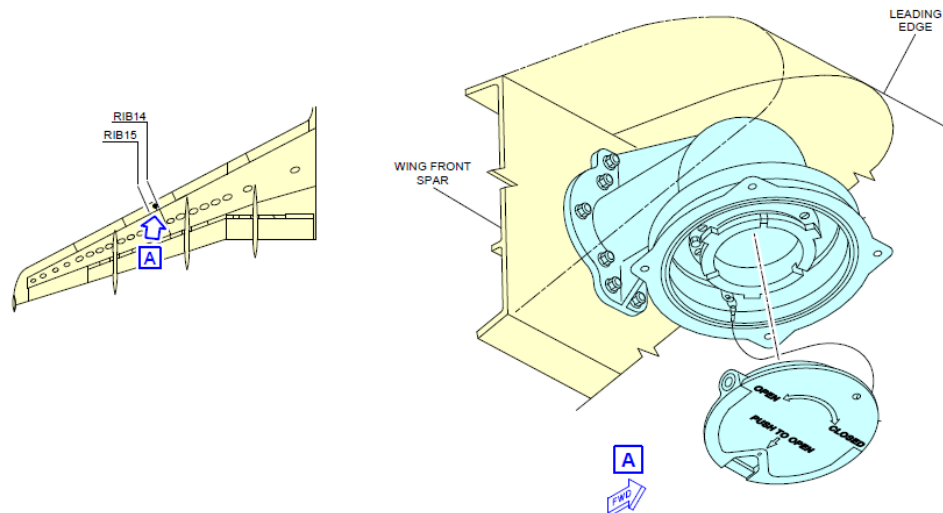


Figure 9.5: Refuel/Defuel Coupling on A320

Commercial jets are using pressure refuelling compared to small aircraft that often use gravity refuelling. A refuel/defuel coupler as present on A320neo can be seen in Figure 9.5. In case of pressure refueling gallery failure, Airbus A320neo has overpressure protectors installed. There are 8 of these valves present; 3 on each wing and 2 in the center tank. Depending on the fuel tank placement that still needs to be determined for the A320-NH3 aircraft, fueling safety zones will be set. A 3-meter safety zone around the region beneath overpressure protectors and refill connections is required by industry standards. There must be no objects or people in these regions. A clear escape lane is also required so that the refueling truck may exit the location in the event of an emergency.⁹ These zones for A320-NEO can be seen in Figure 9.6.¹⁰

⁸<https://www.icao.int/NACC/Documents/Meetings/2012/ICA0FAAAGACertification2012/ICA0FAACertification14.pdf>

⁹<https://www.aviationhunt.com/aircraft-fuel-system/>

¹⁰<https://safetyfirst.airbus.com/safe-aircraft-refuelling/>

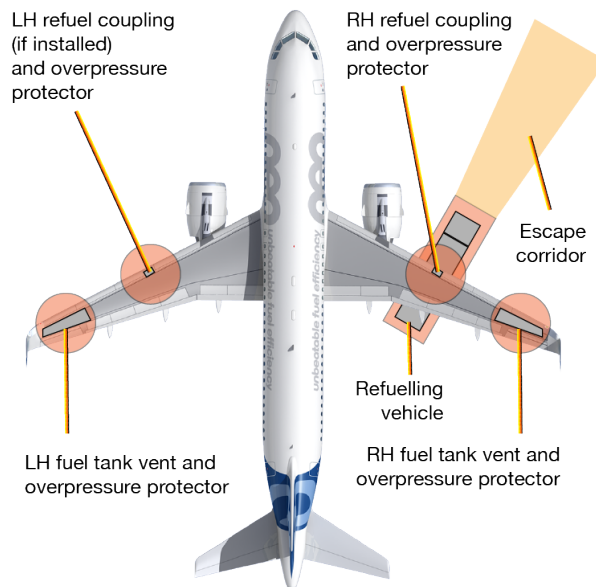


Figure 9.6: Fuelling safety zones on an A320-NEO

Assessing the refueling time of the renewed A320-NH3 aircraft, the following requirement was given: "The impact of refuelling shall not add more than 30 min to the turnaround time.". As already discussed in subsection 9.1.5, the needed kerosene for the given range for this project (which is lower than maximum A320-NEO range) would be 13,000 liters which is also lower than the maximum fuel A320 can carry (23,858 liters). This means that using this range approximately 51,320 liters of liquid ammonia is needed. This is about four times as high as the fuel capacity of the A320 on the same route using kerosene. Since the typical refueling time of an A320 is around 24 minutes, multiplying that time with four would not meet the set requirement not adding more than 30 minutes. However, the refueling rate is mainly limited by the fact that static electricity can build up due to high friction and a spark can be caused resulting in a fire or explosion. Since ammonia is not a flammable gas the refuel rate can be raised resulting in meeting the requirement.

9.2.2. Leakages

All ammonia spills must be reported to Airport Emergency Services, regardless of size or location, so that the spill may be dealt with safely and swiftly. A little drop of liquid ammonia will rapidly evaporate, and the resulting gas cloud will almost certainly be irritating. An ammonia cloud and a liquid ammonia pool might arise from a larger spill. The ammonia will evaporate if it is in liquid form. The heat input from the environment determines the rate of evaporation. The massive vapour cloud has the potential to be hazardous. The cloud will expand and evaporate over time, depending on the weather conditions. A large area downwind might be affected.¹¹ Droplets of extremely cold liquid or exposure to an extremely cold gas may be encountered by emergency personnel working near a breach. Breathing apparatus, a full set of chemical protective clothing, and outside cold-proof protection are all required. In these circumstances, it is hard to make a comprehensive statement regarding the proper safety requirements. When an incident occurs, it is necessary to conduct an analysis.¹²

9.2.3. Fires

Although ammonia gas is flammable, it is extremely difficult to ignite. Experiments and accident observations have revealed that when ammonia is released into the open air, the $\text{NH}_3\text{--O}_2$ combination is typically beyond the flammability limits. As a result, the risk of a fire or explosion outside of structures from an ammonia-air mixture is typically low. However, in limited regions, the situation may be

¹¹[https://www.skyharbor.com/docs/default-source/default-document-library/fuel-handlers-study-guide-\(1\).pdf?](https://www.skyharbor.com/docs/default-source/default-document-library/fuel-handlers-study-guide-(1).pdf?)

¹²https://cefic.org/app/uploads/2018/12/Transporting-Ammonia_ByRail-by-EFMA-2007-GUIDELINES-_ROAD-SUBSTANCE.pdf

different, and the risk of explosion should not be underestimated. Under EU and UN rules, ammonia is not classified as a flammable gas. Under the Global Harmonization System, however, it will be classified as a flammable gas. Ammonia auto-ignites at around 650 °C. The minimum ignition energy by spark is 680 MJ, which is 10,000 times more than hydrogen ignition energy and 1000 times higher than natural gas ignition energy. When ammonia and air combinations within the limitations (16-27 %) are burned in a closed environment, they may explode. In case of fire, the fire extinguishers that use foam, dry powder or CO₂ must be used. It is necessary to use a self-contained breathing device as well as comprehensive protective clothes. Water sprays must also be used to cool fire-exposed items and buildings, disperse vapours, and protect workers, and water must not be sprayed into liquid ammonia. Another requirement that has to be addressed is the evacuation time in case of fire or other emergency. Since the cabin of the A320-NH3 did not undergo a redesign and the amount of passengers decreased compared to the A320neo, the passenger evacuation time of 90 seconds will not be affected by the ammonia storage.

9.2.4. Noise emissions

The noise pollution is big topic in aviation. A report by the International Civil Aviation Organization (ICAO) found that airplanes are 75% quieter than they were in the 1960s. The main reasons for this fact are the modifications that were achieved in the propulsion system - mainly the invention of little honeycomb-shaped mesh pieces fitted on engines to absorb sound, so called liners and high-bypass turbofan engines, which are both quieter and more fuel-efficient, were developed. In this project the propulsion system will mainly be driven by hydrogen. This will have positive effect on the noise emissions since hydrogen turbofan engines produce significantly less noise pollution compared to kerosene turbofan engines.¹³

Another factor responsible for noise emissions is the aerodynamic noise. The higher the surface area, the higher the aerodynamic noise. Biggest part of these is created during the approach and take-off by landing gear and high-lift devices. Only minor changes will be made in these fields and therefore no significant noise pollution increase is expected compared to the A320neo.

Other component that might have a role is a cracking system for converting ammonia to hydrogen which is unique to this aircraft. The high pressure and temperature of the gasses in the reactor may produce loud sounds and possibly vibrations. The exact estimation of the noise emissions for A320-NH3 must be determined in the future and lies outside the scope of this project. After the total design has been iterated, multiple software are used in aerospace for estimation of the precise noise estimations. An example of such outputs can be seen in Figure 9.7¹⁴



Figure 9.7: Noise estimations visualized using 3DExperience software¹⁵

¹³<https://ec.europa.eu/research-and-innovation/en/horizon-magazine/quiet-and-green-why-hydrogen-planes-could-be-future-aviation>, accessed 21/06/2022.

¹⁴<https://events.3ds.com/how-to-reduce-aircraft-noise-emissions>, accessed 21/06/2022.

Material & Manufacturing

10.1. Materials

This section will provide the material composition of different systems and give the different characteristics of these materials. It will first look in the material choice for the structures and then the materials for the fuel storage tanks are explained in subsection 10.1.2.

10.1.1. Material structures

The structures have to sustain the most loads, yet still be lightweight. Therefore, it is important to choose a material with good specific properties. Composites do have very good specific properties. However, composites also have a couple of drawbacks. Firstly, composites are very expensive compared to metals. And because the A320-NH3 has new systems and thus will be more expensive compared to the A320neo, trade-offs need to be made to reduce the cost. Furthermore, composites are harder to manufacture and maintain than metals, and because the A320-NH3 should be easy to incorporate into the current airport infrastructure, it is chosen to use an aluminium alloy for the structures.

The alloy chosen is the: 'Al 7249'. This is an aluminium alloy that consists for 88.5% of Al, 8.2% of Zn, 2% of Mg and 1.3% of Cu. The material properties of the alloy can be seen in Table 10.1, compared with the aluminium alloy that the original A320neo uses for the structures. While the specific stiffness and shear stiffness is slightly higher for the 8090 alloy, the specific yield and tensile strengths are much higher for the 7249 alloy and that's why the 7249 alloy is chosen.

Table 10.1: Material characteristics¹ [15].

Property	Aluminium 7249	Aluminium 8090
Density [kg m^{-3}]	2790	2540
Young's modulus [GPa]	73.6	77.4
Shear modulus [GPa]	27.3	31.8
Yield strength [MPa]	469	211
Ultimate strength [MPa]	524	343
Specific stiffness [MN m kg^{-1}]	26.3	30.5
Specific shear stiffness [MN m kg^{-1}]	9.8	12.5
Specific yield strength [kN m kg^{-1}]	168	83.1
Specific tensile strength [kN m kg^{-1}]	188	135

The aircraft is assumed to fly 10.8 hours a day for 25 years, as mentioned in subsection 11.3.2. This is with maintenance taken into consideration. This then gives an average of 4 flights per day. So the total life cycles of the aircraft will be $4 \cdot 365 \cdot 25 = 36500$ life cycles. However, a conventional aircraft has kerosene in the fuel tank, and this is not heated nor cooled where as the A320-NH3 has liquid ammonia in the fuel tanks and therefore has to be cooled to a minimum of -33°C while the outside of the wing gets warmed up because of the friction. Therefore, the assumption is made that every flight amounts to two flight cycles, and thus the total flight cycles the aircraft has to sustain is 73000 life cycles. In Figure 10.1, it can be seen that with 73000 cycles, the maximum yield stress is 282 MPa.

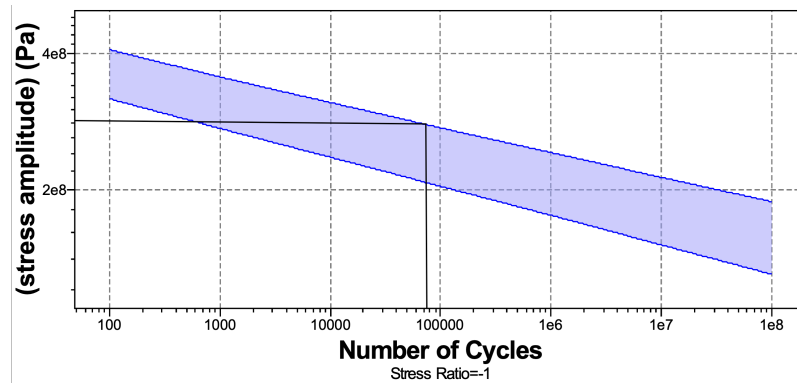


Figure 10.1: Fatigue strength model ² [15].

10.1.2. Material fuel tank

The fuel tanks are designed to be an integral part of the wing and the auxiliary tanks to be conformal with the fuselage. It was therefore chosen to design the tank structure with the same material as the wing skin. Such a choice eliminates problems arising from thermal expansion coefficient differences, which would be significant due to the high expected temperature differences. Additionally, the tanks will be internally insulated with polyurethane spray on foam compatible with liquid ammonia.

10.2. Manufacturing

As with every aircraft, the trinity concept has to be taken into consideration. These are: design, material and manufacturing. It is about taken into account that not all designs are possible if it is impossible to manufacture or there is not a material that is able to withstand the given loads or vice versa. The design and material choice for the wing and structures are explained in chapter 5 above. In this section, the manufacturing of the aircraft will be explained. Firstly, individual parts for the structure of the wing box, for example the outer casing and stringers, are described in subsection 10.2.1. Next, the assembly & rivet spacing is calculated in subsection 10.2.2. Finally, the production plan with the different assemblies is described in subsection 10.2.3

10.2.1. Parts

Firstly, the outer casing has to be manufactured. The most cost effective and fastest way is to create the inner hole with punching. However, the length of each section of the outer case is around 1 m which makes it very hard to punch. Therefore, electrical-discharge wire cutting is used. In this process, metals are eroded by spark discharges. This method has a very high accuracy (of 0.01 mm can be achieved) and is relatively inexpensive compared to other chip separating processes. Moreover, no mechanical energy is involved so properties such as hardness, strength and toughness are not of influence for the removal rate. The only drawback is that the process is slow compared to other manufacturing methods. While the equipment cost are high relatively to other processes, the labour and raw material costs are low. This means that a big upfront investment is needed but with the making of each new aircraft, investment will be worth it as the variable costs are low.

Next, from the material of the inner hole, the stringers can be manufactured to minimize the wasted material. For this, rubber forming is used. The principal is that a sheet is laying on a die and the rubber press presses on it and gives the shape of the stringers. The advantages are that it is cheap, only one product tool is required and due to the soft rubber tool, surfaces of the stringers are not damaged. However, the drawback is that the required press force is large and thus the soft tool wears out over time, but because the soft tool is not expensive, this is seen as a minor liability.

Next, the ribs are manufactured with the process of milling. Face milling is used here as it gives a relatively high accuracy while the process is very easy to accomplish. The cost are medium as the tool need to be replaced more often compared to other processes, however, there are not many ribs

in the wing box and the ribs are thicker compared to the outer casing, thus the face milling process is ideal here fore. Moreover, face milling is widely used in the aerospace industry, thus there are plenty of experienced workers for this manufacturing process and thus reduces the labour costs. For the holes in the ribs, drilling is used as this is the most common used process to make holes.

Moreover, the cracking system needs to be manufactured. As explained in section 6.2, the cracking system is a new of a kind, high end device with much complexity involved in it. Therefore, the best manufacturing process is to use additive manufacturing. Additive manufacturing (also known as 3D printing) is a relative new process. Because the cracking system is made of steel, an additive manufacturing process needs to be used that is compatible with metals. Therefore, selective laser melting is used. There is a basin with metal powder on it. A laser then heats up specific parts of the the powder, and the powder then melts and binds. Layer for layer is than the part created. The advantages here are that very complex parts can be made and no waste is made as the powder that is not bonded to the part, can be reused. Also, preliminary design can be made of thermoplastics to validate the design, and to see if the 3D printer is correctly outputting the CAD design, while no extra equipment is needed to be bought and with very low material costs. The disadvantages are that the process is slower than other processes and that it can be relatively more expensive compared to other processes if a lot of parts need to be manufactured. However, as can be seen in Figure 10.2, there is a trade-off in how much parts need to be manufactured and the complexity. And because the system is new and never been used before, it is chosen to make the trade-off for additive manufacturing.

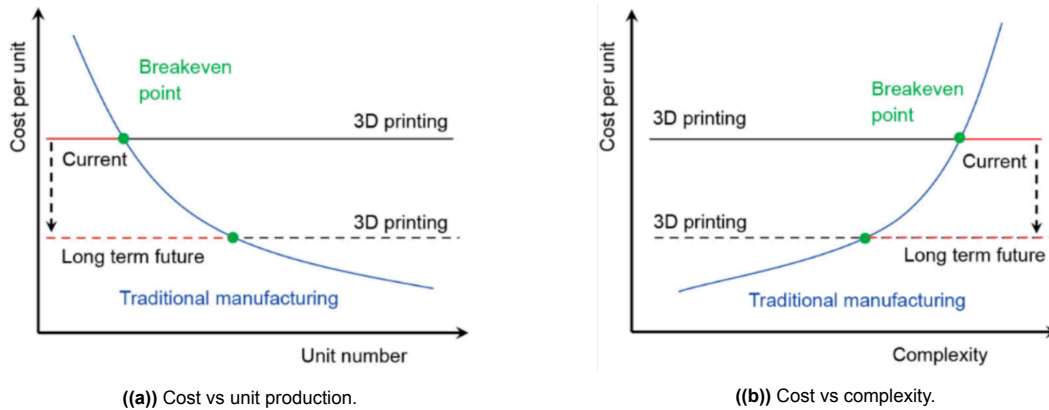


Figure 10.2: Cost vs unit production or complexity.

10.2.2. Assembly

In Equation 10.1 the maximum spacing for rivets is calculated as s is unknown and all other parameters are known. C is a constant that is dependent on the support on the edges. In Figure 10.3, the different values for the different supports are seen. It is chosen to go with line C and thus a value of 4, because it is simply supported and the $a/b = t/s$ is more than 1 %. The final rivet spacing will be 71.6 [mm]

$$\sigma_v = \frac{\pi^2 CE}{12(1 - \nu^2)} \left(\frac{t}{s} \right)^2 \quad (10.1)$$

10.2.3. Production Plan

The production of an aircraft is an essential element during the design phase since a good design still needs to be manufactured. The production line is organized as shown in Figure 10.4. First are the individual parts manufactured or ordered. Then the parts are assembled in sub assemblies and thereafter, all sub assemblies are put together to create the final aircraft. Finally, a layer of paint is painted over the fuselage for more durability and marketing for the airliner. It is opted to use modern production techniques. Furthermore, the production principle of lean manufacturing should be adhered to. 'Lean manufacturing is the dynamics, knowledge driven, and customer-focused process, through

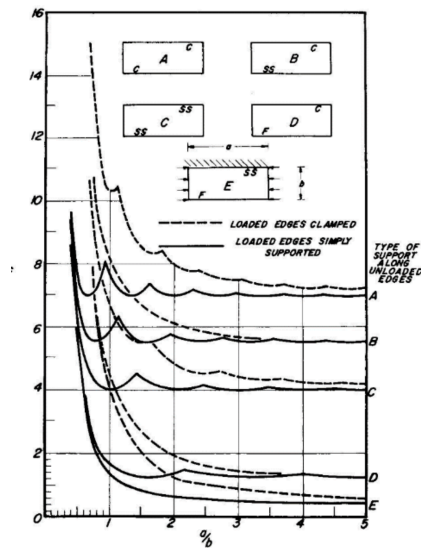


Figure 10.3: Buckling constants[39].

which all people in a defined enterprise continuously eliminate waste with the goal of creating value³. Therefore, lean manufacturing should minimize cost, waste and impact on the environment. Please note that several components are not manufactured by the company but ordered from an external party. Therefore, special attention should be given to this issue since these can impact the production process when delays occur.

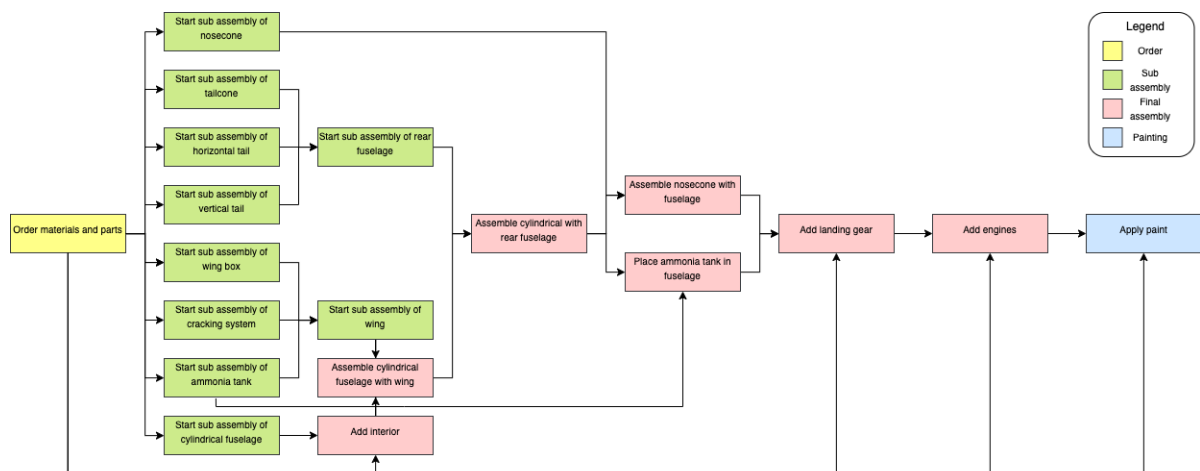


Figure 10.4: Production plan flow chart.

³<https://www.cips.org/knowledge/procurement-topics-and-skills/operations-management/lean-manufacturing/>

Technical Resource Allocation & Budget Breakdown

11.1. Technical Budget Allocation

During the initial phases of designing an aircraft, certain technical performance parameters are estimated and can be assumed to grow or change as the project progresses. In order to prevent these changes from growing out of control, it is useful to give them a certain limiting value. In this section, the resource budgets for range, take-off and fuel mass, fuel capacity, payload mass, take-off length are determined using reference aircraft similar to the A320neo. A budget for the unit price of the A320-NH3 is also allocated. The values for the technical resources are determined by either the mean or the median of these resources of the reference aircraft. The median is considered for resources that are less prone to outlier values in the reference aircraft data, while the mean is used for more conservative values for the resources. Following this, the margins on these budgets are also allocated - they ensure that the budgets are not overshoot by an irreversible extent and that rectification still possible. Note that these margins are only estimates for how much the resource items are expected to vary during the project and the adherence to these budgets shall be overseen by the risk manager.

The following technical items have been given a budget (summarised in Table 11.1):

1. **Design Range:** This budget follows from one of the user requirements and is set as a minimal value. The minimum range specified is 4000km, which is lower than the typical range of Airbus A320neo. This is reasonable, considering hydrogen is less energy dense.
2. **Fuel capacity:** This is an important resource to budget since the fuel used has a lower volumetric energy density than kerosene. It is calculated by multiplying the median fuel capacity by 2.5 to account for the larger volume of liquid Ammonia needed.
3. **Fuel Mass:** This is also an important parameter to budget due to a similar energy performance of liquid Ammonia with respect to mass, compared to that of kerosene. It is calculated by multiplying the Fuel capacity calculated earlier, by the density of liquid Ammonia of 0.674 kg l^{-1} . The resulting value is approximately twice the mass of the median fuel mass of the reference aircraft, which is as expected.
4. **Payload mass:** This parameter has a strong compounding effect on the aircraft sizing and weight estimations, particularly in the preliminary stages. For this reason, over-designing w.r.t to the payload mass is to be avoided. The minimum of the reference aircraft's maximum payload mass is used as the maximum payload mass for the aircraft being designed.
5. **Take-off mass:** This value was obtained by using the higher of the mean and median of the maximum take-off masses of reference aircraft; from which the zero fuel mass is calculated by subtracting the mean maximum fuel mass from it (assuming the aircraft is loaded for maximum fuel). This zero fuel mass is then multiplied by a factor of 1.2 to account for the mass of the ammonia cracking system. The maximum fuel mass for the A320-NH3 is then added to this to obtain the maximum take-off mass for the A320-NH3.
6. **Take-off length:** This parameter has a great influence on the sizing and designing of the wing and propulsion group in the early stages of design. This value is obtained from the mean of

the values of the reference aircraft and multiplied by a factor of 1.1 to account for the increased maximum take-off mass.

7. **Unit cost:** This refers to the price of a single completed aircraft and has been calculated from one of the user requirements, which has been set as a maximal value.

Table 11.1: Technical budget allocation based on reference aircraft data.

	A319neo	A320neo	A321neo	A319	A320	A321	MEDIAN	AVERAGE	Relative Diff [%]	A320 NH3
PERFORMANCE										
Range (km)	-	-	-	-	-	-	-	-	-	4000 km
Max take-off mass (tonnes)	75.50	79.00	97.00	75.50	78.00	93.50	78.50	83.08	5.84	117.11
Max fuel capacity (litres)	26,730.00	26,730.00	32,940.00	30,190.00	27,200.00	30,030.00	28,615.00	28,970.00	1.24	71,537.50
Max fuel mass (kg)	21,384.00	21,384.00	26,352.00	24,152.00	21,760.00	24,024.00	22,892.00	23,176.00	1.24	48,216.28
Max Payload mass (tonnes)	17.70	20.00	25.50	17.70	20.00	25.50	20.00	21.07	5.33	17.7
Takeoff length (m)	2,164.00	1,951.00	1,988.00	1,850.00	1,828.00	1,988.00	1,969.50	1,961.50	0.41	2,157.65
COST										
Unit Cost (million €)	-	95.60	-	-	-	-	-	-	-	109.94

11.1.1. Contingency management

With the technical resources allocated, contingency management has to be performed. These are margins, determined based on the phase of the project and uncertainty regarding technology relevant to the categories. The margins determined are presented as follows:

1. **Design Range:** A margin of 10% is used to allow for under-performance. This should be reasonable considering the early stage of the project, and the new concept of using ammonia as energy carrier for aircraft.
2. **Fuel capacity:** A margin of 15% is enforced due to the early stage of the design process and the uncertainty associated with the sizing regarding the new fuel. This should for example take into account the effect on engine efficiency caused by burning ammonia and hydrogen.
3. **Fuel mass:** Once again a margin of 15% is enforced due to the early stage in the design process and the uncertainty associated with the properties of ammonia.
4. **Payload mass:** A margin of 5% is enforced because large fluctuations in this parameter will have drastic effects on the design of the aircraft in later design changes. There is not much uncertainty about the payload mass that the aircraft is required to carry, because this is given as a requirement with a lenient range. However, considering the early stage of the design, this should be reasonable.
5. **Take-off mass:** A margin of 10% is enforced. The uncertainty caused by using ammonia on fuel mass also influences the take-off mass. This is of course because fuel mass is also part of take-off mass, and the mass of the cracking system also increases the uncertainty.
6. **Take-off length:** With an already conservative estimate for the take-off length, a margin of 7% is used to keep from excessive over-design of the aircraft for take-off.
7. **Unit cost:** A margin of 17% is enforced to account for design changes that will affect this price. There is a relatively large uncertainty concerning the development cost of a new aircraft design concept. However, the margin cannot be set too high to ensure that the design is economically feasible.

From all these margins assigned for contingency management, a table is generated in Table 11.2

Table 11.2: Contingency margins for technical resources.

	Range	Fuel capacity	Fuel mass	Payload mass	Take-off mass	Take-off length	Unit cost
Margin	10%	15%	15%	5%	10%	7%	17%

11.2. Cost Break-Down Structure

The requirement given for the development cost is that it should stay below € 5 billion. After studying the development costs of the A320neo it was estimated that the development costs will probably be lower than this. Of course this is only development costs, where production costs will also add to the total costs. Using the estimated sales in one year, which are around 160 aircraft, the total costs

until that point are about \$20.3 billion. An estimation of how these costs will be distributed was made. This distribution is not set in stone, if there is an overshoot in one department this may be used to compensate another department. Because of this reason it does not go to much into detail, as this would only add inaccuracies in the structure. The cost breakdown structure is given in Figure 11.1 .

11.3. Return on Investment

The return of investment (ROI) is the ratio of net income versus investment. More important for the companies is the break even point. This is the point where the total amount of revenues equals the total amount of costs. Both of these differ for the manufacturing company and the airline. The manufacturing company develops and produces the aircraft and subsequently sells it to the airline. The airline buys the aircraft from the manufacturing company and flies passengers as customers to make revenue. The ROI of the manufacturing company is determined in subsection 11.3.1 and that of the airline in subsection 11.3.2.

11.3.1. Manufacturing company

As manufacturing company, different costs come into place. First, during the development phase of the project, the development costs come into place. In the requirements it is stated that these should be no more than 150% of the development costs of the A320neo. What should also be considered is the cost of production of the aircraft. A limit on these costs was also placed in the requirements; the production costs should not be more than 115% of the A320neo production costs. Considering these extra costs, it was decided that the aircraft price tag will also be about 115% of that of the A320neo. The following estimations, considering inflation over the past couple of years ¹ , were made considering these numbers:

- **Estimated development costs:** The A320neo is an aircraft that is based on the A320ceo. Like stated previously, the main differences are the sharklets added and the use of different engines. Therefore the development costs were quite low compared to other aircraft designs. The A320-NH3 will have a lot of different aspects compared to other aircraft. This will require new aircraft systems and therefore the development costs will be much higher. The development costs are estimated to be around **\$5 billion**.
- **Estimated production price:** The production costs of the aircraft consists of everything in the manufacturing phase. Both part manufacturing and line assembly. For most aircraft in the A320 family the production of one aircraft was around \$100 million [42] . The A320-NH3 will have more complex systems integrated in the aircraft and may require extra reinforcements in order support these systems. Taking into account this additional complexity during the manufacturing process the estimated production price is estimated to be around **\$115 million**.
- **Estimated selling price:** The price tag of the aircraft has to be determined and scaled in such a way that profit can be made after selling a reasonable amount of products. As depicted in the previous point, the production costs are estimated to be around 15% higher than those of the A320neo. The average price tag of the A320neo is lower than the production costs of the A320-NH3. Because of this, the selling price is required to rise as well. The same proportion is taken as for the production costs and with this ratio the most reasonable selling price should be about **\$126.5 million** [60].

With the estimated costs and revenues, the return of investment can be determined. This return of investment graph is plotted in Figure 11.2. On the x-axis it shows the number of aircraft sold and on the y-axis the amount of money in millions of USD (\$) is given.

¹<https://www.usinflationcalculator.com/>, accessed 11-05-2022

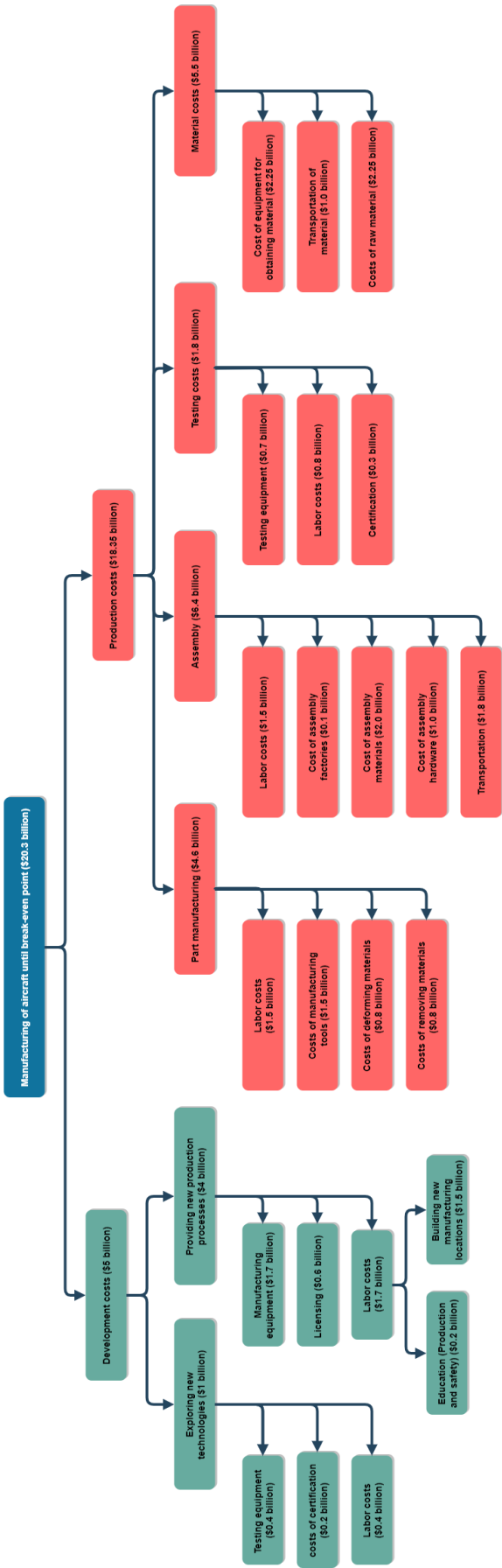


Figure 11.1: Cost breakdown structure.

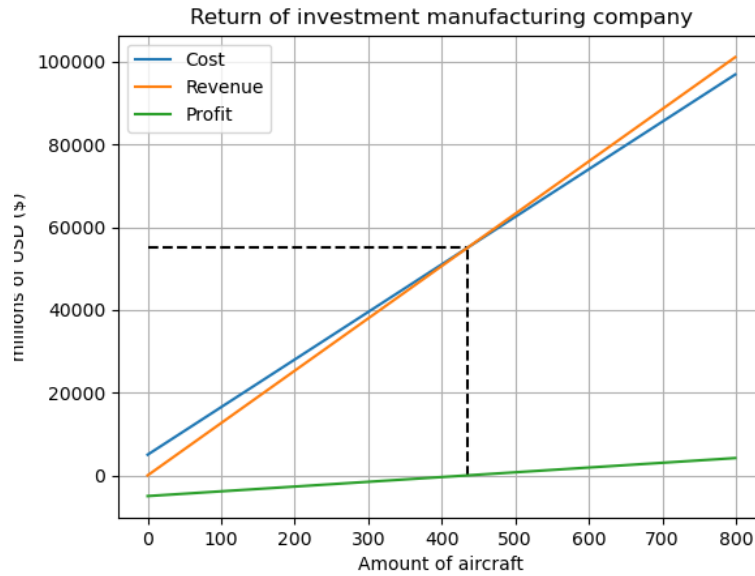


Figure 11.2: Return of investment for the manufacturing company.

What can be seen from the graph is that the break-even point, the location at which all revenues equal all costs, occurs after selling 430 aircraft. This is the point at which the company will start making profit. The total costs made at this point are estimated to be around \$56 billion. Furthermore the profit is plotted as well. The profit at any point can be estimated using Equation 11.1.

$$Profit(millionUSD\$) = AC_{price} \cdot n_{ac,sold} - AC_{cost,p} \cdot n_{ac,sold} - AC_{cost,d} \quad (11.1)$$

Table 11.3: Variables used in Equation 11.1

Definition	Symbol	Value
Aircraft price tag (selling price)	AC_{price}	\$126.5 million
Number of aircraft sold	$n_{ac,sold}$	Variable
Production costs of the aircraft	$AC_{cost,p}$	\$115 million
Development cost of the aircraft	$AC_{cost,d}$	\$5 billion

11.3.2. Airline

For the airline the return of investment point can also be calculated. The airline has a lot of different costs, sometimes divided into maintenance costs and operational costs. These costs depend on the amount of hours flown by the aircraft and sometimes depend on the amount of passengers as well. Therefore the maintenance costs are taken per flight hour and the operational costs are taken per passenger per flight hour ². To determine the return of investment in amount of years, first the amount of flight hours per years needs to be determined [38].

The aircraft will make short to medium range flights throughout the entire day. It is based on a aircraft that is very commonly used by a lot of airlines. The aircraft are assumed to be able to fly between 06.00 and 00.00 and therefore be in service 18 hours a day. The turnaround time needs to be accounted for. Subtracting the turnaround time and assuming a flight is around one and a half hours, we reach a total of 10.8 hours a day. In reality the average flight will very likely be longer than 1.5 hour but this difference can be used to account for maintenance of the aircraft. Throughout the year this means the aircraft will be in service for 3942 hours. This can be used to make the following estimations for the client:

²<https://www.aircraftcostcalculator.com/AircraftOperatingCosts/151/Airbus+320#:~:text=Based%20on%20450%20annual%20owner,down%20to%20%247%2C315.15%20per%20hour.,12-05-2022>

- **Cost of product:** As explained in the previous chapter, the A320-NH3 will have a price tag of **\$ 126.5 million**. This will be the cost per product for the airline. These costs are made on one occasion.
- **Cost of maintenance:** The maintenance costs are the costs of maintenance that has to be done on the aircraft for every hour the aircraft flies. This could be reparations, repainting, refurbishing or replacing items. These maintenance costs for the A320 family add up to about **\$ 509 per flight hour**³.
- **Operational costs:** The operational costs is a big part of the costs consisting of a lot of different categories, all included in the air operations. The operational costs include fuel cost, crew cost, landing fees, non-flying costs and insurance. In total this adds up to around \$ 35 per flight hour per passenger. However, this is the case for kerosene. Taking into account the cheaper price of ammonia compared to kerosene, as well as the difference in energy density between the two fuels, a new operating cost was estimated⁴. This cost was estimated to be around **\$ 36 per flight hour per passenger** [49].
- **Revenue from tickets:** The tickets sold by the airline are the way to make revenue. The ticket is not set in stone and can vary depending on the market. A reasonable price could be **\$ 60 per flight hour**. This means that for every hour a flight takes, \$ 60 will be asked for the ticket. As an example: a flight from Amsterdam to Lisbon (approximately 3 hours) would cost \$ 180 for a ticket.

With the estimated costs and revenues for the airline, the return of investment can be determined. This return of investment is preliminary and is taken for a ticket price of \$60 per flight hour and a occupancy rate of 120 passengers. The capacity will be at least 150 passengers, but the aircraft is rarely fully filled. Using this the plot in Figure 11.3 could be constructed.

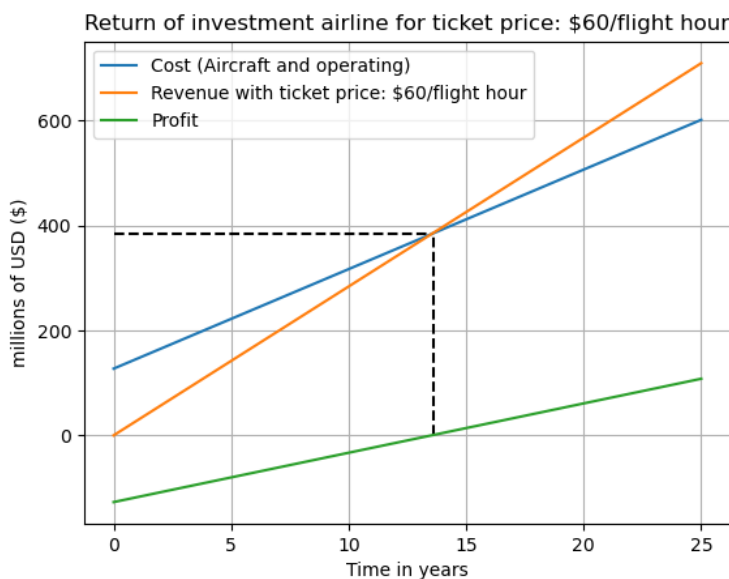


Figure 11.3: Return of investment for the airline, considering 120 passengers and a ticket price of \$60/flight hour.

³https://aviaforum.ams3.cdn.digitaloceanspaces.com/data/attachment-files/2009/03/381226_b979700333d46620bfa45972df7fc637.pdf, 11-05-2022

⁴https://www.globalpetrolprices.com/kerosene_prices/, 30-05-2022

From this plot it can be seen that for this passenger occupation and ticket price the break-even point would occur after about 13.5 years. It is estimated that the aircraft will be able to last an average of 25 years [32], taking into account that maintenance is performed every once in a while. This would mean that the aircraft will make profit for around 11 years for the example case. Of course the case could differ as there are multiple variables taken into account. Figure 11.4 shows the break-even point in years for the ticket prices asked by the airline. It shows this for different amounts of passengers. The reason for this is that the final amount of passengers able to fit in the aircraft is not yet certain and not every flight will be fully booked.

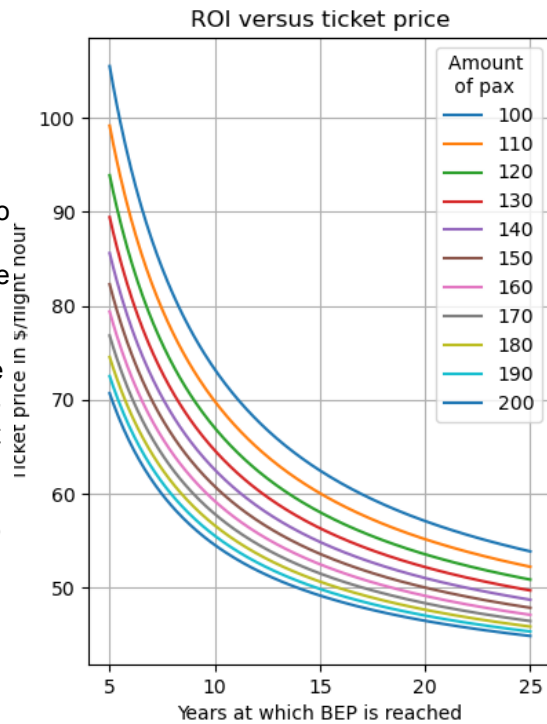


Figure 11.4: Amount of years at which ROI is reached for different ticket prices, assuming sold out flights.

The profit of course also depends on this ticket price. The profit of the airline company, assuming an average occupation of n_{pax} , average ticket price per flight hour of P_t , after yrs amount of years, is given in Equation 11.2.

$$Profit(millionUSD\$) = ((hr_{peryr} \cdot n_{pax} \cdot yrs \cdot P_t) - (AC_{prize} + AC_{cost,m} \cdot hr_{peryr} \cdot yrs + AC_{cost,o} \cdot n_{pax} \cdot hr_{peryr} \cdot yrs)) / 10^6 \quad (11.2)$$

Definition	Symbol	Value
Hours in service per year	hr_{peryr}	3942 hours
Number of passengers (average)	n_{pax}	120
Time in years	yrs	Variable
Ticket price per flight hour	P_t	Variable
Prize of aircraft	AC_{prize}	\$126.5 million
Maintenance cost of aircraft per flight hour	$AC_{cost,m}$	\$509
Operating cost of aircraft per flight hour per passenger	$AC_{cost,o}$	\$36

Table 11.4: Variables used in Equation 11.2.

Verification and Validation Procedures

In this chapter, the verification and validation (V&V) procedure is treated. At first, the program used is divided into parts, which should be verified and validated individually. Then, different verification and validation methods are stated. Finally the V&V plan is illustrated in Table 12.1.

12.1. Design program

In order to verify and validate the program used to design and determine the properties of the concept designs, the program is divided into different functions. At first, these functions will be verified and validated individually using methods described below after which the total code will be treated. The program is divided in the following main functions:

- Weight iteration
- Design update
- Structure
- Engine performance
- Emissions
- Performance

All of the following verification and validation methods are or will be performed on each part of the code. For the parts of the code which are iterative the discretization error has been provided. The verification procedures have been performed as explained, changing certain inputs and checking every block of code. The validation was performed by comparing the results to that of the A320neo. The differences in results should then be logical. For instance: the A320 ammonia will have a higher MTOW, this can be explained by the difference in required fuel. Only the different procedures performed are explained in the different sections.

12.2. Verification

Verification is the process of proving compliance with design solutions specifications and predictive documents. This can be done using several different methods, some of which will be used for this code. The verification methods are described in the ensuing subsections.

12.2.1. Code verification

At first, code verification is performed. Here, the consistency in units should be checked. Furthermore, the input variables should be verified and whether they correspond to the regular formulae inputs. The code is also checked for basic code errors. There are several parts of code that need to be checked using this method. These checks will be performed for all of the formulas present in the code. For example: if the formula is $F = m \cdot a$, then the unit should be Newton ($\text{kg} \cdot \text{m} \cdot \text{s}^{-2}$), this means that the units of the variables on the left hand side and right hand side of the equation should also yield Newton.

12.2.2. Unit tests

To verify individual elements of the code, unit tests are used. This is done to check if the elements perform the intended calculations in the right way. This includes checking whether the calculations

regarding physics are performed in the way they are supposed to be. Other calculations should be checked as well if they serve the intended purpose. Unit tests will be performed according to prescribed procedures stated below.

- Checking the formulae according to literature.
- Checking the calculation for at least 2 input variables.
- Comparing the calculation with calculations performed by hand.

12.2.3. Discretization Error

The refinement of a program has an influence on its accuracy. Therefore, a discretization error analysis should be performed in order to quantify the accuracy of the program. In this analysis, the program runs for different refinements and the results will be compared. During the simulation of the flight used for class 1 weight estimation discretization is used. A certain δt in seconds is considered to determine the mass flow of the fuel on different moments in time and eventually, the total fuel used and MTOW. For the verification on discretization error, graphs will be constructed with on the x-axis the refinement (δt) and on the y-axis the amount of fuel used during the flight, maximum take off thrust and MTOW.

12.2.4. Extreme values

In the extreme value test, extreme values are used as input for the program after which the results of the program will be analysed. These tests are performed to find program errors, which will not be noticed under normal circumstances. Tests that will be performed are putting efficiency numbers to zero and making the OEW very high, among other things. The results will be provided in a table and compared to expected results. For all of the rows in the table, the expected result should be similar to the model result, else there is something wrong in the code. If these extreme inputs are outside of the input range, no rational results will be yielded.

12.3. Validation

Validation is the process of proofing that the product accomplishes the intended purpose based on stakeholder expectations. This will mostly be done by comparing the results to actual aircraft data. For requirements which are not related to aircraft design, the results will be compared with literature. This is applicable to the emissions and the effect on climate change.

12.3.1. Weight Iteration

To validate the weight iteration, both the class 2 as the class 1 weight estimation will be validated individually as they require different approaches. For the class 2 weight estimation, aircraft dimensions of different aircraft serve as an input in the code. In this estimation, the different dimensions are used to determine aircraft parts weights, which will be summed up to get the OEW. Then, by comparing the obtained OEW with the actual OEW, the accuracy of the estimation can be determined and the model can be validated.

Then, class 1, where the MTOW is determined is validated. In this estimation, the OEW, payload weight and the amount of fuel used for the design range are added up to get the MTOW. As the OEW payload weight are already given, the amount of fuel used is the only thing which is treated. The amount of fuel used is a function of the fuel mass flow, which is determined the amount of thrust needed and the engine performance.

To validate the engine performance, the performance of different engines will be simulated and compared to the actual performance. This includes an analysis on maximum thrust and specific mass flow under the different flight conditions and velocities experienced during the simulation. Then, to validate the thrust required, the thrust available is not taken directly into account. Instead, the mass flow is determined using the product of the thrust and the SFC. Then, the obtained mass flow will be validated in a comparison with literature data about the mass flow of the A320neo.

12.3.2. Sizing

For the validation of the aircraft sizing code, the data procession used to come up with the scaling factors will be investigated. Underneath the different procedures used are stated.

- Loading diagram
- Scissor plot

From the loading diagram, the cg range will be determined. To validate these results, an analytical solution will be compared to the result of the code. Furthermore, an existing aircraft will serve as an input for the code and there will be checked whether the cg range obtained by the code is actually similar to the real cg range got from the aircraft data. For the scissor plot, real aircraft data will serve as an input and the obtained horizontal tail area to wing area ratio wing be compared with the actual ratio to see if scissor plot actually shows that the aircraft is stable.”

12.3.3. Structures

The structures of an aircraft is one of the most important parts, because, if the structure of the wing or the structure of the fuselage breaks, all occupants will die. Therefore, it is very important to verify and validate the structures. This is done through multiple methods. First, the loading is verified in subsection 12.3.3. Unfortunately, there will be no validation for the structures. For other properties, the characteristics can be found for the A320neo or similar aircraft, but the structures are all classified. It was planned to do a verification with the help of a finite element method, however, time proved to be too much of a burden.

Unit tests structures

For verifying the structures, it is important that the physical model is correct and verified. As mentioned in subsection 5.7.3, the loadings are, the lift, the weight of the wing and fuel, and the weight of the engine. The forces are calculated at each point of the chord, so this will create an array. The first verification check is to see if the forces in the array will be higher with every step. For the midterm report, it was not seen that this was wrong because the numbers were very close to each other and thus could not be seen in the graph that there was an downwards trend. Therefore, after this mistake, it was seemed necessary to check every minor detail. For the weight of the wing and fuel, the same verification was done. Lastly, the total lift perpendicular on the wing should be slightly more than the half the weight of the total aircraft, as the wing has a dihedral angle, and thus, some lift force is 'lost' to the sideways direction.

Furthermore, the shear forces diagram and moment diagram had to be verified. For here, the shear force diagram need to start at zero as the wingtip is not clamped and thus experience no internal shear and moment, only deflection. Likewise, the final shear force needs to equal half the weight of the total aircraft. Also, there has to be a spike downwards in the internal shear force diagram because of the point load of the engine. Moreover, the moment diagram as well has to start from zero. And because the shear value will always be positive, the moment diagram has to increase from every step. This can all be seen in Figure 5.15(b). A final check has been done to see if the end value of the internal moment is less than Equation 12.1. Equation 12.1 gives the biggest moment if the lift was equally distributed over the wing, but because the lift is bigger closer to the root chord, the final moment also needs to be less than that.

$$M = L \cdot \frac{b}{2} \cdot \frac{b}{4} \quad (12.1)$$

Next, the moment of inertia for every part is tested. This is done with comparing the calculations with hand calculations and with the use of online tools¹. And finally, also the ultimate bending stress is compared with hand calculations and with online tools².

12.4. Verification and Validation plan

For the python code, a verification and validation plan is constructed, which is shown in Table 12.1. As can be seen in the table, the code is divided into several modules, which should be verified and validated individually. For each module, a module test, extreme value test, validation strategy and if applicable, a discretization error test is constructed. Unit tests are not present in this strategy as the unit

¹<https://skyciv.com/free-moment-of-inertia-calculator/> (31-05-2022)

²<https://skyciv.com/free-moment-of-inertia-calculator/> (31-05-2022)

tests are performed on a lower scale (These are parts of the modules). The unit tests will be performed according to the prescribed guidelines stated in Table 12.1.

Table 12.1: Verification and validation table.

Performance				
Part of code	Verification			Validation
	Module test	Extreme values	Discretization error	
Climb performance	Plot the D-V curve and compare with other plots. Plot CL-CD and check with the actual CL-CD plot.	Input T=0, Pa should be horizontal. Input S=0, code should not yield a plot. Input CL/CD=0, range should be 0 at every point.	-	Compare the maximum power (where the lines cross) with that of the A320neo.
Payload-Range	Draw all three parts of the payload range using calculations by hand, compare payload-range diagram.	Change fuel fraction at every stage to infinity. The range for that point should be infinite while the other points do not change.	-	Compare the ranges with the ranges stated in the requirement (e.g design range).
Maneuver	Print velocities and check if fractions make sense. Check the max load factors in diagram with CS25. Compare order of magnitude compared to gust diagram.	Change S=0, the manoeuvre diagram should be flat. Set Vapproach=0. The top of manoeuvre diagram should be a square.	-	Validate using CS25 for the load factors and comparing all of the velocities with the velocities of the a320 neo.
Gust	Print velocities and check if fractions make sense. Check the max load factors in diagram with CS25. Compare order of magnitude compared to manoeuvre diagram.	Set Vb=0, left side of the diagram should be flat, not pointy. Set Vc=0, left side should have two points going back to zero at the highest load factor.	-	Validate using cs25 for the load factors and comparing all of the velocities with the velocities of the a320 neo.
Financial management				
Part of code	Verification			Validation
	Module test	Extreme values	Discretization error	
Return of investment	Change price of aircraft, check whether profits go up/down. Check the linearity of the system, some lines should start at 0, others shouldn't.	Set cost=0, graph should show revenue equal to profit. Set revenue>infinity, the break-even point should be at start of graph.	-	Validate using sources about ticket prices, prices for planes, production costs and operational costs.
BEP vs ticket price	Check when break even point is reached with same ticket price as before. Change the year span to millions, the lines should all converge to the costs/pax/flight hour.	Change passengers to zero, BEP should never be reached.	-	Check regular ticket prices and check whether the plot is reasonable.
Preliminary sizing				
Part of code	Verification			Validation
	Module test	Extreme values	Discretization error	
CG OEW	Print all separate c.g. locations and check the logic. Total c.g. OEW should be in front of main gear	Change one weight component to zero, the c.g. should change. Change one weight component towards infinity. The c.g. should converge to the c.g. of that weight component.	-	The c.g. should lie in front of the main landing gear. The cg should lie somewhere on the MAC.
Loading diagram	Check all of the loading block sizes separately. Check all of the loading blocks weight. Check MTOW and OEW in the loading diagram.	Set the fuel weight=0, this should not create the last added weight. Set number of rows>infinity, the cg should go to -infinity*Mac.	-	The cg range shall lie within the MAC of the wing. The most aft cg shall not lie behind the main landing gear. Furthermore, the MTOW should be compared to other aircraft and data computed by other parts of the code.
Flight performance	Compare all of the results with calculations performed by hand.	Change Vmax=0, the code should not yield any result.	-	Scale the max power with the weight and compare with a320neo.
ISA calculator	Compare with temperature, pressure and density computations with online data at certain altitudes.	Set height to infinity, the density, temperature and pressure should be 0. Set h=0, ISA conditions should appear.	-	Compare with real data.

Aircraft sizing				
Part of code	Verification			Validation
	Module test	Extreme values	Discretization error	
Class 2 weight estimation	Use the inputs from the A320neo and determine analytically the OEW. Then, the analytical result and the result of the python code will be compared.	Input MTOW = 0, OEW should drop. Input b = 0, OEW should drop. Input S=0, OEW should go to infinity.	-	Insert the properties of at least two aircraft and compare the real OEW with the OEW obtained from the code.
Flight profile	Using the velocities and the flight phase data, the distance of the cruise phase will be determined analytically. Then, the analytical result and the result of the python code will be compared.	Input design range = 0km. The flight profile should still include the climb and descent phase, but won't include a cruise phase. Input cruise Mach = 0, program should be stuck in an infinite loop.	Plot a discretization error graph with on the x-axis the refinement (time step) and on the y-axis the maximum acceleration during the flight.	Plot the flight conditions against the distance and check whether the graphs make sense.
Thrust estimation	For every flight phase, the thrust during a random moment in time will be determined analytically and compared with the computed thrust of the program.	Cruise mach will be set to 1, the required thrust should go to infinity. The vertical speed during climb is set to 100m/s. The required thrust should be extremely high (more than 1000kN).	Plot a discretization error graph with on the x-axis the refinement (time step used in the flight profile) and on the y-axis the maximum thrust and the thrust at the beginning of the cruise phase.	Plot the thrust required against the distance and compare it with empirical data about the thrust required for the A320neo.
Fuel mass flow/ engine performance	Determine the SFC during take-off, climb and cruise analytically and compare the results with the SFC found by the code.	Use a LHV of 0, the SFC should go to infinity or the program should give an error due to too high numbers. Use a extremely high LHV, the SFC should be close to zero.	Plot a discretization error graph with on the x-axis the refinement (time step used in the flight profile) and on the y-axis the maximum fuel mass flow and the fuel mass flow at the beginning of the cruise phase.	The fuel mass flow depends in the L/D and the SFC. Compare the obtained L/D with the L/D of an existing aircraft. Then, compare the SFC of the engine with literature data. Finally, compare the determined fuel mass flow during cruise with real data.
Class 1 weight estimation	Using the found fuel used by the program, estimate the range using the Breguet range equation and compare this range with the design range used as input of the program.	Use a LHV of 0, the fuel required should go to infinity or the program should give an error due to too high numbers. Use a extremely high LHV, the MTOW should be close to: OEW+payload weight.	Plot a discretization error graph with on the x-axis the refinement (time step used in the flight profile) and on the y-axis the established MTOW.	Simulate the A320neo and compare the amount of fuel burnt during the flight with real data.
Wing sizing	By dividing the new MTOW by the obtained wing sizing, it will be checked if the wing loading stayed constant.	Input MTOW = 0, S should be 0 m ² .	-	Check whether the wing loading is constant between different existing aircraft to see if scaling the wing linearly with respect to the MTOW makes sense.
Engine sizing	Determine the max thrust of the engine analytically and check whether the engine is sized correctly.	Input max thrust to infinity, engine size should be infinity.	-	Compare the performance of the updated engine with real engines with similar properties.
Fuel Tank Sizing	Determine the tank sizing and location division analytically and compare with the result of the code.	Input amount of fuel = volume of the wing, fuel volume in additional tanks should be zero.	-	Compare the size of the obtained fuel tanks with the fuel tanks of the A320neo and look if the size makes sense.
Cracking system sizing	Determine analytically the required dimensions and weight of the cracking system and compare the results with the results of the code.	Input mass flow in the cracking system = 0, the weight and dimensions should be 0.	-	Compare the size and weight of the cracking system with data obtained from literature study. Furthermore, the scaling method used should be investigated if it is valid. This will be done using literature or by contacting professionals.
Horizontal Tail Sizing, Wing Placement	From the updated tail size and wing position, construct analytically a new scissor plot and loading diagram and check whether the aircraft is stable and controllable for every cg.	Make the cg range very high, the horizontal tail should be very big as well.	-	The size obtained from the code will be compared with the one of the A320neo to see if the horizontal tail is reasonably scaled.
Vertical tail sizing	Check whether the area of the vertical tail is actually linearly scaled with the thrust moment in case of an engine failure.	Input thrust moment = 0, vertical tail should be zero.	-	The size obtained from the code will be compared with the one of the A320neo to see if the vertical tail is reasonably scaled.
Class1 - Class2 weight iteration	Check whether the weights converge.	Set the LHV of the fuel to zero, the weights should diverge to infinity. Set the LHV of the fuel to a very high value, the MTOW should converge to OEW+payload weight.	Plot a discretization error graph with on the x-axis the refinement (time step used in the flight profile) and on the y-axis the converged MTOW, OEW and Fuel mass used.	Run the iteration using the A320neo as input and compare the result with the weights of the A320neo.
Design iteration	Check whether the weights and dimensions of the aircraft converge.	Set the LHV of the fuel to zero, the weights should diverge to infinity. Set the LHV of the fuel to a very high value, the MTOW should converge to OEW+payload weight.	Plot a discretization error graph with on the x-axis the refinement (time step used in the flight profile) and on the y-axis the converged MTOW, OEW and Fuel mass used.	Run the iteration using the A320 neo as input and compare the result with the weights of the A320neo.
Engine Heat Exchangers				
Part of code	Verification			Validation
	Module test	Extreme values	Discretization error	
Heat transfer coefficient estimation	-	Setting air density, velocity or specific heat to 0 should result in an error when calculating overall heat transfer coefficient for helical heat exchanger and 0.3 when calculating overall heat transfer coefficient for annular heat exchanger Setting viscosity of air to 0 should result in an error for Prandtl Number of air		Ensure the Reynolds Numbers, Prandtl Numbers and slenderness ratios calculated are within the validity limits for the formulae for Nusselt numbers

Reliability, Availability, Maintainability, and Safety (RAMS) characteristics

In a RAMS analysis the different aircraft components are analysed and their reliability, availability, maintainability and safety is determined. These values are given from a range of 1 to 5, 5 being the best and 1 being the worst. All of these numbers are estimated using different sources. The first four components, the fuselage, wings, empennage and landing gear will show quite some similarity to the A320neo. Therefore, the A320neo can be analysed for these components.

The reliability of the current A320neo is very high, considering that irregularities in the plane program are rare [13]. Furthermore the materials are all available, since the A320 series is one of the most common in air industry. The same holds for the maintainability. Lastly the safety of the A320neo is very high, this can be concluded from the extremely low hull-loss value compared to other aircraft. Therefore all of these have been given a 5 out of 5. What should be noted is that a lot of the values in the RAMS analysis are high. This is because the different components have been chosen in the trade-off such that they are reliable, available, maintainable and safe. When a RAMS analysis would be performed in a preliminary stage the scores would be much lower.

The fuel tank will be made from aluminium, using insulation around it to control the temperature. Since this is a process that is very common in the aerospace industry the reliability and availability have been set high. The maintainability is acceptable, but more difficult since the fuel tank will be placed within the structure and is therefore harder to reach. Since the process is used more often, but there are some ways it could fail, the safety is expected to be sufficient. The safety is a bit less than the fuel tanks filled with kerosene, because of the new technologies.

For the engines the reliability is not so high, the reason for this is that the design has not yet been developed and therefore the reliability is hard to indicate. The availability is low, the concept does not exist yet and therefore is not available. The concept is however very promising and interesting. The maintainability is sufficient: the engine only has some extra volume which is added between the turbines compared to other engines. The chance that this adds extra difficulties is low. Lastly the safety is sufficient as well. The engine should not bring any difficulties in the design but it has also never been tested. Therefore it is difficult to estimate the outcome. The on ground fuel system is very reliable.

Most of the techniques are already available but need to be redesigned for ammonia use. Furthermore active cooling should be used, this will not be unreliable. The availability for the on ground fueling system is very low. These fueling systems do not yet exist for ammonia and need to be created first, therefore they are not yet available. Despite this, the maintainability is very high. There are a lot of testing methods and ways to maintain systems using ammonia. Some of these protocols use echos or infrared radiation. Lastly, the safety is high as well. Ammonia is not flammable and does not decrease the safety compared to kerosene.

The transportation scores very well on all the RAMS criteria. The reason for this is that all of the systems already exist. Ammonia is used in a lot of other industries and the transportation is happening on a daily basis. One drawback is that the transportation infrastructure might need to be scaled up. Last is the safety, which could be an issue since ammonia brings some difficulties when it leaks. However,

all vehicles are designed to prevent leakage. No casualties have happened since the beginning of ammonia transportation.

The last property to discuss is the feed system, which also includes the cracking process. Since the process of thermal cracking will be used, this process is well established and therefore sufficiently reliable. The system exists and is currently available as well. It will be hard to maintain, since the system is extremely complex. Therefore, it will take time to repair broken parts and expertise is required. Despite this, it is still possible to do so. Lastly, the system is safe. No oxygen is required in the feed system and therefore there is very little risk of combustion. All of the analysis above led to Table 13.1.

Table 13.1: RAMS analysis

	Reliability (1-5)	Availability (1-5)	Maintainability (1-5)	Safety (1-5)
Fuselage	5	5	5	5
Wings	5	5	5	5
Empennage	5	5	5	5
Landing gear	5	5	5	5
Fuel tanks	5	5	4	4
Engines	2	1	4	3
On-ground fuel system	4	1	5	5
Transportation of fuel	5	5	5	5
Feed system	4	5	3	4

Sustainability

14.1. NO_x Emissions

14.1.1. A320-NH3 NO_x Emissions

Because the CO₂ emissions to the flight equal zero, does not indicate that the A320-NH3 is way more sustainable than the A320neo. Before coming to a conclusion about whether this is actually the case, different factors need to be considered. One of the substances being released into the air during the process of combusting hydrogen is NO_x. To determine the severity of these NO_x emissions the emission index should be obtained. This emission index can be calculated using a standard formula which provides the amount of NO_x emissions per kilogram of fuel (H₂). This formula is provided in Equation 14.1 [17]. The inputs for this formula are the pressure and temperature at the inlet of the combustion chamber. These values vary throughout the flight.

$$EINO_x = 33.2 \cdot \left(\frac{P_{t3}}{432.7}\right)^{0.4} \cdot e^{\left(\frac{(T_{t3}-459.67-1027.6)}{349.9}\right) + \left(\frac{6.29-6.30}{53.2}\right)} \left[\frac{g \text{ of } NO_x}{kg \text{ of } Fuel}\right] \quad (14.1)$$

Unfortunately, this formula only holds if the fuel is pure hydrogen. In the case of the A320-NH3 this is not the case. The energy carrier is ammonia, which needs to be cracked into hydrogen. Since this process is not 100% efficient, not all ammonia gets cracked into hydrogen. Therefore, this formula is not valid without first adjusting it. The factor with which the NO_x emissions actually decrease needs to be determined. Mathematically, this value is dependant on the mole fraction of the hydrogen. Therefore, multiple mole fractions are taken and the effect on the emission decrease is researched.

First, the NO_x parts per million in the combustion chamber needs to be determined. These normalized NO_x parts per millions for different hydrogen mole fractions can be determined using Equation 14.2 [48].

$$\bar{y} = \tanh(-0.4193 - 2.0342\tanh(A_1) - 1.8806\tanh(A_2)) \quad (14.2)$$

This formula has two inputs, variables A₁ and A₂. These two values are, like the emission index, dependant on both the the pressure and temperature at the inlet of the combustion chamber. Furthermore, they are dependant on the fuel to air ratio in the combustion chamber and the relative mole concentrations of NH₃, CH₄, H₂ and K_r. Lastly, the premixing ratio is taken into account (α). This results in the equations provided in Equation 14.3 and Equation 14.4 for A₁ and A₂ respectively [48].

$$A_1 = 0.3395 + 0.7475\bar{T} + 0.3464\bar{P} + 0.1009\bar{FAR} - 0.2243\bar{x}_{NH_3} - 0.0689\bar{x}_{CH_4} - 0.7085\bar{x}_{H_2} + 0.3227\bar{x}_{K_r} - 0.7275\alpha \quad (14.3)$$

$$A_2 = 0.6334 + 1.3347\bar{T} + 1.2288\bar{P} + 2.4950\bar{FAR} - 0.5151\bar{x}_{NH_3} - 2547\bar{x}_{CH_4} - 0.5928\bar{x}_{H_2} + 0.4136\bar{x}_{K_r} - 1.2509\alpha \quad (14.4)$$

After this, the normalized parts per million (ȳ) need to be de-normalized. By doing this the parts per million are determined. These parts per million can be rewritten to get the amount of NO_x in kg per kg of hydrogen. Again, this is done for multiple mole fractions. Using this, the relation between the mole fraction and the reduction of NO_x emissions on Equation 14.1 can be determined. This relation differs for every phase of the flight, but the general curve can be seen in Figure 14.1. The emission factor

displayed on the y-axis is a value in between 0 and 1 and this can be multiplied with the NO_x emission index. The mole fraction and the corresponding decrease in NO_x emissions is taken.

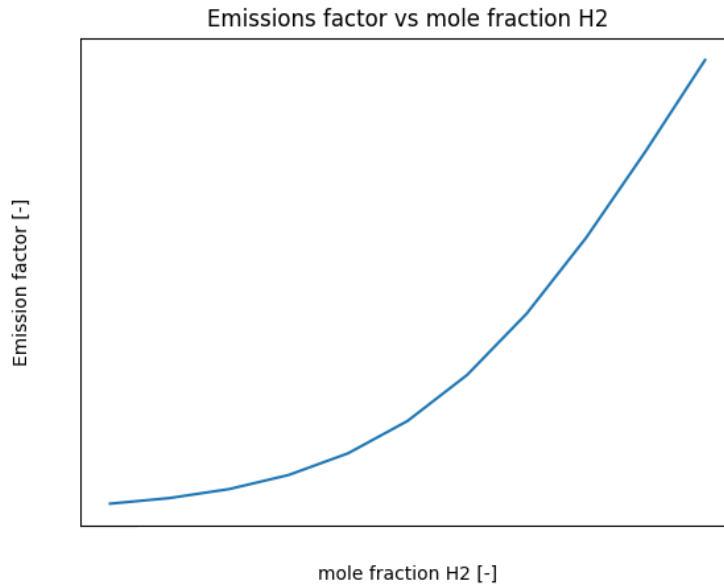


Figure 14.1: The relation between the mole fraction of NH₃/H₂ and emission factor

To further decrease the NO_x emissions, the use of an inter-turbine burner (ITB) in the engine is chosen. The findings of a study investigating the effect of the use of an ITB on the NO_x emissions is shown in Figure 14.2. This plot shows the relative change in NO_x emissions for different inter-turbine burner energy fractions both at the exit of the first combustor as well as at the exit of the ITB. The energy fraction corresponds to the energy fraction of the fuel added in the first combustion chamber to the fuel added in the ITB. What can be concluded is that the difference between the two occurs mostly at higher energy fractions for the ITB. At higher fractions the ITB shows promising results regarding the reduction of NO_x emissions. During the estimation of emissions, relation between the relative change of NO_x to the ITB energy fraction is also considered.

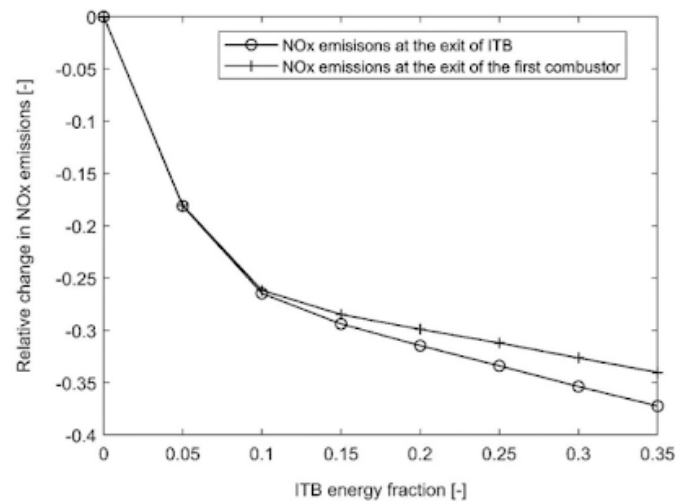


Fig. 16. Normalized reduction in NO_x emission as the energy provided by ITB increases, i.e., the rise in ITB energy fractions.

Figure 14.2: Normalized reduction in NO_x, emissions as the energy provided by ITB increases, i.e. the rise in ITB fractions [59].

After the estimation of the emission index of NO, the amount of NO_x emitted in kilograms when a kilogram of fuel is combusted, the total NO_x emitted during a whole flight is simulated.

Further Improvements for Simulating Emissions In this project, it was chosen to use literature studies to perform emissions analysis, while using reactor mechanism simulations in Cantera and CHEMKIN were also investigated.^{1 2} Cantera and CHEMKIN provide users the opportunity to simulate combustion with different reactor mechanisms and kinetic models. Users can specify parameters for each zone in the combustion chamber, such as the gas molar fractions, the equivalence ratio, the residence time, recirculation rate, geometrical dimensions of the reactors and more. To further improve the emission analysis, such simulations are suggested to be used. However, for this project, the use of literature studies were found to be more reliable sources as it is suggested that there is a lack of accurate kinetic and equilibrium models to predict NO_x emissions and such models are known to give up to 300% prediction error [48]. Another study that compares different kinetic models for different ammonia hydrogen fuel blends suggest that the predicted NO concentration simulation with same conditions can vary up to 600 %. Additionally, the use of an ammonia and hydrogen fuel blend in the engine requires changes in the combustion chamber architecture for optimization purposes. As this was beyond the scope of this project, it is suggested that with improving accuracy of kinetic models and optimized combustion chamber architecture for ammonia hydrogen fuel blend, the accuracy of emission simulation could be improved significantly.

14.1.2. A320neo NO_x Emissions

The A320neo NO_x emissions can be determined using a more simplified method than the one stated above. Statistical data is used to determine the amount of NO_x that is emitted during several phases of the flight. The amount of NO_x emissions are usually given in g/kg of fuel, since the amount of NO_x is little. The most NO_x is emitted during the take-off procedure of the A320neo. Afterwards, during the climb phase the NO_x emissions go down and they are the smallest during the rest of the flight (cruise, descent and landing). These differences in emissions are due to different engine temperatures, air conditions and pressures. The results of these NO_x emissions can be found in Table 14.1. All of these values are the amount of grams of NO_x emitted per kg of kerosene [2].

Table 14.1: NO_x emissions during different flight phases

Phase	Amount	Unit
Take-off	95.74	$g_{NO_x} kg_{kerosene}^{-1}$
Climb	32.35	$g_{NO_x} kg_{kerosene}^{-1}$
Cruise & After	9.95	$g_{NO_x} kg_{kerosene}^{-1}$

14.2. Carbon Dioxide Emissions

14.2.1. A320-NH3 Carbon Dioxide Emissions

During the burning of hydrogen and ammonia, no CO₂ is released into the air. This results in zero CO₂ emissions throughout the entire flight. Although this looks extremely promising, one must not forget the CO₂ emitted during the production process of ammonia. There are multiple ways to produce ammonia, some of which are more sustainable than others. The two methods considered in this study are grey and green ammonia production. Logically, 'green' production is the more sustainable option of the two [52]. During both processes CO₂ is emitted, the amount of CO₂ is provided in Table 14.2. What can be concluded is that green ammonia production emits 78% less CO₂ than grey ammonia production.

Table 14.2: CO₂ emissions during ammonia production processes [52]

Process	Amount	Unit
Grey	2.867	kg_{CO_2}/kg_{NH_3}
Green	0.631	kg_{CO_2}/kg_{NH_3}

¹<https://cantera.org/science/species-thermo.html>

²<https://www.ansys.com/products/fluids/ansys-chemkin-pro>

14.2.2. A320neo CO₂ Emissions

Since the A320neo is fueled by kerosene, CO₂ is emitted during the burning process. The production process of kerosene is extremely efficient and therefore the amount of CO₂ emitted during production can be neglected. The amount of CO₂ emitted during the flight is 3.2 kg_{CO₂}/kg_{kerosene} [26].

14.3. Water Vapour Emissions

Apart from CO₂ and NO_x emissions, H₂O emissions also have a non-negligible effect on the environment. The method for determining these emissions is the same in both the case of the A320-NH3 and the A320neo. In order to determine these emissions, first the amount of H₂ molecules in kerosene, ammonia and hydrogen were determined. This amount can be determined using the mole fraction of H₂ of the total amount of fuel taken aboard. A worst case scenario is taken as it is assumed that all of the H₂ molecules convert into H₂O. In reality the H₂O emissions will be lower than this estimated value.

14.4. Contrail Forming

The contrail forming of the A320-NH3 is taken relative to this forming of the A320neo. It is taken as a fraction of this. The contrail forming of the A320neo is therefore set to 1. The chance that contrails will originate highly depends on the corresponding air conditions. It especially depends on the presence of soot in the air. The contrail forming relative to that of the A320neo can be determined using Equation 14.5 [8].

$$\Delta RF^{contr} = \frac{\arctan(1.9\Delta p_n^{0.74})}{\arctan(1.9)} \quad (14.5)$$

In this formula the Δp_n stands for the amount of soot present in the air compared to the A320neo. The formula holds for a minimum value of $\Delta p_n = 0.1$. Since no soot is emitted during the ignition of ammonia and hydrogen this minimum value is taken. There can be some soot present in the air. The ΔRF^{contr} gives the climate impact of the contrails formed by the A320-NH3 compared to the A320neo.

14.5. Total Emissions

Table 14.3 shows the amount of emissions for both aircraft. One should note that for the contrails cirrus forming, a factor is given instead of the emission in kilogram. This is because the impact of contrails could only be determined relative to the impact of the A320neo

	CO ₂ [kg]	NO _x [kg]	H ₂ O [kg]	Contrail cirrus [-]
A320neo	40578.19	180.29	17434.26	1
A320-NH3, without ammonia production	0	38.33	28960.77	0.31
A320-NH3, green ammonia	14491.12	38.33	28960.77	0.31
A320-NH3, grey ammonia	65868.73	38.33	28960.77	0.31

Table 14.3: Total emissions per aircraft. CO₂ and NO_x are given in [kg] and Contrails is dimensionless.

14.6. Effect on Climate

To quantify the climate effect of the A320-NH3, two methods are used. The reason for this is that it is a complex process and using two methods will help validate the results by comparing them. Additionally, due to the uncertainty both in the amount of emissions and the impact these emissions have on the climate, a sensitivity analysis is implemented in chapter 15 to check whether the requirements regarding climate change are still met in case of changed emissions or climate effect. At last, the change in climate impact for different cruise altitudes is considered.

14.6.1. Weights method

For the first method, Figure 14.3 is used. This table describes the relative forcing per emission. To be able to compare the climate effect between the A320neo and the A320-NH3, the following steps are taken:

1. From Figure 14.3, the relative effect on climate impact, also known as 'forcings', are estimated. These forcings differ per substance which is emitted. The fractions of these emissions can then be divided by the total forcing of all emissions. The result of these calculations will serve as the weights accounted to every emission.
2. For every substance emitted, the amount of emissions during a flight by the A32-NH3 is multiplied by the altitude factor. This factor takes into account the effect of altitude on the impact on the climate. This factor is based on Figure 14.3, according to this table, one should note that this relation only holds between the A320neo cruise altitude (FL370) and 2000ft lower (FL350). When leaving this range, the data obtained from the table can be extrapolated, but this lowers the reliability of this research and therefore makes it less valuable.
3. For every emission and the contrail forming, the amount is divided by the number of passengers on order to take the difference in capacity between the two aircraft into account.
4. For every type of emission, the total amount produced by the A320-NH3 is divided by the one of the A320neo. This results in a emission factor describing the change in emissions.
5. Every emission factor will be multiplied with the corresponding assigned weight to get a normalized contribution to the climate relative to the total climate effect of the A320neo.
6. The sum will be taken of the normalized contributions to get the relative effect of the A320-NH3 on the climate compared to the A320neo.

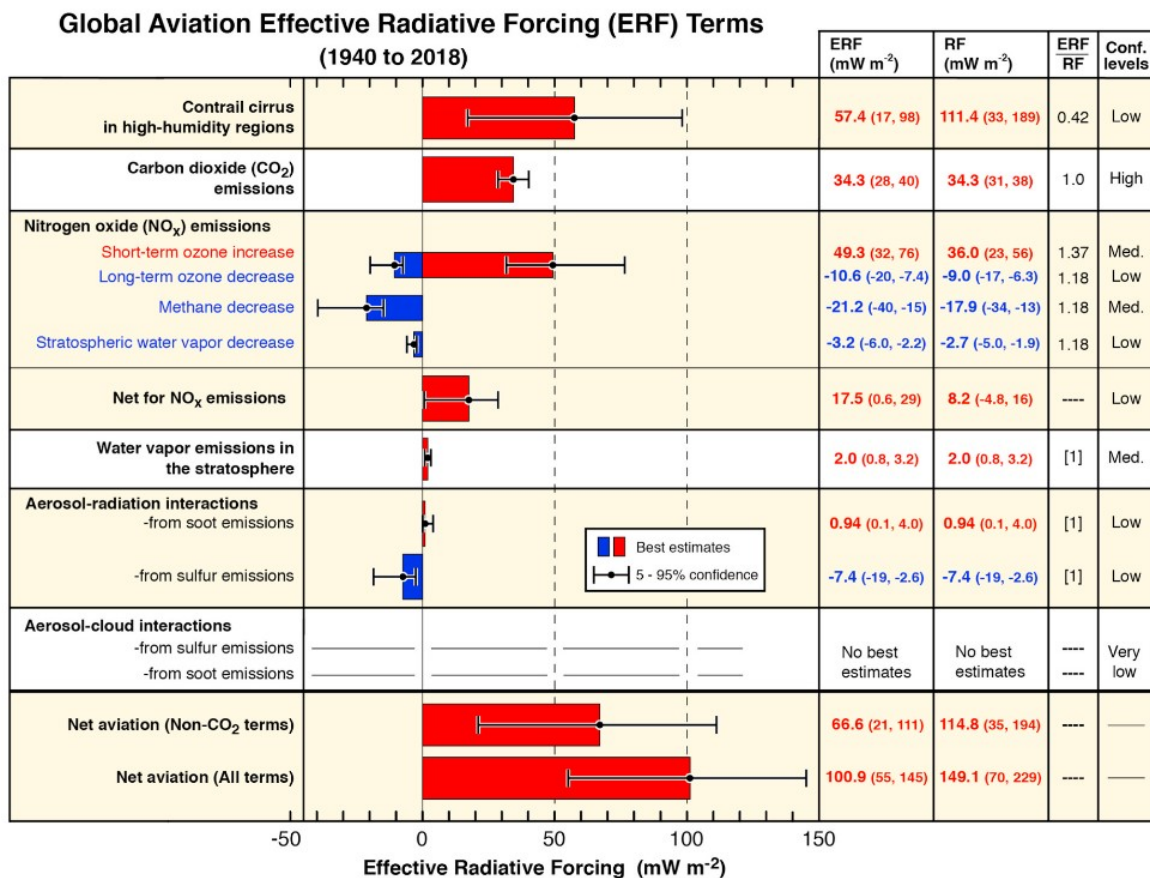


Figure 14.3: Effective radiative forcing (ERF) for contrail cirrus forming and different emissions [6]

14.6.2. CO₂- equivalent method

In this method, the relative climate impact induced by the A320NH3 compared to the A320neo is estimated by determining the total CO₂ - equivalent emissions. In order to do this, Figure 15.1 is used. The CO₂ - equivalent shows what the climate impact of a certain kg of substance is compared to kilograms of CO₂. Regarding contrails, it can be both expressed in kilogram of CO₂ burned during a flight or

per kilometer. To quantify the effect of climate change, both global warming potential (GWP) as global temperature potential (GTP) can be used. Furthermore, the can be looking 20, 50 or 100 into the future. This is because the effect of certain emissions change over time.”The GWP is a measure of the heat absorbed over a given time period due to emissions of a gas in W/m^2 and the GTP is a measure of the temperature change at the end of that time period in K ”³. Scientist usually use GWP for the reason that it can be determined using less assumptions than using GTP. GTP is mostly used by politicians to make policies. In this report, GWP is considered to be more reliable and will therefore, be mainly relied on while analysing the results. For this method the following steps should be taken:

1. Just as in the first method, the emissions and contrails formed during a flight by the A32-NH3 are multiplied by the altitude factor.
2. For every emission and the contrail forming, the amount is divided by the number of passengers on order to take the difference in capacity between the two aircraft into account.
3. The emissions will be multiplied with the according CO₂ equivalent for GWP20, GWP50, GWP100, GTP20, GTP50 and GTP100.
4. For each GWP and GTP, the sum of all CO₂-equivalents is determined for both the A320neo and A320NH3.
5. The CO₂-equivalents of the A320NH3 will be divided by the ones of the A320neo to determine the relative difference in climate impact

Metrics						
ERF term	GWP ₂₀	GWP ₅₀	GWP ₁₀₀	GTP ₂₀	GTP ₅₀	GTP ₁₀₀
CO ₂	1	1	1	1	1	1
Contrail cirrus (Tg CO ₂ basis)	2.32	1.09	0.63	0.67	0.11	0.09
Contrail cirrus (km basis)	39	18	11	11	1.8	1.5
Net NO _x	619	205	114	-222	-69	13
Aerosol-radiation						
Soot emissions	4288	2018	1166	1245	195	161
SO ₂ emissions	-832	-392	-226	-241	-38	-31
Water vapor emissions	0.22	0.10	0.06	0.07	0.01	0.008

Figure 14.4: CO₂-equivalents for contrail cirrus forming and different emissions [6]

14.6.3. Results

Table 14.4 shows the results of the first method. As can be seen in the table, the climate impact during the flight itself is only 26.6% compared to the A320neo. However, the production process of ammonia has a large impact on the climate. Using the grey production process, the requirements are not met as the relative climate impact is 86.7%, while using the green production process, the requirements are met with 43.6%. Finally, if 87% of ammonia is produced using the green method and 13% using the grey method, the requirements are just met. The results of the second method can be seen in Table 14.5. Here, most the findings from the first method are confirmed. However, the requirement regarding GWP20 is not met for green production. This means that it is not possible to lower the climate impact by 50% following GWP20 if the production phase of ammonia is taken into account. Furthermore, if the grey production process is used, the A320-NH3 is performing worse than the A320neo following every ERF term except for GWP20. This means that flying with ammonia as energy carrier is not feasible if a grey production method is used.

Table 14.4: Relative climate impact of the A320-NH3 using method 1.

Ammonia production method	Climate effect A320-NH3
Without production	26.6%
Grey production	86.7%
Green production	43.6%
87% green, 13% grey	50.0%

³<https://www.epa.gov/ghgemissions/understanding-global-warming-potentials#:~:text=While%20the%20GWP%20is%20a,%2C%20relative%20to%20CO2>

Table 14.5: Relative climate impact of the A320-NH3 using method 2.

Ammonia production method	GWP20	GWP50	GWP100	GTP20	GTP50	GTP100
Without production	46.6%	34.4%	27.4%	9.8%	-0.37%	6.57%
Grey production	86.0%	103.4%	119.5%	101.7%	163.8%	175.1%
Green production	55.3%	49.6%	47.7%	30.0%	35.8%	43.7%

14.6.4. Cruise altitude effect

Changing the cruise altitude has an effect on the climate impact. Flying lower reduces the effect of contrail cirrus forming and NO_x and H_2O emissions. However, it also increases drag and therefore, the amount of fuel used. More fuel used will increase the amount of emissions emitted with producing ammonia, so this raises the question: is it preferable to fly at a lower altitude? To determine the amount of extra fuel used in order to fly lower, the Breguet range equation (Equation 14.6) is used⁴. Furthermore, using Figure 14.5, the change in climate impact by flying lower can be determined. Now, looking at Figure 14.6(a), there can be seen that according method 1, flying lower is actually preferable. However, the effect is larger if green ammonia production is used instead of grey production. This is due to the fact that the CO_2 emitted during the production phase is higher if a lower altitude is maintained as it requires more fuel. Looking at Figure 14.6(b), the climate impact according to GTP100 condition, will actually get higher if a lower cruise altitude is maintained. However, it is taking into account that the GWP condition is more reliable than the GTP condition. This shows a decrease in climate impact while changing to a lower cruise altitude. Therefore, the climate impact can be considered to be lower if a lower altitude is maintained⁵.

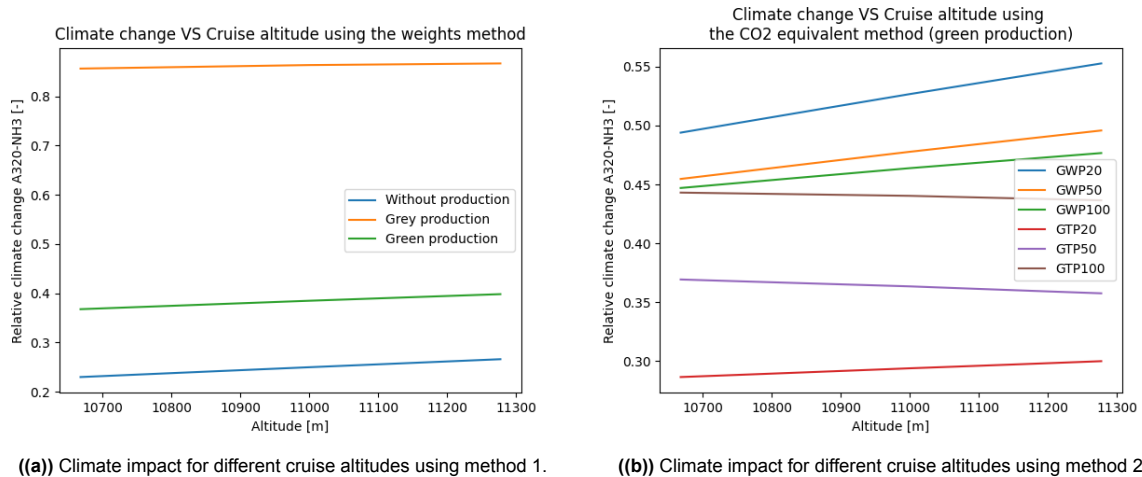
$$R = 2 \cdot \sqrt{\frac{2}{\rho \cdot S}} \cdot \frac{1}{SFC} \cdot \frac{CL^{0.5}}{CD} \cdot (W_{initial}^{0.5} - W_{final}^{0.5}) \quad (14.6)$$

Impact	Reference	Lower	Higher
Net NO_x	8.9	7.3	10.6
<i>NO_x-Ozone</i>	19.5	18.2	21.1
<i>NO_x-Methane</i>	-7.0	-7.1	-6.9
<i>NO_x-PMO</i>	-2.8	-2.9	-2.8
<i>NO_x-H₂O</i>	-0.8	-0.8	-0.8
Direct H_2O	1.5	1.1	2.0
Aerosol indirect warm cloud (AiwC)	-14.8	-21.9	-14.4
Contrail Cirrus (CC)	45	40	48
Total non-CO_2	40.3	26.8	46.1
<i>Total</i> ¹	61.8	48.6	67.4

Figure 14.5: Radiative forcing while flying 2000ft lower and 2000ft higher[7].

⁴<https://present5.com/mae-1202-aerospace-practicum-introduction-to-aircraft-performance/>

⁵<https://present5.com/mae-1202-aerospace-practicum-introduction-to-aircraft-performance/>



14.7. Sustainability approach

In the following part, the project approach with respect to sustainable development is treated. Therefore, it is of main priority to aim for a sustainable design and design process by using a project approach regarding sustainability. This approach will treat the three pillars of sustainability and quantize them in order to be able to make a trade-off between the different design options. The goal is to be 50% more sustainable than the A320neo. In order to compare sustainability in every aspect, a quantification method is introduced. Each priority gets a method to assign a score (from 1 to 10) and an importance rating (1 to 5). For both aircraft, these scores are multiplied and subsequently summed. Every time the most sustainable method, if it fits within the requirements, will be chosen. This way we can use the sustainable methods to produce a more sustainable aircraft than the A320neo. The priorities will have an identifier which can be used in the end of this chapter to give a clear overview of all priorities.

14.7.1. Economical sustainability

The first pillar discussed is the economical sustainability. Economical sustainability is the practice that supports long-term economic growth without negatively impacting social, environmental, and cultural aspects of the community⁶. The main point of economical sustainability is that the design has a feasible rate of investment. As stated in the requirements, the aircraft cannot exceed 115% of the A320neo costs. In addition, the development costs may be no more than 150% of the A320neo. Therefore, manufacturing, development and operating costs should be taken into account throughout the entire process. The problem that this drives is that cheap manufacturing methods and resources are usually only available in countries where working conditions are poor and environmental pollution are still common⁷. Therefore, the main aim of the economical sustainability plan is to not contribute to these problems whilst staying within 115% of the A320neo production and 150% of the development costs.

In order to clearly monitor the economical sustainability of the design whilst also comparing it to the other pillars of sustainability, it needs to be quantified. This means using priorities to give rankings of importance to the categories discussed. First the categories are stated and then the way of quantification is given. Taking into account that the costs will adhere to the requirements stated previously while minimising the impact made on people and environment, the following categories are considered when talking about economical sustainability:

- **PRI-EC-01:** The development costs should stay within 150% of that of the A320neo. This will be quantified in the following way: the 150% is a score of 5, every 10% below this limit will raise the score with 1 point. Every 10% above this limit will decrease the score with 1 point. This requirement is not that important for economical sustainability on the long term, as it only delays the break-even point, but does not affect the profit per sale, it will get an importance rating of **3 out of 5**. This can be achieved by constantly monitoring the development costs, and predicting

⁶<https://sustainability.umw.edu/areas-of-sustainability/economic-sustainability/>, 2022-4-21

⁷<https://www.u-earth.eu/post/world-most-least-polluted-countries>, 2022-04-29

the total development costs at all time. If it seems like the goal will not be reached, actions could be taken to reduce the development costs.

- **PRI-EC-02:** The costs of the aircraft shall stay within 115% of the A320neo costs. To quantify this the same method is used as for the development costs. A score of 5 is given to this limit. Every 3% below the limit will add 1 point to this score. Every 3% above this limit will reduce the score by 1 point. Considering that it is important to keep the costs of the aircraft limited in order to achieve economical sustainability, but that is not a driving factor behind this project, it will get an importance rating of **3 out of 5**. The production costs could be reduced by choosing more common manufacturing methods, or using less transportation in assembly.

14.7.2. Social sustainability

The next pillar that needs to be discussed is the social sustainability of the design. Social sustainability is defined as "identifying and managing business impacts, both positive and negative, on people"⁸. Therefore we look at the social aspect of our design. New innovations in the air industry lay focus upon the progressive caring side of people. This can be seen by the CO₂ compensation which can be bought when buying almost any aircraft ticket. This way airlines share part of the responsibility with their passengers⁹. What is seen is that over the past years, more and more people pick this option as the results of global warming are getting more serious every day.

This is why it is of great importance to promote the green initiative taken by the ammonia aircraft design. This means marketing methods need to be established which enhance the image of the aircraft. Many people are willing to pay slightly more than they would for different tickets if the flight does not contribute to global warming. Therefore the 'green initiative' needs to be the main point of advertising. Another social consideration which should be taken into account is the trust people have in the airplane. In comparison to the A320neo, the ammonia aircraft is new and therefore does not have the image of reliability that the A320neo does have. This trust needs to be created by bringing the right information to the public. These are the two main priorities for social sustainability. An explanation of how they are quantified are presented below:

- **PRI-SO-01:** The aircraft shall represent the 'green' initiative. This can be measured by sending out a questionnaire to a Representative group of people and asking them what their thoughts are on emissions. For instance: you can ask people whether they think certain substances are harmful for the environment. Then we could inform them about ammonia and our aircraft. After that they will have to take the questionnaire again and we can compare. From this questionnaire a score of 1-10 can be obtained to see how environmental sustainable people think the ammonia aircraft is at the moment and during the same time, what the public opinion will be when a large amount of people are informed about the emission. Since the tickets for flying in this aircraft will probably be more expensive compared to the tickets of kerosene powered aircraft, people should be aware of the environmental advantages. Therefore it is given an importance of **3 out of 5**. This score can be improved by providing more advertisements to educate potential clients about the aircraft.
- **PRI-SO-02:** The aircraft shall represent a certain reliability. Once again, this can be measured using a questionnaire. First the information about the aircraft can be given, then the questionnaire can be taken and a score from 1 to 10 comes out. Since most people trust in aircraft in general and are not afraid to fly this is given an importance of **1 out of 5**. This score can be improved by providing more advertisements to educate potential clients about the aircraft.

14.7.3. Environmental sustainability

The last pillar of sustainability is the environmental sustainability. Environmental sustainability is defined as the responsibility to conserve natural resources and protect global ecosystems to support health and well-being, now and in the future¹⁰. This pillar is undoubtedly the one with the highest priority for the ammonia aircraft design. The sustainability of an aircraft is not only determined by the emission during the flight, but also by the manufacturing process and the fuel resource. These three aspects

⁸<https://www.unglobalcompact.org/what-is-gc/our-work/social>, 2022-4-29

⁹<https://www.greentripper.org/en/aboutus/whyaco2neutralflight>, 2022-4-29

¹⁰<https://sphaera.com/glossary/what-is-environmental-sustainability/>, 2022-04-21

will be examined on different parameters regarding sustainability, which are treated below. These parameters will be quantified in order to be suitable for the trade-off. To optimize the design options, lean manufacturing will be used to minimize the waste.

Every year Earth Overshoot Day indicates the day the renewable energy sources are used for that year. From that day on the world is practically using up the reserves the world has. In 2021 this day was on July 29¹¹. In order to not exhaust the world any further renewable energy sources need to be used in the production process, such that it does not contribute much to global warming. Therefore it is also a priority that minimum to no fossil fuels are used in the production, operation and fuel production processes.

The next thing that needs to be considered is the pollution created in all three of the aforementioned processes. This does not only include the CO₂ that is expelled but this will also include other harmful substances. What should not be forgotten is that the aircraft can be extremely green while the production process of the fuel is not green at all. There are also emissions which do not look harmful at first sight, but once reacting with the atmosphere could have serious consequences. Another thing that should not be forgotten are the contrails emitted at high altitudes. These factors need to be combined to come up with the best combination of fuel and aircraft design.

Another consideration is the recyclability of the fuselage (parts) and the materials used in manufacturing. A high recyclability means that the aircraft is less harmful for the environment. The same holds for the reliability. The higher the reliability, the longer the aircraft can be in use without requiring maintenance. This results in less manufacturing processes and therefore less pollution.

The last thing that needs to be considered is the ammonia cracking process in which a lot of catalysts are used. Often, these catalysts are bad for the environment as well. Therefore the total emission for the use of these catalysts needs to be considered as well. All in all these categories lead to two different categories related to environmental sustainability. The first one is the emissions released only once:

- **PRI-EN-01:** The environmental footprint during manufacturing must be analysed. These should be compared to that of the A320neo. For every 10% that the environmental impact of the ammonia plane during manufacturing is lower than that of the A320neo 1 point will be added. Since this environmental impact only occurs once the importance rating is chosen to be **2 out of 5**. Possible methods of reducing emissions would include reusing certain processes or materials. Another way to accomplish this is replacing polluting production methods in the process with less polluting methods.

The next category is the once that do have an environmental impact throughout the use of the airplane:

- **PRI-EN-02:** The environmental footprint during operation of the aircraft must be analysed. These should be compared to that of the A320neo. For every 10% that the environmental impact of the ammonia plane during operation is lower than that of the A320neo 1 point will be added. This includes everything like the cracking of ammonia, burning of ammonia and all other emissions involved during operation. Since this environmental impact occurs every time the plane takes off it has been given a rating of **5 out of 5**. The environmental footprint can be reduced by using green fuel. Furthermore taking as little weight as possible is beneficial for this. The pilots can also be trained to fly saving fuel.
- **PRI-EN-03:** The environmental footprint during production of ammonia must be analysed. These should be compared to the production of other fuels (most likely kerosene). For every 10% that the environmental impact of ammonia production is lower than that of alternative fuels 1 point will be added. This includes everything concerning the production of the fuel. Since this environmental impact occurs every time the plane takes off, it has been given a rating of **4 out of 5**. The emissions could be reduced by choosing the most green option for ammonia and regularly checking the conditions under which ammonia is being produced.

¹¹<https://www.overshootday.org/>, 22-04-29

14.7.4. Sustainability quantification

In this section all of the previous sustainability methods are once again shown including their identifier, a short description of the grading method and the corresponding importance. All of these are provided in Table 14.6.

Table 14.6: All sustainability priorities, the ways to measure them and importance.

Sustainability priority	Grading method	Importance (1-5)
PRI-EC-01	Development costs	3
PRI-EC-02	Aircraft costs	3
PRI-SO-01	Questionnaire of 'green' image	3
PRI-SO-02	Questionnaire of trust	1
PRI-EN-01	Comparison with A320neo manufacturing footprint	2
PRI-EN-02	Comparison with A320neo operational footprint	5
PRI-EN-03	Comparison with production of alternative fuels	4

Sensitivity Analysis

The design of the aircraft subsystems often depend on other related subsystems. This means that a different result from one subsystem may influence the design of another subsystem. It is therefore, important that sensitivity analysis is performed to assess how the design will change if different parameters are used.

15.1. Cracking System Design

The main input for the cracking system is the amount of H_2 needed by the aircraft. A change in this value will influence the amount of NH_3 that need to be decomposed. The amount of ammonia that can be processed depends on the number of reactors that is used in the system, which will influence the power that the N_2 circuit needs to supply. In short, the principal design of the cracking system should not change much with a different parameter. It simply has to be scaled up by using more reactors, which will increase the weight and volume of the system.

15.2. Engine Heat Exchanger Design

In this section, the effect on the sizing of the helical heat exchanger in the engine will be discussed. This sensitivity analysis will assume the parameter values discussed in subsection 6.2.5 in addition to the engine core flow parameters presented in Table 15.1. For these values the length and weight of the helical heat exchanger was found to be 56 cm and 12.37 kg respectively (see chapter 8).

Table 15.1: Engine parameters used for engine heat exchanger size sensitivity analysis.

Parameter	Symbol	Value	Units
Engine core mass flow	\dot{m}_{core}	33.93	$[kg \cdot s^{-1}]$
Air density in combustion chamber	ρ_{core}	4.08	$[kg \cdot m^{-3}]$
Air temperature in combustion chamber	T_{core}	2100	$[K]$
Airflow velocity in combustion chamber	V_{core}	39.22	$[m \cdot s^{-1}]$

15.2.1. Effect of nitrogen mass flow

A 10% increment in the nitrogen mass flow results in 61.65 cm and 13.6 kg for the heat exchanger length and mass respectively. This corresponds to a roughly 10% increase in both of these parameters. If the nitrogen mass flow, \dot{m}_{N_2} , is doubled, the heat exchanger length is changes to 112 cm, doubling the initial heat exchanger length. This is expected because - assuming the heat extracted from the engine flow is the same as the heat absorbed by the nitrogen flow - the area of the heat exchanger (and consequently the helix length) is indeed directly proportional to the nitrogen mass flow. The doubling of the helix mass to 24.69 kg also follows the same logic.

15.2.2. Effect of combustion chamber temperature

A 10% increment in the combustion chamber temperature results in 48.96 cm and 10.8 kg being the new helix length and mass respectively. This corresponds to a 12.65% decrease in both the parameters of the heat exchanger. Similarly a 20% increase in the combustion chamber temperature results in 43.46 cm and 9.59 kg for the helix length and mass respectively. This also corresponds to 22.4%

decrease in both the parameters of the heat exchanger.

This brief analysis suggests that the helical heat exchanger sizing parameters are coupled slightly stronger to the combustion chamber temperature than they are to the mass flow of the nitrogen through the heat exchangers.

15.3. Emissions Analysis

This sensitivity analysis consists of two parts. In the first part, it is determined what the climate effect will be if the ERF of NO_x and contrail cirrus are varied over the 95% interval stated in Figure 14.3. NO_x and NO_x ERF will stay constant. NO_x stays constant, because the 95% interval is relatively small and NO_x stays constant as the climate impact is relatively small. Because of this, only the NO_x , contrails and soot is taken into account. In Figure 15.1, the sensitivity in effective radiative forcing (ERF) of both NO_x and contrails can be determined. If these values would change the climate impact compared to that of the A320neo would also change. That is what is displayed by the different colours in the graph. On the right, the relative climate impact of the A320-NH3 compared to the A320neo is given (A320-NH3/A320neo). In all cases in the plot the relative climate impact stays under 0.48. This means that the requirement regarding climate change is met regardless of what the ERF is within the 95% uncertainty boundaries.

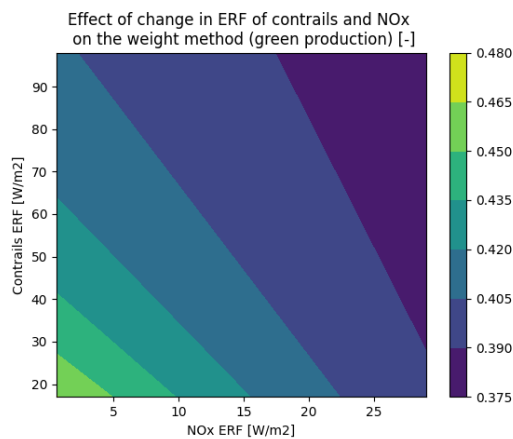
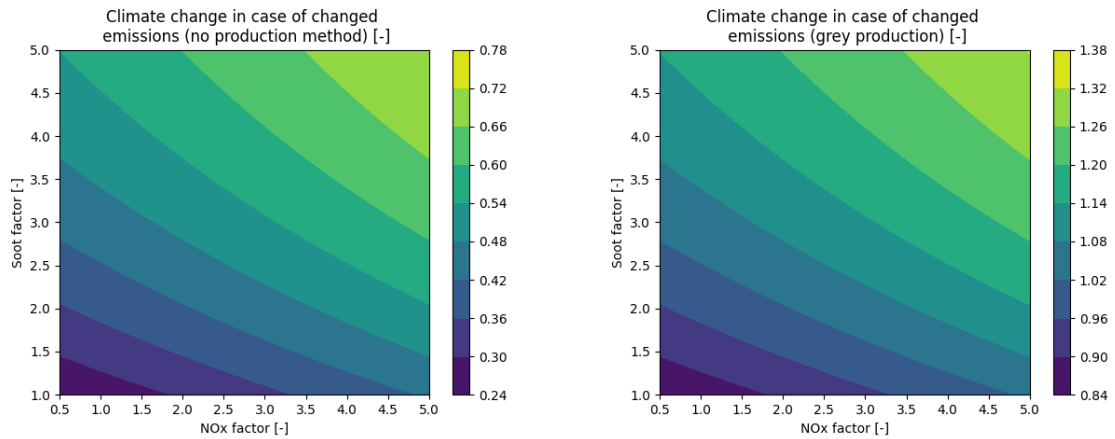


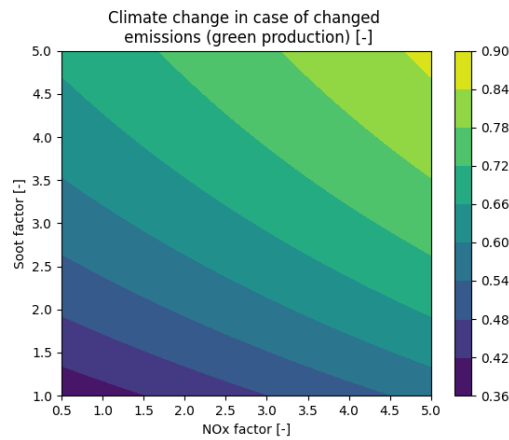
Figure 15.1: CO_2 -equivalents for contrail cirrus forming and different emissions[6].

The sensitivity of the NO_x and soot factor is also relevant. These factors are compared to the previously estimated emissions of the A320-NH3. The soot is present in the air whilst the NO_x is emitted by the aircraft. For clarification: if the NO_x factor is equal to 2, the NO_x emissions are twice as much as the estimated value in the report. Once again, the relative impact compared to the A320neo is displayed using the colour scheme. Logically, the relative impact also depends whether the production process is taken into consideration. It also depends on which production process is used. In Figure 15.2(a) the sensitivity of the effect on climate change is given in the case where production is not accounted for. The second figure (15.2(b)) provides a sensitivity in the case of grey ammonia production. Lastly, in Figure 15.2(c), the green ammonia production case is provided. This entire sensitivity analysis is provided for the weights method (the first estimation method). In the following plots, it can be seen that the requirement concerning sustainability is met for every combination of NO_x and soot factor which gives a relative climate effect lower than 0.5.



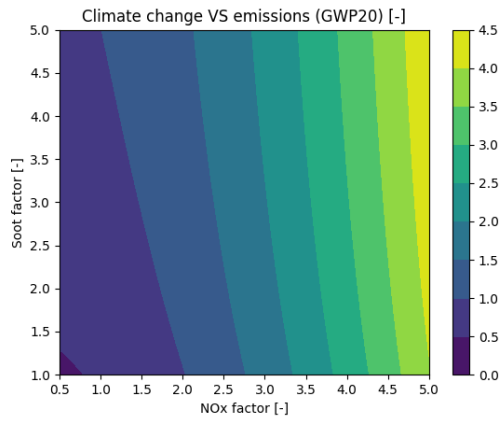
((a)) Sensitivity of NO_x and soot in climate change relative to the A320neo, without production

((b)) Sensitivity of NO_x and soot in climate change relative to the A320neo, with grey production

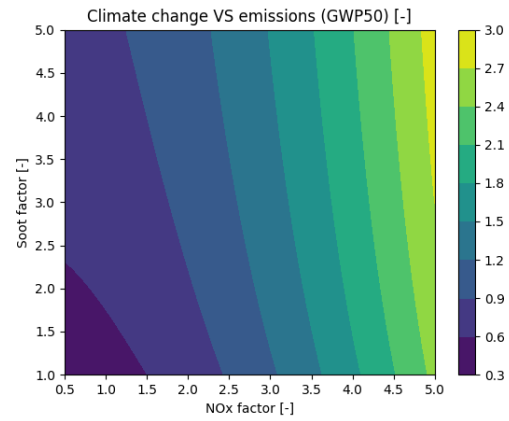


((c)) Sensitivity of NO_x and soot in climate change relative to the A320neo, with green production, using the weight method (method 1)

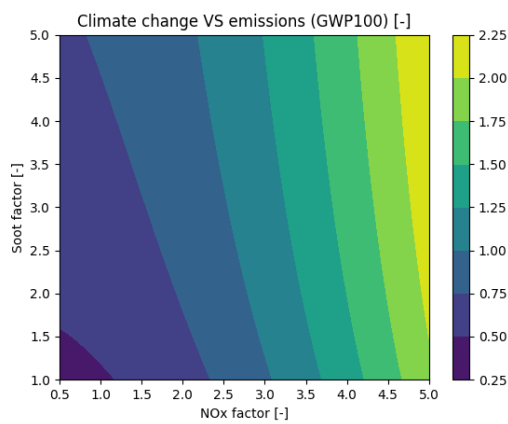
A similar sensitivity analysis was performed for the CO₂-equivalent method. In these graphs, the sensitivity in NO_x and soot factors for the different GWP and GTP time spans are provided. It should be noted that the GWP is more relevant in this case, as less assumptions are taken. This means that the values are more accurate than the GTP. However, the GTP is more commonly used in policies. The plots corresponding to the sensitivity analysis of GWP are provided in Figure 15.3(a), Figure 15.3(b) and Figure 15.3(c) for 20, 50 and 100 years respectively. Those for the GTP are provided in Figure 15.3(d), Figure 15.3(e) and Figure 15.3(f) for 20, 50 and 100 years respectively.



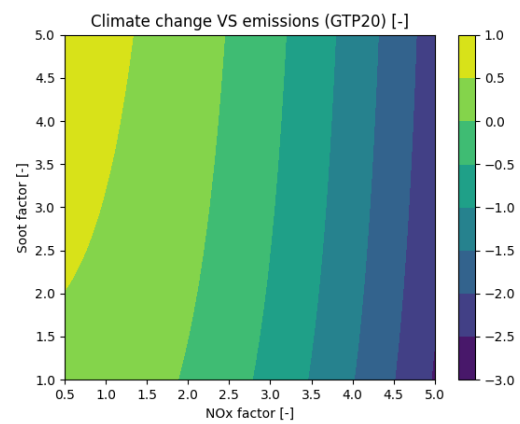
((a)) Sensitivity of NO_x and soot in climate change relative to the A320neo, for the GWP over 20 years



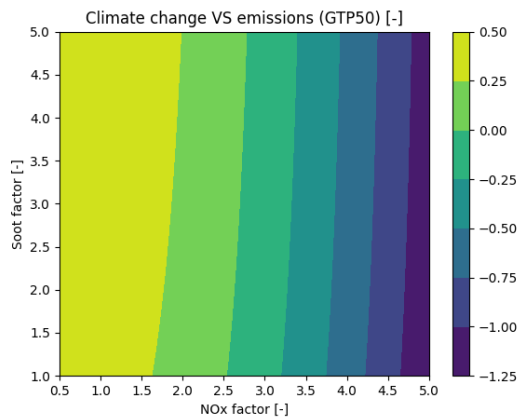
((b)) Sensitivity of NO_x and soot in climate change relative to the A320neo, for the GWP over 50 years



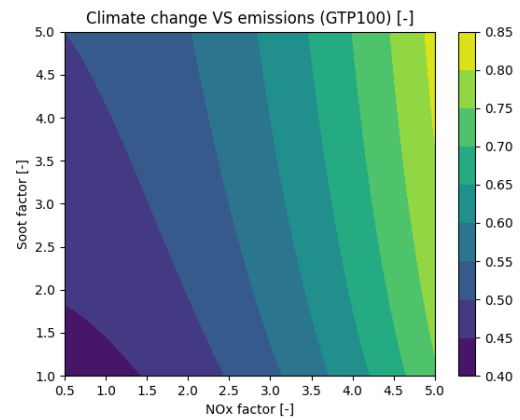
((c)) Sensitivity of NO_x and soot in climate change relative to the A320neo, for the GWP over 100 years



((d)) Sensitivity of NO_x and soot in climate change relative to the A320neo, for the GTP over 20 years



((e)) Sensitivity of NO_x and soot in climate change relative to the A320neo, for the GTP over 50 years



((f)) Sensitivity of NO_x and soot in climate change relative to the A320neo, for the GTP over 100 years

Figure 15.3: Sensitivity of NO_x and soot in climate change relative to the A320neo, with green production, using the weight method (method 1)

Requirements and Budgets Compliance

In this section the stakeholder requirements, often known as user requirements, will be discussed. This will be followed by the budget analysis of technical and financial resources which were assigned at the beginning of the design process. The user requirements have been stated by the client in their own language, which were then translated into technical specifications. If the user requirements were impractical owing to their complexity or if they conflicted with the mission statement, they have been discussed with the customers. The user requirements are negotiable with the client if they are unfeasible due to a high level of complexity or they do interfere with the mission statement. The identifier is structured as **US-[subgroup]-[#]** and are divided into subgroups, respectively: performance (PER), safety and reliability (SAR), sustainability (SUS), engineering budget (ENB) and cost (CST).

The user requirements can be presented in the so-called requirements compliance matrix. In this table the given requirements shall be presented, followed by confirmation whether these have been met. The Requirements Compliance Matrix can be found in Table 16.1. In this table the requirement identifiers are given for each of the given requirements. Then this requirement is explained and indicated whether it has been met. In the last column the corresponding chapter is mentioned where the elucidation for the given condition can be found.

Table 16.1: Requirements Compliance Matrix.

<u>Identifier</u>	<u>Explanation</u>	<u>Met</u>	<u>Elucidation</u>
<i>PERFORMANCE</i>			
US-PER-01	The students shall have a quantification of the performance gain due to ammonia usage	✓	subsection 6.1.2
US-PER-02	The aircraft shall have a refuelling system compatible with ammonia	✓	subsection 9.2.1
US-PER-03	The flight mechanics characteristics of the aircraft shall be evaluated	✓	section 5.6
US-PER-04	The flight performance of the aircraft shall be compared to the A320neo	✓	section 12.4
US-PER-05	The climate impact of the aircraft shall be compared to the A320neo	✓	chapter 14
US-PER-06	The operating cost of the aircraft shall be compared to the A320neo	✓	section 11.2
US-PER-07	The propulsion system shall be powered by ammonia	✓	section 6.2
US-PER-08	The aircraft shall satisfy the CS25 rules	✓	section 5.7
US-PER-09	The aircraft shall have a minimum range of 4000 km	✓	section 5.6
US-PER-10	The aircraft shall have a passenger capacity between 150-200 passengers	✓	section 5.1

US-PER-11	The impact of refuelling shall not add more than 30 min to the turnaround time	✓	subsection 9.2.1
SAFETY AND RELIABILITY			
US-SAR-01	The aircraft refuelling system shall be safe, following the CS-25 rules	✓	subsection 9.2.1
US-SAR-02	The ammonia storage system shall be safely separated from the passenger cabin	✓	subsection 6.2.6
US-SAR-03	The safety of ammonia refuelling system shall be addressed	✓	subsection 9.2.1
US-SAR-04	The storage of ammonia at the airport shall be addressed	✓	subsection 9.1.3
US-SAR-05	The ammonia storage system must be able to store the fuel for at least 48 hours without boil-off at an outside temperature of 45 [Celsius]	✓	subsection 6.2.6
US-SAR-06	The passenger evacuation time of 90 seconds shall not be affected by the ammonia storage	✓	subsection 9.2.3
SUSTAINABILITY			
US-SUS-01	The supply and production of green hydrogen at the airport shall be investigated	✓	subsection 9.1.1
US-SUS-02	The life cycle of the aircraft shall be analysed	✓	section 11.2
US-SUS-03	The climate impact of the aircraft shall be at least 50% lower than A320neo	✓	chapter 14
US-SUS-04	The NO_x , CO , unburnt hydrocarbon and soot emission for the LTO cycle shall be reduced by at least 50% when compared to A320neo	✓	chapter 14
ENGINEERING BUDGET			
US-ENB-01	The TRL road-map for the development of the designed aircraft shall be made	✓	chapter 14
US-ENB-02	The EIS of the aircraft shall be in 2035	✓	chapter 14
COST			
US-CST-01	The total development cost of the aircraft must not exceed €5 billion	✓	section 11.2
US-CST-02	The cost of the A320-NH3 aircraft shall not be 15% more than that of the A320neo	✓	section 11.2

In addition to the user requirements stated earlier, some technical resources such as design range, mass, aircraft cost were budgeted in the beginning weeks of the project. These budgets needed to ensure that the growth in such parameters is controlled. As such these parameters were tracked and enforced by the Risk Manager. All the budgeted items have been compared to the attained values of the final design in Table 16.2 (obtained from chapter 8 and section 11.2).

Table 16.2: Technical budget compliance matrix

Budget Items (margin)	Values excl. Margins	Values incl. Margins	Final Design Values	Units
PERFORMANCE				
Range (10%)	4000	3600	4000	[km]
Max take-off mass (10%)	117.11	128.82	91.6	[tonnes]
Max fuel capacity (15%)	71.54	82.27	39.84	[m ³]
Max fuel mass (15%)	48.22	55.43	24.67	[tonnes]
Max Payload mass (5%)	17.70	18.6	17.63	[tonnes]
Takeoff length (7%)	2157.65	2308.68	1951	[m]
COST				
Unit Cost (17%)	109.94	128.63	126.50	[million€]

As can be seen, all the budgeted items have been attained well within the allocated margins. Note that the difference in values between the budget values and the final attained values are particularly high for the maximum take-off mass, maximum fuel mass and maximum fuel capacity. This is due to the fact

that these budgeted items were estimated under the assumption that only hydrogen would be burned in the engines, thus a large amount of hydrogen, and consequently ammonia, was required.

Conclusion

This report aims to give an outline on the final design done by Group 10 to develop the concept of a new generation A320 aircraft. The crucial departments that require significant modifications over the current A320neo design are described and analysed. Overall, the fuel storage, cracking system and propulsion department are extensively changed compared to the A320neo. The fuselage dimension are kept the same, while the wing and tail area are changed marginally while still meeting the user requirements.

The market for aviation is still growing rapidly. Airbus expects to double their fleet in 20 years. However, with this expansion, the CO₂ emissions emitted by the aviation industry will also increase. There is an incentive and need for technological advancements to decrease the CO₂ emissions. With ammonia as energy carrier, no CO₂ will be emitted and this can decrease the effect this aircraft will have on the climate. Our mission statement need is therefore: 'Design an aircraft that is power driven by ammonia'. However, it is a challenge to reduce the costs for development, operation and fuel while staying ahead of the competition.

The client had given user requirements. All these requirements were met with some trade-offs. Moreover, technical requirements were created to make sure the aircraft will be feasible and safe. For these requirements, trade-offs have been made in order to meet the wishes of the client. Thereby, a technical risk assessment had been performed in order to not fail the design of the aircraft, as a couple of departments of the aircraft will include new technologies and new risks attached to that.

With the requirements, it was important to design and evaluate the propulsion system. This included the cracking system, fuel storage, engine and heat exchanger. New technologies and advancements were used to realise the design. However, it was still chosen to use a thermal cracking system instead of a plasma cracking system, as this cracking system is technologically proven, and more feasible for the aircraft. Possibly, in the future, plasma cracking will be used, because it can be more efficient than thermal cracking, but there are challenges in scaling up for now. The design of the engine also utilise an inter-turbine burner (ITB), which is introduced to improve emission performance. Heat exchangers are also used in the engine to recycle heat from the engine for use in the cracking system.

With the propulsion system designed, the rest of the aircraft can be designed around it. Fuel tanks required by the propulsion system is larger than the standard capacity the aircraft is able to carry, and some of them has to be placed in the cargo. The cabin design account for this by reducing passenger capacity, using the additional space for cargo. The aerodynamic performance was studied by first calculating the total weight of the aircraft, and then designing the wing, airfoil, and high lift devices for this. The tail of the aircraft was also redesigned for the new longitudinal and lateral stability.

With the design process established, the iteration for the design can be performed. This results in cracking system with mass of 4172 [kg], volume of .715 [m³]; engine of with thrust of 133.6 [kN] and mass of 2540 [kg]. It is also estimated that the aircraft's MTOW will be 91,600 [kg] and OEW of 49,300 [kg]; the wing surface area will increase to 141.93 [m²], with the vertical and horizontal tail surface area 21.5 [m²] and 35.908, respectively. As can be seen, the dimensions are not changed much compared to the original A320neo

Aluminium alloy is the main material used for the aircraft, including the wing box and fuselage. However, the cracking system will use steel because of the higher temperature tolerance. With development cost of the aircraft of the aircraft being 5 billion \$, and profit from each aircraft about 11.5 million \$, it is estimated that the break even point will be at 430 aircraft sold. For the airline, this break even point will be at about 13.5 years into the operation of an aircraft.

With regard to emission, the aircraft total climate effect including emission generated from ammonia production will be about 86.7% of the one generated by the current A320-neo. This is assuming grey ammonia production, which is the only feasible option for now, but can be further improved to about 43.6% if green ammonia production can be achieved fully.

References

- [1] *A320 AIRCRAFT CHARACTERISTICS AIRPORT AND MAINTENANCE PLANNING*. Rev 41. AIRBUS S.A.S. Jan. 2022.
- [2] European Aviation Safety Agency. *ICAO Aircraft Engine Emissions Databank*. July 2021. URL: <https://www.easa.europa.eu/domains/environment/icao-aircraft-engine-emissions-databank>.
- [3] European Aviation Safety Agency. *Type-Certificate Data Sheet for LEAP-1A & LEAP-1C Series Engine*. May 2018.
- [4] AIRBUS. *A320 FAMILY: the most successful aircraft family ever*. 2021. URL: <https://www.airbus.com/sites/g/files/jlcbta136/files/2021-12/EN-Airbus-A320-Facts-and-Figures-December-2021.pdf>.
- [5] Initial Airworthiness. *Certification Specifications and Acceptable Means of Compliance for Large Aeroplanes (CS-25)*. URL: <https://www.easa.europa.eu/downloads/134259/en>.
- [6] D.S.Lee et al. "The contribution of global aviation to anthropogenic climate forcing for 2000 to 2018". In: *Atmospheric Environment* 244 (2011), pp. 117–834. URL: <https://www.sciencedirect.com/science/article/pii/S1352231020305689?via%5C%3Dihub>.
- [7] Sigrun Matthes et al. "Mitigation of Non-CO2 Aviation's Climate Impact by Changing Cruise Altitudes". In: *Aerospace* 36 (2020). DOI: <https://doi.org/10.3390/aerospace8020036>. URL: <https://www.mdpi.com/2226-4310/8/2/36>.
- [8] Volker Grewe et al. "Evaluating the climate impact of aviation emission scenarios towards the Paris agreement including COVID-19 effects". In: *Nature communications* 12.3841 (2021). DOI: <https://doi.org/10.1038/s41467-021-24091-y>.
- [9] Gael Baldissin et al. "Synthesis of Pure Lithium Amide Nanoparticles". In: *European Journal of Inorganic Chemistry* 2013 (Apr. 2013). DOI: 10.1002/ejic.201201535.
- [10] T. E. Bell. "H2 Production via Ammonia Decomposition Using Non-Noble Metal Catalysts: A Review". In: *Topics in Catalysis* 59 (2016). DOI: <https://doi.org/10.1007/s11244-016-0653-4>.
- [11] Paula H. Blanco, Chunfei Wu, and Paul T. Williams. "Influence of Ni/SiO2 catalyst preparation methods on hydrogen production from the pyrolysis/reforming of refuse derived fuel". In: *International Journal of Hydrogen Energy* 39.11 (2014), pp. 5723–5732. ISSN: 0360-3199. DOI: <https://doi.org/10.1016/j.ijhydene.2014.01.150>. URL: <https://www.sciencedirect.com/science/article/pii/S0360319914002304>.
- [12] Aircraft Cost Calculator. *AIRBUS 320 Price and Operating Costs*. 2022. URL: <https://www.aircraftcostcalculator.com/AircraftOperatingCosts/151/Airbus+320>.
- [13] Simon Calder. "AIRBUS A320: WELL-REGARDED WORKHORSE OF SHORT-HAUL FLYING". In: *Travel correspondent* (2020). URL: <https://www.independent.co.uk/travel/news-and-advice/airbus-a320-karachi-crash-pakistan-international-airways-a9528736.html>.
- [14] *Certification Specifications for Large Aeroplanes*. Amendment 3. European Aviation Safety Agency. Sept. 2007.
- [15] *CES EduPAck 2017 User Manual & Getting Started Guide*. the 2022 granta edupack version was used, not the 2017 version. ANSYS inc. June 2022.
- [16] Airbus Company. *Airbus Global Market Forecast 2021-2040*. 2021.
- [17] Parisa Derakhshandeh, Abolfazl Ahmadi, and Reza Dashti. "Simulation and technical-economic-environmental optimization of the General Electric GE90 hydrogen turbofan engine". In: *International journal of hydrogen energy* 46 (2021), pp. 3303–3318.

- [18] St. Louis Division. "THE USAF STABILITY AND CONTROL DATCOM". In: *McDonnell Douglas Astronautics Company Volume I; Users Manual*. AFFDL-TR-79-3032 (Apr. 1979).
- [19] Group 10 DSE. "Midterm Report for the Design Synthesis Exercise AE3200". In: (2022).
- [20] I. E. Fesmire et al. *Spray-On Foam Insulations for Launch Vehicle Cryogenic Tanks*. 2011.
- [21] DAN WEBB MGR.; ENG. and TECH. SVCS; CF INDUSTRIES; INC. LONG GROVE. *Large Scale Ammonia Storage And Handling*. 2022.
- [22] F.Oliviero. *AE3211-I Systems Engineering and Aerospace Design*. Mar. 2021.
- [23] Dr.ir. M.I. Gerritsma. *Chap. 4 Incompressible Flow over Airfoils*. Study course. 2020.
- [24] V. Gnielinski. "New equations for heat and mass transfer in the turbulent flow in pipes and channels". In: *NASA STI/Recon Technical Report A 41.1* (Jan. 1975), pp. 8–16.
- [25] G. Gonçalves et al. "Preparation and characterization of nickel based catalysts on silica; alumina and titania obtained by sol–gel method". In: *Journal of Non-Crystalline Solids* 352.32 (2006). Glasses and Related Materials 7, pp. 3697–3704. ISSN: 0022-3093. DOI: <https://doi.org/10.1016/j.jnoncrysol.2006.02.120>. URL: <https://www.sciencedirect.com/science/article/pii/S0022309306007472>.
- [26] Carbon Offset Guide. *CO2 Emissions*. 2017. URL: <https://www.offsetguide.org/undersanding-carbon-offsets/air-travel-climate/climate-impacts-from-aviation/co2-emissions/>.
- [27] J.P. Holman. "Heat Transfer". In: Tenth. McGraw-Hill, 2010.
- [28] Denis Howe. "Aircraft Conceptual Design Synthesis". In: *Professional Engineering Publications Limited* (2000), equation 6–14a.
- [29] ICAO. *Future of Aviation*. 2022. URL: <https://www.icao.int/Meetings/FutureOfAviation/Pages/default.aspx?%5C#:~:text=The%5C%20aviation%5C%20sector%5C%20is%5C%20growing,over%20%5C%5C%20%5C%20the%5C%20next%5C%2020%5C%20years.>
- [30] C. Jackson et al. "Ammonia to Green Hydrogen Project". In: (2020).
- [31] Ward Jacobs et al. "Applied Computational Aerodynamics". In: *NACA Report* (Mar. 1933), Appendix A, 4.
- [32] Max Kingsley-Jones. "Airbus begins tests to extend service life of A320 family". In: *Flight Global* (2008). URL: <https://www.flightglobal.com/airbus-begins-tests-to-extend-service-life-of-a320-family/78350.article>.
- [33] Dittus; P.W.; Boelter; L.M. In: *Publications in Engineering* 1.13 (1985), pp. 443–461.
- [34] Stian T. Magnusson and Danielle Murphy-Cannella. *AMMONIA – WHAT IS IT, AND HOW CAN IT BE APPLIED TO THE ENERGY AND SHIPPING SECTORS?* 2021. URL: <https://www.econnectenergy.com/articles/ammonia-what-is-it-and-how-can-it-be-applied-to-the-energy-sector#:~:text=Ammonia%5C%20can%5C%20be%5C%20used%5C%20as%5C%20a%5C%20transport%5C%20fuel%5C%20by%5C%20engine,liquid%5C%20to%5C%20gas%5C%20phase%5C%20changes..>
- [35] Tippawan Markmaitree, Ruiming Ren, and Leon L. Shaw. "Enhancement of Lithium Amide to Lithium Imide Transition via Mechanical Activation". In: *J. Phys. Chem. B* 100 (2006). DOI: <https://doi.org/10.1021/jp060181c>.
- [36] Tippawan Markmaitree, Ruiming Ren, and Leon L. Shaw. "Enhancement of Lithium Amide to Lithium Imide Transition via Mechanical Activation". In: *The Journal of Physical Chemistry B* 110.41 (2006). PMID: 17034263, pp. 20710–20718. DOI: 10.1021/jp060181c.
- [37] Orlita Martin and Vos Roelof. "Cruise Performance Optimization of the Airbus A320 through Flap Morphing". In: *AIAA Aviation Technology, Integration, and Operations Conference* 17 (2017). DOI: 10.2514/6.2017-3264. URL: <chrome-extension://efaidnbmninnibpcajpcglclefindmkaj/https://pure.tudelft.nl/ws/files/20290950/template.pdf>.
- [38] G. S. McDouGALL and D. W. Cho. *Estimating Practical Maximum Flight Hours for General Aviation Turboprop and Jet Aircraft*. 2022. URL: <https://onlinepubs.trb.org/Onlinepubs/trr/1989/1214/1214-007.pdf> (visited on 05/11/2022).

- [39] T.H.G. Megson. *Aircraft Structures for Engineering Students*. sixth. Elsevier, 2017.
- [40] Ir. Joris Melkert. *Lecture 4: Aero Engines - Theory*. 2020.
- [41] J.A. Mulder et al. *Flight Dynamics*. 2013. URL: <https://brightspace.tudelft.nl/d2l/le/content/419895/viewContent/2369208/View> (visited on 04/28/2022).
- [42] C. Nally. "How Much Does A Boeing 737 Engine Cost?" In: *McNally Institute* (2022). URL: <https://www.mcnallyinstitute.com/how-much-does-a-boeing-737-engine-cost/>.
- [43] Fabrizio Oliviero. "AE3211-I Systems Engineering Aerospace Design". In: *TUDeft* (2021).
- [44] Arvind Gangoli Rao and Ivan Langella. *Project Guide DSE A320-H3N*. 2022.
- [45] Dr. Arvind Gangoli Rao and Dr. Ivan Langella. *Project Description*. 2022. URL: <https://brightspace.tudelft.nl/d2l/le/content/397908/viewContent/2629322/View> (visited on 04/28/2022).
- [46] Lorenz Ratke. "Aerogels: Structure, properties and applications". In: Oct. 2011.
- [47] Daniel P. Raymer. "Aircraft Design: A Conceptual Approach". In: *President; Conceptual Research Corporation I* (1992), p. 279.
- [48] Abdullah Saleem, Iftekhar A. Karimi, and Shamsuzzaman Farooq. "Estimating NOx emissions of useful two-fuel blends from literature data". In: *Fuel* 316 (2022), pp. 123–213.
- [49] Gary Schnitkey et al. "Nitrogen Fertilizer Prices and Supply in Light of the Ukraine-Russia Conflict". In: (2022). URL: <https://farmdocdaily.illinois.edu/2022/04/nitrogen-fertilizer-prices-and-supply-in-light-of-the-ukraine-russia-conflict.html#:~:text=According%5C%20to%5C%20the%5C%20Agricultural%5C%20Marketing%5C,per%5C%20ton%5C%20in%5C%20October%5C%202021..>
- [50] Manel Sghairi et al. "Architecture Optimization Based on Incremental Approach for Airplane Digital Distributed Flight Control System". In: (October 2008). URL: https://www.researchgate.net/publication/232632092_Architecture_Optimization_Based_on_Incremental_Approach_for_Airplane_Digital_Distributed_Flight_Control_System.
- [51] Skybrary. *Emergency Evacuation on Land*. 2022. URL: <https://skybrary.aero/articles/emergency-evacuation-land#:~:text=those%5C%20on%5C%20board.-Certification,total%5C%20number%5C%20of%5C%20emergency%5C%20exits> (visited on 04/28/2022).
- [52] Smith et al. "Current and future role of Haber–Bosch ammonia in a carbon-free energy landscape". In: *Energy Environ. Sci.* 13 (2 2020), pp. 331–344. DOI: 10.1039/C9EE02873K. URL: <http://dx.doi.org/10.1039/C9EE02873K>.
- [53] Bryan H. R. Suryanto et al. "Nitrogen reduction to ammonia at high efficiency and rates based on a phosphonium proton shuttle". In: *SCIENCE*.372 (2021). URL: <https://www.sciencedaily.com/releases/2021/06/210610150110.htm>.
- [54] "The Jet Engine". In: fifth. Rolls-Royce plc, 1986.
- [55] Egbert Torenbeek. "Synthesis of subsonic airplane design". In: *Delft University Press* 90-247-2724-3 (Dec. 1982).
- [56] P.P. Walsh and P. Fletscher. "Gas Turbine Performance". In: second. Blackwell Science, 2004.
- [57] Thomas J. Wood and Joshua W. Makepeace. "Assessing Potential Supports for Lithium Amide-imide Ammonia Decomposition Catalysts". In: *ACS Applied Energy Materials* 1.6 (2018), pp. 2657–2663. DOI: 10.1021/acsaem.8b00351.
- [58] Yihao Xu et al. "Optimization and design of heat recovery system for aviation". In: *Applied Thermal Engineering* 165 (2020), p. 114581. ISSN: 1359-4311. DOI: <https://doi.org/10.1016/j.applthermaleng.2019.114581>. URL: <https://www.sciencedirect.com/science/article/pii/S1359431119315650>.
- [59] Feijia Yin and Arvind Gangoli Rao. "A review of gas turbine engine with inter-stage turbine burner". In: *Progress in Aerospace Sciences* 121 (2020).
- [60] Benjamin Zhang. "The amazing story of how the Airbus A320 became the Boeing 737's greatest rival". In: *Business Insider Nederland* (2019). URL: <https://www.businessinsider.nl/airbus-a320-history-boeing-737-rival-2018-9?international=true&r=US>.

- [61] Cheng; Zhe et al. "Experimental observation of high intrinsic thermal conductivity of AlN". In: *Phys. Rev. Materials* 4 (4 Apr. 2020), p. 044602. DOI: 10.1103/PhysRevMaterials.4.044602. URL: <https://link.aps.org/doi/10.1103/PhysRevMaterials.4.044602>.

A

Diagrams

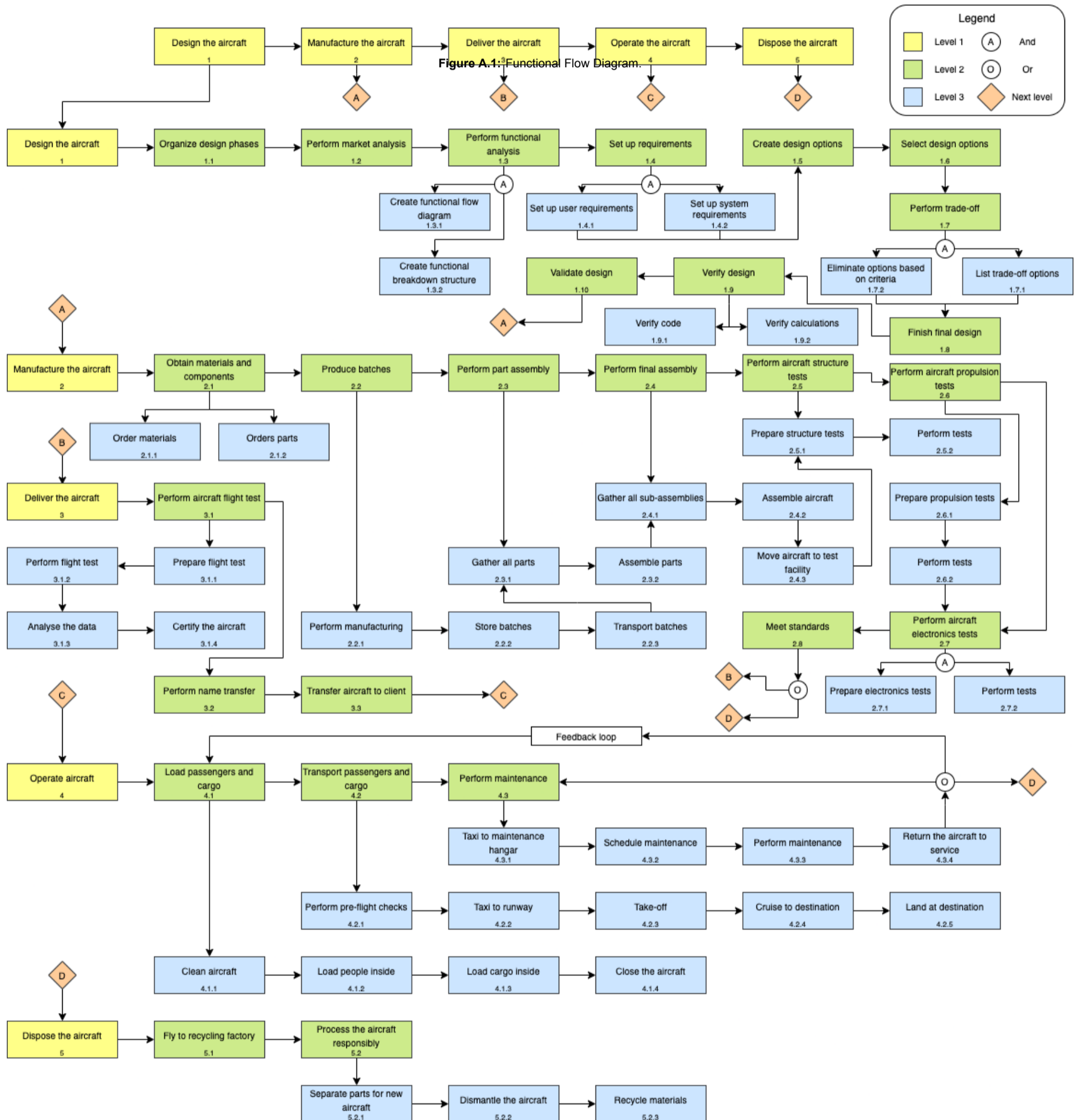
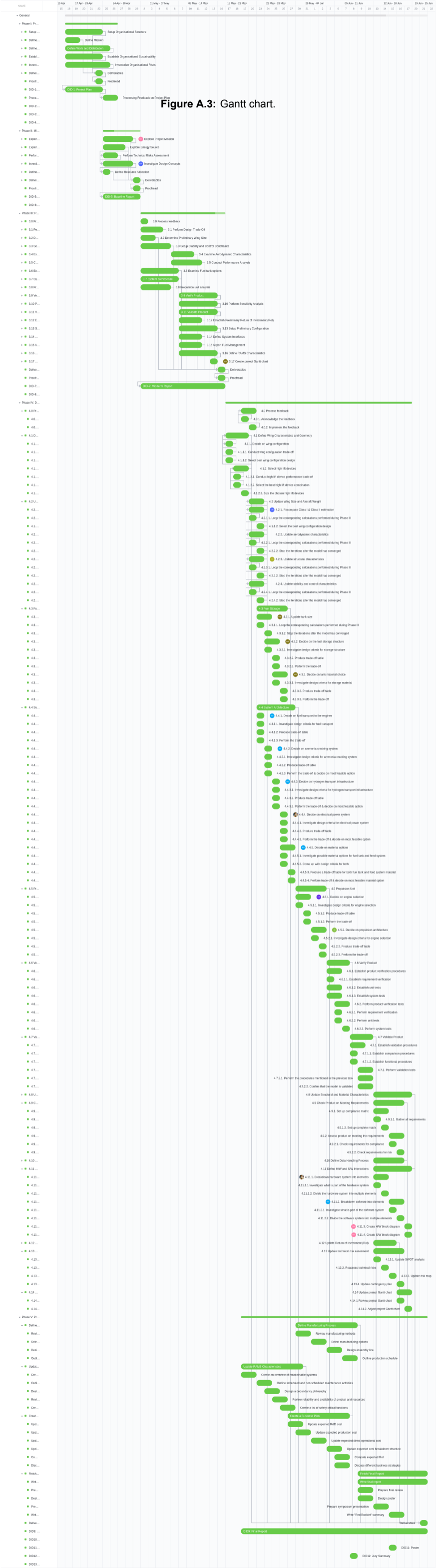


Figure A.2: Functional Breakdown Structure.





B

Design figures

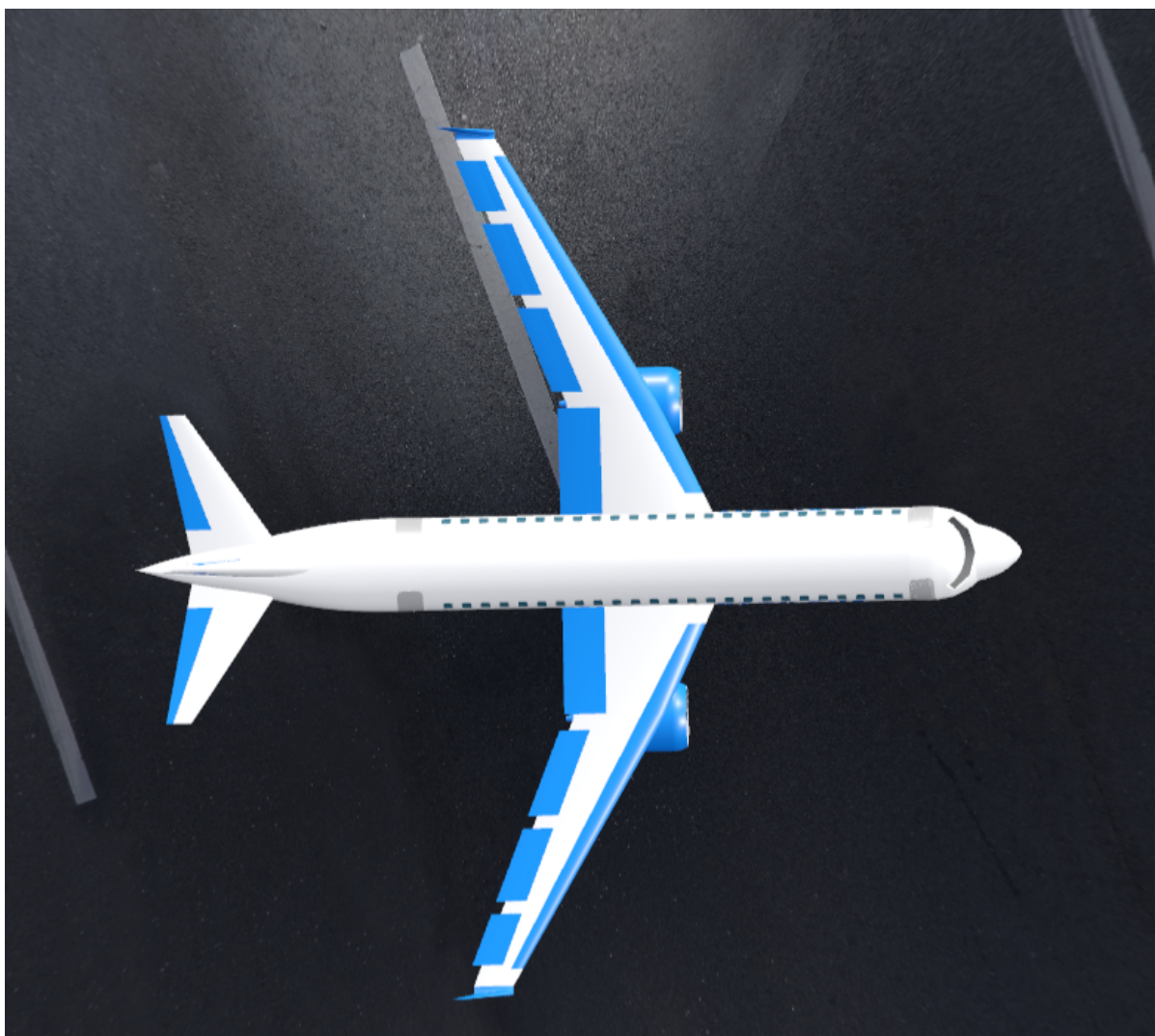


Figure B.1: Top view of the A320-NH3.



Figure B.2: Front-side view of the A320-NH3.



Figure B.3: Back-side view of the A320-NH3.

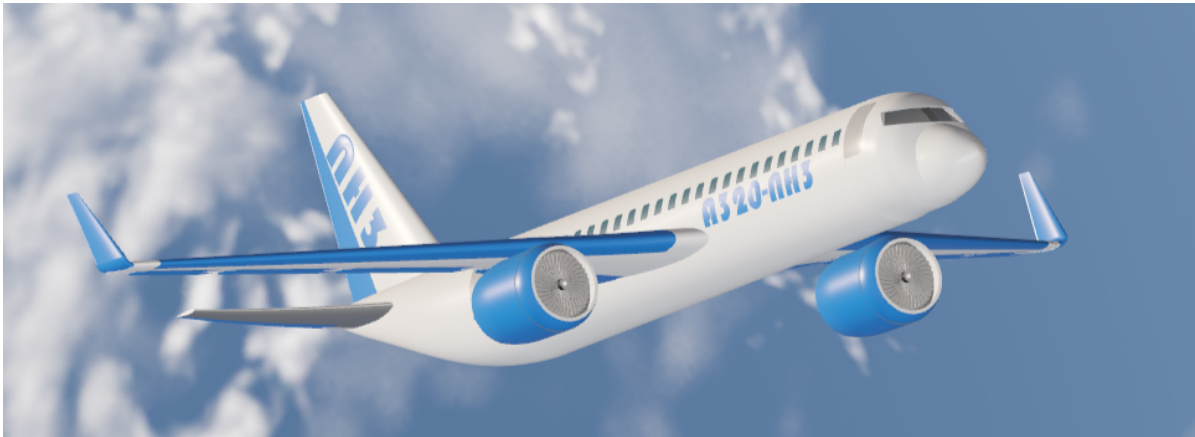


Figure B.4: Bottom view of the A320-NH3 while in flight.

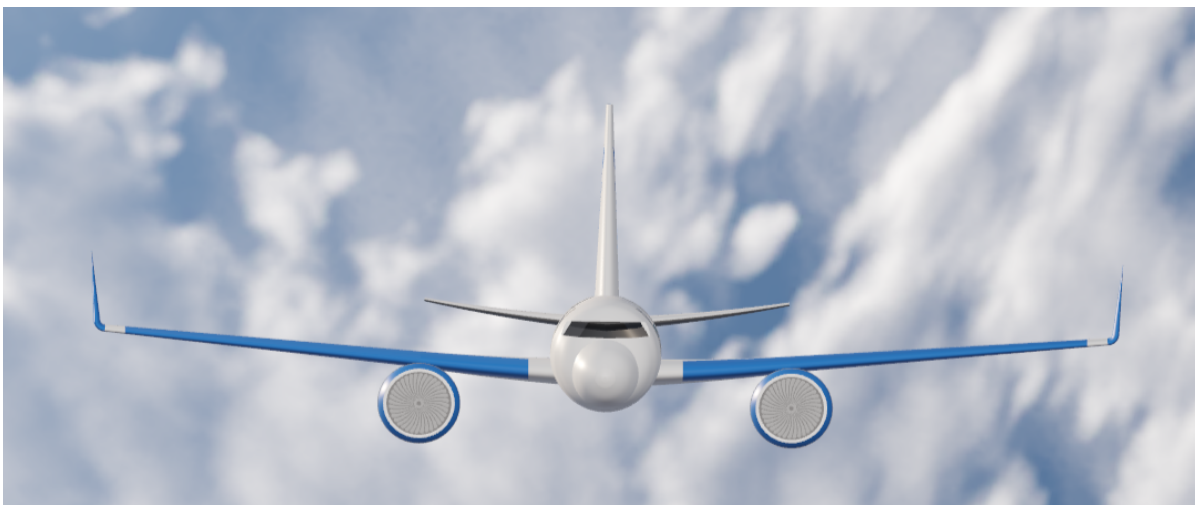


Figure B.5: Front view of the A320-NH3 while in flight.

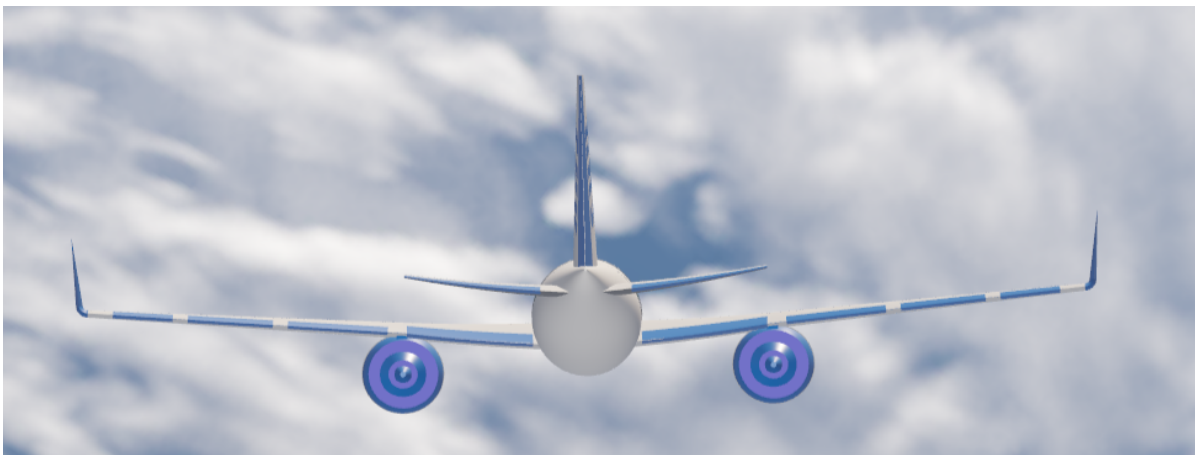


Figure B.6: Back view of the A320-NH3 while in flight.

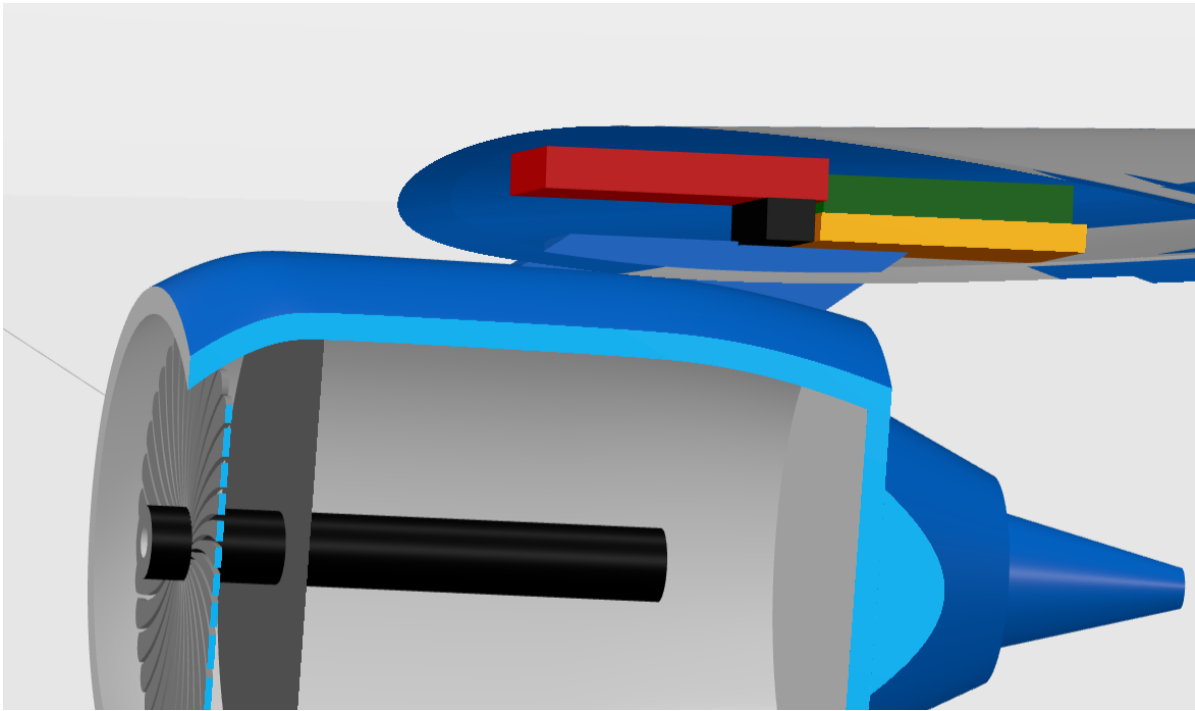
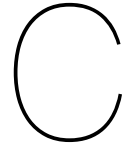


Figure B.7: The visualization of the placement of the cracking system with respect to the wing and the engine. Green: Evaporators, Orange: Preheaters, Red: Reactors, Black: Heat exchangers 2.



Task Division

Table C.1: Distribution of the workload.

	Task	Student Name(s)
	Executive Overview	I. Burdo, W. Biegański
Chapter 1	Introduction	P. Haanen
Chapter 2	Market Analysis	P. Haanen, D.Rhode, I. Burdo
Chapter 3	Requirements and Constraints	P. Haanen, S. Hersbach
Chapter 4	Technical Risk Assessment	B. Sutar, W. Biegański
Chapter 5	Engineering Design & Analysis	S. Hersbach, P. Haanen, C. Cotovanu, J. Brusche, I. Burdo
Chapter 6	Propulsion Design	D.Rhode, B. Sutar, D. Amrane, J. Shi, I. Burdo, J.Brusche, W. Biegański
Chapter 7	A320-NH3 Design Optimization	S. Hersbach, J. Brusche
Chapter 8	Final Design Parameters	D.Rhode, B. Sutar, S. Hersbach, J. Brusche
Chapter 9	Operations & Logistic Concept	I. Burdo
Chapter 10	Material & Manufacturing	C. Cotovanu
Chapter 11	Technical Resource Allocation & Budget Breakdown	B. Sutar
Chapter 12	Verification and Validation Procedures	J. Brusche, P. Haanen, C. Cotovanu
Chapter 13	Reliability, Availability, Maintainability, and Safety (RAMS) characteristics	P. Haanen
Chapter 14	Sustainability	J. Brusche
Chapter 15	Sensitivity Analysis	B. Sutar, J. Brusche, J. Shi
Chapter 16	Requirements and Budgets Compliance	I. Burdo, B. Sutar
Chapter 17	Conclusion	J. Shi, C. Cotovanu
	Editors	C. Cotovanu, S. Hersbach
	Document Design and Layout	D. Amrane, I. Burdo, S. Hersbach , B. Sutar